

Christer Fureby, Peter Eliasson (Eds.)

Proceedings from
FOI Workshop on Computational Fluid Dynamics

SWEDISH DEFENCE RESEARCH AGENCY

Weapons and Protection
SE-147 25 Tumba
Aeronautics
SE-172 90 Stockholm

FOI-R--0456--SE

Mars 2002

ISSN 1650-1942

Lägesrapport

Christer Fureby, Peter Eliasson (Eds.)

Proceedings from

FOI Workshop on Computational Fluid Dynamics

Issuing organization FOI – Swedish Defence Research Agency Weapons and Protection SE-147 25 Tumba Aeronautics SE-172 90 Stockholm	Report number, ISRN FOI-R--0456--SE	Report type Status report
	Research area code 987, 3	
	Month year March 2002	Project no. I235 / I807
	Customers code 5, 3	
	Sub area code ?, 31	
Author/s (editor/s) Christer Fureby Peter Eliasson (Eds.)	Project manager Christer Fureby, Peter Eliasson	
	Approved by	
	Scientifically and technically responsible Christer Fureby, Peter Eliasson	
Report title Proceedings from FOI Workshop on Computational Fluid Dynamics		
Abstract (not more than 200 words) <p>This report is the result of a workshop on Computational Fluid Dynamics, held at FOI Ursvik, 2001-10-30 with participation from Computational Aerodynamics at the Aeronautics Division and Computational Physics at the Weapons & Protection Division. The workshop indicates that FOI is active in a very wide range of activities within the field of Computational Fluid Dynamics, ranging from basic research on numerical methods and turbulence to real-world problem solving relevant to the Swedish defence and the Swedish defence industry. The current state-of-the-art at FOI holds strong promises for the future, and synergistic effects can be achieved by collaboration in new projects utilizing the respective competences of the two groups.</p>		
Keywords workshop, computational fluid dynamics, turbulence modelling, combustion, solid-fluid interactions, electrodynamics, aeroacoustics, IR-calculations, cavitation		
Further bibliographic information	Language English	
ISSN 1650-1942	Pages 240 p.	
	Price acc. to pricelist	
	Security classification	

Utgivare Totalförsvarets Forskningsinstitut - FOI Vapen och skydd 147 25 Tumba Flygteknik 172 90 Stockholm	Rapportnummer, ISRN FOI-R--0456--SE	Klassificering Lägesrapport
	Forskningsområde 987, 7	
	Månad, år Mars 2002	Projektnummer I235 / I807
	Verksamhetsgren 5, 3	
Författare/redaktör Christer Fureby Peter Eliasson (Eds.)	Delområde ?, 31	
	Projektledare Christer Fureby, Peter Eliasson	
	Godkänd av	
	Tekniskt och/eller vetenskapligt ansvarig Christer Fureby, Peter Eliasson	
	Rapportens titel (i översättning) Proceedings from FOI Workshop om numerisk strömningsmekanik	
Sammanfattning (högst 200 ord) Föreliggande rapport är resultatet av en workshop in numerisk strömningsmekanik som hölls i Ursvik 2001-10-30 med deltagande från Beräkningsaerodynamik vid avdelningen för Flygteknik och Beräkningsfysik vid avdelningen för Vapen och skydd. Workshopen visade att FOI har en bred verksamhet inom området numerisk strömningsmekanik, från grundläggande forskning om numeriska metoder och turbulens till praktisk problemlösning som är relevant för Totalförsvaret och försvarsindustrin i Sverige. I dagsläget visar FOI goda framtidsutsikter och synergierffekter kan uppnås genom samverkan i nya projekt som tillvaratar gruppernas respektive kompetenser.		
Nyckelord Workshop, numerisk strömningsmekanik, turbulensmodellering, förbränning, solid-fluidinteraktioner, elektrodynamik, numerisk analys, aeroakustik, IR-beräkningar, kavitation		
Övriga bibliografiska uppgifter	Språk engelska	
ISSN 1650-1942	Antal sidor: 240 s.	
Distribution enligt missiv	Pris: Enligt prislista Sekretess	

Contents

Introduction (C. Fureby & P. Eliasson)	5
Introduction to FOI/ FFA's CFD software (P. Eliasson)	8
Grid generation software (L. Thysell)	27
Introduction to FOAM, FOI/ VS's CFD software (C. Fureby)	32
Flow problems involving moving boundaries and interfaces (E. Lillberg, L. Olovsson)	39
Turbulence modeling in RANS and LES (C. Fureby, L. Persson & U. Svennberg)	51
Turbulence modeling (S. Wallin)	60
Transition prediction (A. Hanifi)	76
Optimal design and control (M. Berggren)	89
High speed turbulent combustion (C. Fureby)	96
Solid rocket propellant combustion and launch technology (M. Berglund)	106
The pulse detonation engine (J. Tegnér)	113
Ram jet robot calculations (M. Tormalm)	123
Conceptual study of a supersonic heavy, low observable missile (J. Johansson)	128
Numerical analysis (J. Nordström)	141
Aeroacoustics (G. Efraimsson)	182
The interaction between a lightning flash and an aircraft in flight (A. Larsson)	188
IR calculations (M. Andersson)	196
Low speed applications (S. Peng)	201
Tip vortex cavitation modeling (N. Wikström)	215
Underwater vehicle hydrodynamics (N. Alin)	228
Surface ship hydrodynamics (E. Lillberg & U. Svennberg)	239

Introduction

The main aim of the FOI Workshop on Computational Fluid Dynamics, held at FOI Ursvik, 2001-10-30 was to bring researchers together from Computational Aerodynamics at the Aeronautics Division in Bromma and from Computational Physics, Dept. of Warheads and Propulsion, Weapons & Protection Division at the Grindsjön Research Center. This joint initiative was an opportunity for the two groups to identify each other's current research areas as well as areas of mutual interest for the future, in order to coordinate their activities and facilitate the integration process between old FFA and old FOA. The workshop indicates that FOI is active in a very wide range of activities within the field of Computational Fluid Dynamics, ranging from basic research on numerical methods, turbulence and turbulence modeling to real-world problems relevant to the Swedish defence and the Swedish defence industry. In many of these areas the research at FOI is of high international quality which is corroborated by the large number of national and international collaborations shared by the two groups. The current state-of-the-art at FOI holds strong promises for the future, and synergistic effects can be achieved by collaboration in new projects utilizing the respective competences of the two groups. These proceedings consist of a collection of slides presented at the workshop. Further information regarding specific research topics is available from the individual researchers.

Christer Fureby Peter Eliasson

FOI Workshop on Computational Fluid Dynamics

2001-10-30

Beräkningsaerodynamik (Flygteknik) –
Beräkningsfysik (Vapen och Skydd)
FOI Ursvik, Konferensrum Frej

FOI

Introduction to FOI/FFA's CFD software (*P.Eliasson*)

Grid generation software (*L.Thysell*)

Introduction to FOAM, FOI/VIS's CFD software
(*C.Fureby*)

Aeroelastic activities (*J.Smith*)

Flow problems involving moving boundaries and
interfaces (*E.Lillberg*)

Turbulence modeling in RANS and LES (*C.Fureby*,
L.Persson & U.Svennberg)

- Turbulence modeling (*S.Wallin*)

Transition prediction (*A.Hanifi*)

Optimal design and control (*M.Berggren*)

High speed turbulent combustion (*C.Fureby*)

Solid rocket propellant combustion and launch
technology (*M.Berglund*)

The pulse detonation engine (*J.Tegnér*)

Applied aerodynamics (*O.Hamér*)

Ram jet robot calculations (*M.Tormalm*)

Conceptual study of a supersonic heavy, low observable
missile (*J.Johansson*)

Numerical analysis (*J.Nordström*)

Aeroacoustics (*G.Efraimsson*)

The interaction between a lightning flash and an aircraft
in flight (*A.Larsson*)

IR calculations (*M.Andersson*)

Low speed applications (*S.Peng*)

Tip vortex cavitation modeling (*N.Wikström*)

Underwater vehicle hydrodynamics (*N.Alin*)

Surface ship hydrodynamics (*E.Lillberg & U.Svennberg*)

Introduction to FOI/FFA's CFD software

P. Eliasson

Euranus

Euranus : European Numerical Aerodynamic Simulator, developed at FFA and VUB, developed for ESA

- 3D RANS compressible Navier-Stokes cell centred finite-volume solver for structured multiblock grids
 - Steady state solver/time accurate solver with/without moving grids
 - Convergence acceleration like multigrid and implicit residual smoothing
 - Originally designed for high-speed flows, contains thermally perfect gas models, equilibrium chemistry, chemical and thermal non-equilibrium models
- Several turbulence models
 - Rotating frame of reference, block-wise
 - Large variety of numerical models and b.c. for external/internal flows
 - Sequential/parallel (PVM)

Turbulence models

- Baldwin-Lomax turbulence model (algebraic)
 - Spalart Almaraas turbulence model (one equation)
 - $k-\varepsilon$ turbulence model, near wall treatment by Chien (two equations)
 - $k-\omega$ turbulence model (two equations)
 - Wilcox standard model
 - Wilcox low-Reynolds model
 - BSL model by Menter
 - SST model by Menter
 - Explicit Algebraic Reynolds Stress Models (two equations)
 - New model by Wallin & Johansson
 - Model by Gatski & Speziale; Shih Zhu & Lamley
 - Linear model
 - RANS/LES based on Spalart Almaraas
 - LES, dynamic SGS model
- Transition may be imposed along grid lines (by requiring $P=0$)

Additional options

- Spatial discretizations, 2nd order accurate
 - Central discretization with artificial dissipation
 - Upwind schemes with TVD limiters
- Boundary conditions
 - Characteristic b.c., inlet and outlet b.c., spec. fields on boundary ...
 - Wall (viscous or Euler)
 - Connectivity, periodicity, translation, rotation, ...
 - Non-matching boundary conditions
 - Preconditioning for low Mach numbers
- Gas options
 - Calorically perfect gas
 - Thermally perfect gas
 - Equilibrium thermo chemistry
 - Chemical and thermo chemical non-equilibrium

Steady state solver

- FAS multigrid
 - Saw-tooth, V-, or W-cycles
 - Simplification on coarser grids
 - Full multigrid
 - Different transfer operators between coarse/fine grids
 - Simplification on coarser grids
- N-stage explicit Runge-Kutta scheme as smoother
- Implicit residual smoothing
 - Constant or variable coefficients, explicit contribution
 - Usually gives a doubling of possible CFL number
- Point implicit treatment of turbulent and chemical source terms

Unsteady Solver

- Explicit 4th order Runge-Kutta
- Implicit 2nd order backward difference with explicit pseudo time iteration

$$\frac{1.5(qV)^{n+1} - 2(qV)^n + 0.5(qV)^{n-1}}{\Delta t} + R(q^{n+1}) = 0$$
$$V^n + \frac{1}{\Delta t} \frac{dq^*}{d\tau} + R^*(q^*) = 0 \quad R^*(q^*) = \frac{1.5V^{n+1}}{\Delta t} q^* + R(q^*) + \frac{-2(qV)^n + 0.5(qV)^{n-1}}{\Delta t} \frac{dq^*}{d\tau} \rightarrow 0 \Rightarrow q^* \rightarrow q^{n+1}$$

Typically: 10-20 multigrid cycles for about 3 orders of residual reduction

- Moving grids

Grid movement from analytical expressions or perturbation grids
GCL

Block wise rotation/steady blocks

Aeroelastic computations with linear eigenmodes as input perturbation grids

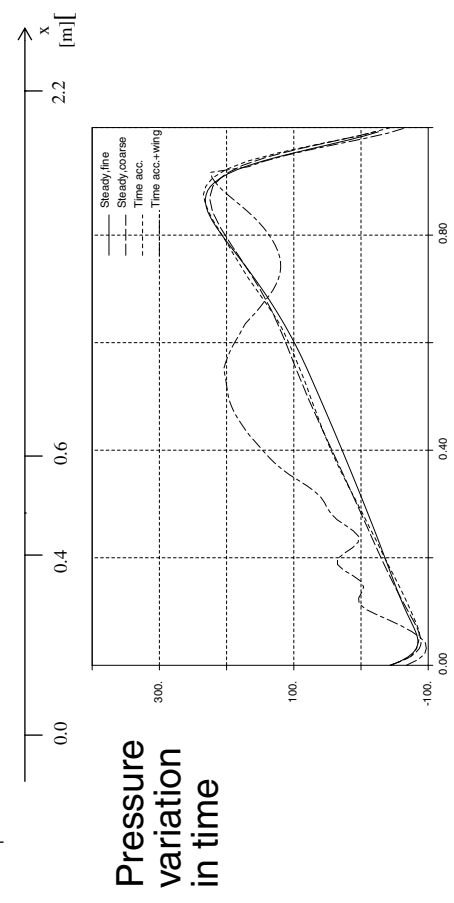
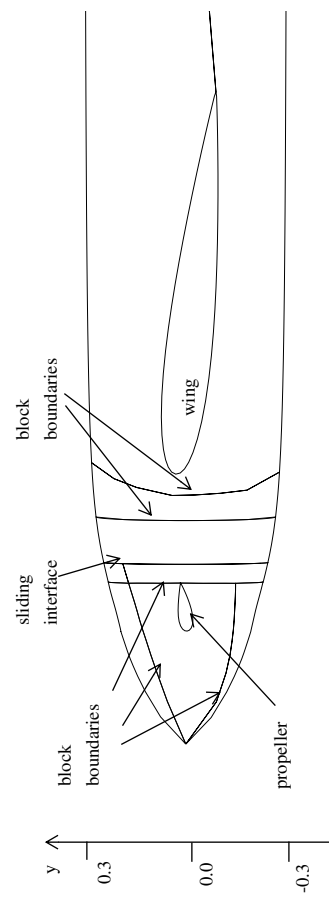
- Manoeuvres, e.g. acceleration

Non-matching boundary conditions

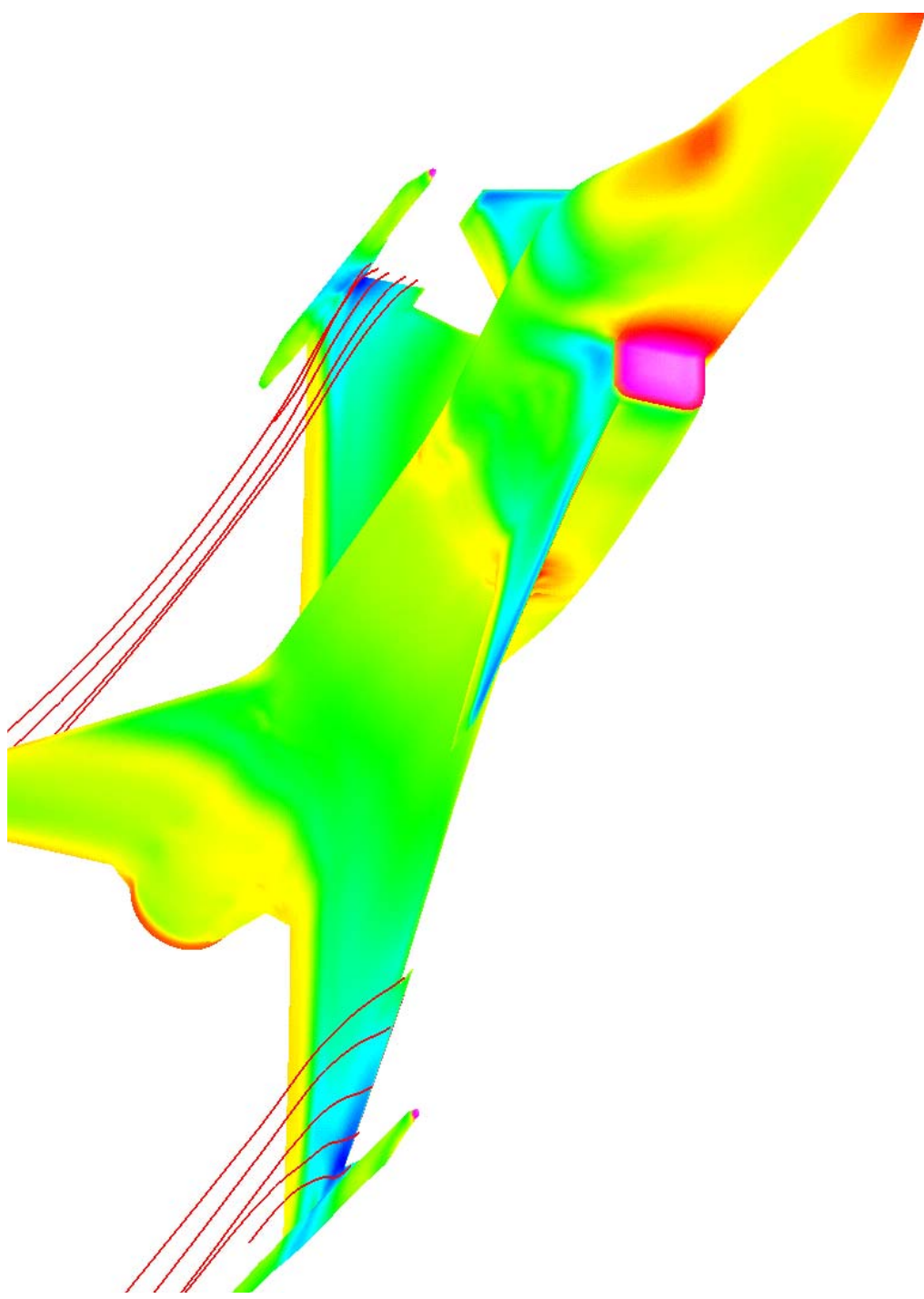
Non-matching options available, matched grids with grid discontinuity normal to the boundary. Useful for local refinement or rotating - non-rotating calculations

- The same grid topology in the two non-matching blocks
- No topology requirement (more expensive)

Example, propeller-wing calculation AlAA-98-0371



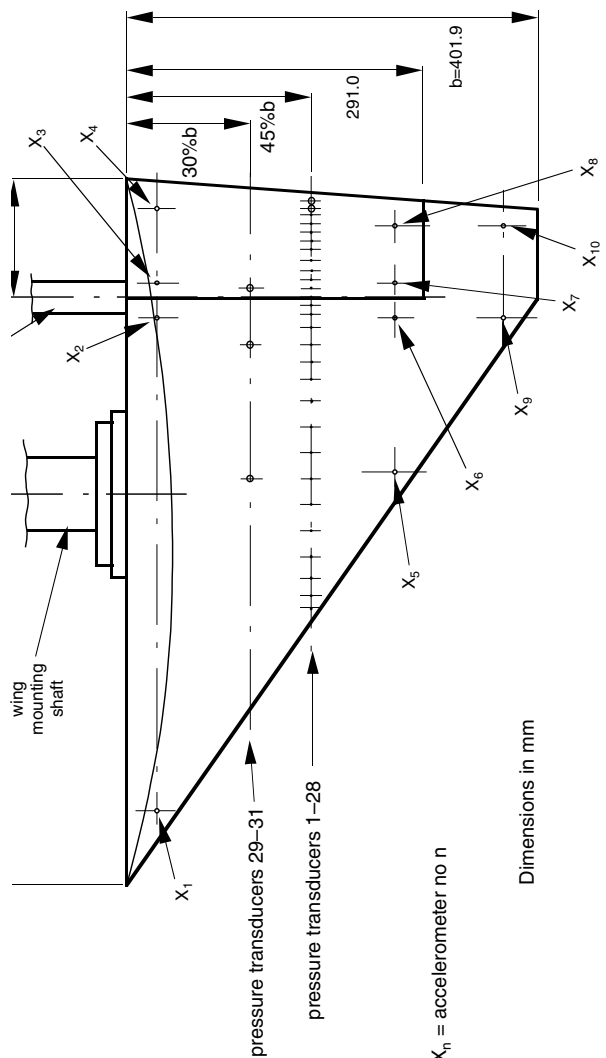
JAS computation



JAS at transonic
conditions
Mach number
distribution

FOI

3D delta wing with oscillating flap



55° delta wing

Pressure measurements at FFA T1500

Euler calculations at SAAB

Navier-Stokes computations at FFA

FOI

Unsteady Euler results

Unsteady Cp-distribution

Computations-Experiments

$$M_{\infty} = 0.94, \alpha = 0^\circ, \delta_{mean} = 0^\circ$$

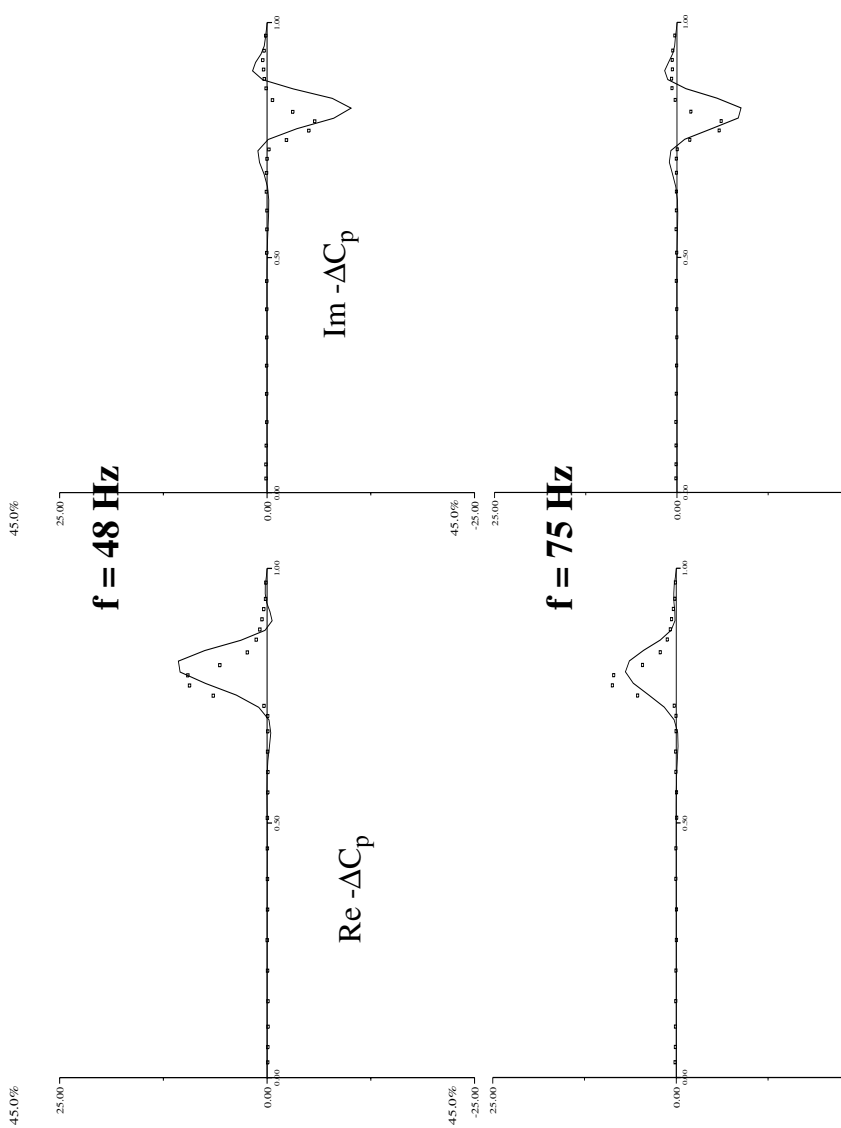
Real: in-phase

Imaginary: out-of-phase
(damping)

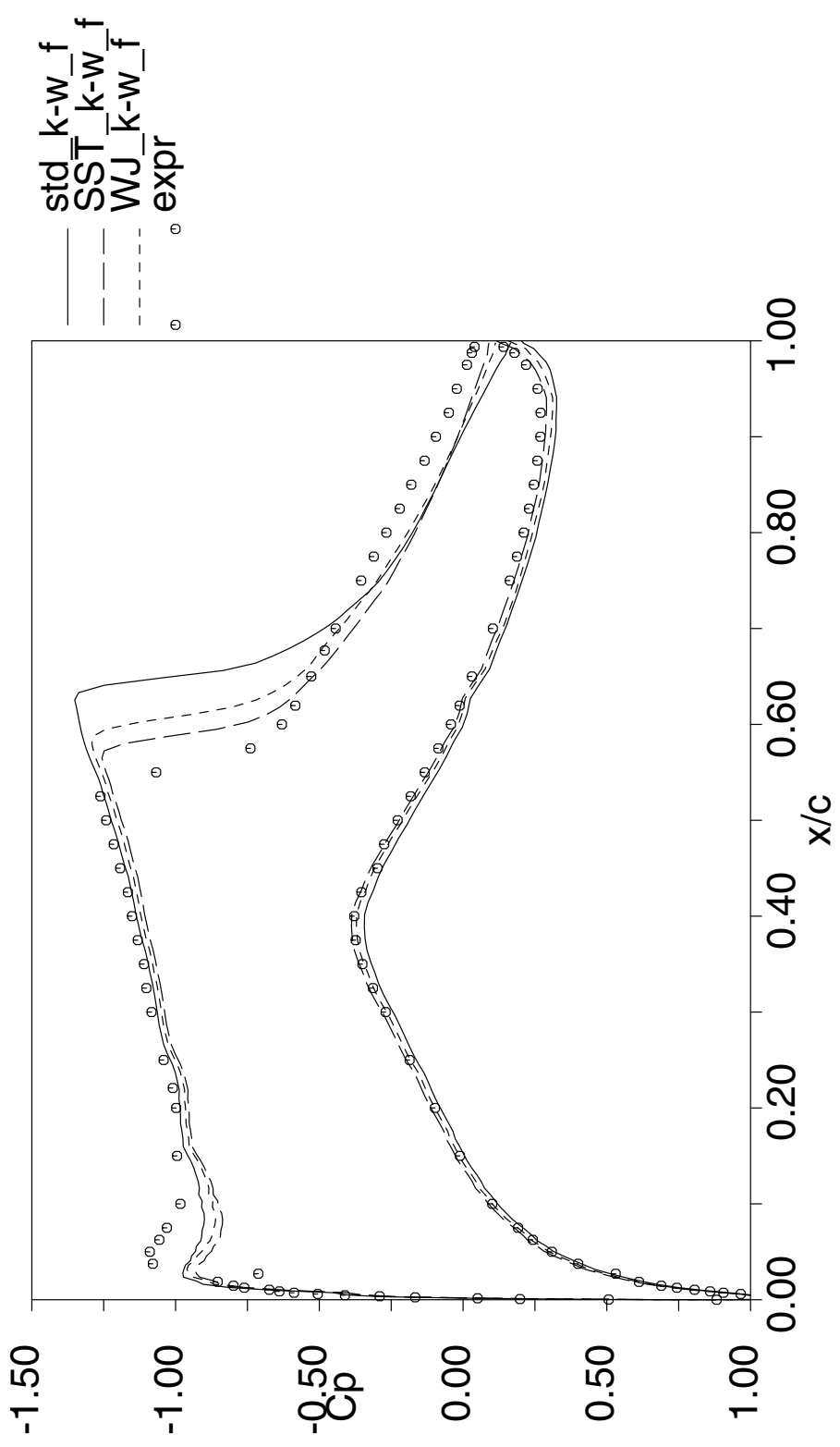
References:

AIAA-96-2417

ECCOMAS 1996, pp.478-484



RAE2822 Case 10



Mach 0.754, $a_0 \cdot a = 2.57$, $Re=6.2 \cdot 10^6$, C-mesh 273*81

FOI

European Cooperation

Ongoing European projects (5th F.W)

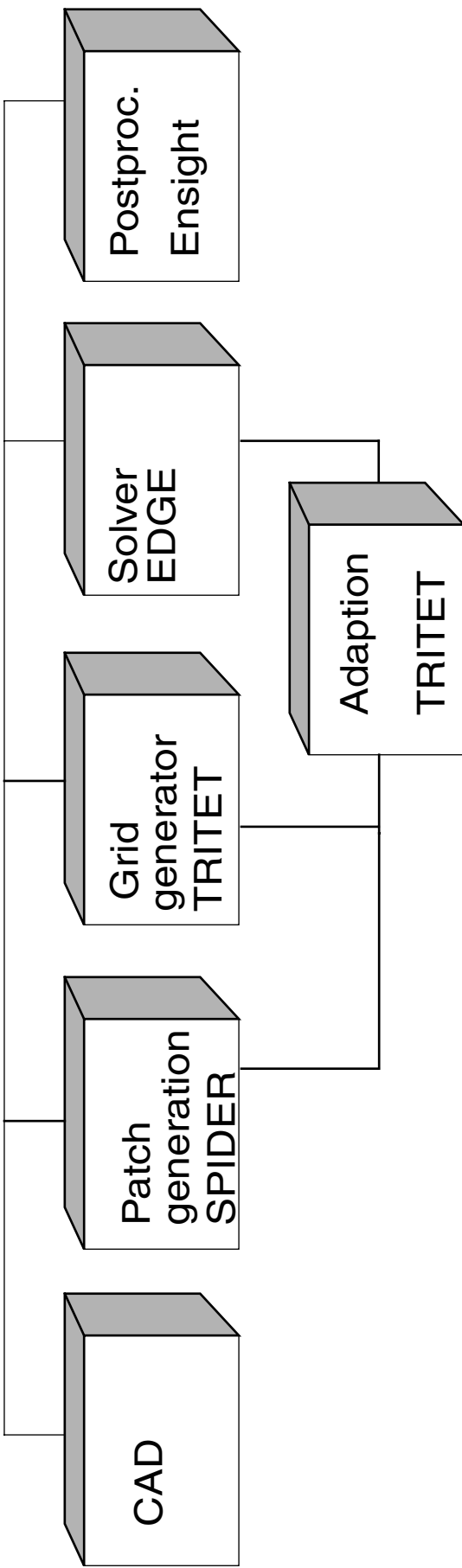
- Eurolift - high lift project, industrially oriented
- HiAer - high lift research oriented
- Helix - high lift, new concepts
- HyLtec - Laminar flow technologies
- ALTA - Laminar flow technologies
- Aeroshape - shape optimization
- TurboNoiseCFD - Aero acoustics in jet engines
- Taurus - Aero elasticity

Project starting 2002

- FloMania - turbulence modelling
- KnowBlade - wind turbine project

FOI

System for computations on unstructured grids



SPIDER - in-house program for creation of patched surface patches from IGES files

TRITET - Surface and volume generator. Includes also adaption modules

EDGE - Flow solver

Post processing: commercial tools, programs for simpler plotting exists

Hybrid grid generation

TRITET

- Generation of unstructured grids
- 2D - triangles and quadrilaterals
- 3D - prisms (varying # layers), pyramids (transitional) and tetrahedra
- Grid adaptation (remeshing) embedded in Tritet
- Grid adaption uses original surface descr.
- Common file format with Edge solver

Ongoing development of Tritet

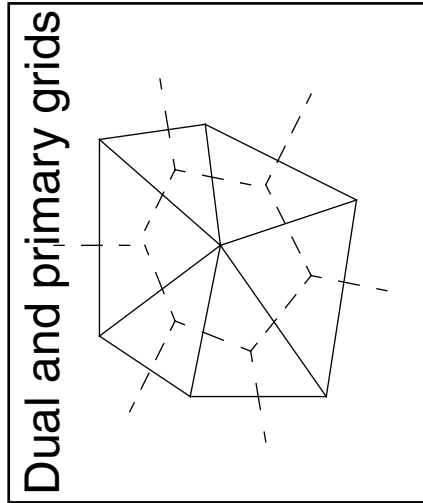
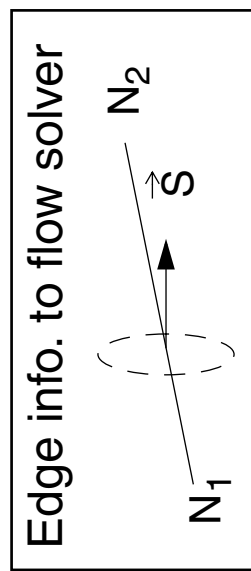
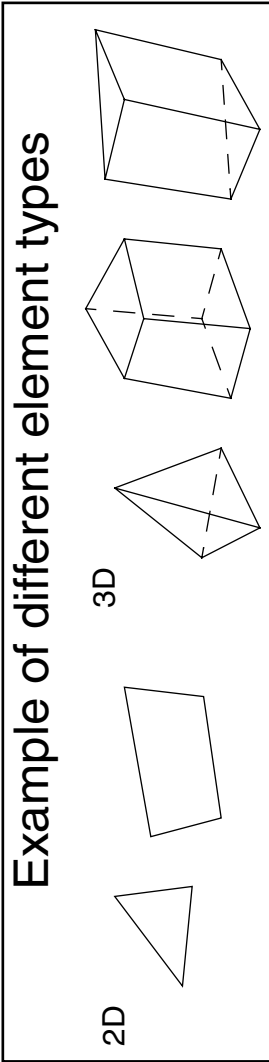
- Moving grids with retained topology
- Local adaptation based on h-refinement
- Local remeshing



Overview EDGE solver

EDGE solver based on: Finite volume, node centred, hybrid grids - arbitrary elements, agglomeration multigrid

- Preprocessor
 - Generates dual grid
 - Agglomerates coarser grids
 - Blocking for parallel computations
- Flow solver
 - Reads preprocessed grid containing node and edge data
 - Makes the flow computation
- Help programs
 - Sets boundary condition
 - Lists contents of files
 - Exports to different file formats
 - Plot programs
 - etc...



EDGE flow solver code characteristics

- Code in FORTRAN 90
 - Data stored in linked list - stored data may be retrieved everywhere
 - Dynamic memory allocation
 - Recursion, derived types, structures ...
- Similarities with EURANUS
 - EURANUS uses the same data structure in Fortran 77
 - Same name of routine names
 - ...
- FFA file format
 - General file format in common with EURANUS
- Strategy to extend and implement most promising options in EURANUS to EDGE

Status of Edge

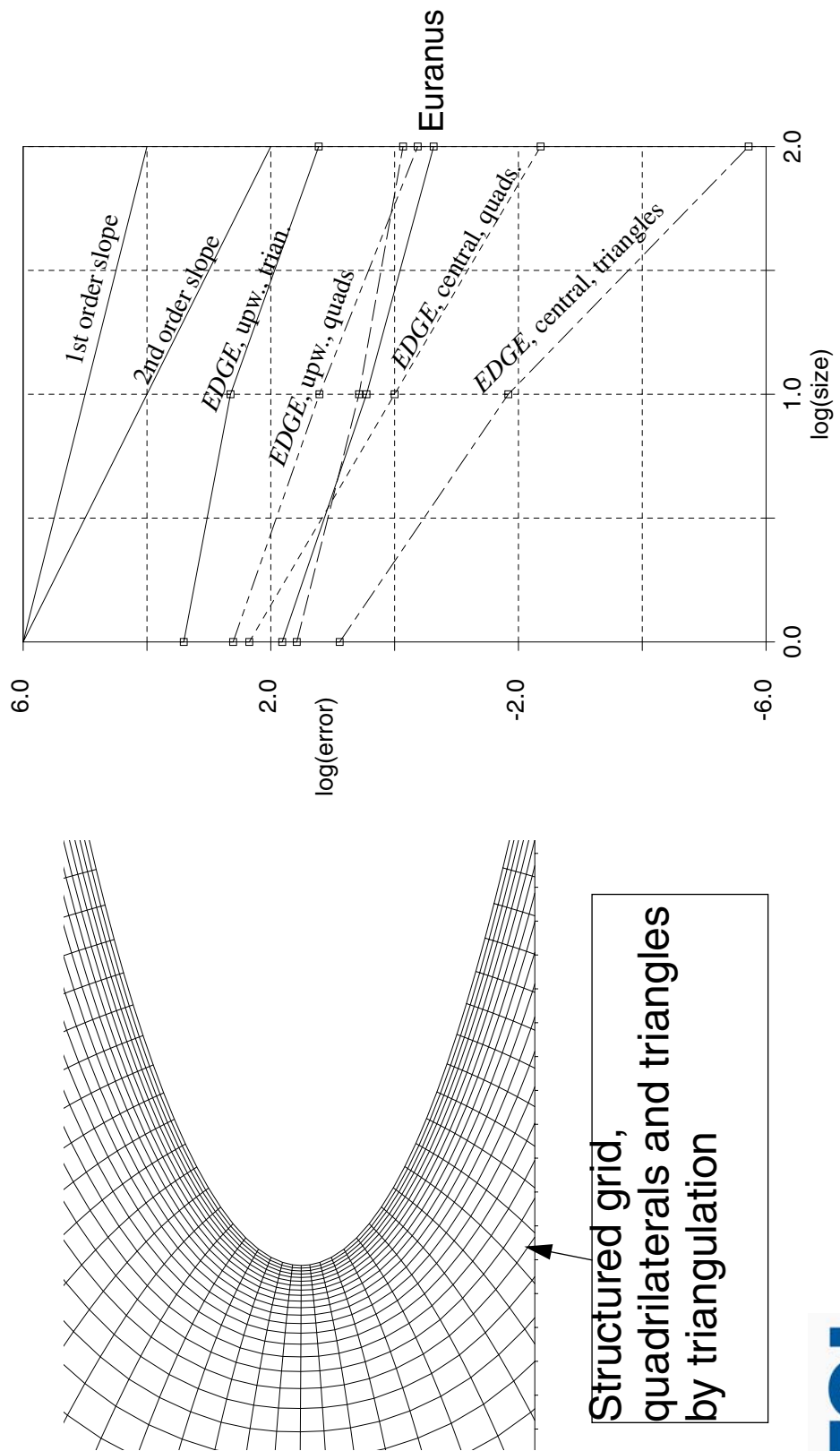
Included and validated features of Edge (2001-10-29)

- Euler and NS, laminar and RANS
- Explicit, steady state, residual smoothing
- Agglomeration multigrid
- Central spatial discretization with artificial viscosity, 2nd order upwind scheme
- Rotation in a rotating frame of reference
- Turbulence: Wilcox k- ω and Explicit Algebraic Reynolds stress model (EARSM)
- Block partitioning with message passing using MPI
- Unsteady ‘dual time stepping’
- Preconditioning for low Mach numbers (Choi & Merkle)
- GUI

Validation of Edge

Total pressure loss, RAE2822 airfoil. $M=0.5$, $\alpha = 2.8$

3 structured grids, 545×97 , 273×49 , 137×25



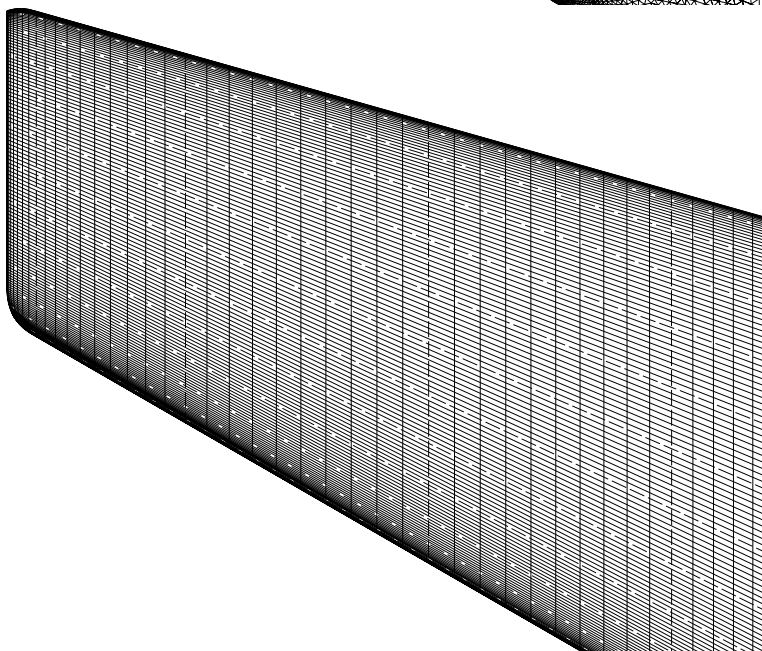
M6-wing: Structured - unstructured

Transonic flow on M6-wing, $M=0.84$, $\alpha=3.06$, $Re=11 \cdot 10^6$

Cp distribution:

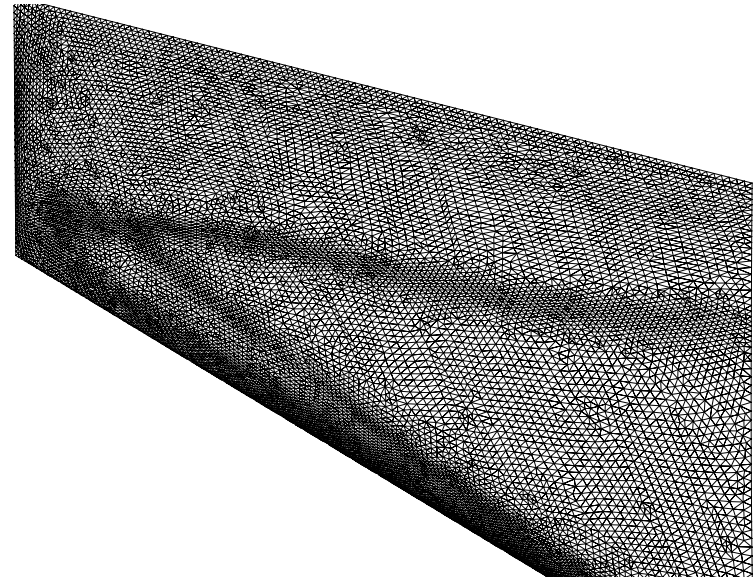
Structured surface grid

1.2 Mpoints



Unstructured surface grid

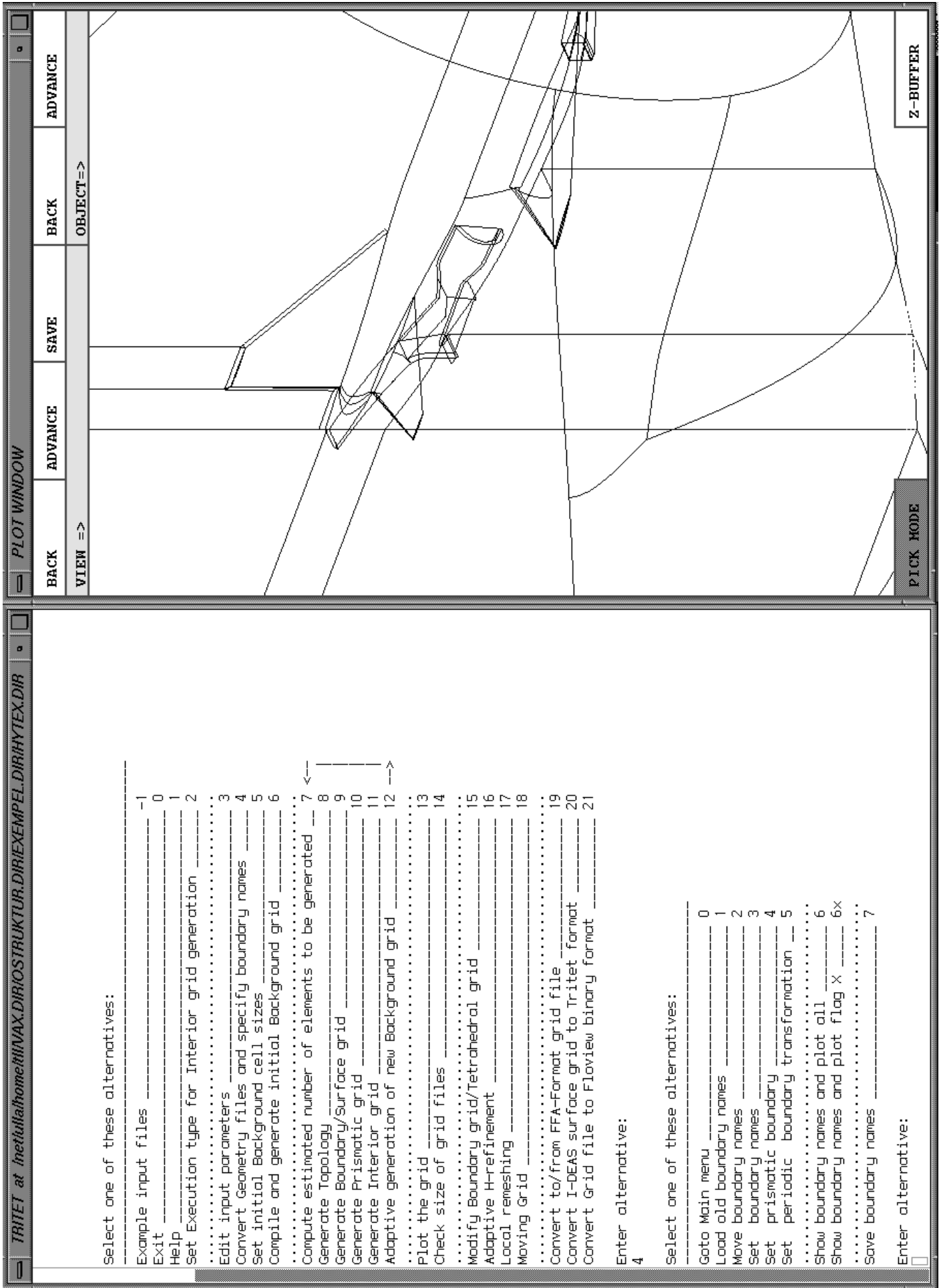
0.9 Mpoints

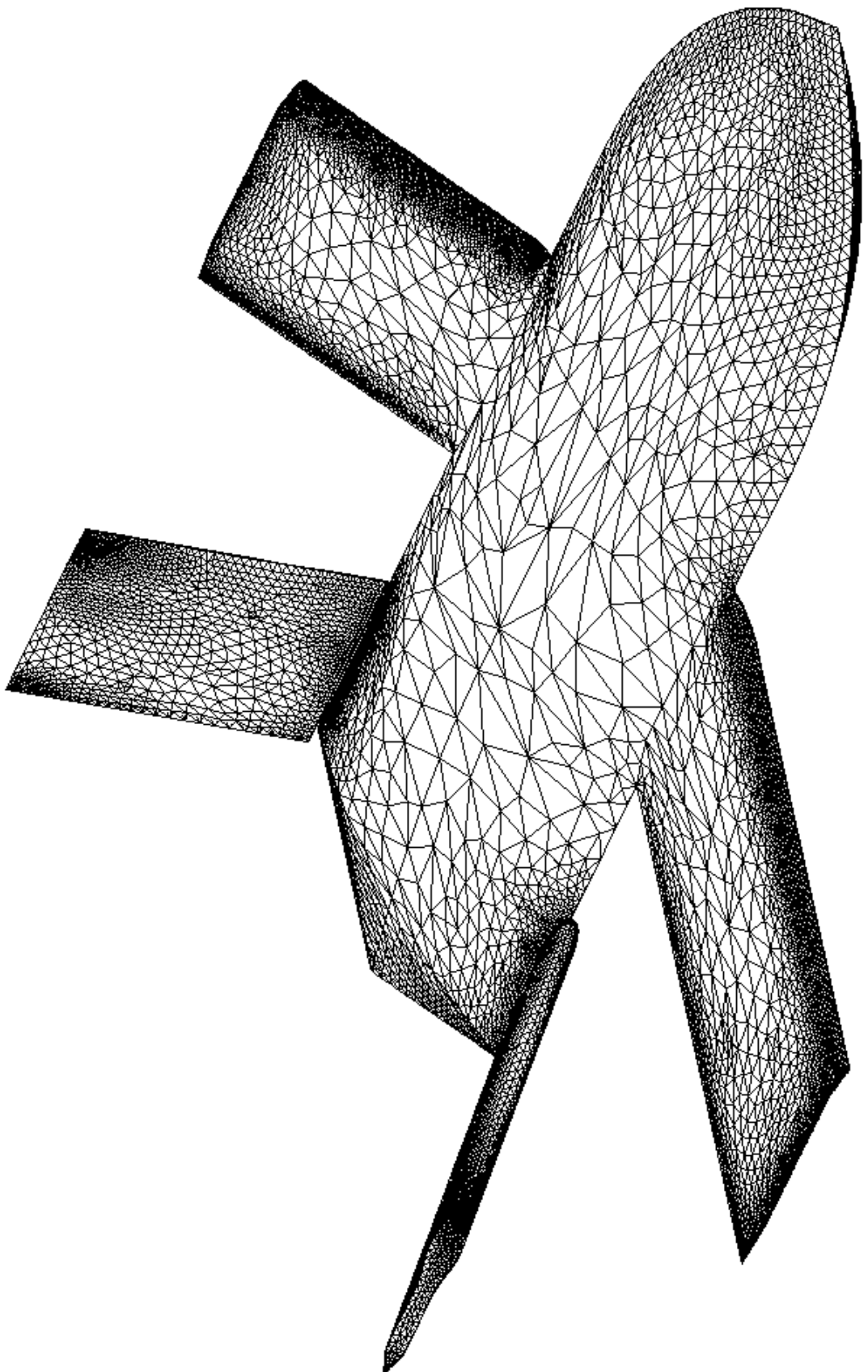


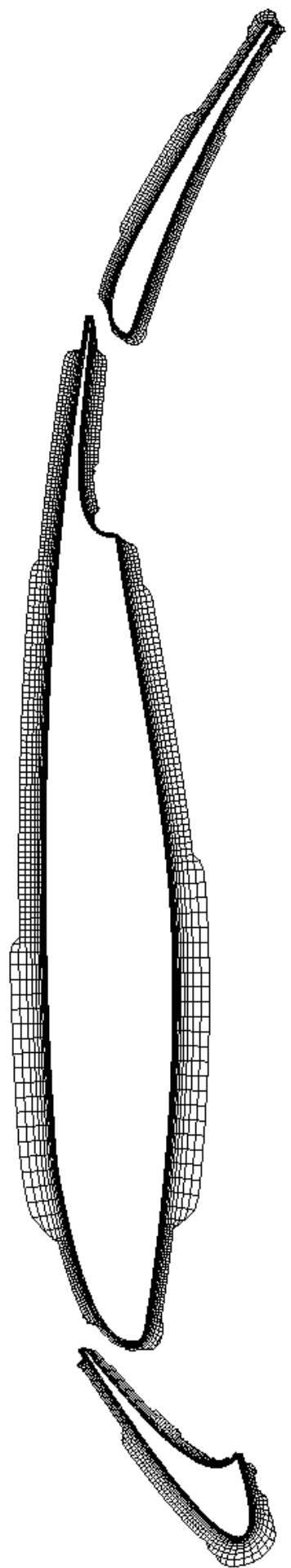
FoI

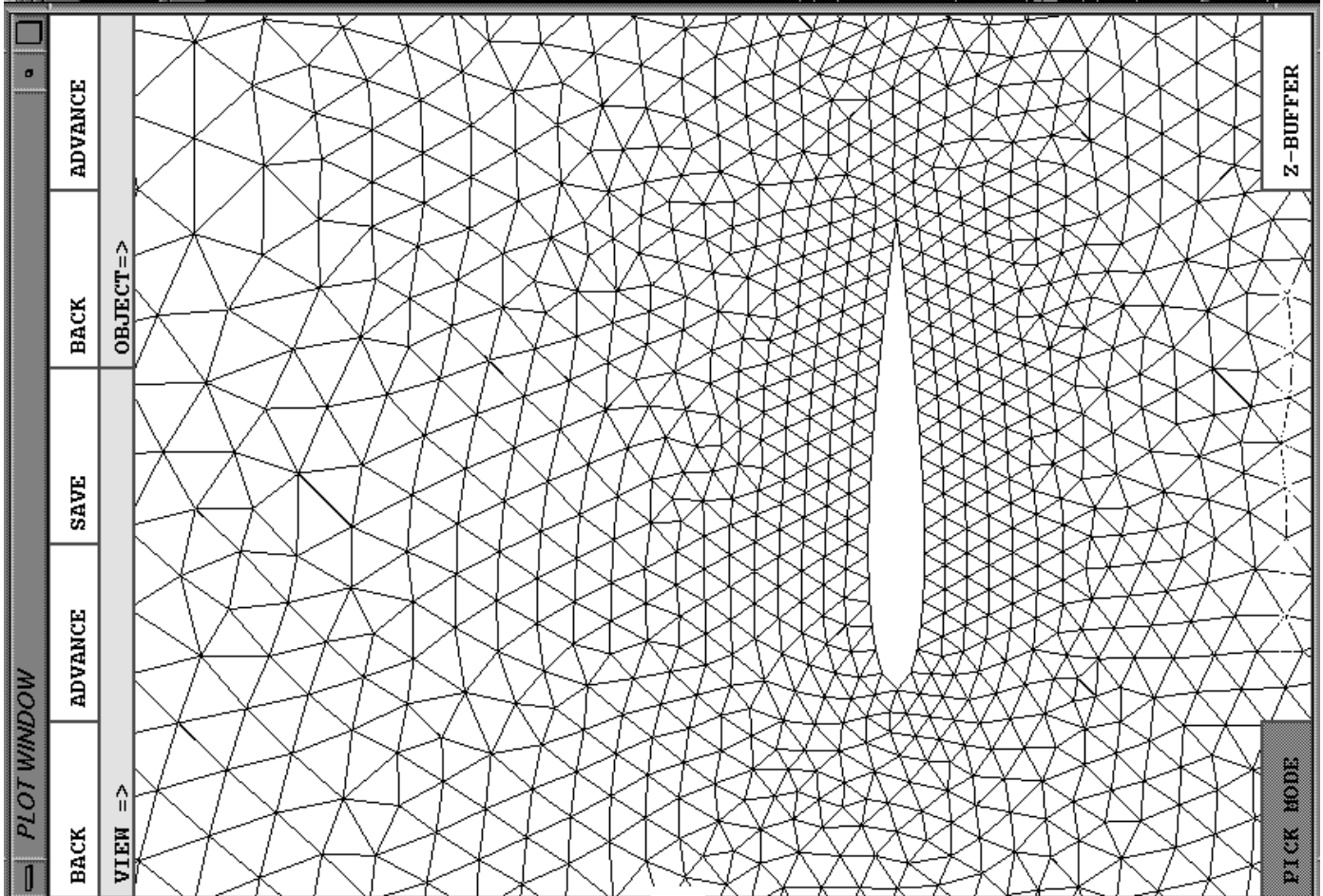
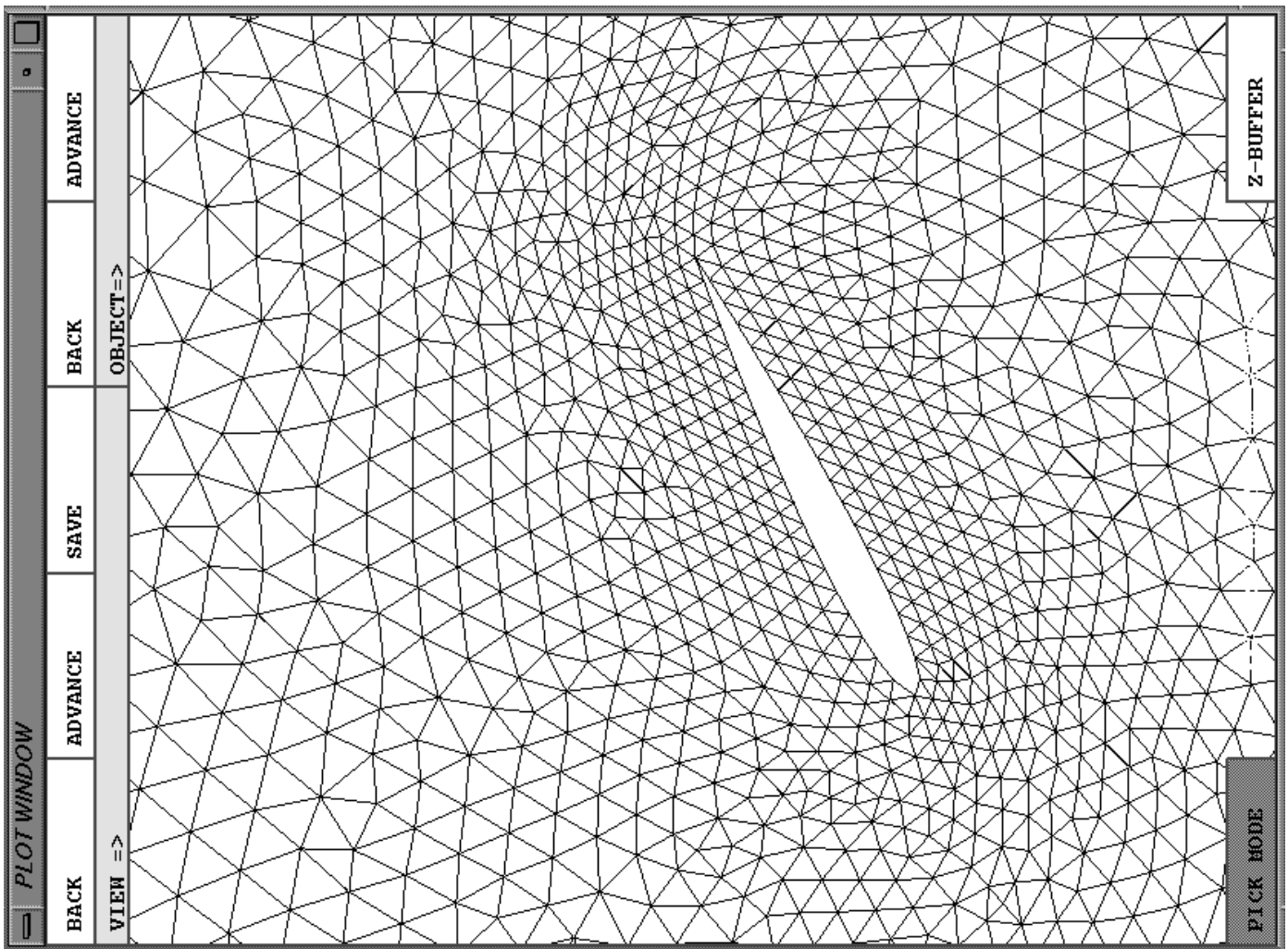
Grid Generation Software

L. Tysell









FOAM™ Field Operation And Manipulation

Christer Fureby
Totalförsvarets Forskningsinstitut, FOI
Vapen & Skydd
Grindsjöns forskningscentrum



History

- 1989 Henry got tired of FORTRAN and started to play around with OOP and particularly C++
- 1990-93 Intense development of the core of FOAM (Hrvoje & Dave) skeletal classes for field manipulation + numerics
- 1994 Gavin joins the group at IC and starts adding more physics
- 1995 Christer & Onno join the group at IC, further physics, turbulence, combustion, electromagnetics → publications
- 1995-98 FOAM grows into a full-bodied CCM package (group of 5-7 people)
- 1999 Academic research code → Commercial code?
- 2000 Foundation of Nabla Ltd.
- 2001- Marketing of FOAM on LINUX PC's as a 'package solution' to CFD

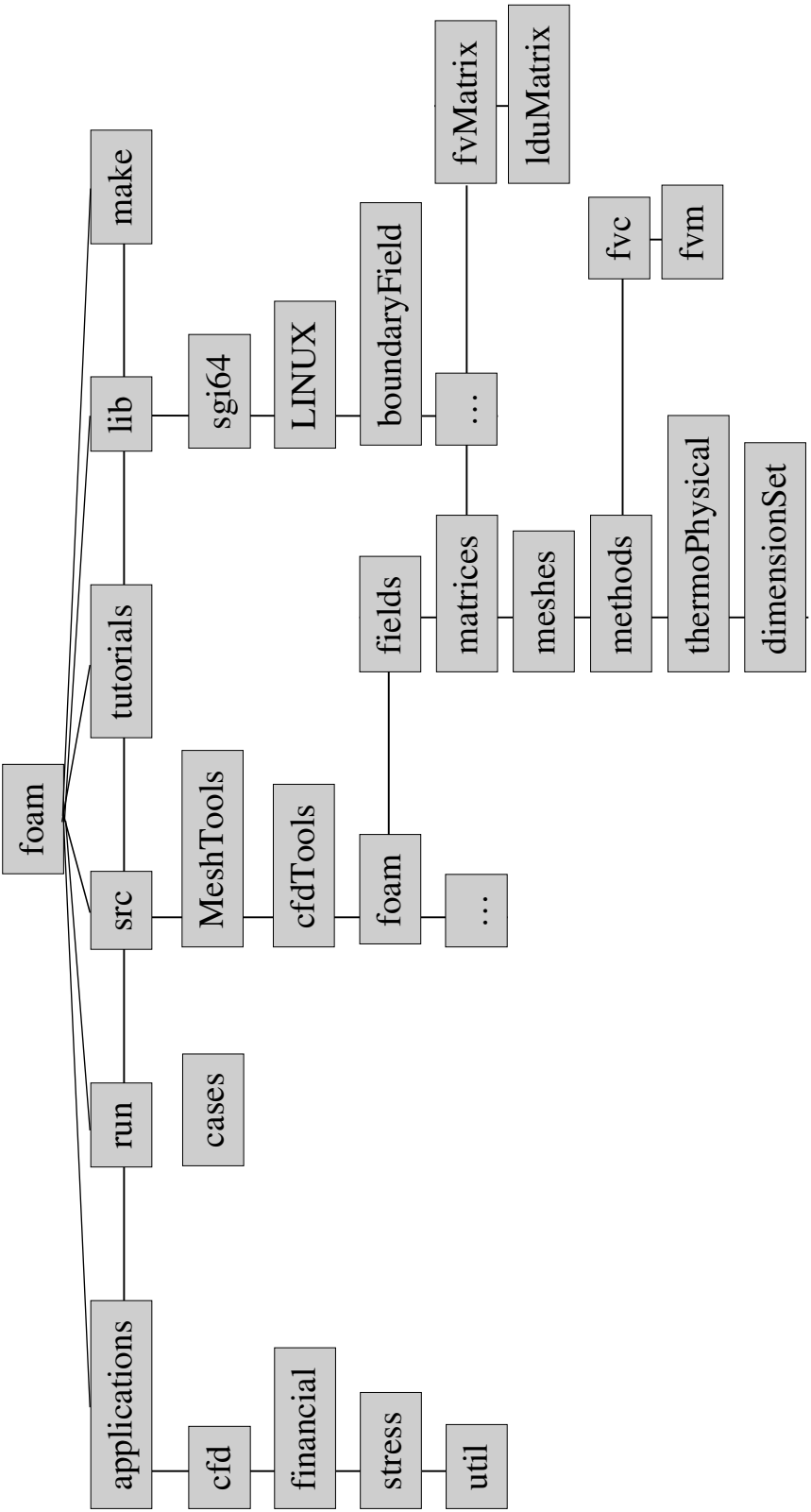
Contact: Nabla Ltd.

e-mail H.Weller@nabla.co.uk



Weller H.G., Tabor G., Jasak H. & Fureby C.; 1997, "A Tensorial Approach to CFD using Object Oriented Techniques", Comp. in Physics, **12**, p 629.

Overall Structure



Platforms: UNIX, UNICOS:
SUN, IBM, CRAY, SGI, HP, DEC
PC

Parallelization: pvm and mpi
Linux



Discretization and Numerics

The NSE can be discretized as

$$\begin{cases} \sum_f (\mathbf{v} \cdot d\mathbf{A})_f = 0 \\ \sum_{i=0}^m (\alpha_i (\mathbf{v})_P^{n+i} + \frac{\beta_i \Delta t}{\delta v_p} \sum_f [\mathbf{F}_f^C + \mathbf{F}_f^D]^{n+i}) = -\beta_i (\nabla p)_P^{n+i} \Delta t \end{cases}$$

where $\begin{cases} \mathbf{F}_f^C = F_f \mathbf{v}_f \approx F_f (1 \mathbf{v}_P + (1-1) \mathbf{v}_N \\ \mathbf{F}_f^D \approx v_f d\mathbf{A} |(\mathbf{v}_N - \mathbf{v}_P)| / |\mathbf{d}| \end{cases}$

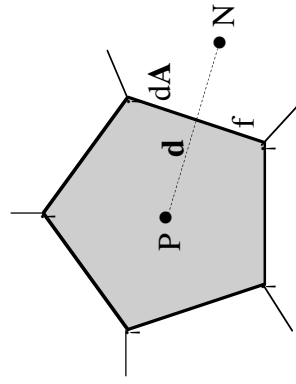
for CD. In other words,

$$\begin{cases} a_P \mathbf{v}_P^{n+2} = H(\mathbf{v}) - (\nabla p)_P^{n+2} \\ \sum_f [(a_P^{-1})_f (\nabla p)_f^{n+2} = \sum_f [(H(\mathbf{v})/a_p)_f \cdot d\mathbf{A}_f] \end{cases}$$

and

$$F_f \approx [(H(\mathbf{v})/a_p)_f - (a_p^{-1})_f (\nabla p)_f^{n+2}] \cdot d\mathbf{A}_f$$

Equations are solved in sequence using
a PISO-type loop



```

for(runTime++; !runTime.end(); runTime++)
{
    Info << "Time = "<<runTime.curTime() nl<<endl;
    fvm Ueqn
    (
        fvm::ddt(U)+fvm::div(phi,U,scheme)
        -fvm::laplacian(nu,U)
    );
    solve(Ueqn == -fvc::grad(p));
    // --- PISO loop
    for (int corr=0; corr<nCorr; corr++)
    {
        phi=interp(Ueqn.H)/Ueqn.A()&mesh.areas();
        fvm peqn
        (
            phi::laplacian(1.0/Ueqn.A(),p)==fvc::div(phi)
        );
        peqn.solve();
        phi=peqn.flux();
        U=(Ueqn.H)-fvc::grad(p))/Ueqn.A();
        U.correctBoundaryConditions();
    }
}

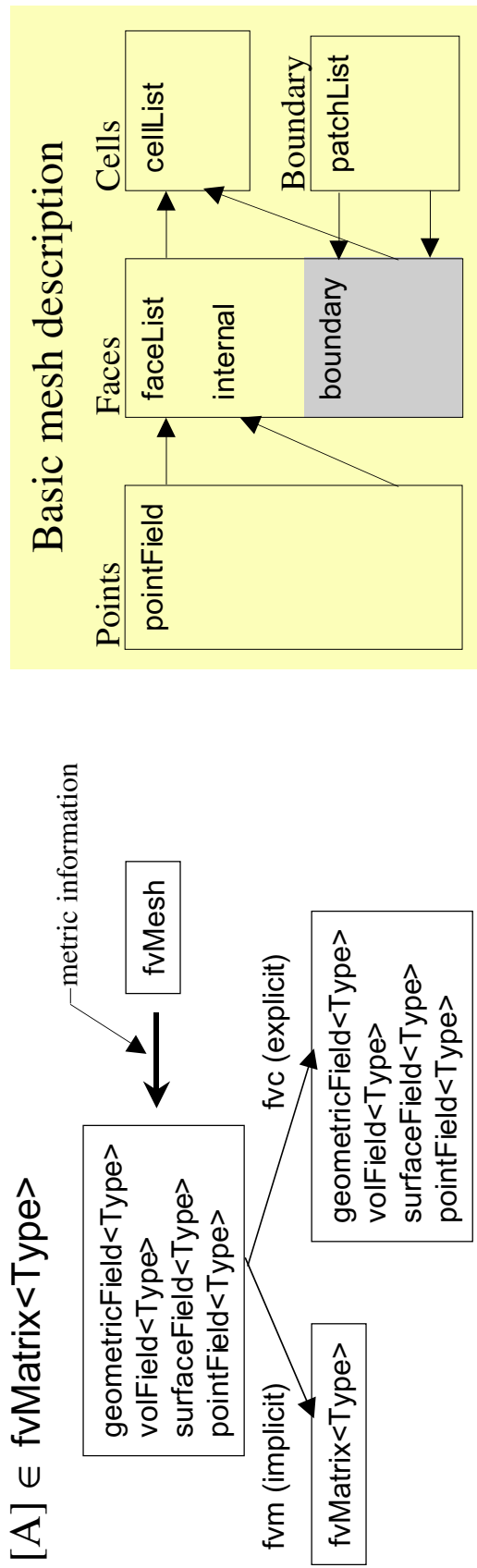
```

Equation Discretization

The discretized equations can be compactly expressed by [A]{x} = {y}

$\{\cdot\} \in \text{geometricField}<\text{Type}>$

$[\mathbf{A}] \in \text{fvMatrix}<\text{Type}>$

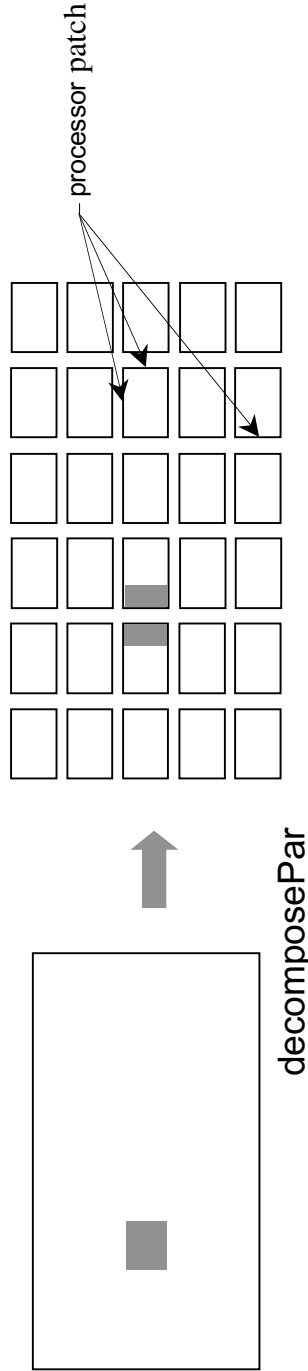


Additional features

- syntax that closely mimics the notation of written mathematics (+, symm, pow, &)
- written in C++
- automatic dimension checking
- tensor mathematics (scalar, vector, tensor, tensorThird)
- all transcendental functions available

Parallelization Strategies

Parallelisation of FOAM is via domain decomposition i.e. the domain is split up into sub-domains, one for each processor, and a copy of the code run on each domain.



The processor patch class caters for the inter-processor information within the solver.

On decomposition, internal boundaries within the complete mesh are given processor patches which know about the inter-processor topology, and which hide the inter-processor calls (pvm or SHMEM).

⇒ since the interprocessor communication is at the level of the field classes, any geometric field will automatically parallelise.

High-Level Language Codes – a short selection

Basic CFD codes

icoFoam	incompressible laminar flow code for Newtonian and Non-newtonian fluids
potentialFoam	potential flow code
turbFoam	incompressible turbulent flow code (algebraic, 2 eqn, & Reynolds stress)

Compressible Flow

sonicFoam	compressible transsonic/supersonic laminar gas flow code
sonicTurbFoam	compressible transsonic/supersonic turbulent gas flow code

Heat Transfer

chtFoam	incompressible code with conjugate heat transfer
---------	--

DNS and LES codes

dnsFoam	direct numerical simulation code
oodles	incompressible large eddy simulation code
sonicOodles	compressible large eddy simulation code

Combustion

Xoodles	compressible turbulent combustion code using the FW-model
reactingOodles	compressible turbulent combustion code a range of combustion models

Electromagnetics

Finance

Stress Analysis



Moving Boundary and Interface Methods for Computational Fluid and Solid Mechanics

Eric Lillberg och Lars Olosson

The Swedish Defence Research Agency, FOI
Weapons and Protection Division



Eric Lillberg, Computational Physics
FOI Defence Research Agency

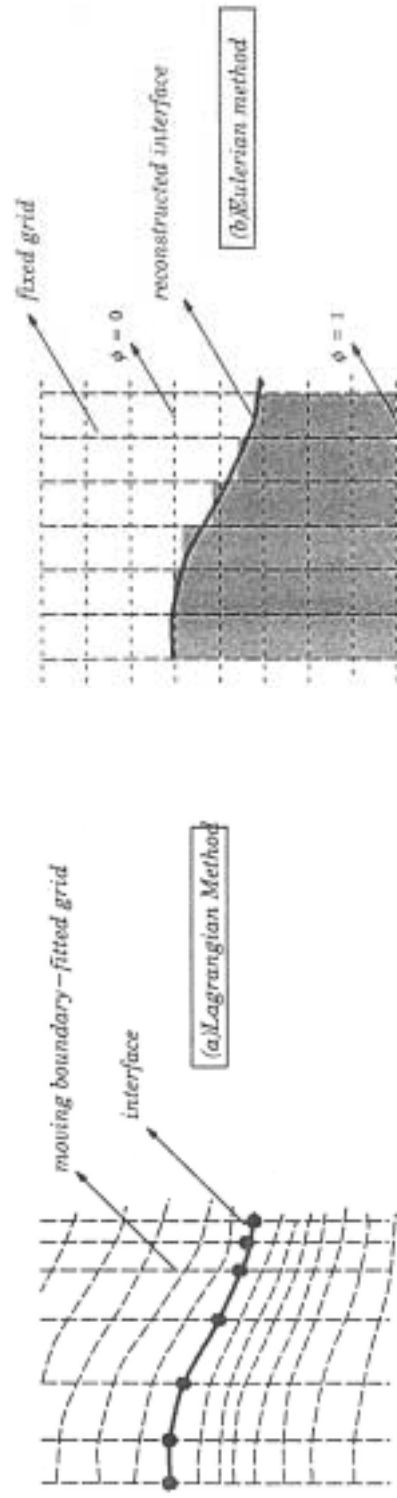
Moving Boundary and Interface Problems in Fluid Mechanics

- Many physical phenomena of interest must contend with moving boundaries and interfaces, e.g. free surface flows, penetration mechanics, flow induced vibrations, bodies with relative motion.
- Different methods needed to solve different problems.
- Fluid/solid, fluid/fluid and solid/solid interactions leads to highly coupled, nonlinear systems.
- LES is suitable for the transient non-linear coupling between fluid and structure where time accuracy is important.
- “Several numerical solutions have been found to such problems, and this leads one to believe that the problems are well posed.”

Floryan and Rasmussen, “Numerical methods for viscous flows”, Appl. Mech Rev vol 42, no 12, Dec 1989

Interface Representations

- Lagragian methods (a)
Maintain the interface as a discontinuity and explicitly track its evolution.
The grid is configured to conform to the shape of the interface and adapts continually to it.
- Eulerian methods (b)
Employs a fixed grid.
The interface is reconstructed from the properties of appropriate field variables such as fluid fractions or a level-set



General methods at hand

ALE - Arbitrary Lagrangian-Eulerian

Transformation methods

- + Explicit tracking of the interface
- + Boundary conditions
- Complex geometries
- Breakups/Mergers
- Large deformations

Volume of Fluid

Volume of Solid

Cut-Cell Techniques

Virtual Boundary methods

Level-Set methods

- + “Any” geometry
- + Complex interfacial behavior
- + Large deformations
- Interface not explicitly defined
- Complex boundary conditions
- Interface reconstruction

Over Set Grid Methods

- + Multiple geometries with relative motion

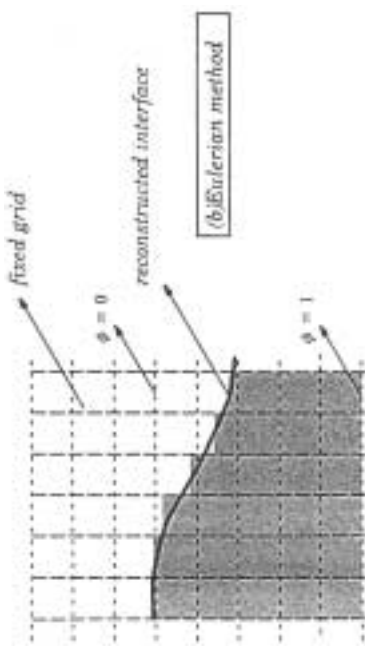
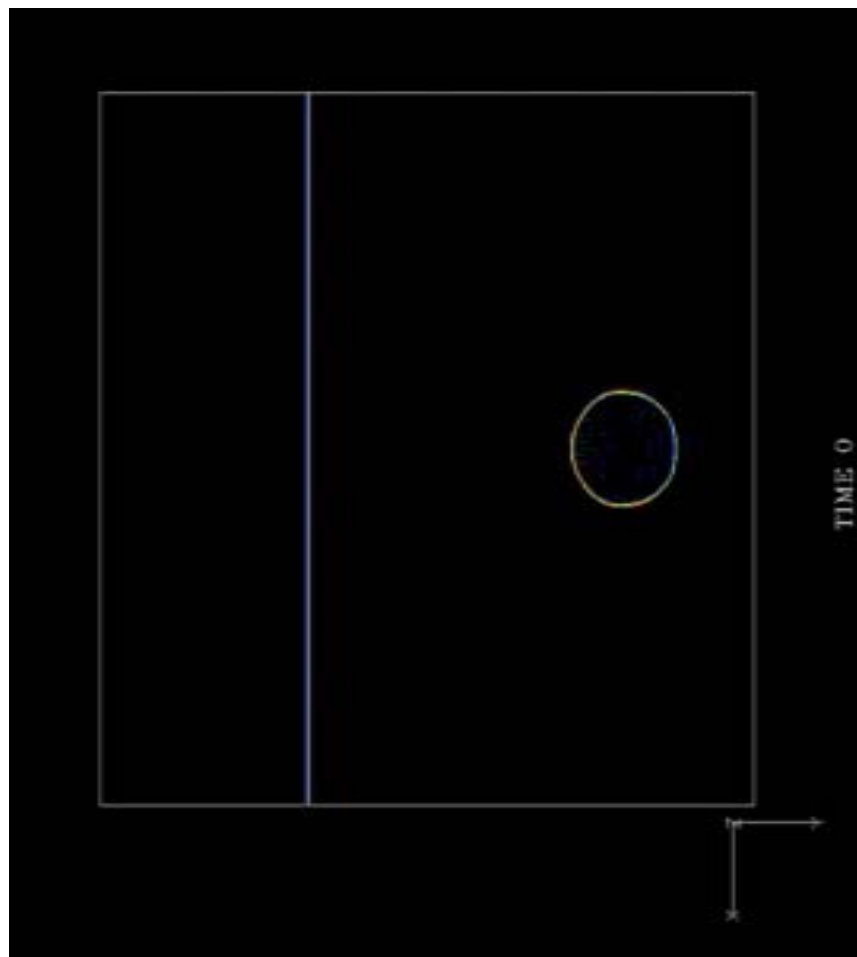
VOF Methods for Fluid Interfaces

- Bubble dynamics as an example of interface capturing for large, general deformations, using a Volume of Fluid (VOF) method

$$\begin{cases} \operatorname{div} \mathbf{v} = 0 \\ \partial_t (\rho \mathbf{v}) + \operatorname{div}(\rho \mathbf{v} \otimes \mathbf{v}) = -\operatorname{grad} p + \operatorname{div} \mathbf{S} + \rho \mathbf{g} + \mathbf{f} \\ \partial_t (\alpha) + \operatorname{div}(\alpha \mathbf{v}) = 0 \end{cases}$$

$$\rho = \alpha \rho_1 + (1-\alpha) \rho_2, \quad \mu = \alpha \mu_1 + (1-\alpha) \mu_2$$

$$\mathbf{f} = -\sigma \operatorname{div}(\operatorname{grad} \alpha / |\operatorname{grad} \alpha|) \operatorname{grad} \alpha$$

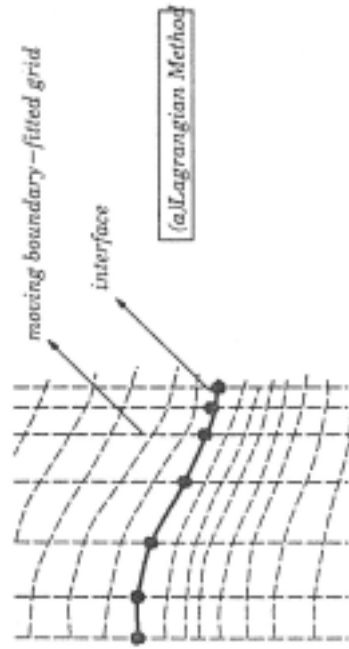
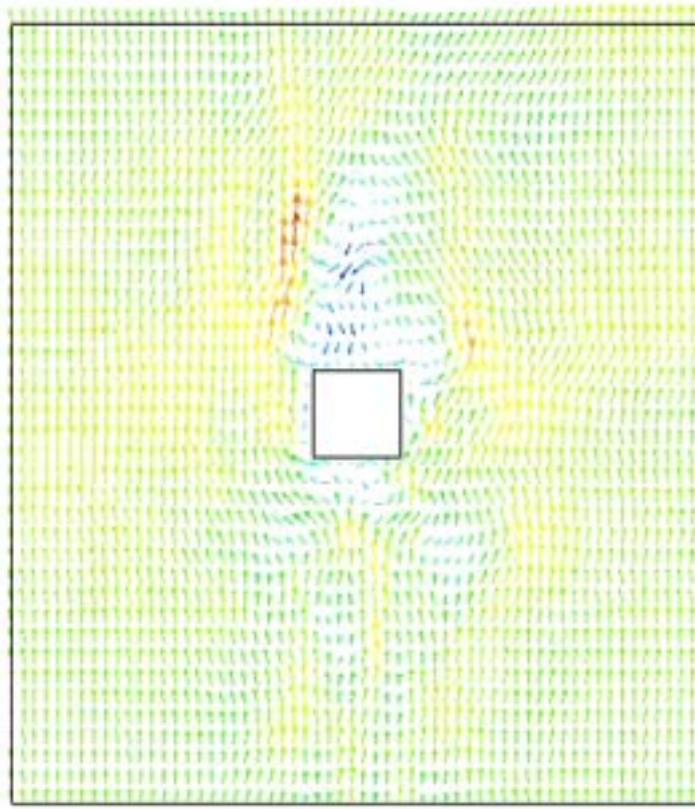


ALE Methods for Fluid/Structure Interaction

- Grid moves with the geometry while the N-S equations are solved in a fixed grid approach compensated for the mesh-motion fluxes \mathbf{U} .
- Suitable for accurate fluid/structure interaction problems with limited deformations.

- Geometric conservation.

$$\begin{cases} \operatorname{div}(\mathbf{v} - \mathbf{U}) = 0 \\ \partial_t(\mathbf{v}) + \operatorname{div}((\mathbf{v} - \mathbf{U}) \otimes \mathbf{v}) = -\operatorname{grad} p + \operatorname{div} \mathbf{S} \end{cases}$$



Några ord om penaltybaserad Euler-Lagrangekoppling

Lars Olovsson

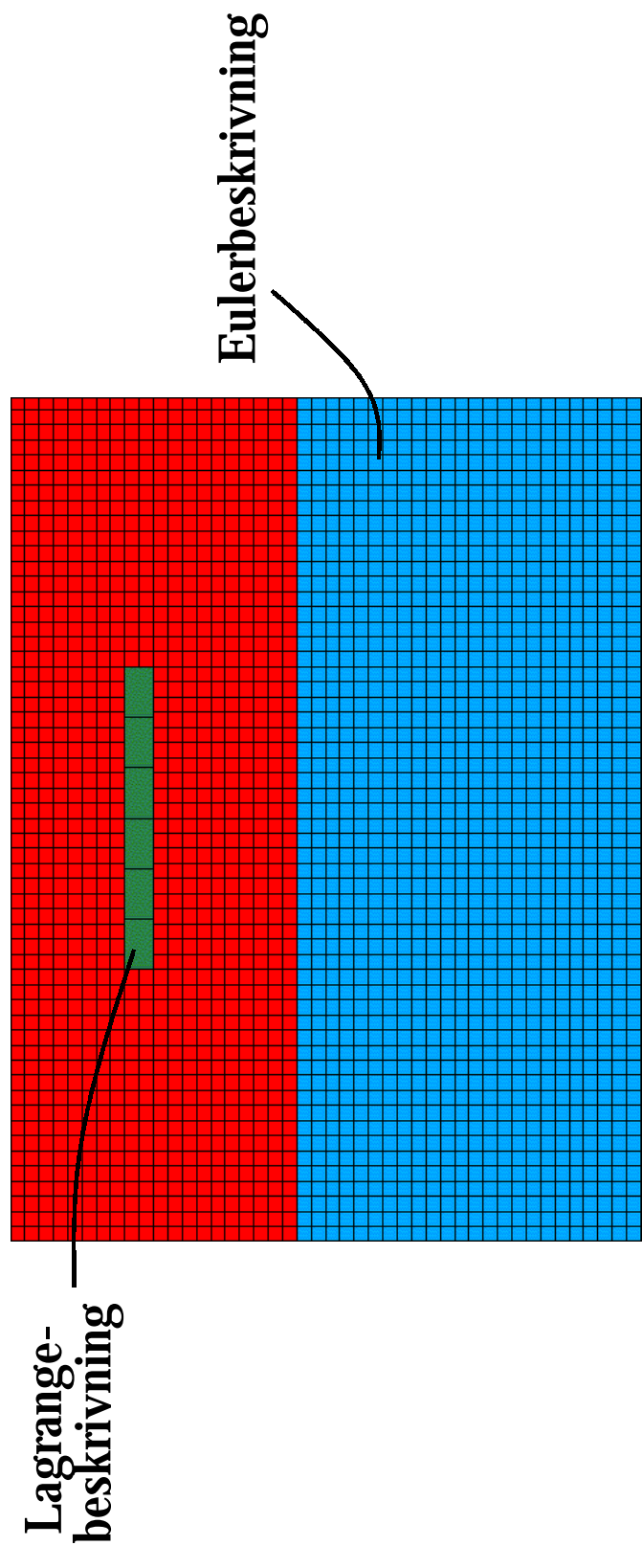
The Swedish Defence Research Agency, FOI
Weapons and Protection Division



Varför Euler-Lagrangekoppling?

Det är ofta lämpligt att beskriva en del av en modell med en Lagrangesformulerings och en del med en Eulerformulerings.

En kopplingsalgoritm krävs för kommunikationen mellan modellens olika komponenter.

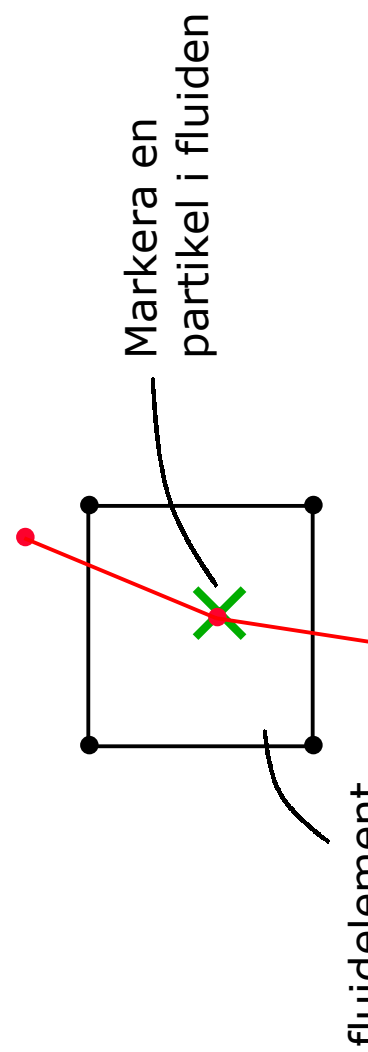


Penaltybaserad metod

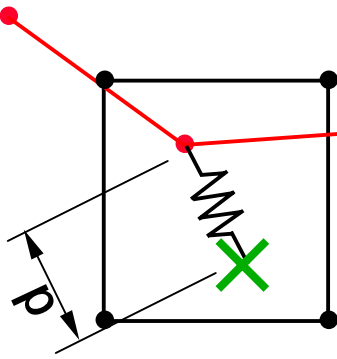
En penaltybaserad kopplingsalgoritm håller koll på relativa förskjutningen mellan fluid och struktur.

Nodkrafter, proportionella mot relativa förskjutningen, tvingar fluid och struktur att följas åt.

Kontakt detekteras

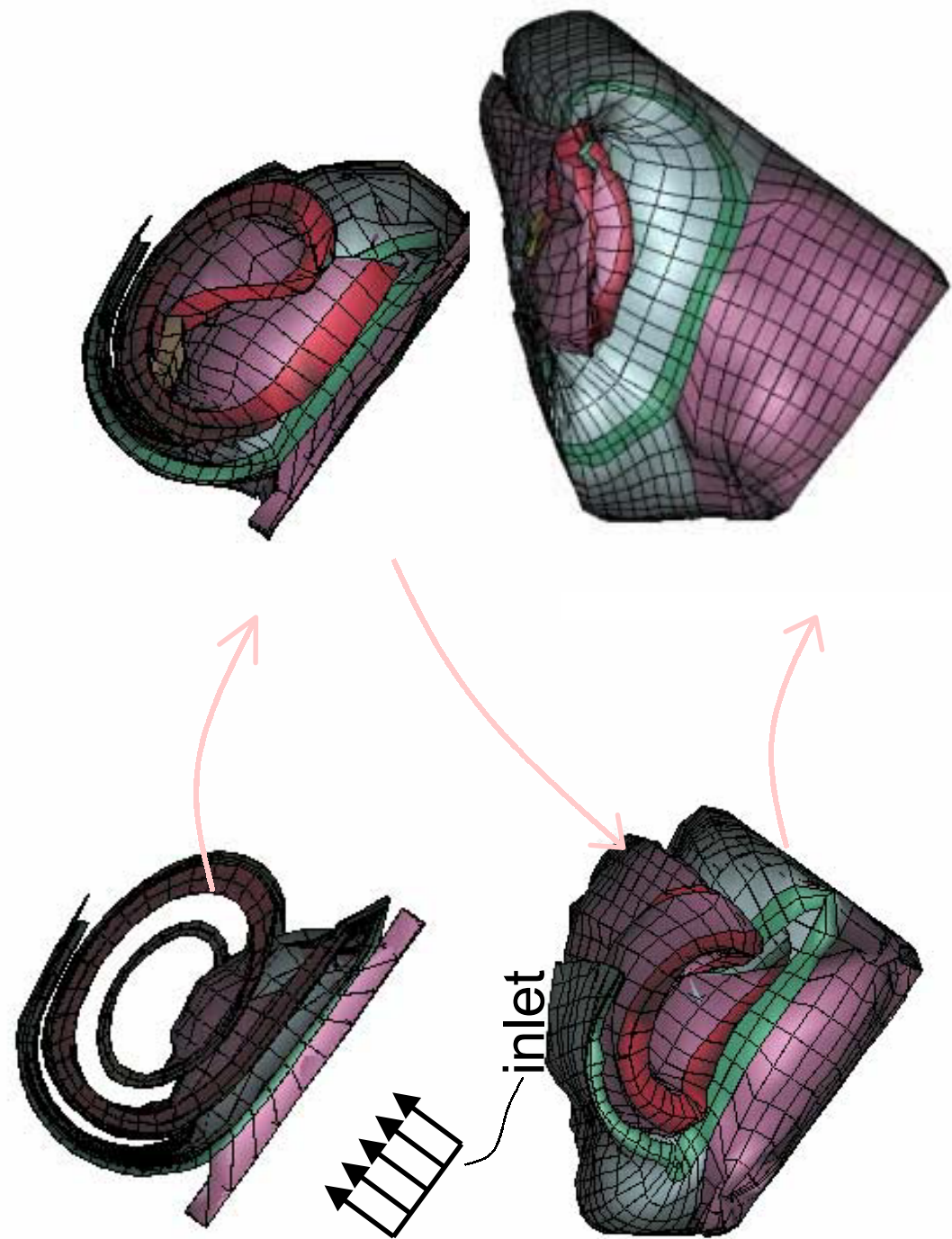


Senare



Följ partikeln, **X**, och applicera en kraft proportionell mot d .

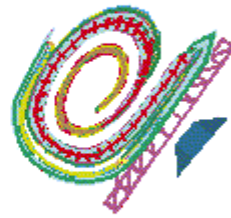
Airbag



Airbag



Airbag

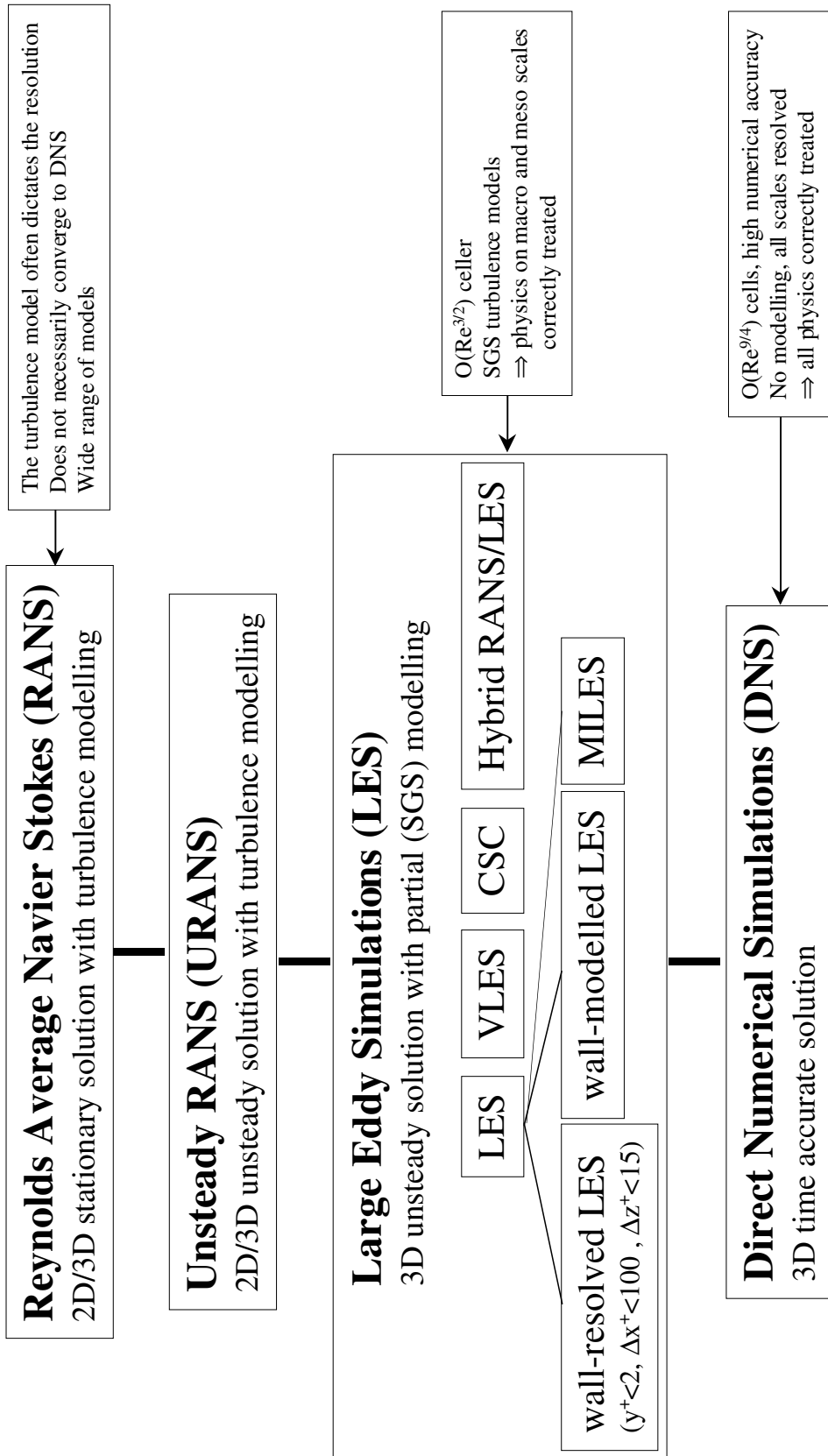


TURBULENCE MODELLING IN RANS AND LES

Urban Svennberg, Leif Persson & Christer Fureby
Totalförsvarets Forskningsinstitut, FOI
Vapen & Skydd
Grindsjöns forskningscentrum



RANS, URANS, ..., LES, DNS and all that



RANS

Average the NSE over time or across an ensemble of flows (ergodicity)

$$\nabla \cdot (\langle \mathbf{v} \rangle \otimes \langle \mathbf{v} \rangle) = -\nabla \langle p \rangle + \nabla \cdot (\langle \mathbf{S} \rangle - \mathbf{R}) + \langle \mathbf{f} \rangle, \quad \nabla \cdot \langle \mathbf{v} \rangle = 0$$

where $\mathbf{R} = \langle \mathbf{v}' \otimes \mathbf{v}' \rangle$

Need to close these equations by modelling \mathbf{R}

Different levels of modeling – different cost and accuracy

- Two-equation models ($\mathbf{R} = v_t \langle \mathbf{D} \rangle$, $v_t = c_\mu k^2 / \varepsilon$)

$$\begin{cases} \nabla \cdot (k \langle \mathbf{v} \rangle) = 2v_t \langle \mathbf{D} \rangle^2 + \nabla \cdot ((v + v_t / \sigma_k) \nabla k) - \varepsilon \\ \nabla \cdot (\varepsilon \langle \mathbf{v} \rangle) = P_\varepsilon + \nabla \cdot ((v + v_t / \sigma_\varepsilon) \nabla \varepsilon) - R \end{cases}$$

¥ Non-linear two-equation models

¥ Differential stress models

$$\nabla \cdot (\mathbf{R} \otimes \langle \mathbf{v} \rangle) = \mathbf{R} \langle \mathbf{D} \rangle^T + \langle \mathbf{D} \rangle \mathbf{R} + \nabla \cdot (v_k \mathbf{R} \nabla \mathbf{R}) + c_1(\varepsilon/k) \mathbf{R} - \frac{2}{3} c_2 \varepsilon \mathbf{I}$$

More complex models → more physics → better resolution

The Filtering Approach to LES

Convolving the NSE with the filter kernel $G(\mathbf{x}, \Delta)$ yields the LES equations

$$\partial_t (\bar{\mathbf{v}}) + \nabla \cdot (\bar{\mathbf{v}} \otimes \bar{\mathbf{v}}) = -\nabla \bar{p} + \nabla \cdot (\bar{\mathbf{S}} - \mathbf{B}) + \bar{\mathbf{f}} + \mathbf{m}^v; \quad \nabla \cdot \bar{\mathbf{v}} = 0$$

where $\begin{cases} \mathbf{B} \equiv (\mathbf{v} \otimes \mathbf{v} - \bar{\mathbf{v}} \otimes \bar{\mathbf{v}}) = (\overline{\mathbf{v} \otimes \mathbf{v}} - \bar{\mathbf{v}} \otimes \bar{\mathbf{v}}) + (\overline{\mathbf{v}' \otimes \bar{\mathbf{v}}} + \overline{\bar{\mathbf{v}} \otimes \mathbf{v}'}) + (\overline{\mathbf{v}' \otimes \mathbf{v}'}) \\ \mathbf{m}^v = [\nabla, G^*](\mathbf{v} \otimes \mathbf{v} + p\mathbf{I} - \mathbf{S}) \end{cases}$ in which $[\nabla, G^*]\Phi = \overline{\nabla \Phi} - \nabla \overline{\Phi}$

Need to close these equations by modelling \mathbf{B} and \mathbf{m}^v , or \mathbf{B} neglecting \mathbf{m}^v
SGS models usually based on *isotropy* assumptions
 \Rightarrow some physics not included (e.g. near wall effects)

- EVM $\mathbf{B} = -2\mathbf{v}_k \overline{\mathbf{D}}$
- SSM & MM $\mathbf{B} = \overline{\mathbf{v} \otimes \mathbf{v}} - \bar{\mathbf{v}} \otimes \bar{\mathbf{v}} - 2\mathbf{v}_k \overline{\mathbf{D}}$
- DRSM $\partial_t(\mathbf{B}) + \nabla \cdot (\mathbf{B} \otimes \bar{\mathbf{v}}) = -(\overline{\mathbf{L}} \mathbf{B}^T + \mathbf{B} \overline{\mathbf{L}}^T) + \nabla \cdot \mathbf{M} + \Pi + \mathbf{E}$

Improvements (modifications) necessary for high Re complex flows.

- E.g.
- | | | | | |
|-------------------|---|---|---|---------------------|
| wall-resolved LES | — | wall-modelled LES | — | MILES |
| $y^+ < 2$ | | $v_{BC} = v_{BC}(\tau_w, y_p, \bar{v}_p)$ | | particular numerics |

Monotone Integrated LES (MILES)

Alternative concept for LES introduced by Boris *et al*, (1992) and under rapid development: Fureby & Grinstein, (1998, 1999, 2000), Karniadakis *et al* (2000), Knight *et al* (1998, 2000).

- Idea* MILES uses the features of particular numerical methods to construct implicit (built-in) SGS models by means of the leading order truncation error
- + no commutation error
 - + improved generality
 - no parameters
 - +/- strong coupling with the numerics

The FV, FD or FE discretization acts as an implicit low-pass filter

- same temporal scheme as in conventional LES
- same treatment of diffusive and source terms as in conventional LES
- Monotonicity preserving or TVD schemes for the convective terms (often using flux limiters Γ)

$$\text{Modified equations} \Rightarrow \mathbf{B} = \mathbf{C}\mathbf{L}^T + \mathbf{L}\mathbf{C}^T + \chi^2 \mathbf{L}\mathbf{d} \otimes \mathbf{L}\mathbf{d}, \quad \mathbf{C} = \mathbf{C}(\bar{\mathbf{v}}, \Gamma), \quad \chi = \chi(\Gamma)$$

Free Shear Flows

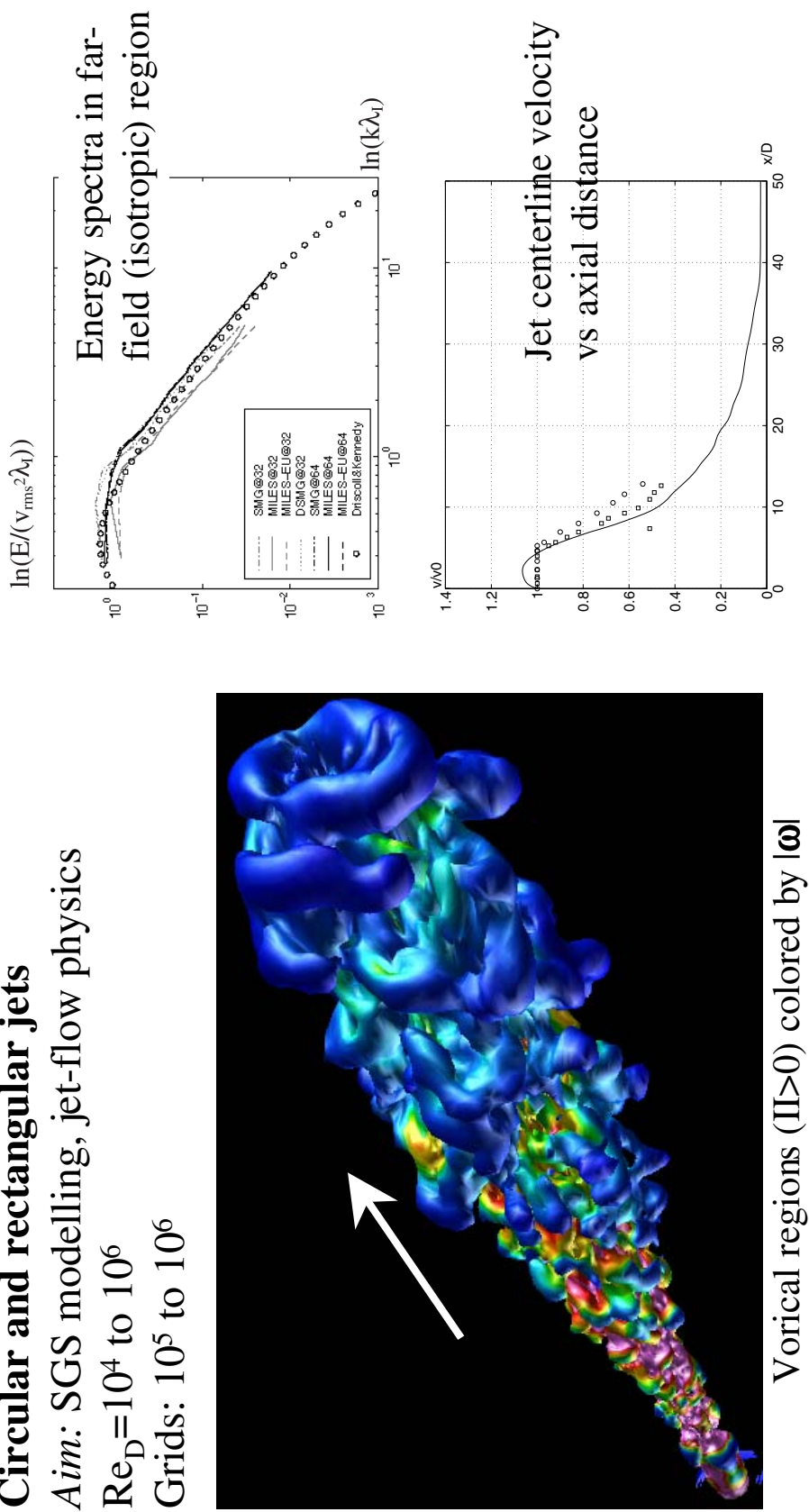
Spatially Developing Transitional Jet

Circular and rectangular jets

Aim: SGS modelling, jet-flow physics

$Re_D = 10^4$ to 10^6

Grids: 10^5 to 10^6



In collaboration with NRL, SBD & KTH

Fureby C. & Grinstein F.F.; 1998, AIAA Paper No 98-0537, AIAA J., 37, p 544.
Fureby C. & Grinstein F.F.; 2000, 8th European Turb. Conf., Barcelona, Spain.

Wall Bounded Flows

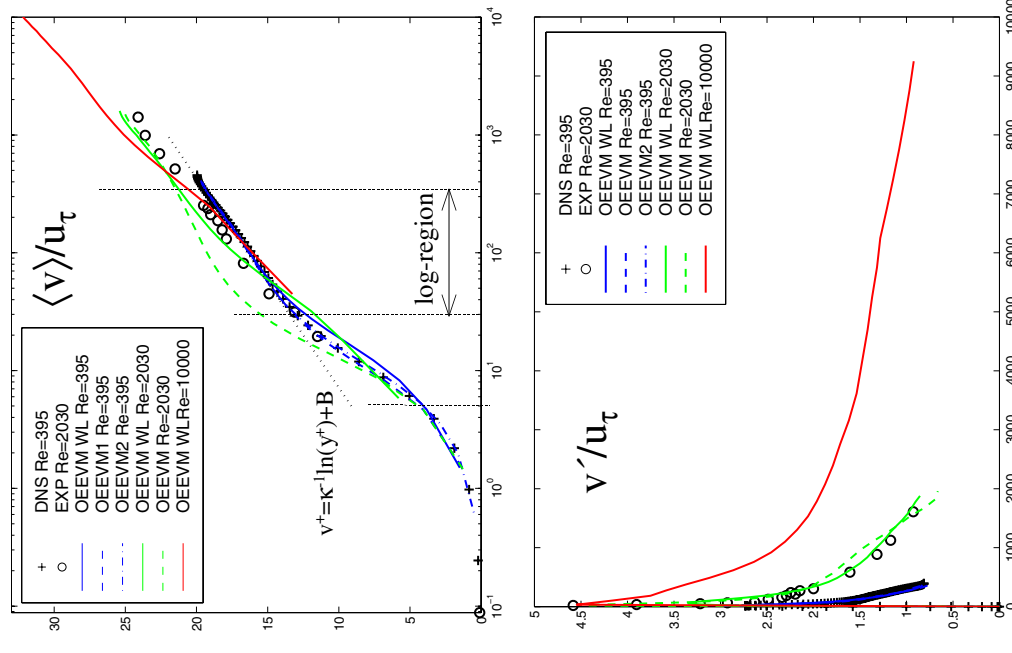
Fully Developed Turbulent Channel Flow

$Re_\tau = 180, 395, 590$ (DNS), 2030 (EXP) and 10000

Grids: $60^3, 60^2 \times 90$ and 90^3

LES: SMG, DSMG, OEEVM, DSM

MILES
wall-resolved and wall modelled LES

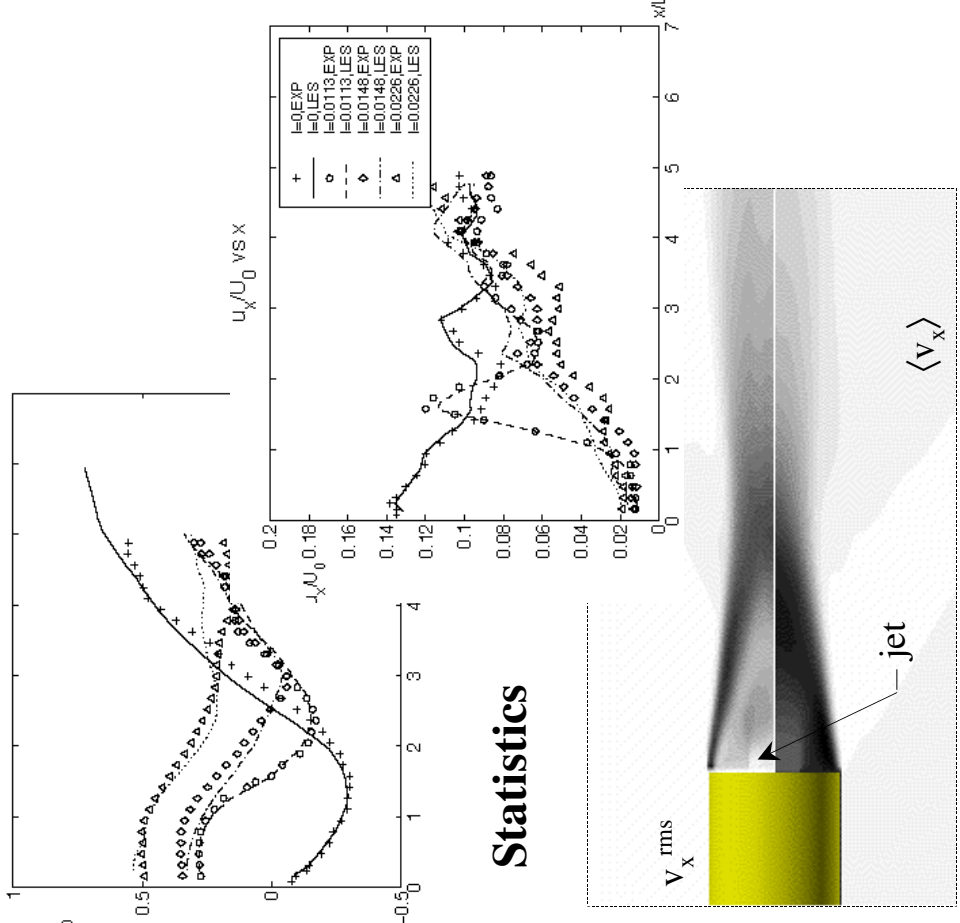
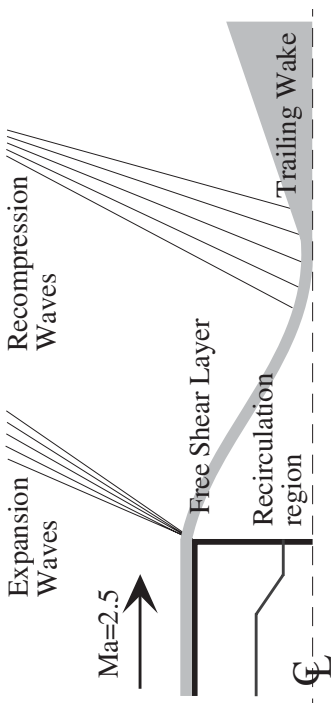


wall-modelled
OEEVM, 60^3

Fureby C., Gosman A.D., Sandham N., Tabor G., Weller H.G., & Wolfstein M.; 1997, TSF 11
Fureby C. & Grinstein F.F.; 2000, AIAA Paper No 00-2307, J. Comp. Phys

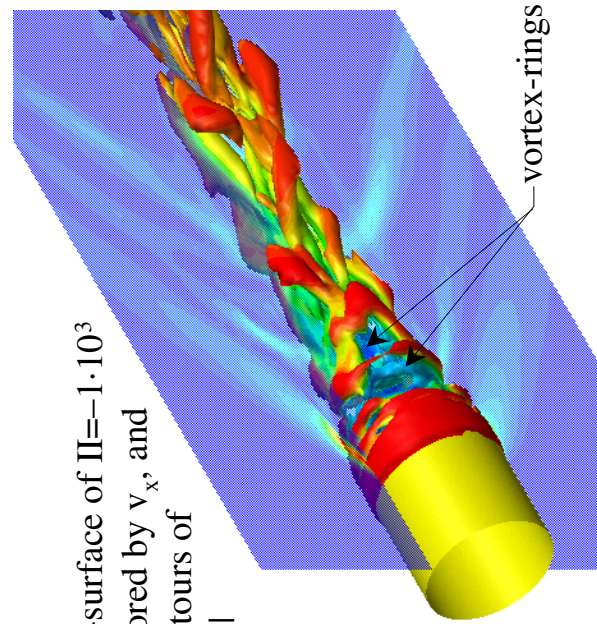
Supersonic Flows

Base Flow at $\text{Ma}=1.5$



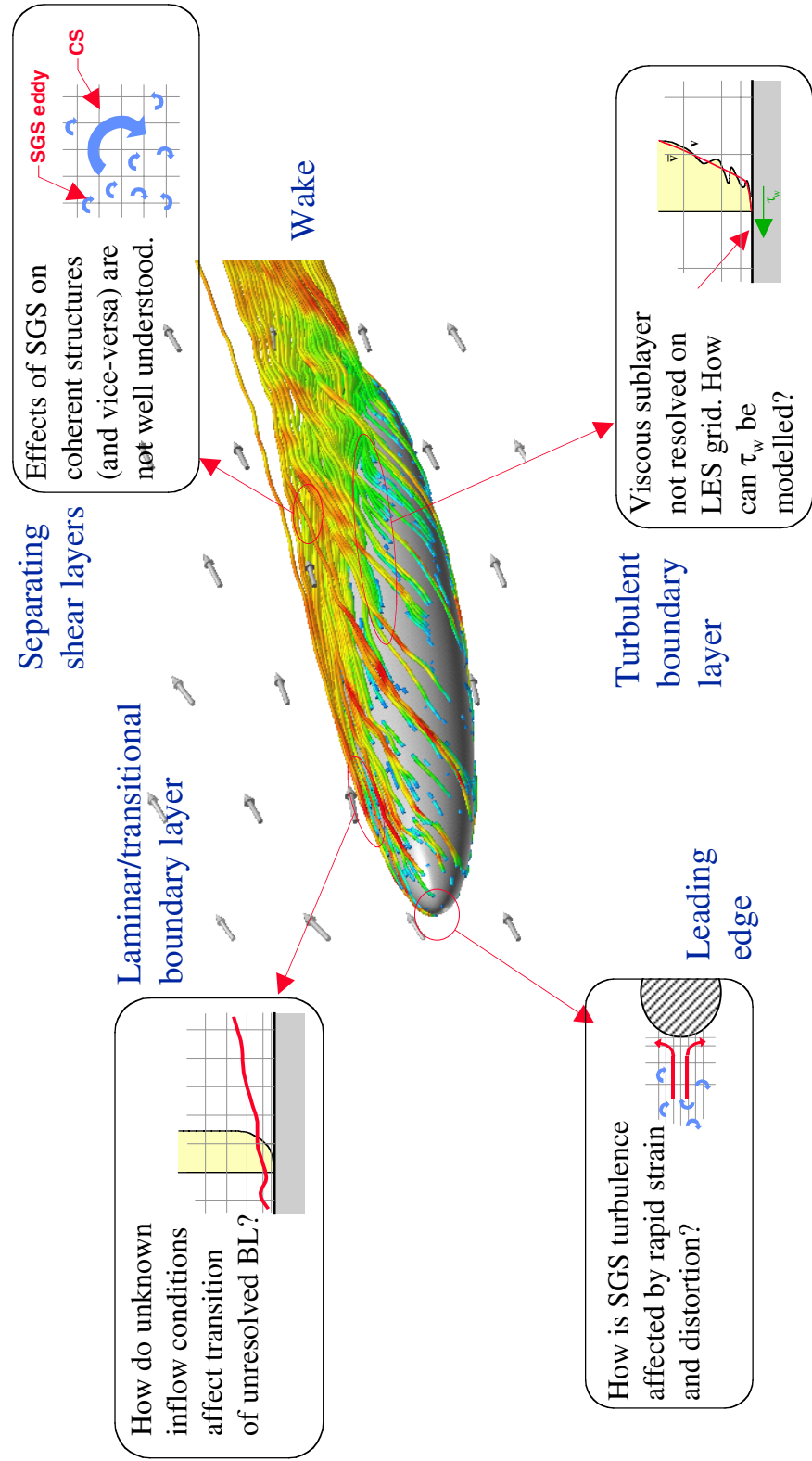
Statistics

Iso-surface of $\Pi = -1 \cdot 10^3$
 colored by V_x , and
 contours of
 $|V_p|$



Concluding Remarks

LES is not currently fully developed, a few pacing items remain to be solved before LES is useful for engineering calculations



Turbulence Modeling

S. Wallin

FoI

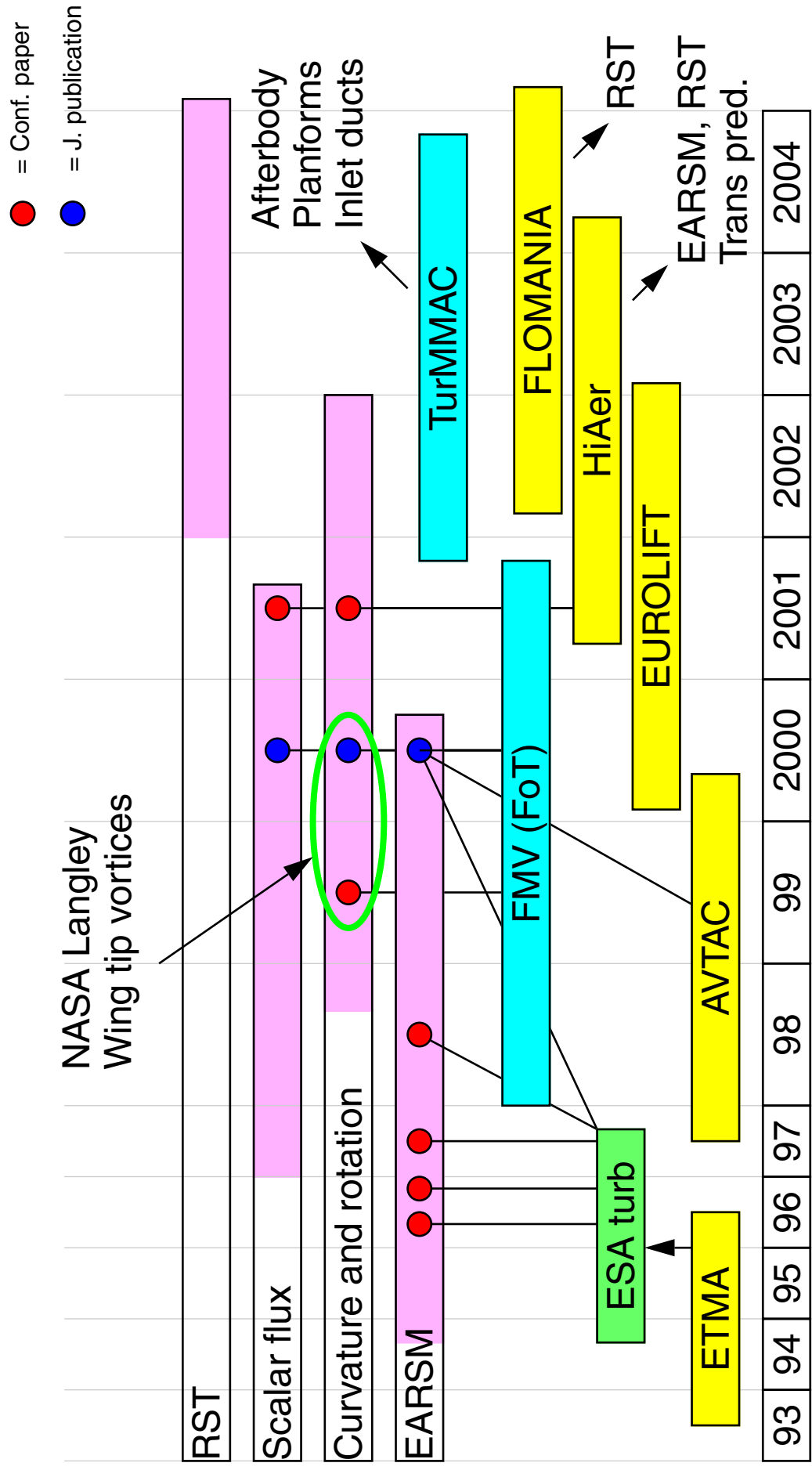
RANS modelling activities at “Flygteknik, FFA”

Stefan Wallin
Aeronautics Division, FFA, FOI, Sweden

Contents:

- Overview
- Some theory and examples of EARSM
- Curvature effects
- Passive scalar flux

Overview



Statistical approach

- Time dependent Navier-Stokes equations

$$\frac{\partial}{\partial t} \tilde{u}_i = \text{NS}_i(\tilde{u}_j)$$

- Reynolds decomposition

$$\tilde{u}_i(x, t) = U_i(x) + u_i(x, t)$$

- Reynolds averaged Navier-Stokes (RANS) equations

$$\overline{\frac{\partial}{\partial t} \tilde{u}_i} = \text{NS}_i(\tilde{u}_j) \quad \Rightarrow \quad \frac{\partial}{\partial t} U_i = \text{NS}_i(U_j) - \frac{\partial}{\partial x_j} (\overline{u_i u_j})$$

- Reynolds stress tensor

$$\overline{u_i u_j}$$

Some definitions

- Reynolds stress anisotropy tensor
$$a \equiv a_{ij} \equiv \overline{u_i u_j} - \frac{2}{3} \delta_{ij}$$
- Mean flow strain and rotation rate tensors (normalized)

$$\mathbf{S} \equiv S_{ij} \equiv \frac{1}{2} \frac{K}{\varepsilon} \left(\frac{\partial U_i}{\partial x_j} + \frac{\partial U_j}{\partial x_i} \right) \quad \Omega \equiv \Omega_{ij} \equiv \frac{1}{2} \frac{K}{\varepsilon} \left(\frac{\partial U_i}{\partial x_j} - \frac{\partial U_j}{\partial x_i} \right)$$

- Turbulent kinetic energy

$$K \equiv \frac{1}{2} \overline{u_i u_i} \quad \varepsilon$$

- Dissipation rate of turbulent kinetic energy

Modelling approaches

- RST

$$\text{Tr}(\boldsymbol{a}) = f_a(\boldsymbol{S}, \boldsymbol{\Omega}, \boldsymbol{a})$$

- ARSM

$$0 = f_a(\boldsymbol{S}, \boldsymbol{\Omega}, \boldsymbol{a})$$

- EARSM

$$\boldsymbol{a} = f_e(\boldsymbol{S}, \boldsymbol{\Omega})$$

- Non-linear eddy-viscosity models

$$\boldsymbol{a} = f_{\text{N-L}}(\boldsymbol{S}, \boldsymbol{\Omega})$$

- Linear eddy-viscosity models

$$\boldsymbol{a} = -2C_\mu \boldsymbol{S}$$

- Boussinesq (1877)

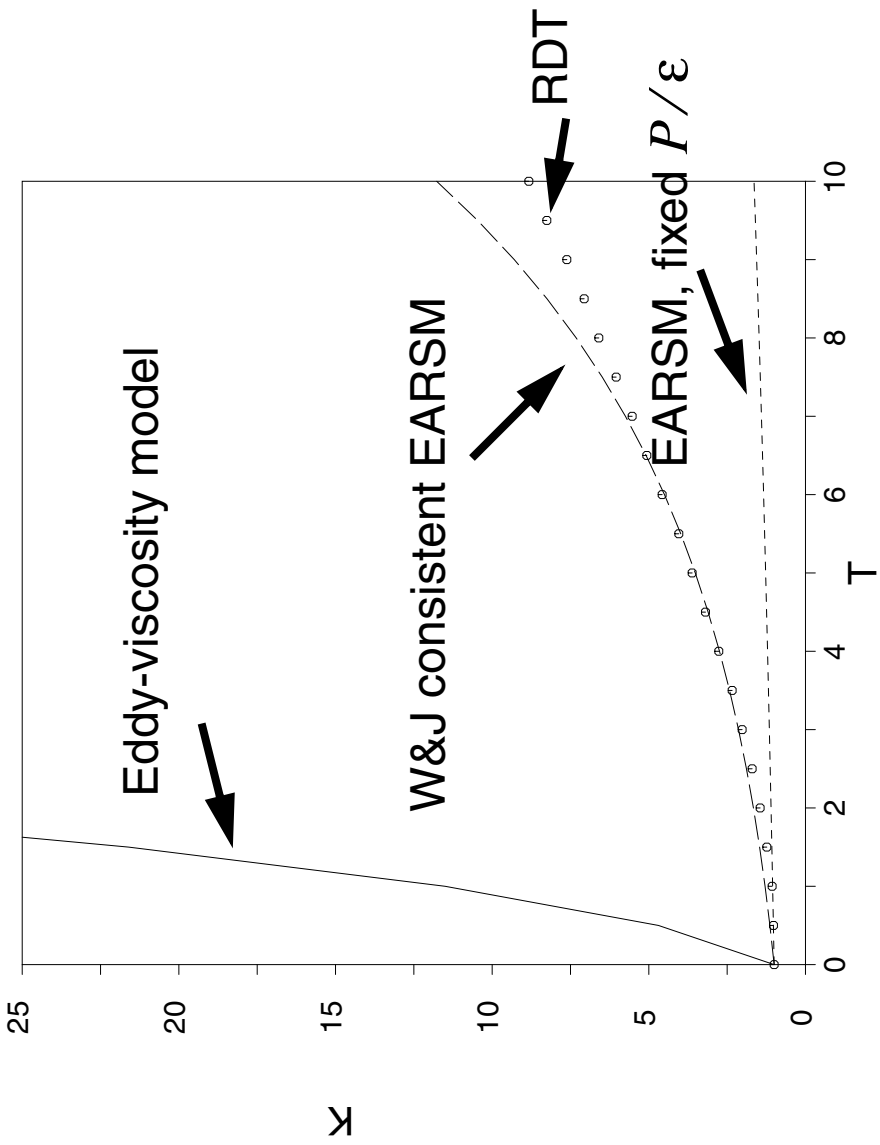
$$-\bar{u}\bar{v} = v_t \frac{\partial U}{\partial y}$$

- Turbulence scales

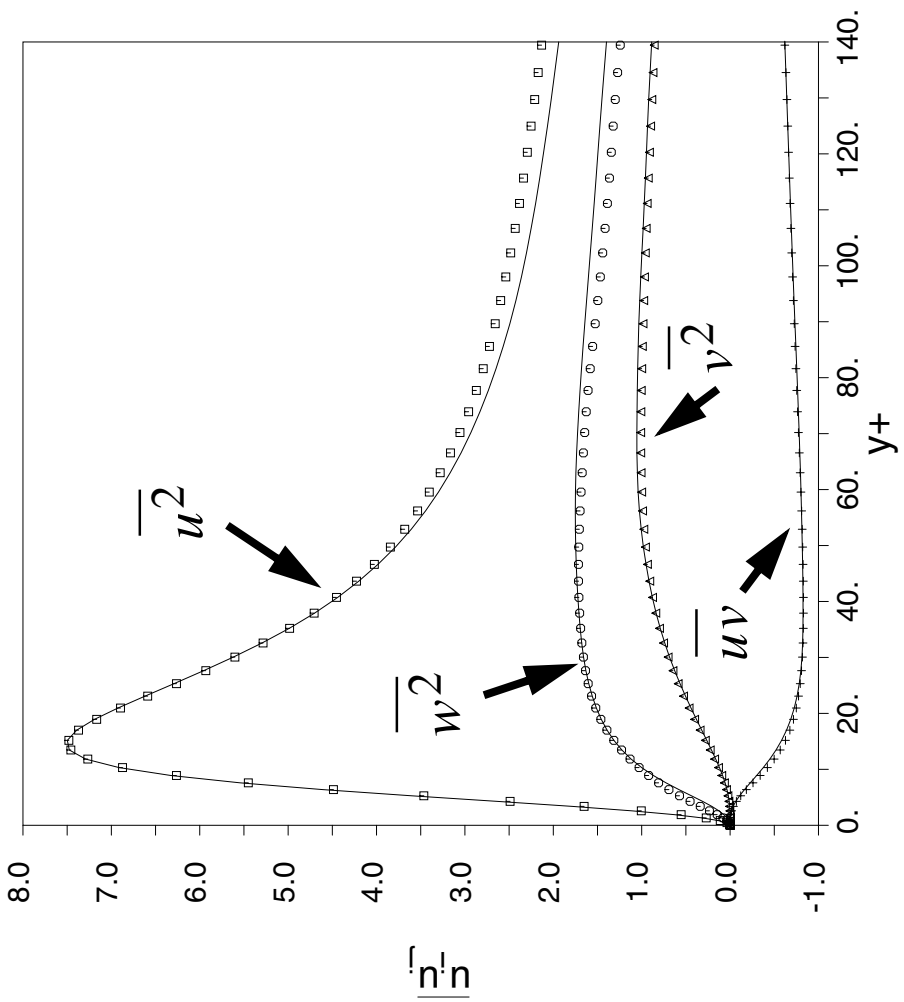
$$\text{Tr}(K) = f_K(K, \varepsilon, \boldsymbol{S}, \boldsymbol{a})$$

$$\text{Tr}(\varepsilon) = f_\varepsilon(K, \varepsilon, \boldsymbol{S}, \boldsymbol{a})$$

Rapidly sheared homogeneous flow

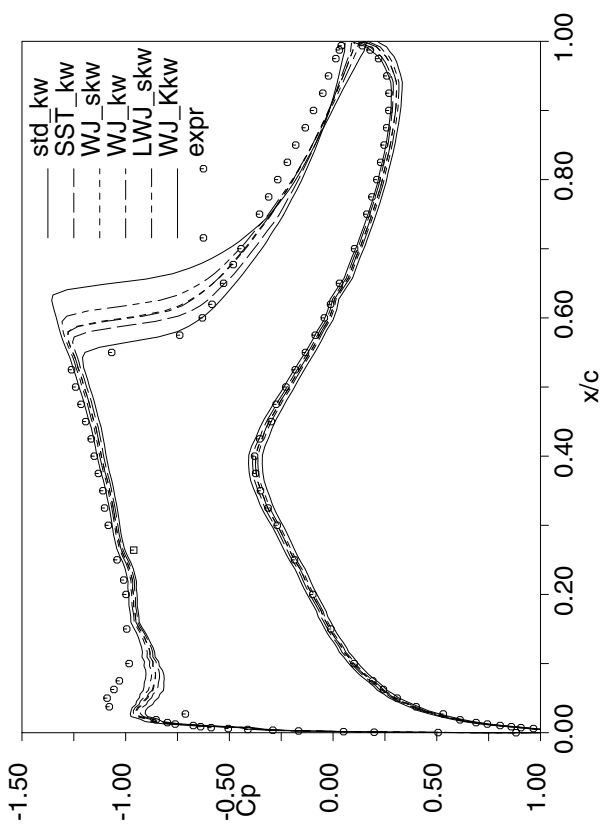


Channel flow

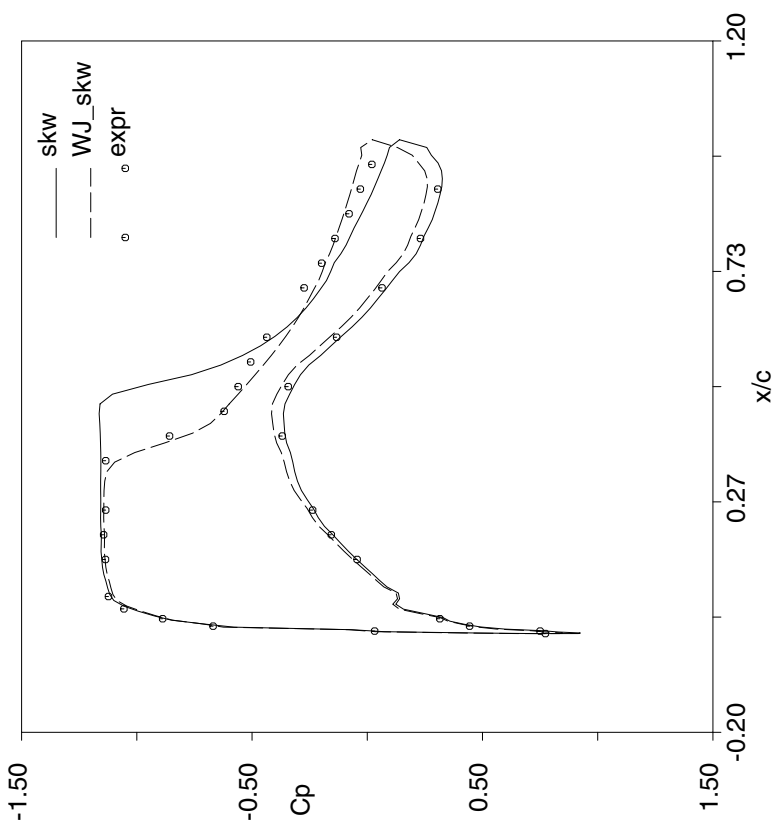


Shock induced separation

RAE2822, Case10 2D transonic profile



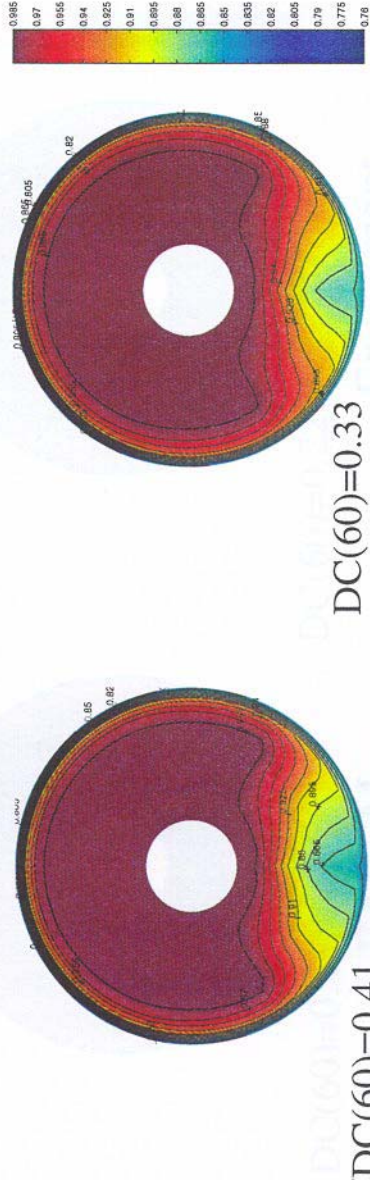
LANN 3D transonic wing, 47.5% span



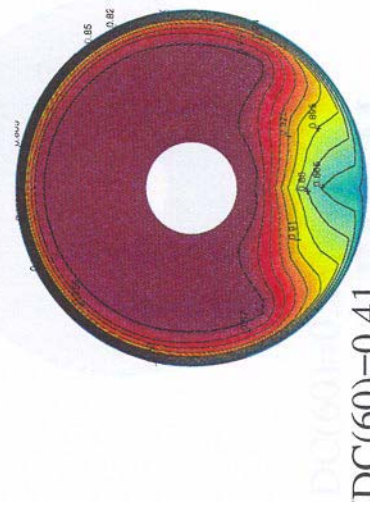
Inlet ducts (M2129 by SAAAB)

Total pressure distribution at AIP, $M_t = 0.79$

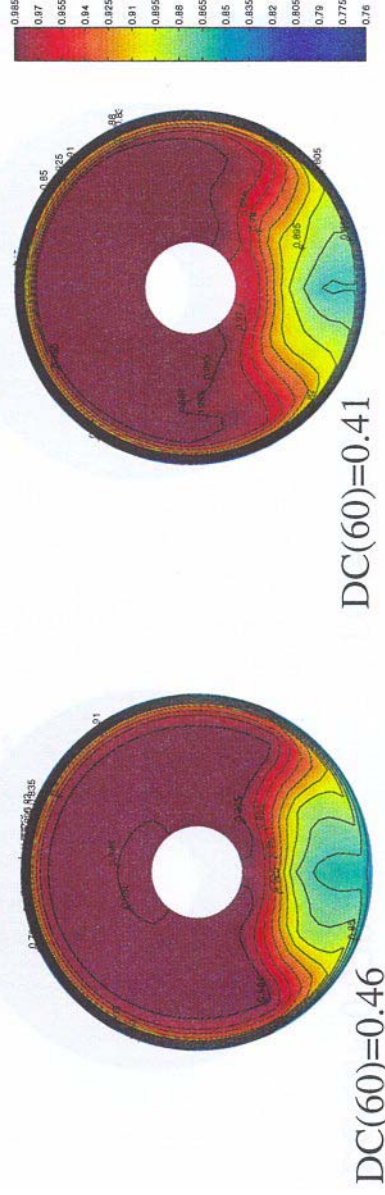
k- ω Wilcox



k- ε Chien



Experiment



taken from Ericsson, J. 2000, Master thesis, SAAAB, GDFP-00.0025

Curvature effects

- Weak-equilibrium assumption

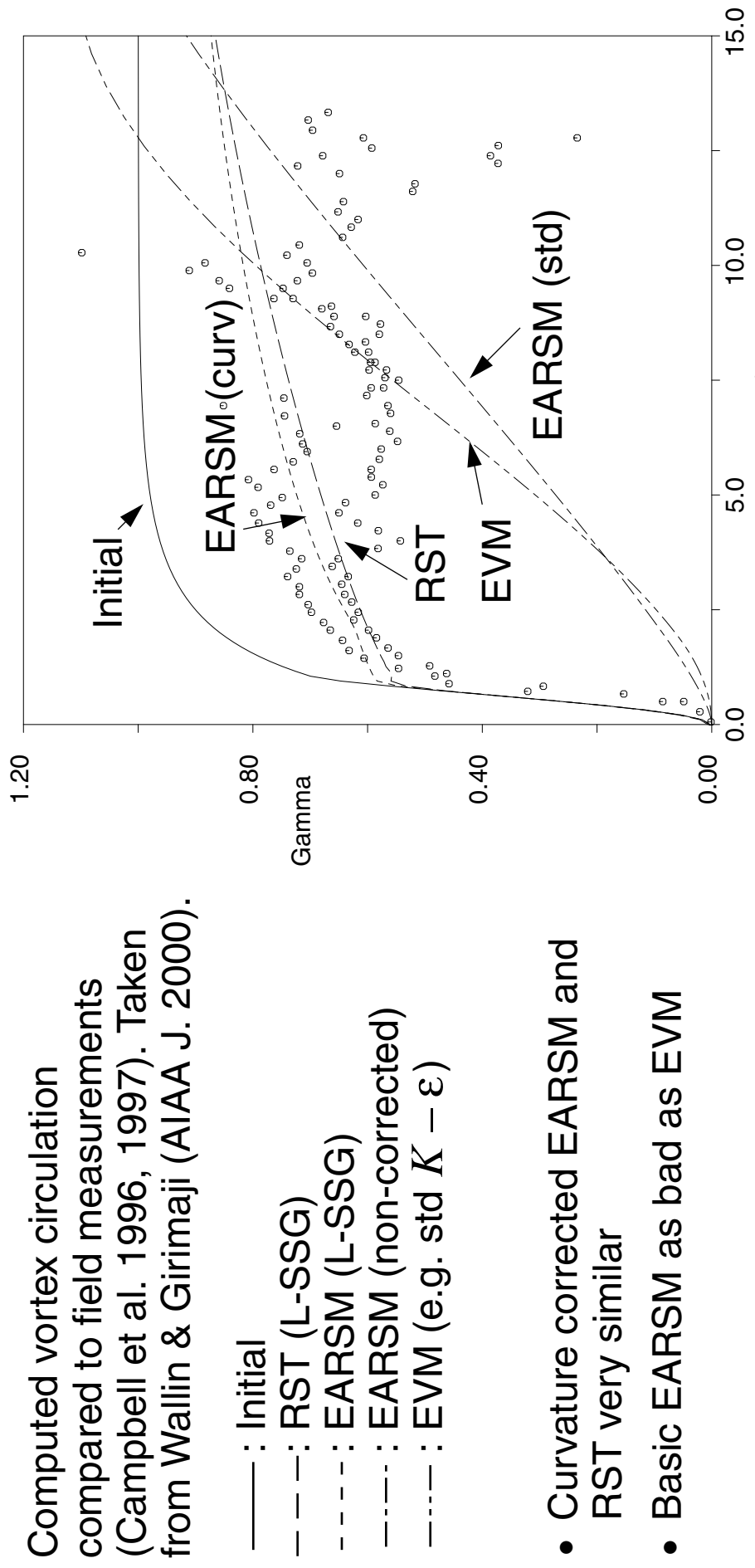
$$\frac{D\boldsymbol{a}}{Dt} = \boldsymbol{0} \rightarrow \text{algebraic relation}$$

- The advection $D\boldsymbol{a}/Dt$, and consequently also the algebraic model, depend on the coordinate system representing the \boldsymbol{a}_{ij} components.
- Most generic cases can be transformed so that $D\boldsymbol{a}/Dt = \boldsymbol{0}$ (rotating homogeneous shear, rotating channel, vortices, rotating pipe, ...)
- Complex flows do not have a general transformation.
- Streamline-based advection

$$\frac{D\boldsymbol{a}}{Dt} = \underbrace{\boldsymbol{T}^t \frac{DT^t}{Dt} \boldsymbol{T} - \left(\boldsymbol{a} \frac{DT^t}{Dt} \boldsymbol{T} - \boldsymbol{T}^t \frac{DT}{Dt} \boldsymbol{a} \right)}_{A} (\boldsymbol{a} \boldsymbol{\Omega}^{(r)} - \boldsymbol{\Omega}^{(r)} \boldsymbol{a})$$

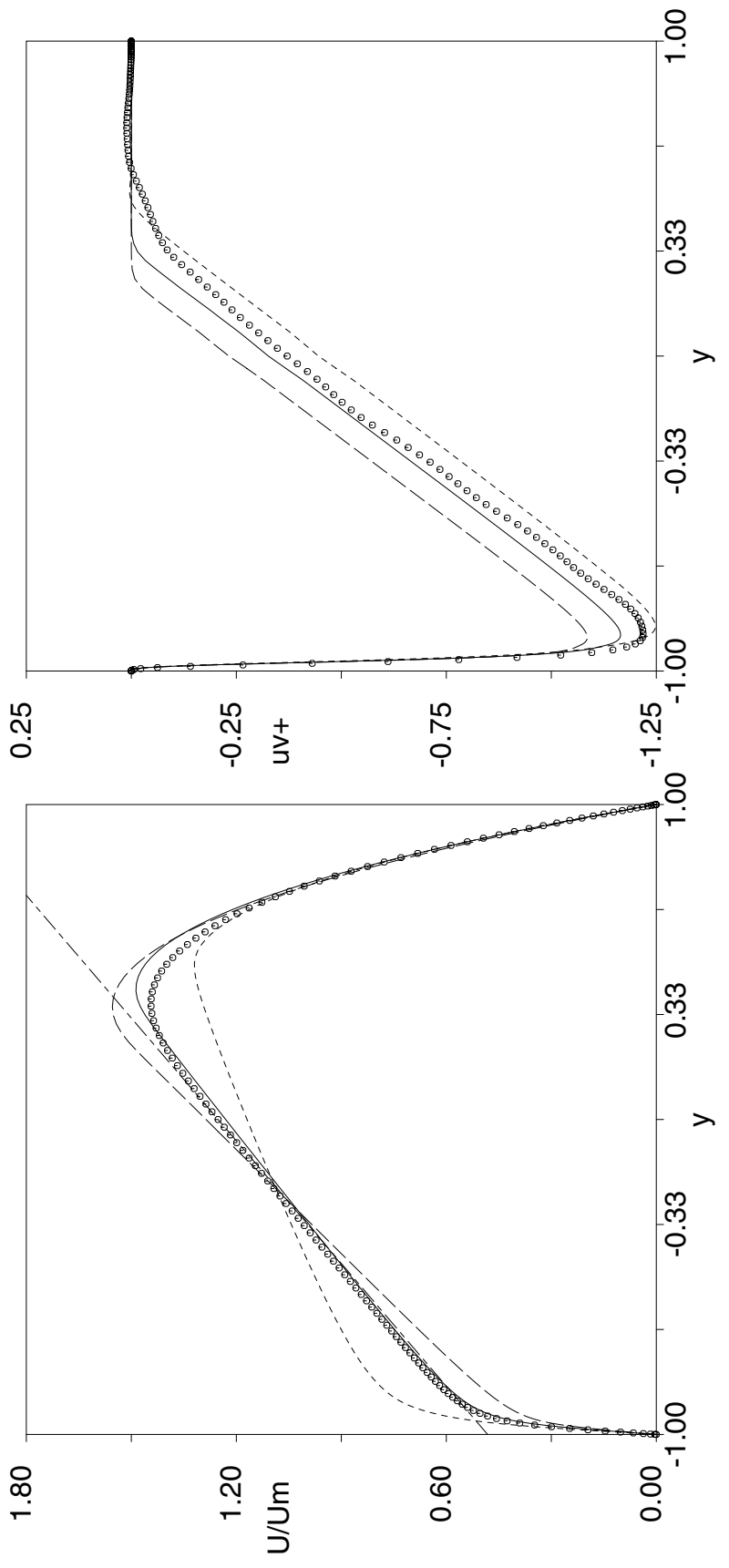
Isolated wing-tip vortex

Computed vortex circulation compared to field measurements (Campbell et al. 1996, 1997). Taken from Wallin & Girimaji (AIAA J. 2000).



- Curvature corrected EARSM and RST very similar
- Basic EARSM as bad as EVM

Rotating channel, $\text{Ro}=0.77$



Fully developed channel flow, DNS Alvelius & Johansson (2000).

- - - : WJ
- : CC-WJ
- - - : non-corrected CC-WJ.

Scalar turbulent flux

- Turbulent mixing of temperature, species concentration, pollutants, etc.
- Usually modelled by a eddy diffusivity model (EDM)

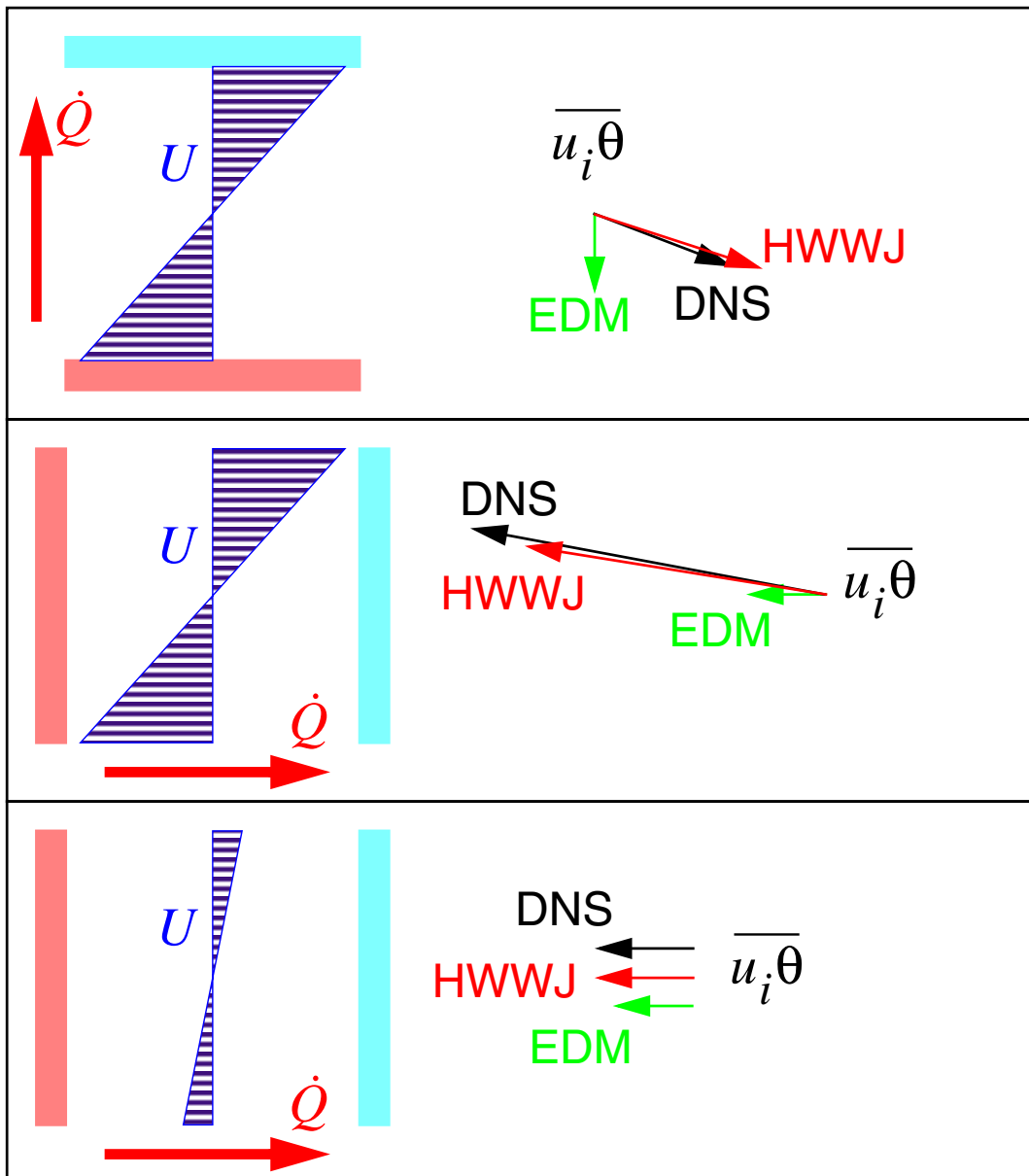
$$\overline{u_i \theta} = -\frac{v_t}{Pr_t} \frac{\partial \Theta}{\partial x_i}$$

- EDM gives the flux aligned with the gradient
- Even in simple shear flows the flux is not aligned with the gradient (se homogeneous shear)
- Need for improvements
-
-
- The explicit algebraic model HWWJ, (Wikström, Wallin & Johansson, Phys. Fluids, 2000)

$$\overline{u_i \theta} = -(1 - c_{\theta 4}) B_{ij}(S, \Omega) \overline{u_j u_k} \frac{K}{\varepsilon} \frac{\partial \Theta}{\partial x_k}$$

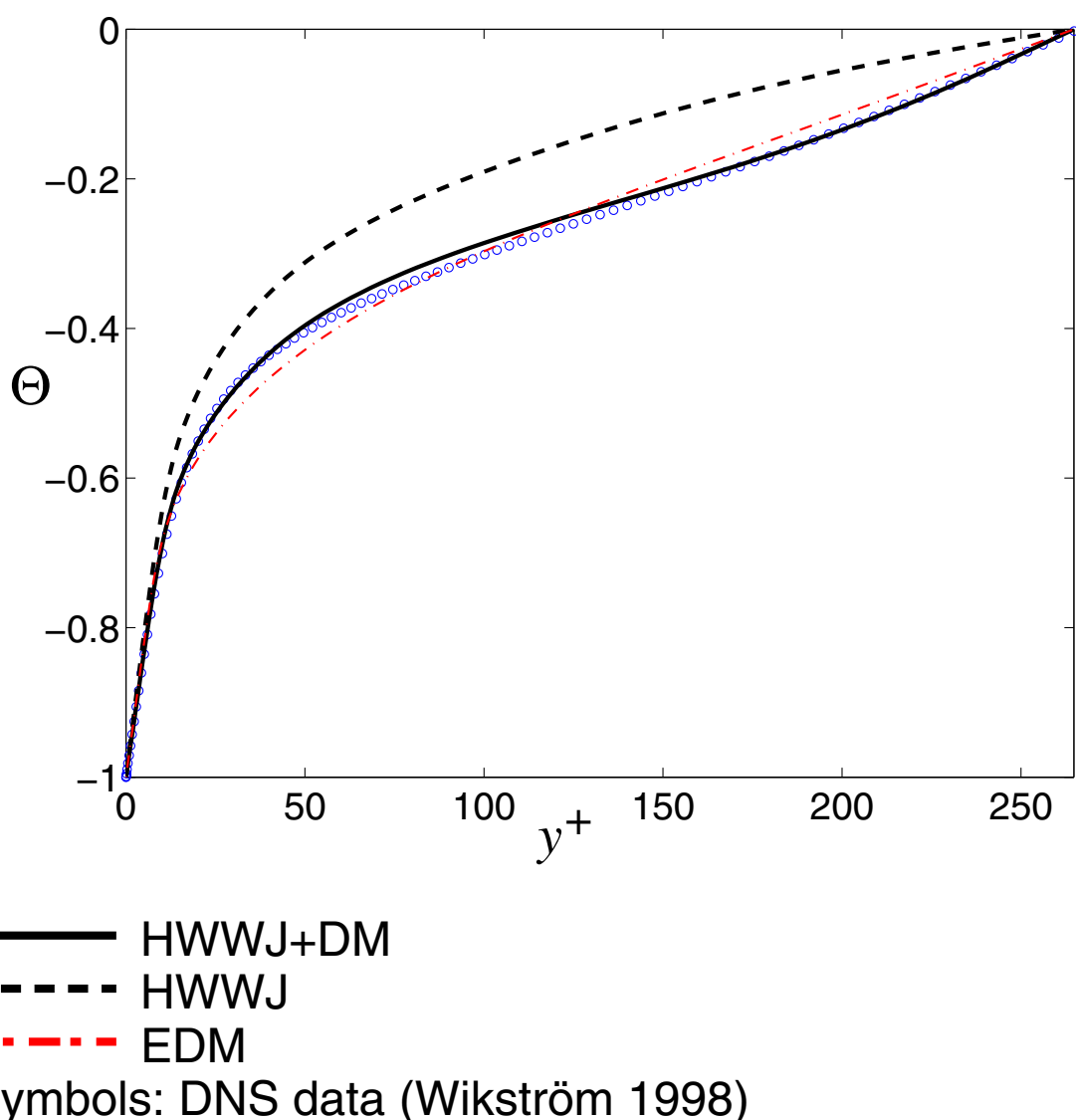
Homogeneous shear flow

- Mean scalar gradient in three different directions.
- Proposed model (HWWJ) compared with DNS (Rogers et al. 1986) and standard eddy diffusivity model (EDM)
- Proposed model (HWWJ) captures the flux direction (not aligned with the gradient)



Channel flow

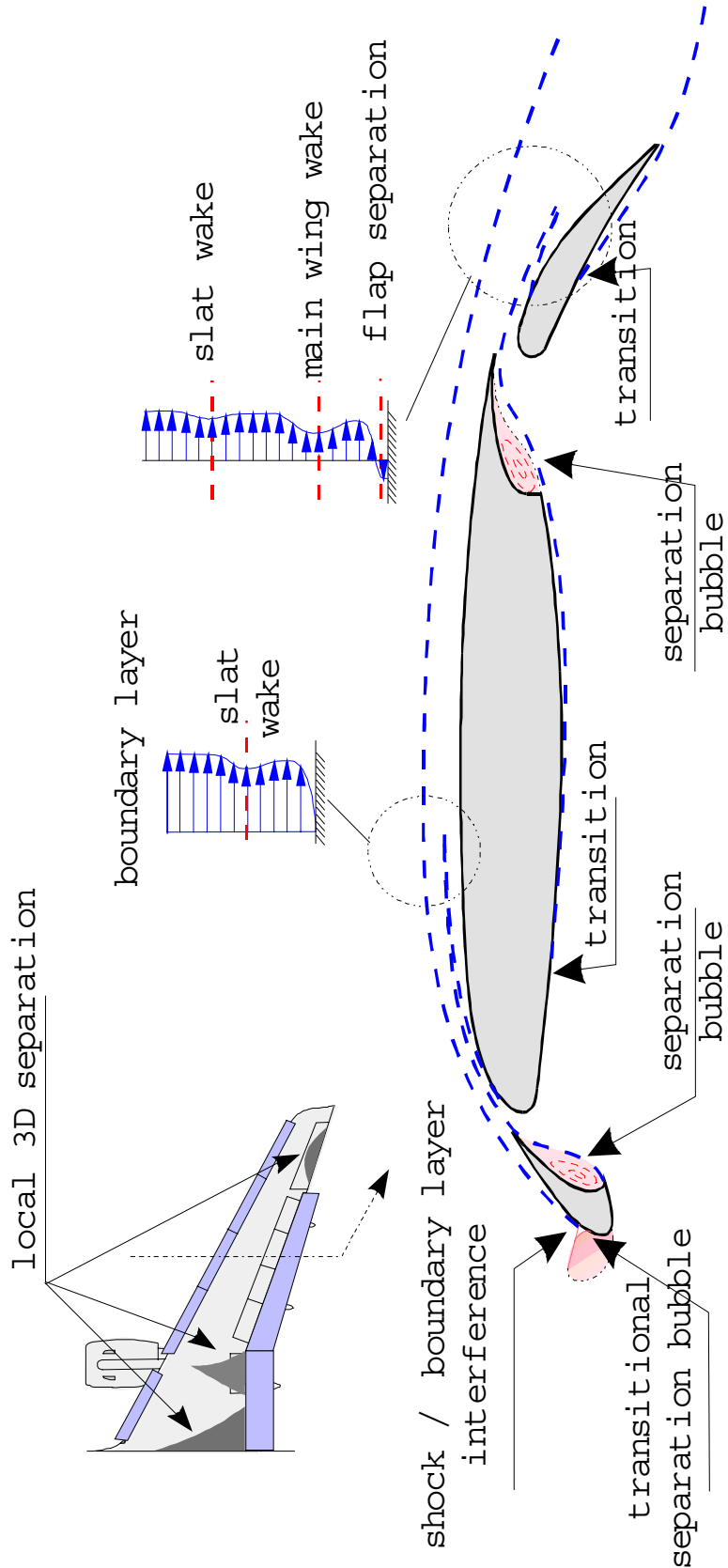
- The HWWJ model solved together with the low Reynolds number EARSM and the $K - \omega$ model.
- Comparision of the HWWJ model with and without diffusion model (DM) model and the eddy-diffusivity model model (EDM).

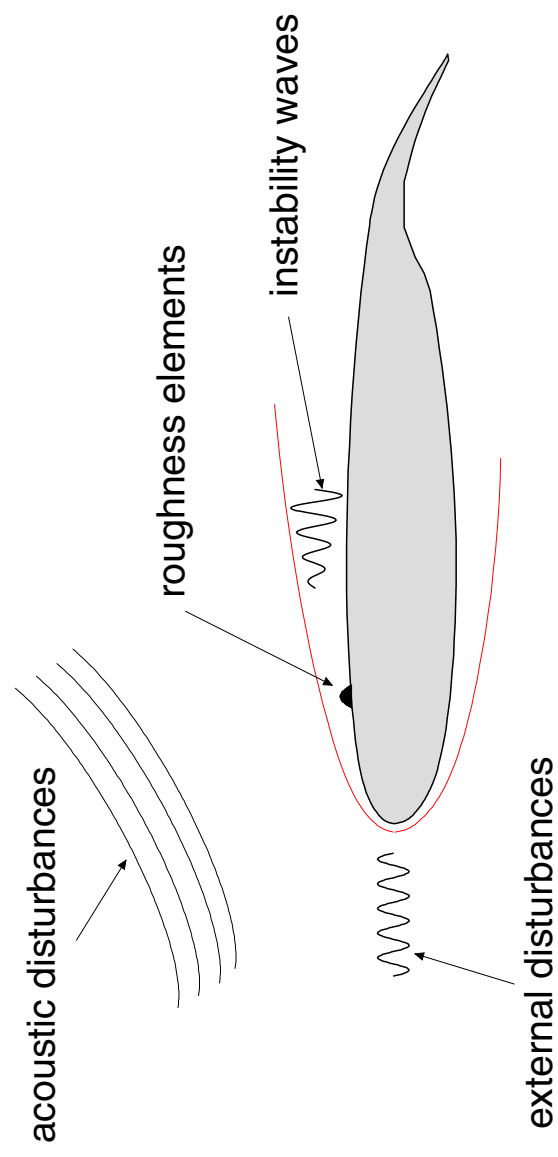


Transition prediction

Ardeshir Hanifi

FOI/FFA





Instability Theory

Laminar-Turbulence transition is assumed to be caused by breakdown of small disturbances inside the boundary layer.

$$Q(x, y, z, t) = \bar{Q}(x, y, z) + q(x, y, z, t)$$

Fourier expansion

$$q(x, y, z, t) = \sum_{m=-\infty}^{\infty} \sum_{n=-\infty}^{\infty} \tilde{q}_{m,n}(x, y) e^{i(n\beta z - m\omega t)}$$

Governing equations

- Mean flow with weak streamwise-variation,
- WKB or Multiple scales type:

$$\tilde{q}_{m,n}(x, y) = \hat{q}_{m,n}(x, y) e^{i \int_{x_0}^x \alpha_{m,n}(x') dx'}.$$

- scale separation:

$$\frac{\partial}{\partial x} = O(R^{-1}), \quad V = O(R^{-1}).$$

Collecting terms up to $O(R^{-1})$ gives a set of 'nearly' parabolic differential equations

$$A\hat{q}_{m,n} + B\frac{\partial \hat{q}_{m,n}}{\partial y} + C\frac{\partial^2 \hat{q}_{m,n}}{\partial y^2} + D\frac{\partial \hat{q}_{m,n}}{\partial x} = F_{m,n},$$

Solution is obtained by marching along x direction with $\hat{q}(x = x_0) = \hat{q}_0$.

Different level of approximation:

- Local theory:

$$\frac{\partial}{\partial x} = 0 \quad \rightarrow \quad \text{Eigenvalue problem}$$

- Linear non-local theory:

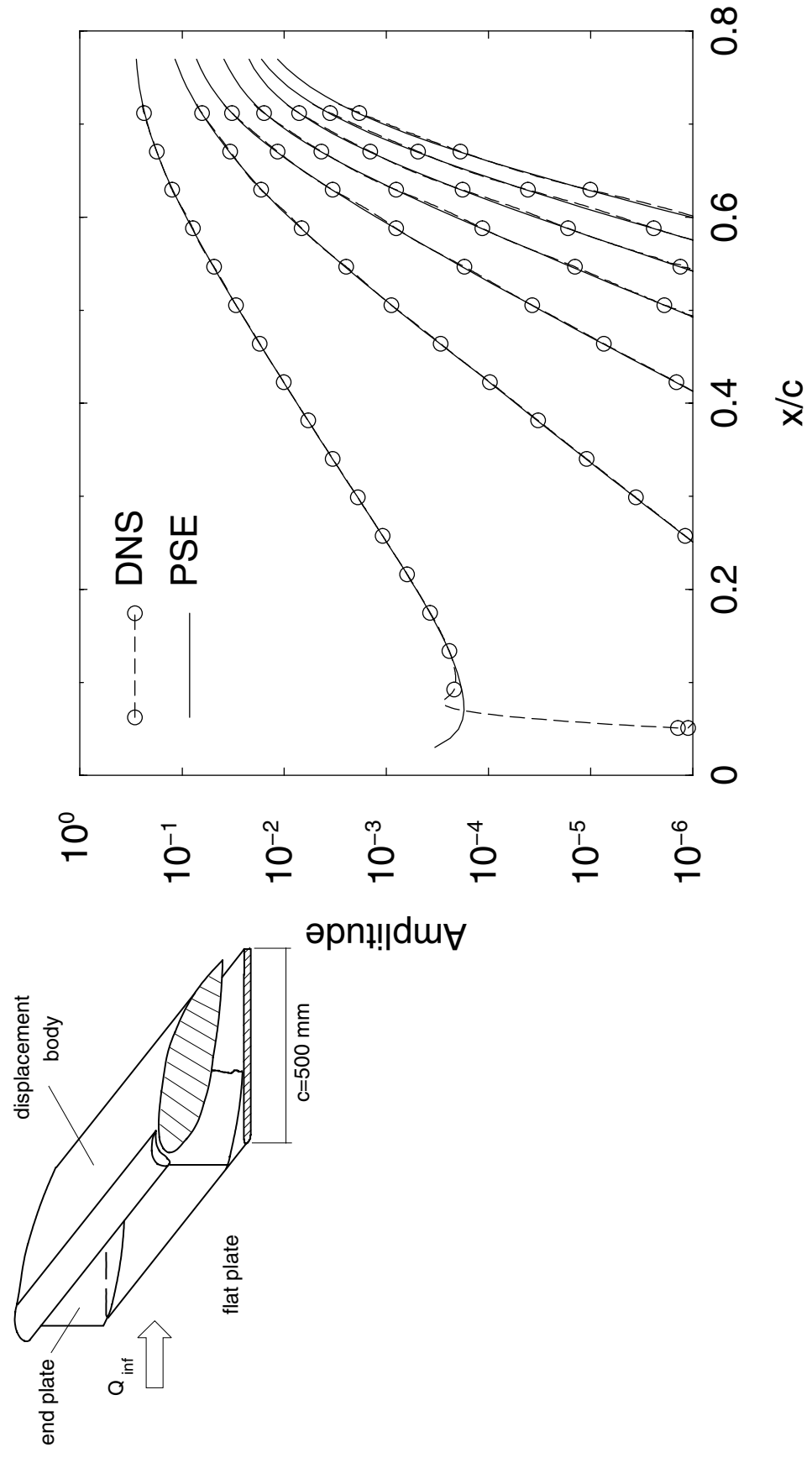
$$F_{m,n} = 0 \quad \rightarrow \quad \text{Linear parabolic eqs.}$$

- Non-linear non-local theory:

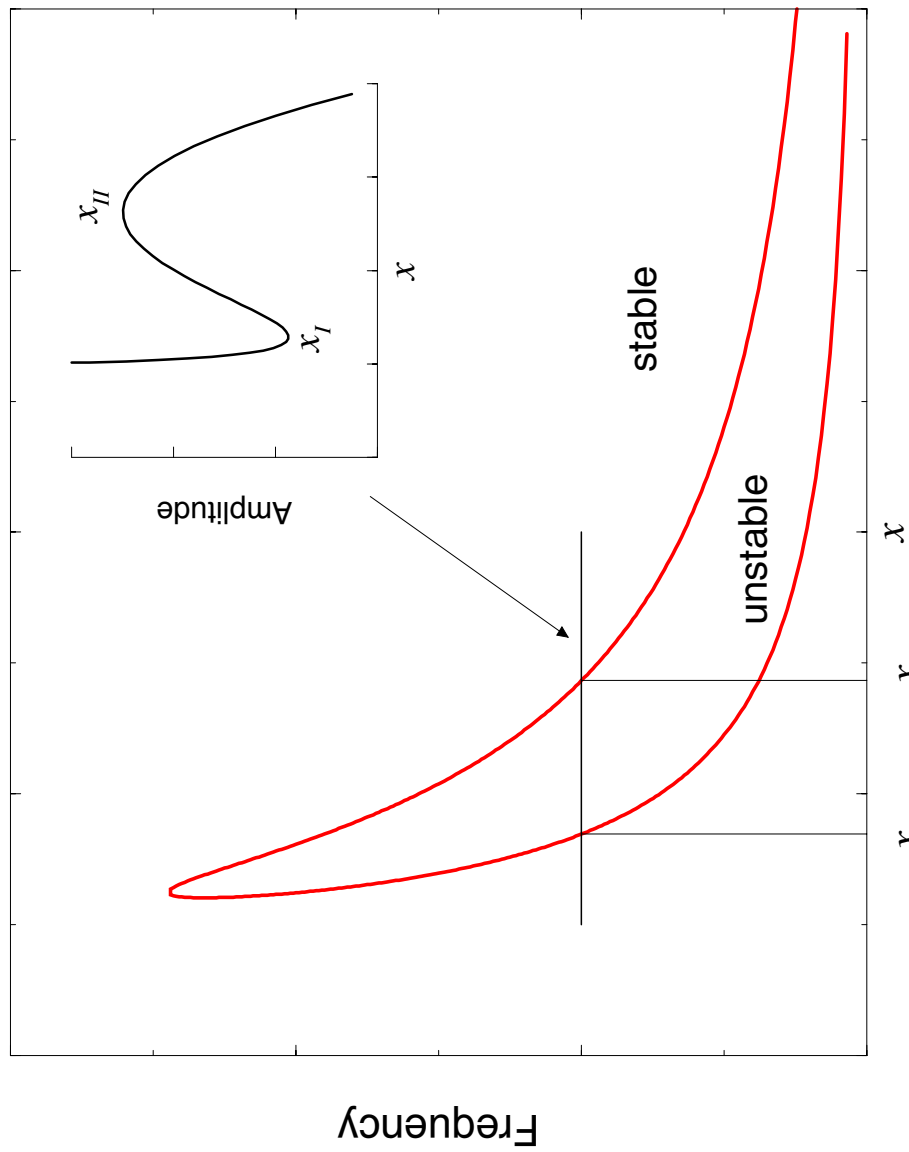
$$\text{All terms are kept} \quad \rightarrow \quad \text{Non-linear parabolic eqs.}$$

NoLoT-code (Developed at FFA and DLR)

- Solves Parabolized Stability Equations (PSE)
- Local / non-local theory
- Linear / non-linear equations
- Compressible / incompressible
- General orthogonal curvilinear coord.



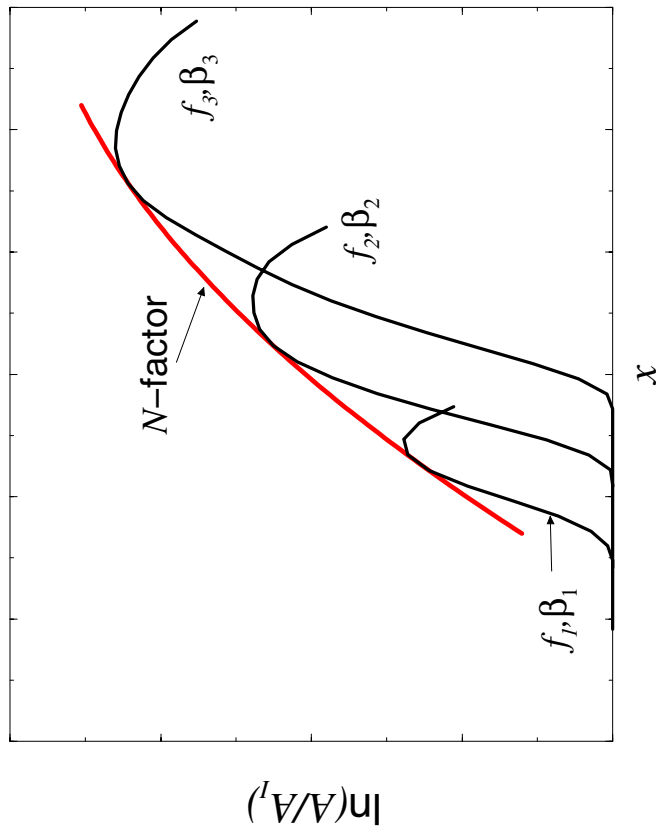
Nonlinear PSE vs DNS (Högberg & Henningson). Stationary crossflow mode (0,1) and its higher harmonics (0,2)-(0,7).



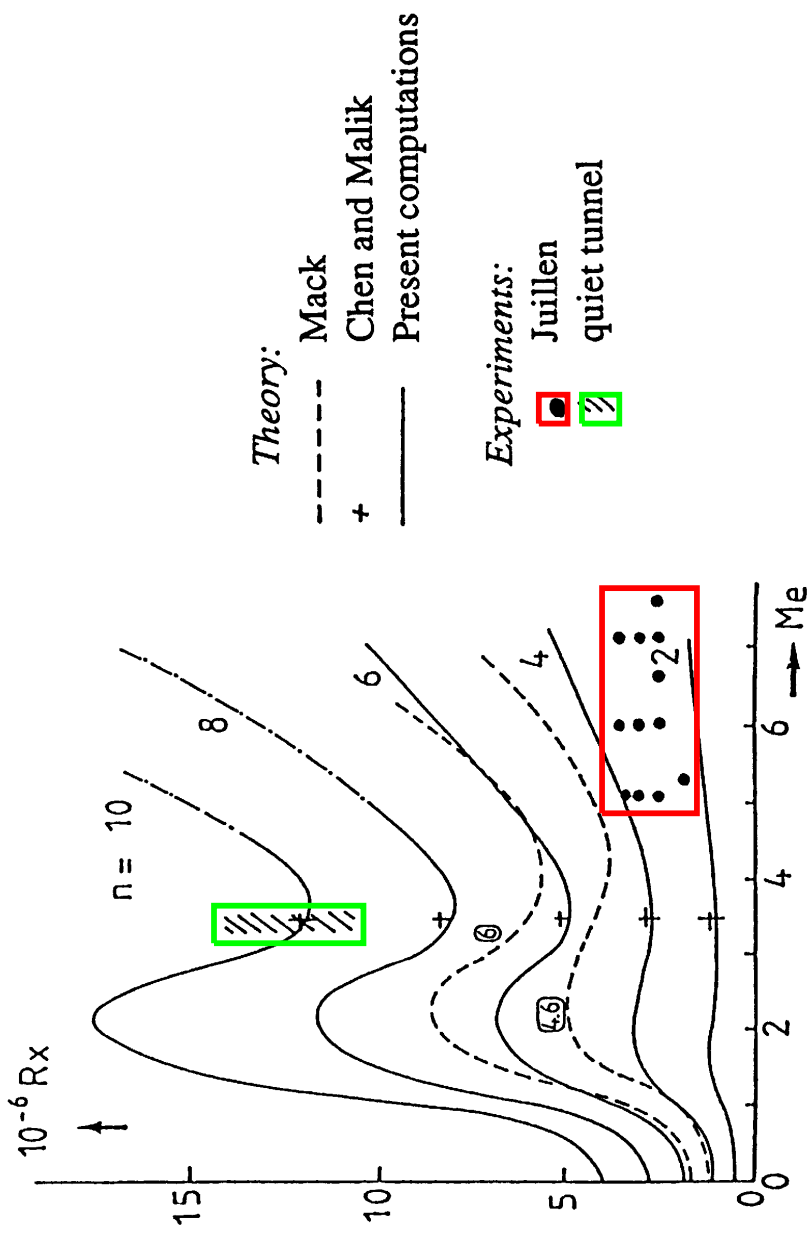
Schematic of neutral stability curve.

Transition prediction: e^N -method

$$\begin{aligned}
 N &= \max_{f,\beta} \left(\ln \frac{A}{A_I} \right) \\
 &= \max_{f,\beta} \left(\int_{x_I} -\alpha_i \, dx \right)
 \end{aligned}$$

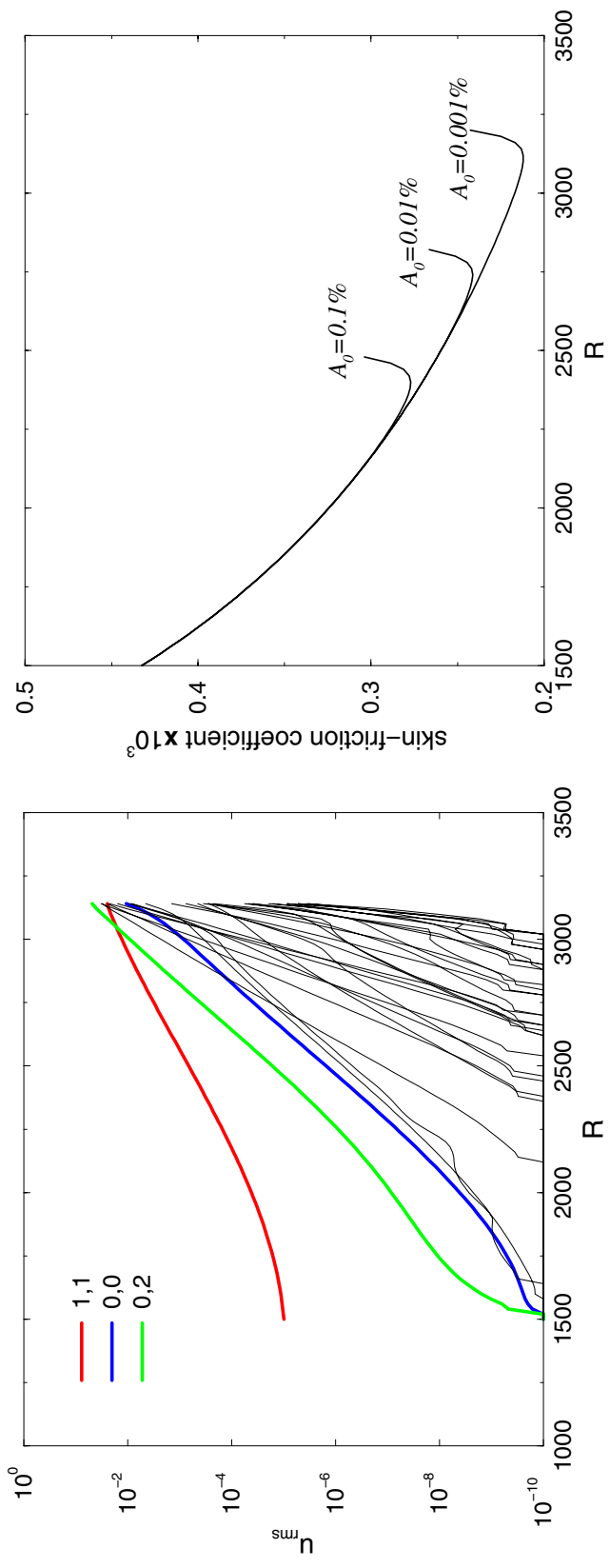


The value of N at onset of transition is obtained by correlation of computational and experimental data.



Application of the e^N method (flat plate, adiabatic wall). From Mack (1975), Arnal (1989).

Oblique-mode breakdown in supersonic boundary layer

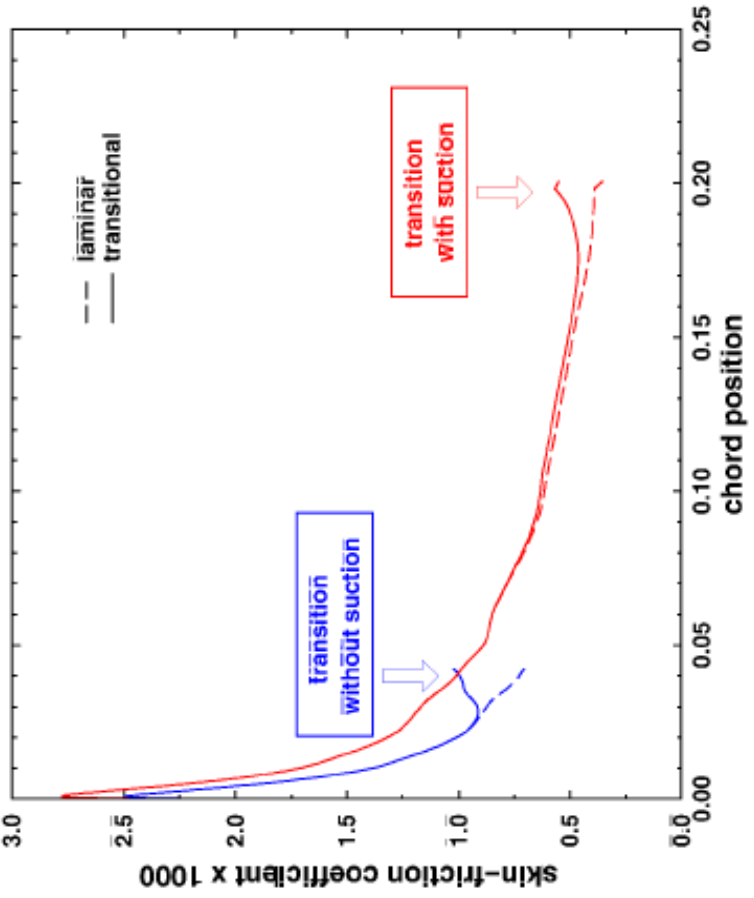


Mach number=1.6, $F = 6 \times 10^{-6}$, $\beta/R = 0.25 \times 10^{-4}$

Flight test



Non-linear, non-local transition analysis



Calculations performed by S. Hein using NOLLOT/PSE (DLR/FFA) code.

Strömningsstyrning och aerodynamisk optimering

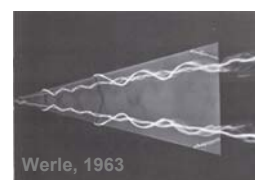
Martin Berggren
Flygteknik, FFA

FOI

Flow Control

Utilize flow instabilities/sensitivities to accomplish
large effects by small efforts, e.g.

- Vortex control

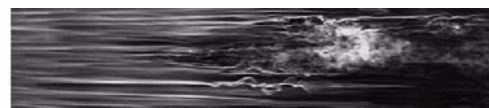


- Separation control



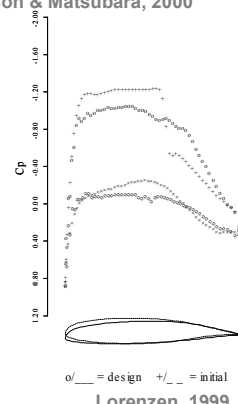
FOI

- Transition control



Alfredsson & Matsubara, 2000

- Transonic wave drag control

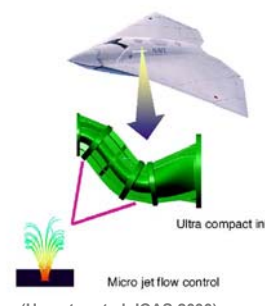


$\circ/-\cdots$ = design $+/-\cdots$ = initial
Lorenzen, 1999

FOI

Aeronautical Applications of Flow Control

- Active inlets
- Fluidic thrust vector control
- Nose vortex control
- Active Core Exhaust (ACE)
- Drag reduction, increased lift



FOI

FOI project: Optimal Design and Control of Fluid Flows

Project leader: Dan Henningson

Computational Aerodynamics: Martin Berggren,
Mattias Chevalier, Ardesir Hanifi, Jan Pralits,
Olivier Amoignon

Experimental Aerodynamics: Jens Österlund etc.

Systems Control: Martin Hagström,
Sven-Lennart Wirkander

FOI

Activities in the FOI project

Computational/Theoretical

- Algorithm development for control and optimization
- Methods development for automated design
- Supercomputer simulation of complete flow control systems (incl. sensors, actuators), currently for CF-instability control

Experimental

- Active control of flow in S-duct diffusor

FOI

PhD Projects in cooperation with KTH and UU

Mattias Chevalier	<i>Optimal control of boundary layers</i>	FOI
Jan Pralits	<i>Optimal design wrt low drag</i>	SSF:IVS, FOI/EU
Olivier Amoignon	<i>Aerodynamic shape optimization</i>	PSCI, FOI/EU
Markus Högberg	<i>Optimal control of channel flows</i>	VR ramprogram
Ori Levin	<i>Flow control in boundary layers</i>	STEM
Astrid Herbst	<i>Flow control in diffusor flows</i>	PSCI, SAAB

FOI

Optimal control/design using Navier-Stokes eq.

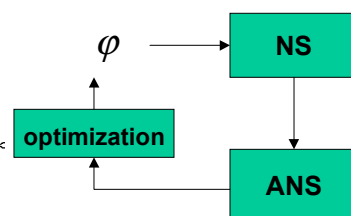
$$\frac{du}{dt} = A(u) + B(u, \varphi), \quad u(t=0) = u_0$$

$$J(\varphi) = \int_0^T \int_{\Omega} [c(u) + l^2 d(\varphi)] d\Omega$$

$$\nabla_{\varphi} J = \nabla_u B(u, \varphi)^* p + l^2 \nabla_{\varphi} d(\varphi)^*$$

where

$$\begin{cases} -\frac{dp}{dt} = \nabla_u A(u)^* p + \nabla_u B(u, \varphi)^* p + \nabla_u c(u)^* \\ p(t=T) = 0 \end{cases}$$



FOI

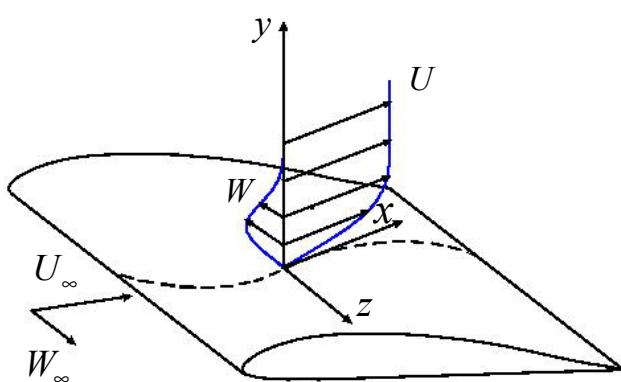
This scheme is applied to

- Optimal control in boundary layers (Chevalier, Högberg)
- Drag minimization in Edge (Amoignon, Berggren)
- Design of optimal suction on wings (Hanifi, Pralits)
- Natural laminar flow technology (Hanifi, Pralits)

The control can sometimes be expressed
in terms of a pre-computed *feed-back law*.
⇒ No iterations needed

FOI

Boundary layer on a swept wing

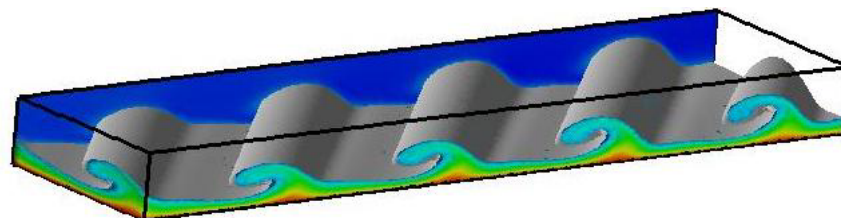
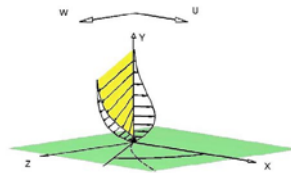


FOI

Cross-flow vortices on a swept wing

Direct numerical simulation using the
Navier-Stokes equations

Slice of a periodic array of vortices
in a Falkner-Skan-Cooke boundary-layer

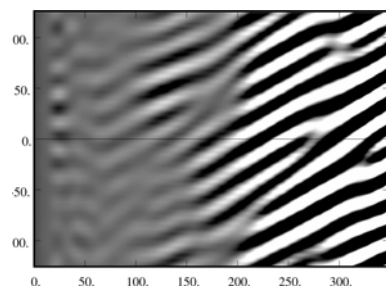


FOI

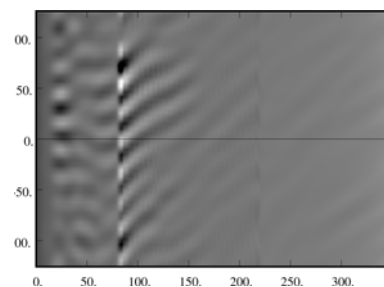
Control of CF-vortices

Direct Numerical Simulation of FSC-flow with/without control

Control off



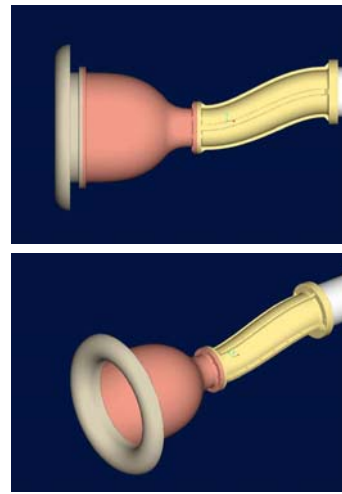
Control on



FOI

FOI S-duct experiment

- Test bed for actuators and sensors
(pulsed micro jets, pressure shear stress)
 - Test bed for control concepts
(system identification, optimal control)
 - Fan for low speed operation
 - Rock chamber for high speeds
 - CAD geometry, under construction
- $L = 1548\text{mm}$, $H = 464.4\text{mm}$,
 $\phi_1 = 218\text{mm}$, $\phi_2 = 258\text{mm}$



FOI

HIGH SPEED TURBULENT COMBUSTION

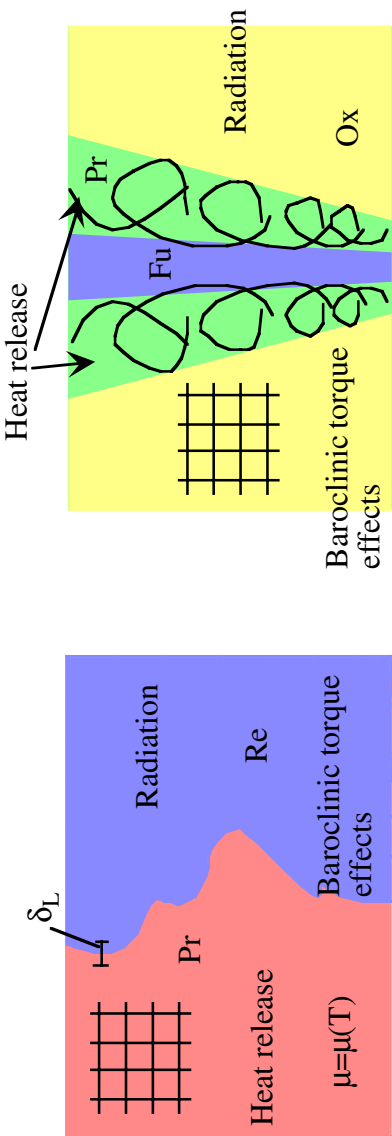
Christer Fureby, Per Walmerdahl & Marco Kupiainen
Totalförsvarets Forskningsinstitut, FOI
Vapen & Skydd
Grindsjöns forskningscentrum



Introduction

Multi-disciplinary field involving: (i) fluid dynamics, (ii) thermodynamics, (iii) chemical kinetics and (iv) thermal radiation

Premixed Combustion



Areas of research

- Premixed turbulent combustion (jet-engine afterburners, LPP combustors)
- Non-premixed turbulent flames (engine flames, gas turbines)
- Supersonic combustion (ram- and scramjets)
- Fire spread in confined spaces
- Pool fires
- Explosions and ignition effects

Governing Equations of Reacting Flow

The governing equations for the reactive flow problem consists of

$$\sum_{i=1}^N (P'_{ij} \mathcal{S}_i) \Leftrightarrow \sum_{i=1}^N (P''_{ij} \mathcal{S}_i) \quad \begin{cases} \partial_t(\rho) + \nabla \cdot (\rho \mathbf{v}) = 0 \\ \partial_t(\rho \mathbf{v}) + \nabla \cdot (\rho \mathbf{v} \otimes \mathbf{v}) = -\nabla p + \nabla \cdot \mathbf{S} + \rho \mathbf{f} \\ \partial_t(\rho h) + \nabla \cdot (\rho v h) = \dot{p} + \mathbf{S} \cdot \mathbf{D} + \nabla \cdot \mathbf{h} + \rho \sigma \end{cases}$$

$$[\partial_t(\rho Y_i) + \nabla \cdot (\rho \mathbf{v} Y_i)] = \nabla \cdot \mathbf{j}_i + w_i$$

$$\begin{cases} p = \rho R T \sum_{i=1}^n [Y_i / M_i], & h = \sum_{i=1}^n [Y_i (h_{i,f}^\theta + \int_{T_0}^T C_{P,i} dT)], \quad S = 2\mu D_D, \quad h = \kappa \nabla T \\ \mathbf{j}_i = \lambda_i \nabla Y_i; \quad \sum_{i=1}^n [Y_i] = 0, \quad \sum_{i=1}^n [\mathbf{j}_i] = 0 \\ w_i = [P''_{ij} - P'_{ij}] w_j; \quad w_j = \rho^{\sum_{i=1}^n (P'_{ij} - P''_{ij})} k_j \prod_{i=1}^n [Y_i^{P'_{ij}}]; \quad k_j = \Lambda_j T^{\alpha_j} e^{-T_{A,j}/T} \end{cases}$$

- complex physics (turbulence, chemical reactions, volume expansion, heat release)
 - wide range of length & time scales
 - hard to estimate all parameters
 - very large system of equations to solve for practical fuels
 - equations generally stiff
- ∴ Simplifications required !

Premixed Turbulent Combustion

Global or simplified reaction mechanisms with Arrhenius chemistry using MILES

$$\sum_{i=1}^N (P'_{ij} \mathfrak{I}_i) \Leftrightarrow \sum_{\substack{i=1 \\ j < 4, i < 10}}^N (P''_{ij} \mathfrak{I}_i)$$

$$\begin{cases} \partial_t(\rho) + \nabla \cdot (\rho \mathbf{v}) = 0 \\ \partial_t(\rho \mathbf{v}) + \nabla \cdot (\rho \mathbf{v} \otimes \mathbf{v}) = -\nabla p + \nabla \cdot (2\mu \mathbf{D}_D) + \rho \mathbf{f} \\ \partial_t(\rho h) + \nabla \cdot (\rho v h) = \dot{p} + \mathbf{S} \cdot \mathbf{D} + \nabla \cdot (\kappa \nabla T) + \rho \sigma \\ \partial_t(\rho Y_i) + \nabla \cdot (\rho \mathbf{v} Y_i) = \nabla \cdot (\lambda_i \nabla Y_i) + P_{ij} w_j, \quad i=1,\dots,5, \quad j=1,2 \end{cases}$$

If carried out with *explicit filtering* (LES) several additional terms needs to be modeled.

Flamelet models using LES

The flame is assumed to be a thin wrinkled interface

$$\begin{cases} \partial_t(\bar{\rho}) + \nabla \cdot (\bar{\rho} \tilde{\mathbf{v}}) = 0 \\ \partial_t(\bar{\rho} \tilde{\mathbf{v}}) + \nabla \cdot (\bar{\rho} \tilde{\mathbf{v}} \otimes \tilde{\mathbf{v}}) = -\nabla \bar{p} + \nabla \cdot (2\mu \tilde{\mathbf{D}}_D + \mathbf{B}) + \bar{\rho} \tilde{\mathbf{f}} \\ \partial_t(\bar{\rho} \tilde{h}) + \nabla \cdot (\bar{\rho} \tilde{\mathbf{v}} \tilde{h}) = \bar{\dot{p}} + \bar{\mathbf{S}} \cdot \tilde{\mathbf{D}} + \varepsilon + \nabla \cdot (\kappa \nabla \tilde{T} + \mathbf{b}_h) + \bar{\rho} \tilde{\sigma} \\ \partial_t(\bar{\rho} \tilde{\xi}) + \nabla \cdot (\bar{\rho} \tilde{\mathbf{v}} \tilde{\xi}) = \nabla \cdot \mathbf{b}_{\xi} - \rho_u \langle S_u \rangle \Xi |\nabla \tilde{\xi}| \end{cases}$$

SGS models required for \mathbf{B} , \mathbf{b}_h , \mathbf{b}_ξ and ε !

Ξ and S_u require modelling
 Ξ by a *modelled* transport equation
 S_u by correlations

Non-Premixed Turbulent Combustion

Global or simplified reaction mechanisms with Arrhenius chemistry using MILES

$$\sum_{i=1}^N (P'_{ij} \mathfrak{I}_i) \Leftrightarrow \sum_{\substack{i=1 \\ j < 4, i < 10}}^N (P''_{ij} \mathfrak{I}_i)$$

$$\begin{cases} \partial_t(\rho) + \nabla \cdot (\rho \mathbf{v}) = 0 \\ \partial_t(\rho \mathbf{v}) + \nabla \cdot (\rho \mathbf{v} \otimes \mathbf{v}) = -\nabla p + \nabla \cdot (2\mu \mathbf{D}_D) + \rho \mathbf{f} \\ \partial_t(\rho h) + \nabla \cdot (\rho v h) = \dot{p} + \mathbf{S} \cdot \mathbf{D} + \nabla \cdot (\kappa \nabla T) + \rho \sigma \\ \partial_t(\rho Y_i) + \nabla \cdot (\rho \mathbf{v} Y_i) = \nabla \cdot (\lambda_i \nabla Y_i) + P_{ij} w_j, \quad i=1,\dots,5, \quad j=1,2 \end{cases}$$

If carried out with *explicit filtering* (LES) several additional terms needs to be modeled.

Flamelet models using LES

Introduce a mixture fraction, such that $z=z(Y_i)$. The eqns' can then be expressed

$$\begin{cases} \partial_t(\bar{\rho}) + \nabla \cdot (\bar{\rho} \tilde{\mathbf{v}}) = 0 \\ \partial_t(\bar{\rho} \tilde{\mathbf{v}}) + \nabla \cdot (\bar{\rho} \tilde{\mathbf{v}} \otimes \tilde{\mathbf{v}}) = -\nabla \bar{p} + \nabla \cdot (2\mu \tilde{\mathbf{D}}_D + \bar{\mathbf{B}}) + \bar{\rho} \tilde{\mathbf{f}} \\ \partial_t(\bar{\rho} \tilde{h}) + \nabla \cdot (\bar{\rho} \tilde{\mathbf{v}} \tilde{h}) = \bar{\dot{p}} + \bar{\mathbf{S}} \cdot \tilde{\mathbf{D}} + \varepsilon + \nabla \cdot (\kappa \nabla \tilde{T} + \mathbf{b}_h) + \bar{\rho} \tilde{\sigma} \\ \partial_t(\bar{\rho} \tilde{z}) + \nabla \cdot (\bar{\rho} \tilde{\mathbf{v}} \tilde{z}) = \nabla \cdot (\lambda \nabla \tilde{z} + \mathbf{b}_z) \end{cases}$$

$$\tilde{Y}_i = \int_0^1 \int_0^\infty \mathcal{O}_\beta(z, \chi) Y_i(z) dz d\chi$$

SGS models required for \mathbf{B} , \mathbf{b}_h , \mathbf{b}_z and ε ! Thin flame located at $z=z_{st}$.

Numerical Methods in Reacting Flow

Stiffness avoided by using either global schemes or flamelet models!

Finite-Volume (FV) discretization

Continuity and momentum equations combined to form a Poisson equation for p

Convective fluxes reconstructed with 2nd order CD

For MILES a 2nd order FCT scheme is used

Diffusive/viscous fluxes represented by 2nd order CD

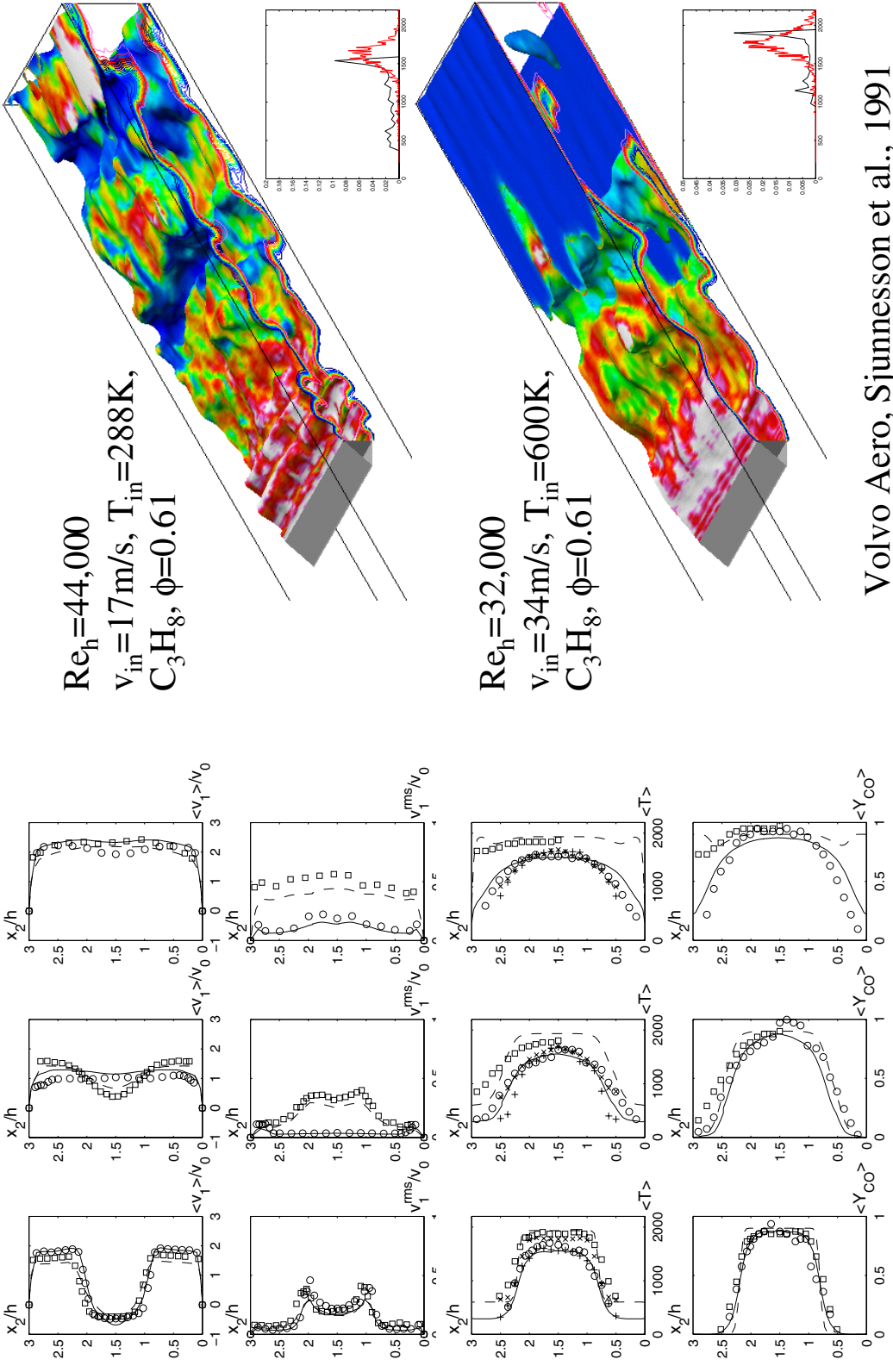
Crank Nicolson time integration

⇒ Scheme of $O(\Delta t^2, \Delta x^2)$

PISO-type loop adopted for the p-equation

Segregated solution approach ($Co < 0.2$)

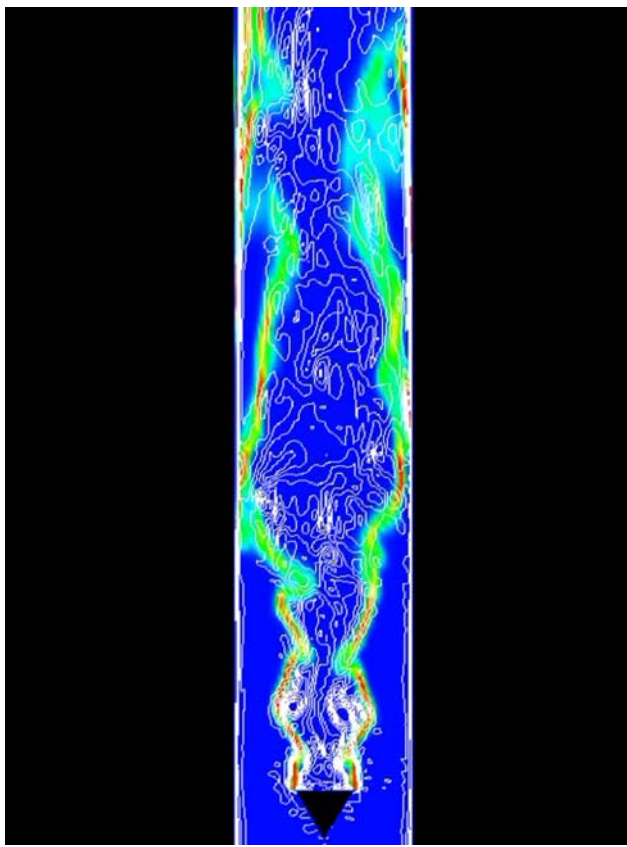
Combustion in a Jet-Engine Afterburner



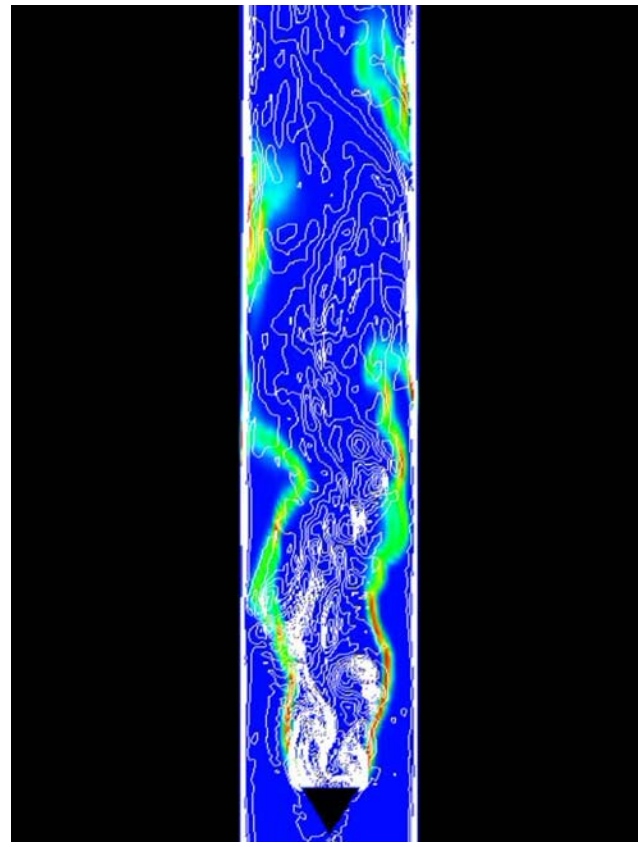
Volvo Aero, Sjunnesson et al., 1991

Weller H.G., Tabor G., Gosman A.D. & Fureby C.; 1998, 27th Int. Symp. on Comb., p 899.
 Fureby C., Grinstein F.F. & Kailasanth K.; 2000, AIAA Paper No 00-0863
 Fureby C.; 2000, Comb. Sci & Tech, **161**, p 213.
 Fureby C., Grinstein F.F., Menon S. & Weller H.G.; 2001, 2nd Int. Conf. on Turb. Shear Flow Phen., Stockholm.

Combustion in a Jet-Engine Afterburner cont.

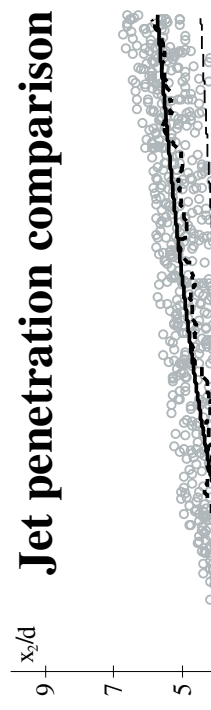
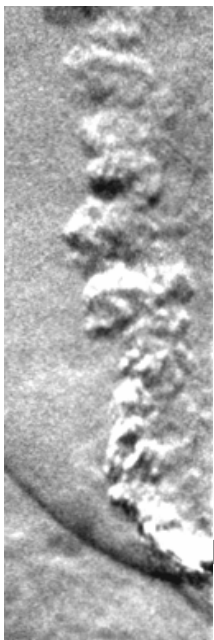


$Re_h=44,000$
 $V_{in}=17\text{ m/s}, T_{in}=288\text{ K}$,
 $C_3H_8, \phi=0.61$

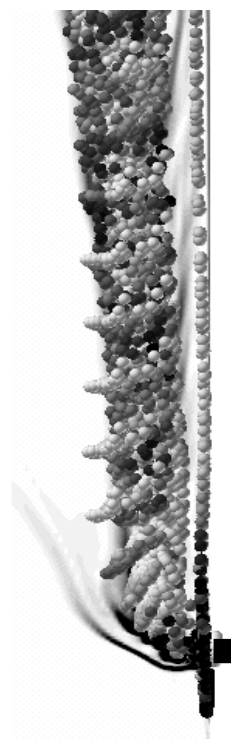


$Re_h=32,000$
 $V_{in}=34\text{ m/s}, T_{in}=600\text{ K}$,
 $C_3H_8, \phi=0.61$

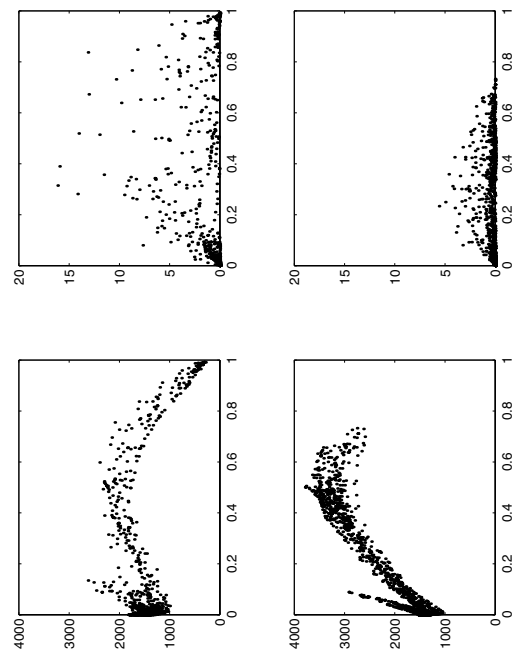
Scramjet Combustion



Schlieren (Ben-Yakbar & Hansen, 1998)



LES with Arrhenius chemistry



Scalar statistics

Concluding Remarks

Simulations of reacting flows very complicated

- more complex physics (reactions, turbulence, radiation, ...)
 - a wider range of scales (spatial and temporal) to consider
- ⇒ Specific treatment of different combustion regimes (non-premixed / premixed)
- ⇒ Families of models

RANS out of the question due to the strong interactions between the flame and the reactions.

Much research (experimentally, theoretically & computationally) to be done!

Important military applications

Solid Rocket Propellant Combustion and Launch Technology

Magnus Berglund
Weapons and Protection Division
Warheads and Propulsion

Outline

- Motivation
- Flow Modeling
- Some Qualitative Results
- Summary / Outlook

Motivation

- Better understanding of reacting/ non-reacting gas-solid flows and their simulation
 - Modeling and model limitations
 - Numerical techniques
- Design considerations for gas-solid systems.
 - For the SRM case e.g.
 - Propellant grain
 - Rocket chamber
 - Nozzle
- For the gun case e.g.
 - Propellant grain size distribution and geometry
 - Geometry of barrel and muzzle brakes

Flow Modeling

Starting point, SRM

Euler (multifluid) approach to multiphase flow, giving a set of phase-averaged Navier–Stokes equations via volume-averaging; similar to a volume of fluid (VOF) approach.

Simplifying assumptions, SRM

Non-moving, non-porous, incompressible solid; zero fluid velocity at the phase boundary, local thermodynamic equilibrium between the phases, burn rate obey a Vielle type law: $u_b = ap^n$, radiation neglected.

Starting point and simplifying assumptions, gun

Not yet considered in detail. A lot of similarities with SRM flows which thus can act as a “platform” for simulations of interior ballistics flows in guns.

Flow Modeling (cont'd)

Governing equations (simplified), **SRM**

$$\left\{ \begin{array}{l} \partial_t \langle \rho \rangle_i + \operatorname{div} (\langle \rho \rangle_i \langle \mathbf{u} \rangle_i) = 0 \\ \\ \partial_t (\widetilde{\langle \rho \rangle_i \langle \mathbf{u} \rangle_i}) + \operatorname{div} (\widetilde{\langle \rho \rangle_i \langle \mathbf{u} \rangle_i \langle \mathbf{u} \rangle_i}) = -\operatorname{grad} \langle p \rangle_i + \operatorname{div} \langle \mathbf{S} \rangle_i + \frac{1}{V} \int_{A_1} \mathbf{S}_1 \cdot \mathbf{n}_1 dA \\ \\ \partial_t (\widetilde{\langle \rho \rangle_i \langle h \rangle_i}) + \operatorname{div} (\widetilde{\langle \rho \rangle_i \langle \mathbf{u} \rangle_i \langle h \rangle_i}) = \dot{\langle p \rangle}_i - \operatorname{div} (\alpha_1 \langle \mathbf{j}_{q,1} \rangle_i + \alpha_2 \langle \mathbf{j}_{q,2} \rangle_i) \\ \quad + \alpha_1 \langle \phi_1 \rangle_i + \alpha_2 \langle \phi_2 \rangle_i - \frac{1}{V} \int_{A_1} (\rho_2 h_2 - \rho_1 h_1) \mathbf{u}_s \cdot \mathbf{n}_1 dA \\ \\ \partial_t \alpha_2 = -\frac{1}{V} \int_{A_1} \mathbf{u}_s \cdot \mathbf{n}_1 dA \end{array} \right.$$

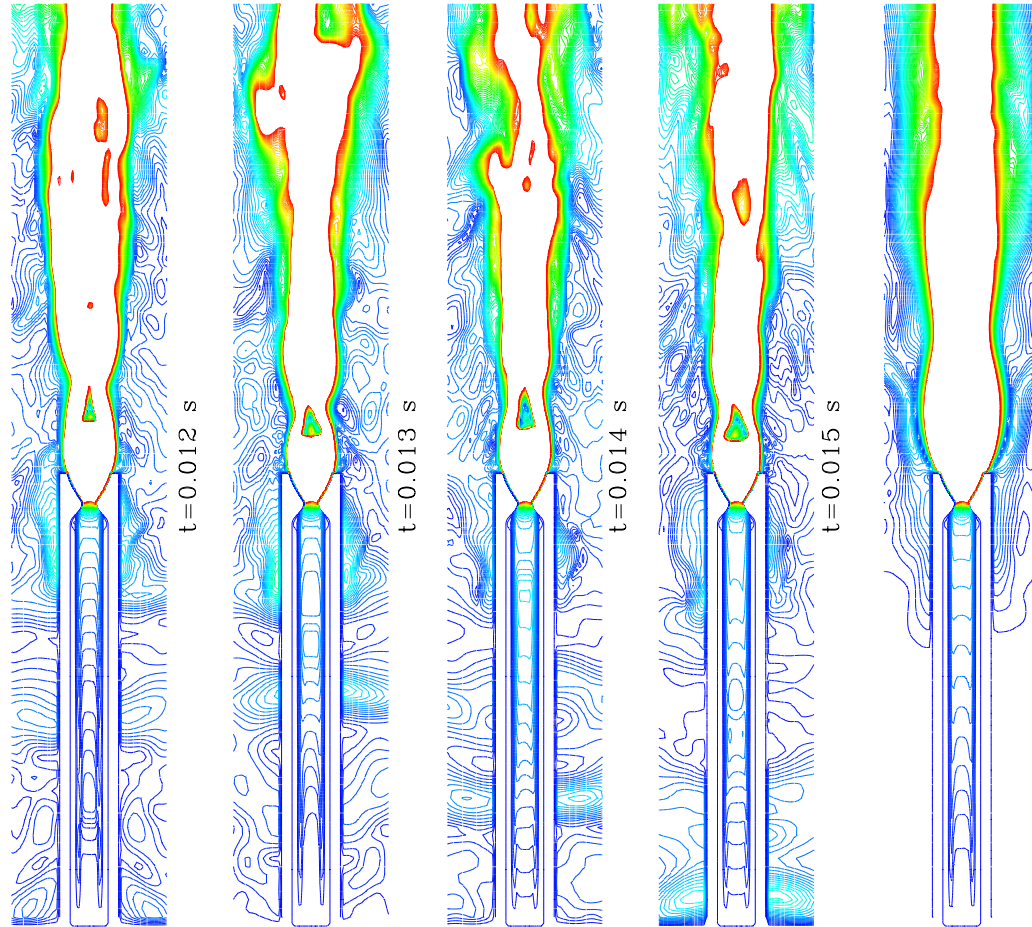
Boltzmann virial expansion used for the equation of state for the gas.

Solution strategy, SRM

Large Eddy Simulation (LES); especially Monotone Integrated LES, viz. using intrinsic properties of high-resolution schemes for construction of implicit (or built-in) subgrid scale models by means of the leading order truncation errors.

Some Qualitative Results

Contour plots of Mach number (below one) at different times and mean Mach number



Perspective view of instantaneous iso-surfaces of the magnitude of the velocity at 1000 m/s and 125 m/s, colored with temperature

Summary / Outlook

Summary

- A reduced set of flow equations have been derived from a general Euler formulation of multiphase flows. In this derivation a number of specializing assumptions have been used
- A Monotone Integrated LES approach has been used for solving the governing equations applied to a static firing of a solid rocket motor
- Qualitatively good results has been obtained, implying that this computational approach has the potential to mature into a valuable tool for quantitative predictions of reacting gas-solid flows
- Qualitative results presented as AIAA Paper 2001-0895, Reno, NV, USA
- Loosening the simplifying assumptions and study effects from this on the SRM case
- Study effects of using different combustion models and different phase boundary capturing on the SRM case
- Relevant modeling issues for interior ballistics flows in guns

Outlook

Swedish PDE-Program

Jon Tegnér

Swedish Defence Research Agency, FOI
Stockholm, Sweden

Purpose

- Demonstrate the PDE as a potential propulsion system/subsystem for air vehicles.
- Evaluate the potential of PDE powered systems.

Goal

- A flying demonstrator.

Funded by The Swedish Defence Forces.

Agencies:

- Swedish Defence Materiel Administration, FMV.
- Swedish Defence Research Agency, FOI.

Subcontractors:

- Volvo Aero Corporation, VAC.
- Royal Institute of Technology, KTH.
- Ultratech.

Swedish Defence Materiel Administration, FMV

- Management of the PDE technology demonstrator program.
- International cooperations.
- Erik Prisell and Björn Jonsson.

Volvo Aero Corporation, VAC

- Design and realization the engine.
- Study fuels and components (pre-detonators, valves, fuel injectors ...).
- CFD analysis of the PDE cycle.
- Göran Jonsson and Patrik Johansson.

Swedish Defence Research Agency, FOI

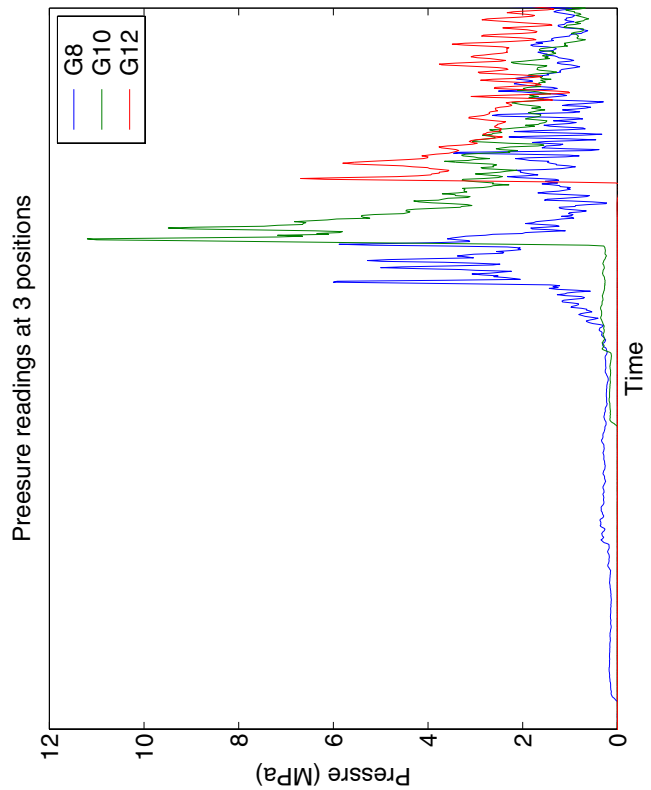
- Numerical calculations of detonations in one, two and three dimensions in cooperation with the Royal Institute of Technology, KTH.
- Analysis of Deflagration to Detonation Transitions (DDTs).
- Single pulse experiments using acetylene/air and hydrogen/air.
- Experiments on pre-detonators and DDT-enhancing devices.
- Multi-cycle experiments on hydrogen/air.

Numerical Approximation

- TVD, ENO, or centered approx.
 - Explicit RK in time.
 - One sided operators at boundary points.
 - Point values.
 - Straight channel, no geometry.
 - Extension to 3D and O-H chemistry.
- Implementation
- MPI.
 - C and f77.
 - IBM/SP2, SGI, Cray J90, Linux cluster.

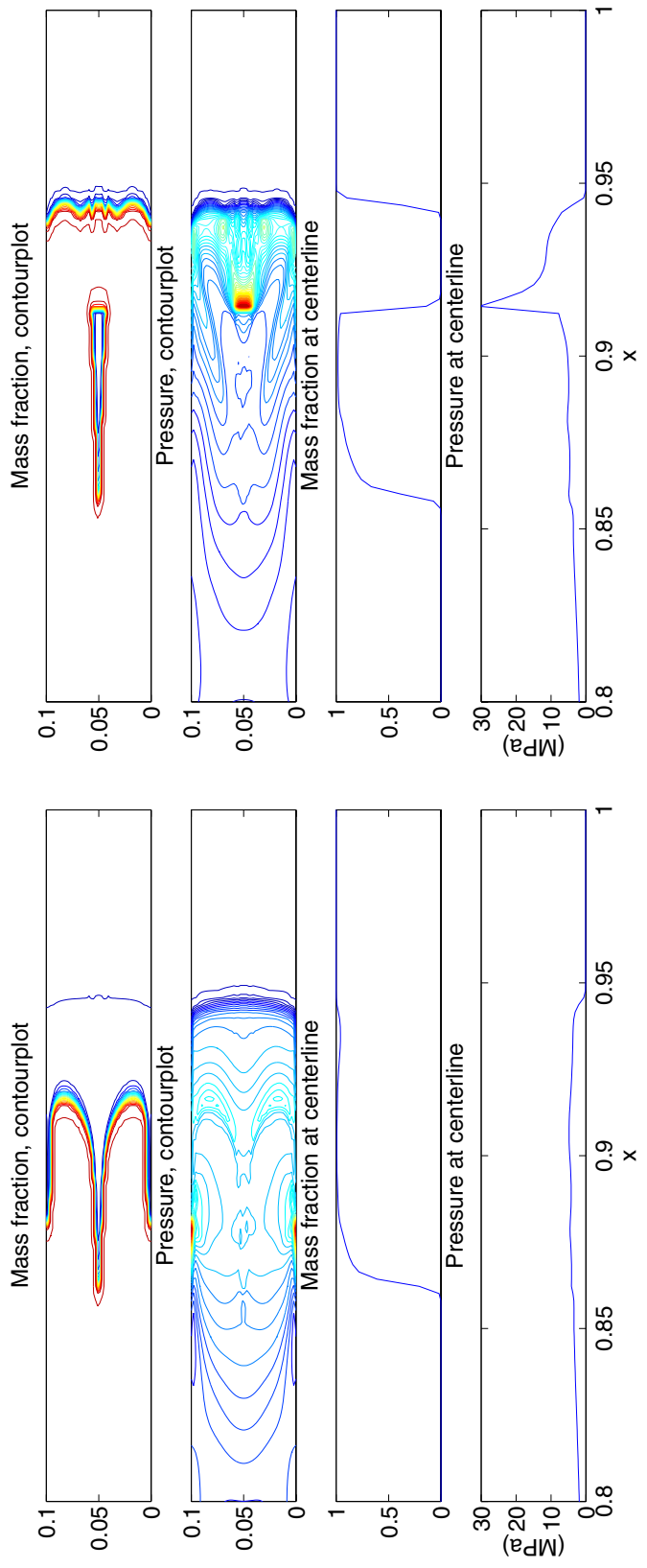
Single pulse, results from experiment

One example. Shock waves are important in DDTs and extreme pressures are often obtained.



High peak pressure in a DDT.

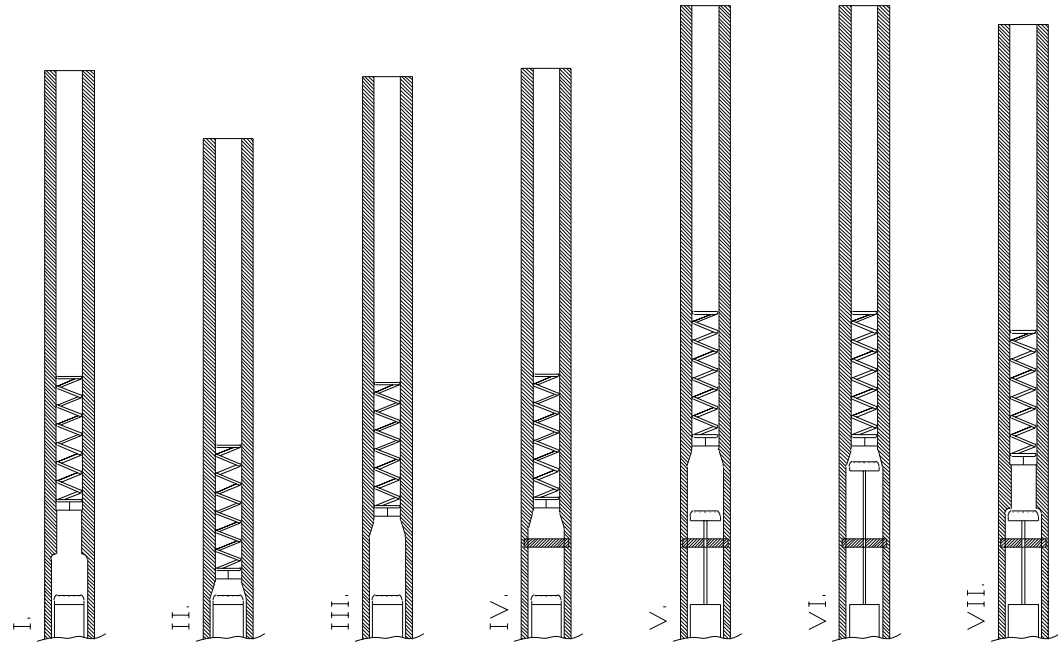
Single pulse, results from CFD



A retonation wave with very high peak pressure is developed in a pocket of unburnt mixture.

Multi-cycle experiments

- Inspired by work by Schauer et al., and similar to experiment by Nicholls et al.
- Valveless and reed valve.
- Capable of operation up to 40 Hz.
- Pressures exceeding ZND-peaks detected.
- No “clean” detonations.



Results from multi-cycle experiments indicate that it is a lot easier to initiate the detonation in multi-cycle than in single pulse mode.

Multi-cycle

- Can be initiated at $\Phi = 0.5$
- Need more than 10% extra O_2 to initiate (FOI).
- Can “almost” be initiated at $\Phi = 0.6$ (FOI).

Single pulse

Why?

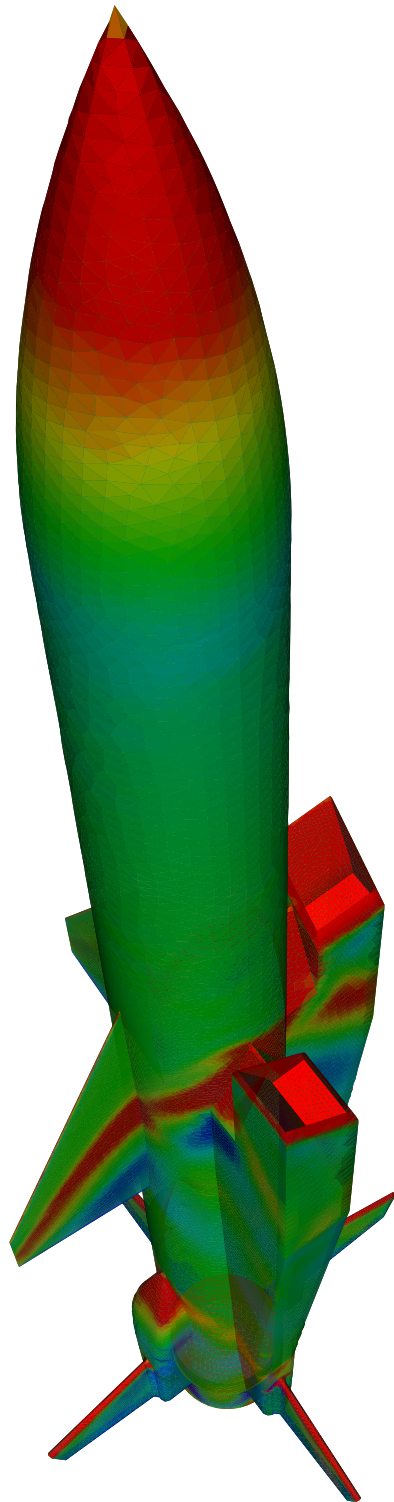
Dynamic effects? Heated tube? Small differences in geometry?

Ram Jet Robot Calculations

M. Tormalm

FoI

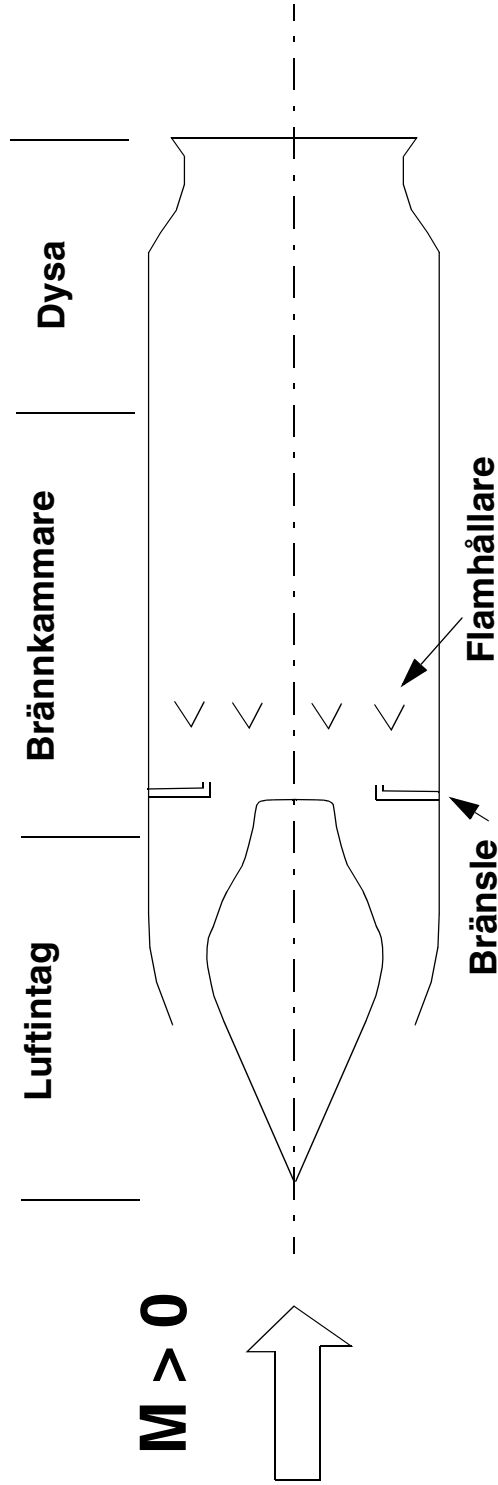
Ramjetrobotberäkningar vid FFA



Målsättning:

Att med hjälp av CFD beräkningar skapa ett aerodynamiskt simuleringsunderlag för en ramjetmotordriven robot.

Ramjet motorn



Fördelar:

Enkel konstruktion

Bra bränsleekonomi vid höga Machtal

Reglerbar

Nackdelar:

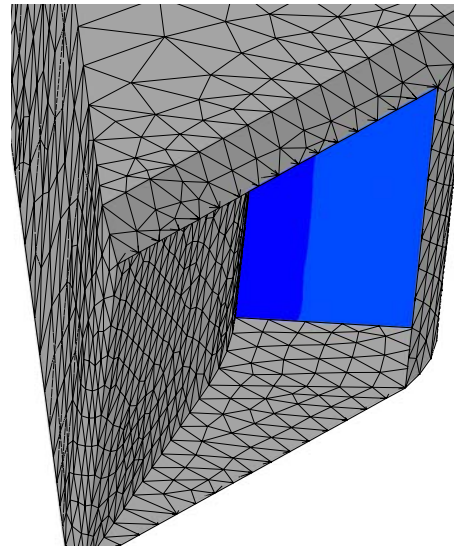
Kräver initial hastighet för att starta
Dålig bränsleekonomi vid låga Machtal

Implementation av VAC:s motormodell i EDGE

Två nya randvillkor

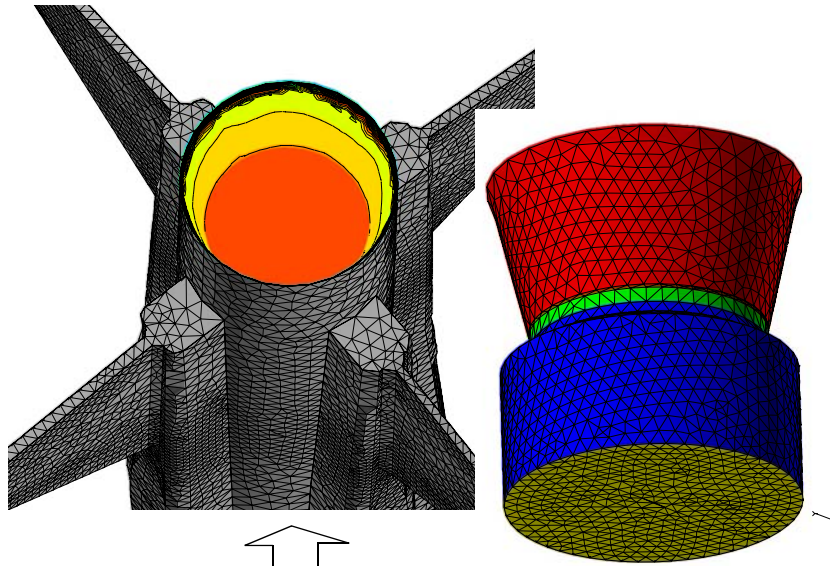
Intagsytan

(Massflöde, medeltryck och -temperatur)



VAC:s
ramjetmotor
modell 1D
CET89

utloppsytan
(Massflöde, tryck och -temperatur)



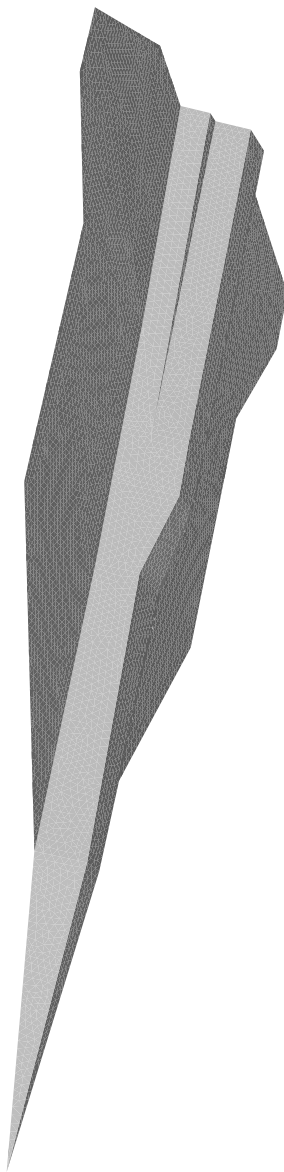
Status Ramjetrobotberäkningar

2001-10-30:

- VAC:s motormodul implementerad i EDGE
- Underlag framtaget för RB73_m2 och jämfört med vindtunneldata.
God överensstämmelse! Jämförelse med VAC:s simuleringsdata ej möjlig pga olika intagsareor.
- Separata luftintagsräkningar med bledd genomförda i Euler.
- Nya beräkningar med modifierat luftintag genomförda. Jämförelse med VAC:s simuleringsdata gav stora motståndsskillnader. Simuleringsdata ej möjlig med FFA:s underlag.
- Undersökning av skillnader pågår.

Tvärteknikprojektet

A multi-disciplinary project involving the design
of a stealthy supersonic strike missile



Johannes Johansson

FFA
AERONAUTICS DIVISION



Agenda

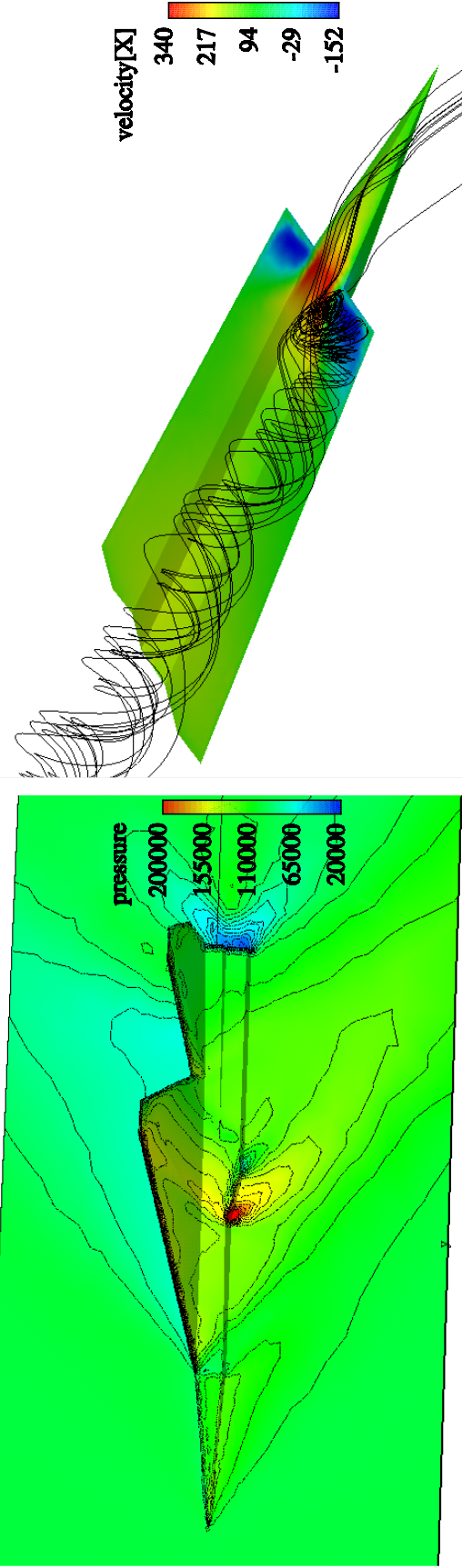
What is "Tvärteknikprojektet"?

Design requirements

Aerodynamic calculations

RCS calculations

Current and future work



Configuration U0, Mach 0.5



SWEDISH DEFENCE
RESEARCH AGENCY



What is "Tvärteknikprojektet"?

"Tvärteknikprojektet" is a multi-disciplinary project involving:

Computational aerodynamics

Experimental aerodynamics

Structures

Radar signature

IR signature

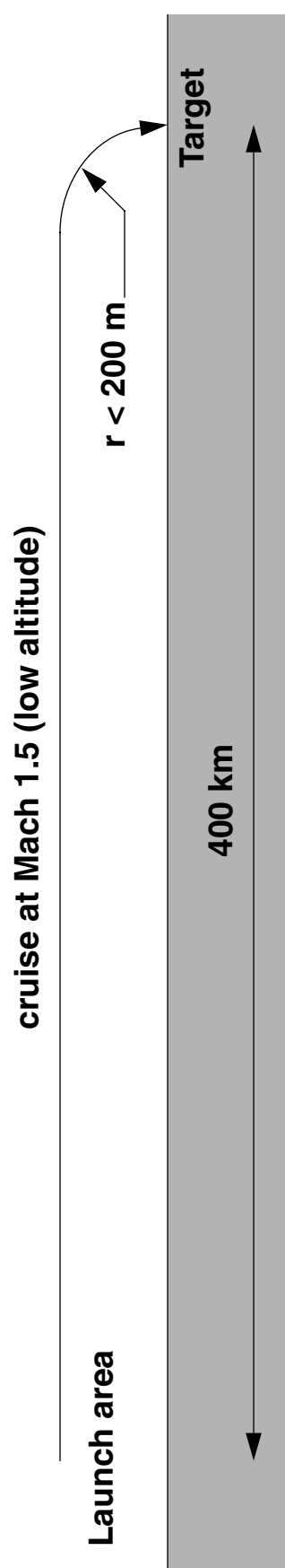
Flight simulations

Goal is to design a stealthy supersonic strike missile
capable of given design requirements



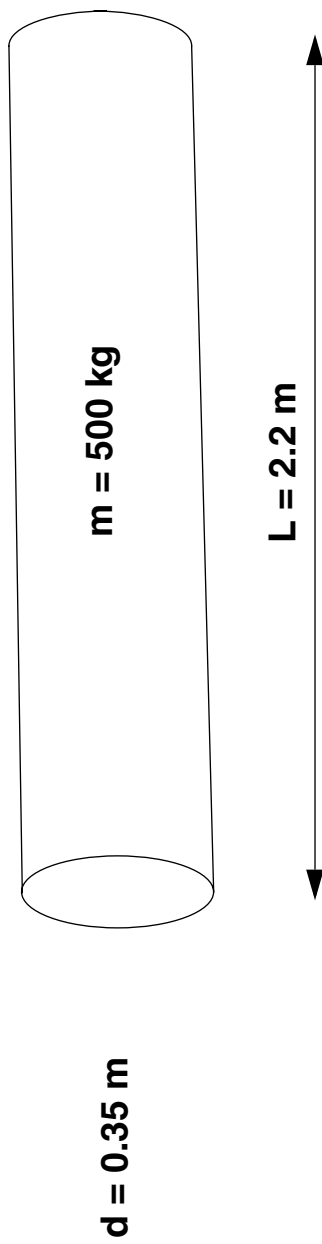
Design requirements

Mission profile



Design requirements

Payload



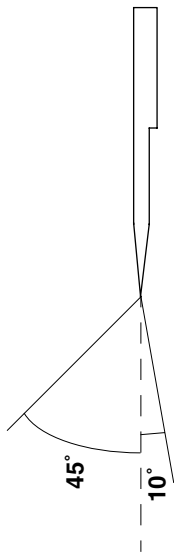
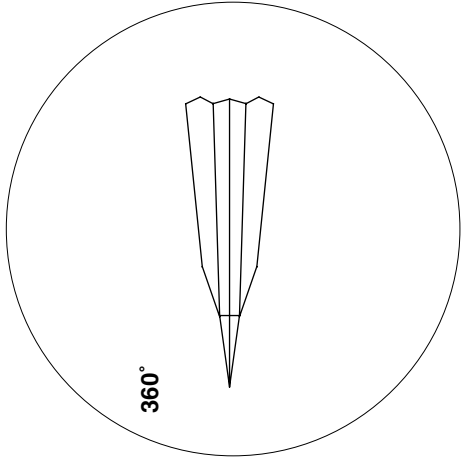
Warhead from KEPD 350

Design requirements

Signature

Radar:

Missile should have "low RCS" in given sector



IR:

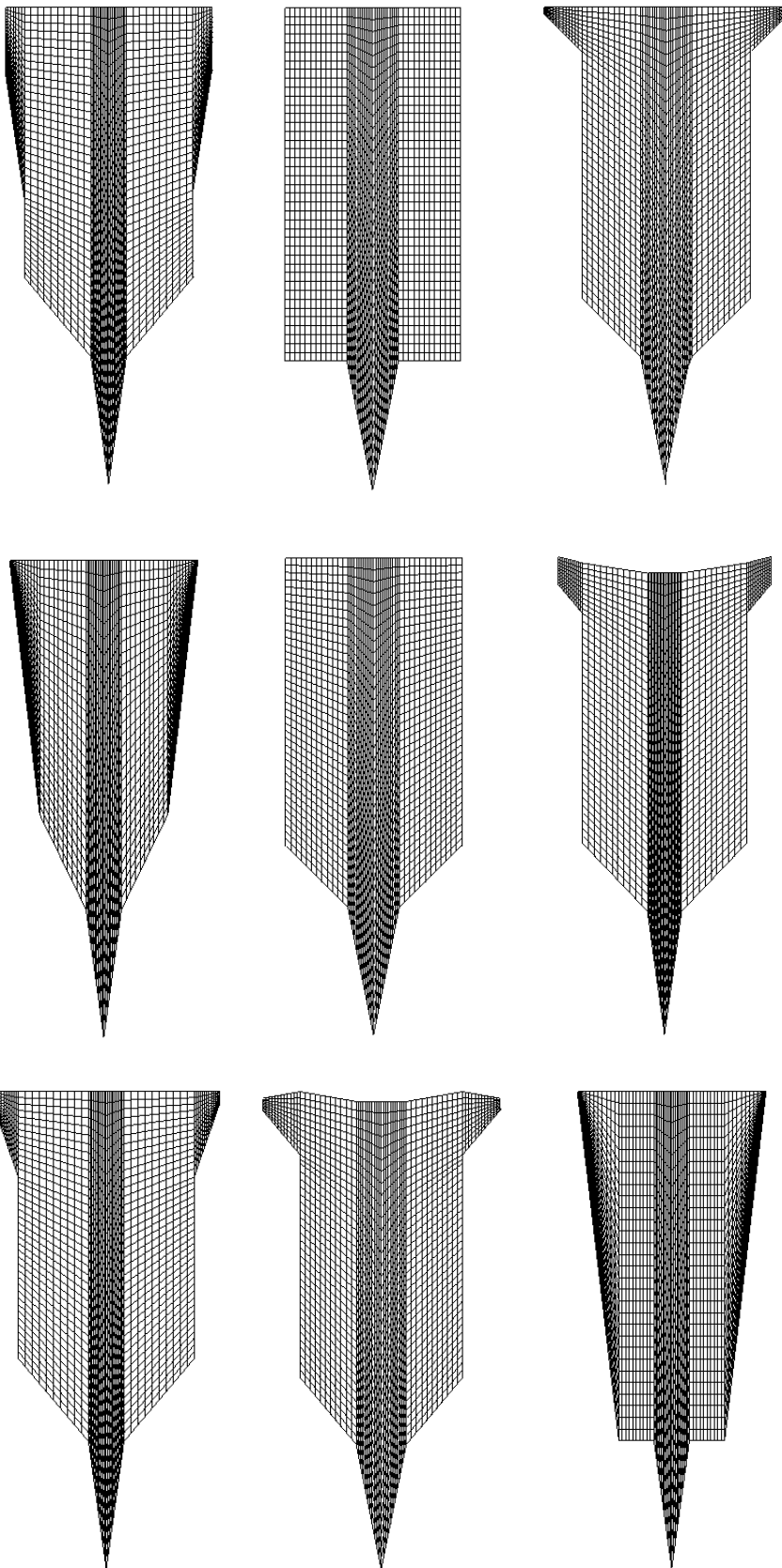
Missile should have "low IR signature"

Initial design

Wing planform design

Developing planform using Wingbody panel method program

Example shows some of the evaluated planforms.

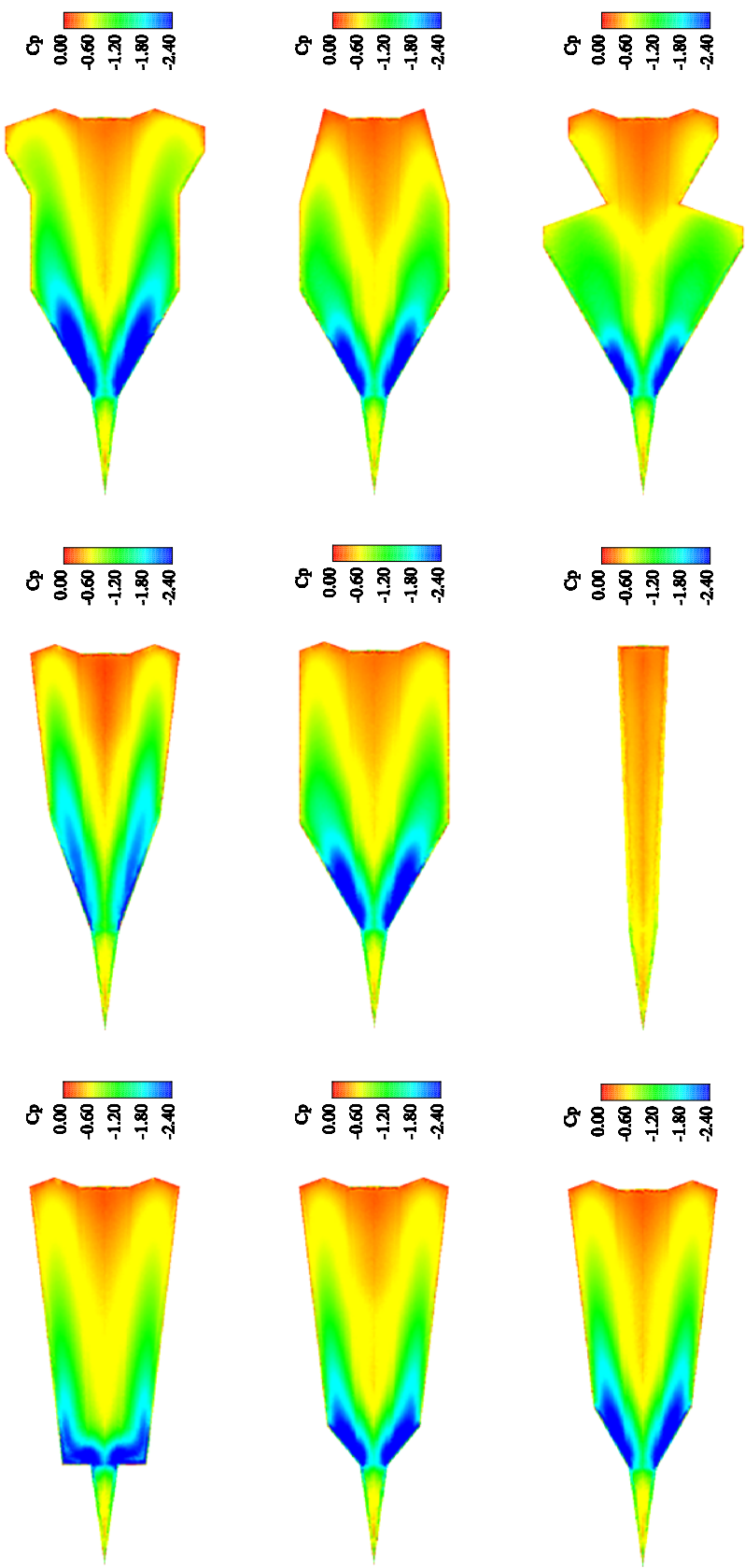


Aerodynamic calculations

CFD Euler calculations using Edge

Unstructured mesh (generated with Tritet)

Example shown: Pressure coefficient at Mach 0.5, 30° angle of attack



Aerodynamic calculations

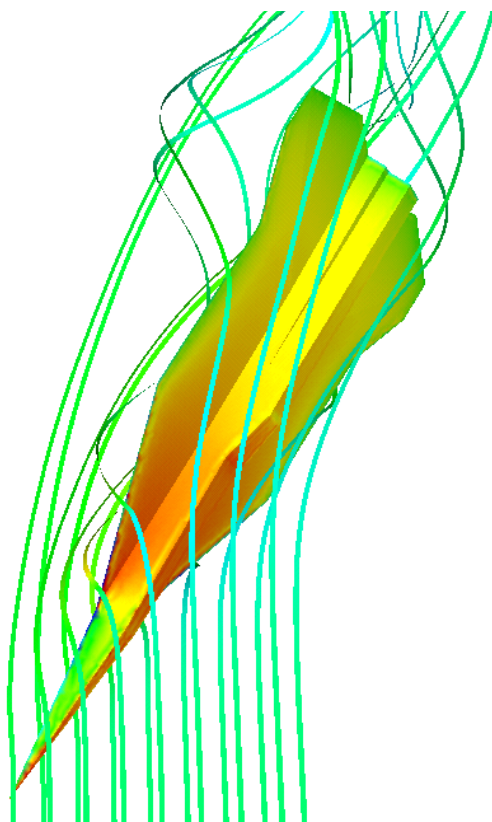
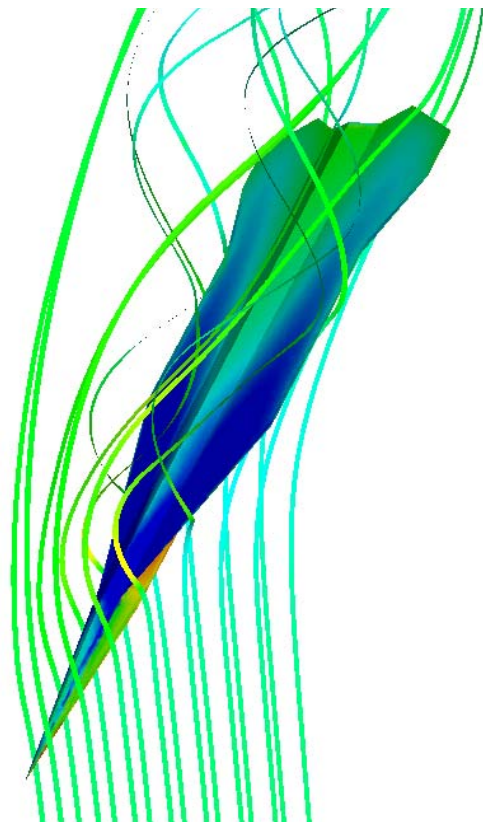
9 different configurations

2 main Mach numbers plus sweep

Angles of attack up to 50°

Sideslip at low and high angles of attack

About 200 different cases calculated



RCS calculations

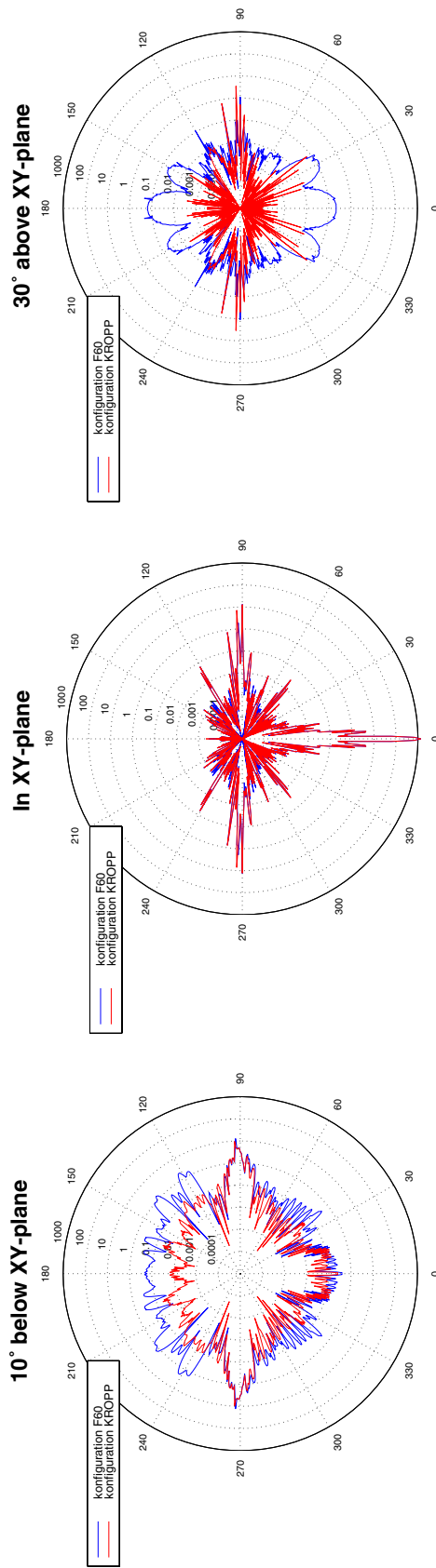
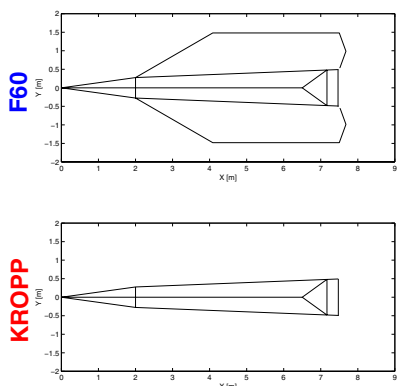
Calculations with FOPOL (using physical optics)

Uses same surface mesh as CFD calculations

Example shows RCS calculations with
and without wing.

10 GHz

Horizontal polarisation



Current and future work

Structures

Structural design of body and wings

Flutter and other aeroelastic effects

Wind-tunnel testing

Testing in S4 at FFA

14 different wing configurations

2 fin sizes

Deflection of elevators, ailerons and fin

Mach 1.52 (cruise), Mach 0.5 (final turn) and transition Mach numbers

Small angles of attack and sideslip at Mach 1.52

Large angles of attack and sideslip at Mach 0.5

Current and future work

Development process

- Analyse of wind-tunnel test**
- Evaluate stability and control characteristics**
- Refine wing design**
- Improve sizing of control surfaces**
- Simulate to prove concept**

Numerisk Analys på Institutionen för Beräkningsaerodynamik

Jan Nordström, Karl Forsberg, Gunilla Efraimsson

Högre ordningens finita differens metoder

- Euler, Navier-Stokes, Maxwell's . (NASA,UU)

Finita volyms metoder

- Stabilitet och nogrannhet. (UU)

Speciella problem

- Artificiell viskositet och randvillkor (KTH,UNM)

High Order Finite Difference Methods for the Euler, Navier-Stokes and Maxwell's Equations

Jan Nordström, Karl Forsberg, Mark H. Carpenter^a,
Ken Mattsson^b Magnus Svärd^c & Rikard Gustafsson^d

Journal of Computational Physics, Vol 148 No. 2 1999, pp. 341-365
Journal of Computational Physics, Vol 148 No. 2 1999, pp. 621-645
Journal of Computational Physics, Vol 173 2001, pp. 149-174
FOI-R-0120-SE, submitted

^aModelling and Simulation Methods Branch, NASA Langley Research Center

^bThe Department of Information Technology, Scientific Computing, Uppsala University

^cThe Department of Information Technology, Scientific Computing, Uppsala University

^dThe Department of Information Technology, Scientific Computing, Uppsala University

Ambition

- Develop new methods.
- Relate the mathematics and numerics.
- Proofs for all numerical techniques implemented.

1D, Basic theory, SBP (summation by parts) operators

Continuous case

$$(u, v_x) = \int_0^1 u v_x dx = (uv)_{x=1} - (uv)_{x=0} - (u_x, v)$$

Discrete case

$$(U, \mathcal{D}V)_P = U^T P \mathcal{D}V = U_N V_N - U_0 V_0 - (\mathcal{D}U, V)_P$$

$$\mathcal{D}U = P^{-1} Q U, \quad P = P^T, \quad Q + Q^T = D, \quad D = diag[-1, 0 \dots 0, 1]$$

Proof:

$$(U, \mathcal{D}V)_P = U^T Q V = U^T (-Q^T + D)V = -(P^{-1} Q U)^T P V + U^T D V$$

1D, Basic theory, Example

The SBP operator in the second order case.

$$\mathcal{D} = \frac{1}{2\Delta x} \begin{pmatrix} -2 & 2 & & & \\ -1 & 0 & 1 & & \\ & . & . & . & \\ & & . & . & . \\ & & & . & . \\ & & & & 1 \end{pmatrix}, \quad P = \Delta x \begin{pmatrix} \frac{1}{2} & & & & \\ & 1 & & & \\ & & . & & \\ & & & . & \\ & & & & 1 \end{pmatrix} \frac{1}{2}$$

1D, Basic theory, Example

The norm in the general case.

$$P = \begin{bmatrix} H_L & & & \\ & 0 & & \\ & & \ddots & \\ & & & 0 \\ & 1 & & \\ \end{bmatrix}$$

m:th order scheme $\rightarrow (H_L, H_R)$ are symmetrical $m \times m$ blocks

Penalty formulation for boundary conditions

The continuous problem

$$U_t + U_x = 0, \quad t \geq 0, \quad 0 \leq x \leq 1, \quad U(0, t) = g(t).$$

The energy-method yields:

$$\|U\|_t^2 = g(t)^2 - U(1, t)^2.$$

The semi-discrete approximation

$$\vec{U}_t + P^{-1} Q \vec{U} = \frac{P^{-1} [\sigma(U_0(t) - g(t))] \vec{e}_0}{}$$

The energy-method ($\sigma = -1$) yields:

$$\|\vec{U}\|_t^2 = g(t)^2 - U_N(t)^2 - \frac{(U_0(t) - g(t))^2}{}.$$

2D formulation

Continuous

$$u_t + F_x + G_y = 0$$

Semi-discrete

$$U_t + \underbrace{\left(P_x^{-1} Q_x \otimes I_y \right) F}_{D_x} + \underbrace{\left(I_x \otimes P_y^{-1} Q_y \right) G}_{D_y} = 0$$

Integration by parts

$$U^T P_x \otimes P_y U_t + U^T (Q_x \otimes P_y) F + U^T (P_x \otimes Q_y) G = 0$$

$$Q_x = -Q_x^T + B_x, \quad Q_y = -Q_y^T + B_y \Rightarrow$$

$$U^T P_x \otimes P_y U_t - (D_x U)^T P_x \otimes P_y F + U^T (B_x \otimes P_y) F + \dots = 0$$

Artificial Dissipation and Accuracy Downstream of
Slightly Viscous Shocks

Gunilla Efraimsson, Jan Nordström & Gunilla Kreiss ^a

SIAM Journal of Numerical Analysis, Vol 38 No. 6 2001, pp. 1986-1998
AIAA CFD Conference, paper No. 2001-2608, Anaheim Ca, June 2001

^aNADA, KTH

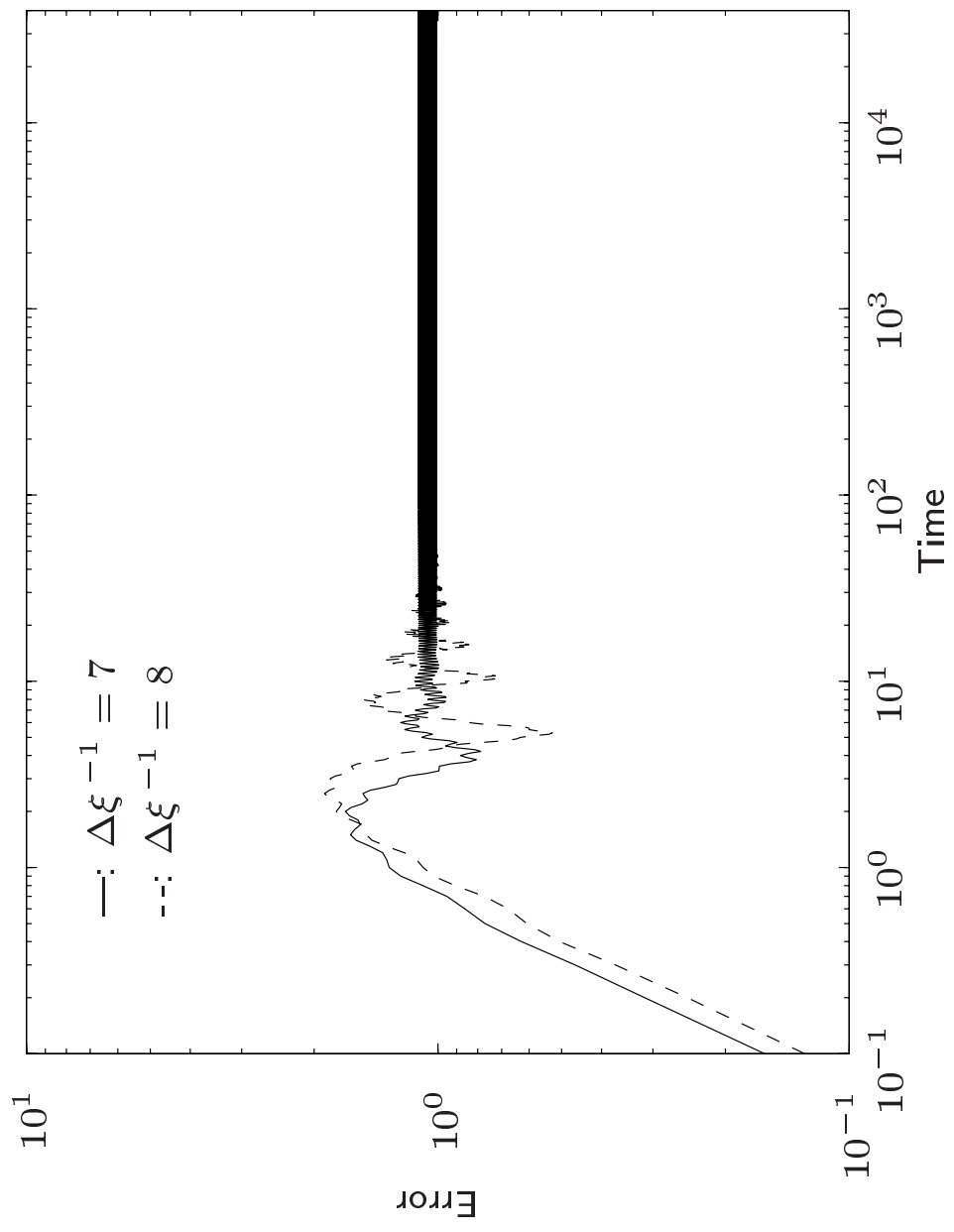


Figure 1: Error in the numerical solution, as a function of time. Cell centered strictly stable formulation, varying $\Delta\xi$.

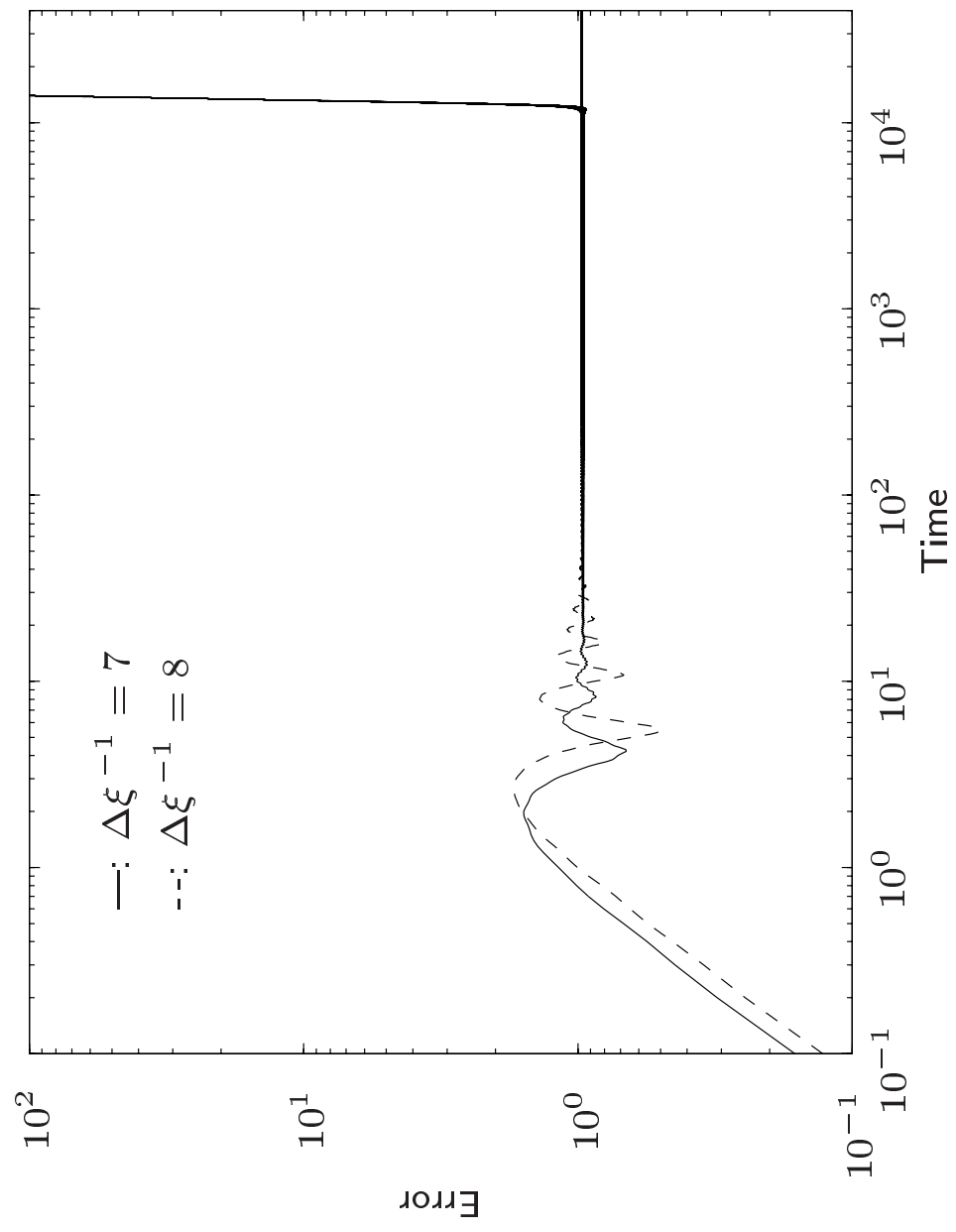


Figure 1: Error in the numerical solution, as a function of time. Cell centered *not strictly stable formulation*, varying $\Delta\xi$.

High Order Finite Difference Approximations of Electromagnetic Wave Propagation Close to Material Discontinuities

Rikard Gustafsson & Jan Nordström

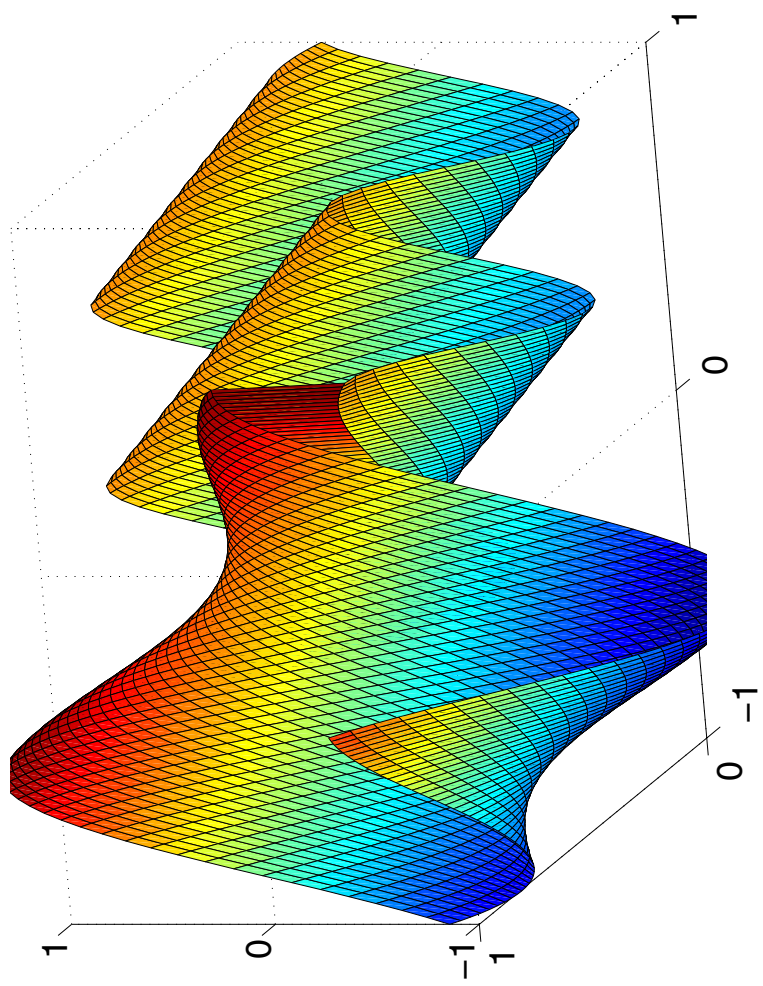
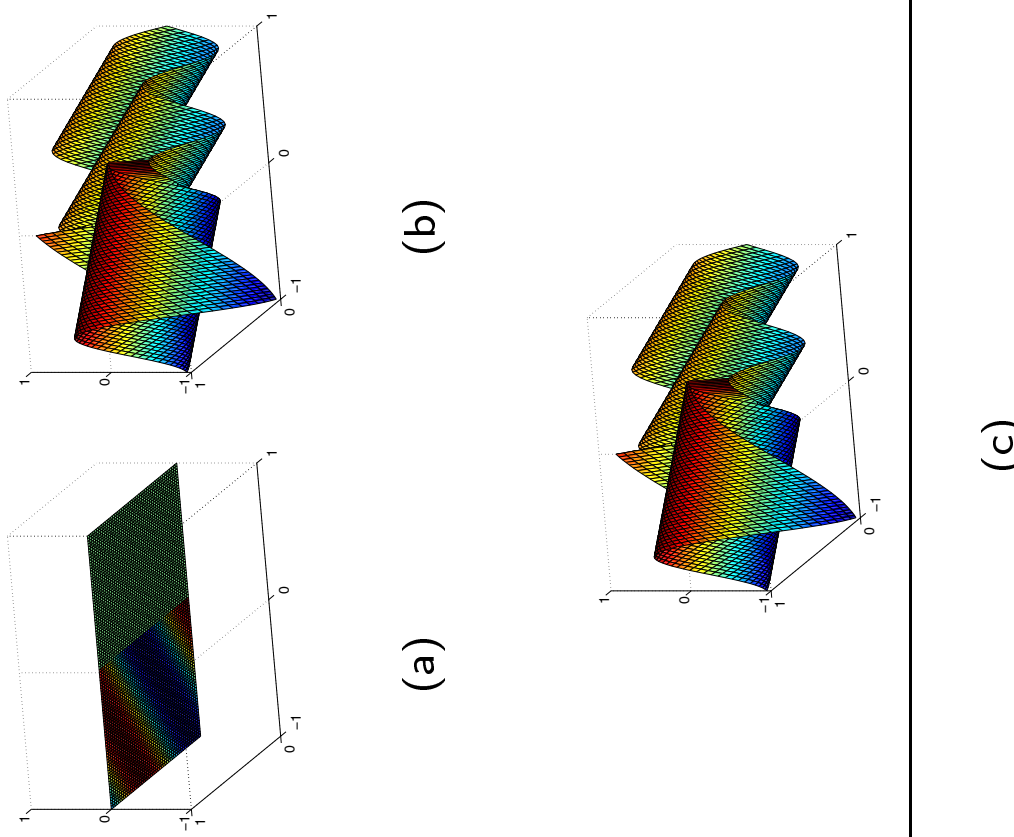


Figure 1: The wave in the domain, for $\Theta_i = \Theta_p$. (a) the wave propagating to the left, (b) the wave propagating to the right, (c) the total wave



Finite Volume Methods and Strict Stability

Jan Nordström, Karl Forsberg, Martin Björck^a, & Carl Adamsson^b

Applied Numerical Mathematics, Vol 38, 2001, pp. 237-255
FOI-R-0121-SE, submitted.

^aThe Department of Information Technology, Scientific Computing, Uppsala University

^bThe Department of Information Technology, Scientific Computing, Uppsala University

Ambition

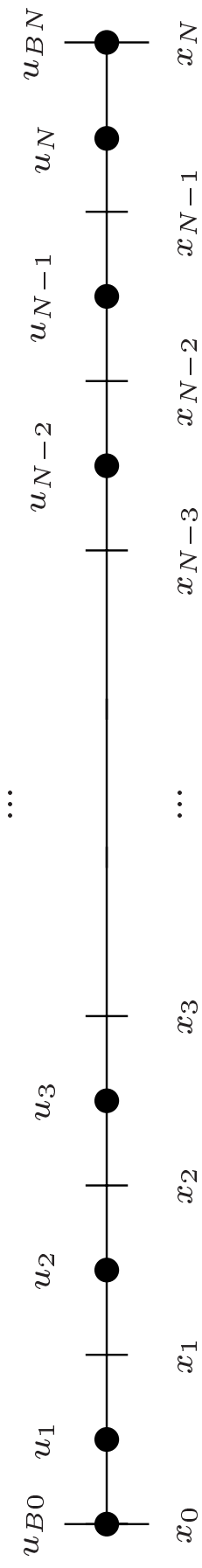
- Analyze the stability and accuracy of our “production codes”
- Suggest improvements.

Cell centered structured approximations (**EURANUS**)

Moving the dummy points to the boundaries yield the SBP formulation:

$$\vec{U}_t + P^{-1} Q \vec{U} = P^{-1} [\sigma(U_0(t) - g(t))] \vec{e}_0,$$

which lead to strict stability.



$$P = \Delta x \begin{pmatrix} r_0 & -r_0 + \frac{1}{4} & & \\ -r_0 + \frac{1}{4} & r_0 + \frac{1}{2} & & \\ & & \ddots & \\ & & & 1 \end{pmatrix},$$
$$\begin{pmatrix} r_N + \frac{1}{2} & -r_N + \frac{1}{4} & & \\ -r_N + \frac{1}{4} & r_N & & \\ & & \ddots & \\ & & & 1 \end{pmatrix},$$

$$Q = \begin{pmatrix} -1/2 & 1/2 & & \\ -1/2 & 0 & 1/2 & \\ & \ddots & \ddots & \ddots \\ & & -1/2 & 0 & 1/2 \\ & & & -1/2 & 1/2 \end{pmatrix}.$$

A 2D hyperbolic problem

Consider

$$v_t + v_x + v_y = 0, \quad 0 \leq x \leq 1, \quad 0 \leq y \leq 1, \quad t \geq 0,$$

with the boundary conditions $v(0, y, t) = g(y, t)$, $v(x, 0, t) = h(x, t)$.

The cell centered formulation becomes,

$$\vec{U}_t + (P_x^{-1}Q_x \otimes I_M)\vec{U} + (I_N \otimes P_y^{-1}Q_y)\vec{U} = BT,$$

where

$$BT = (P_x^{-1}E_{0N} \otimes \Sigma_{0y})(\vec{U} - e_{0N} \otimes \vec{g}) + (\Sigma_{0x} \otimes P_y^{-1}E_{0M})(\vec{U} - \vec{h} \otimes e_{0M}).$$

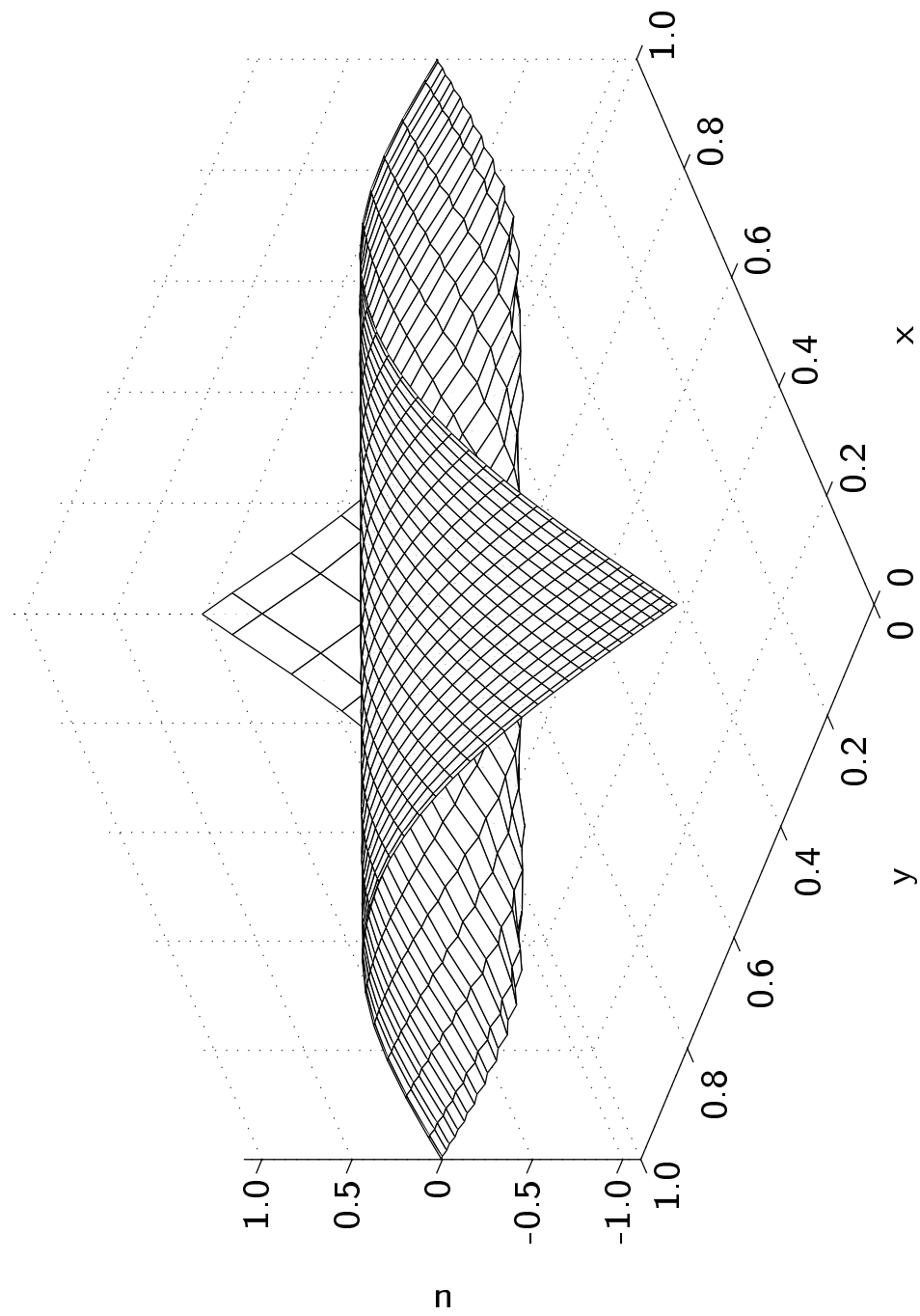


Figure 1: Numerical solution at $t = 1$. $\Delta\xi^{-1} = \Delta\eta^{-1} = 30$, an exponentially stretched grid (G3) is used. Cell centered formulation.

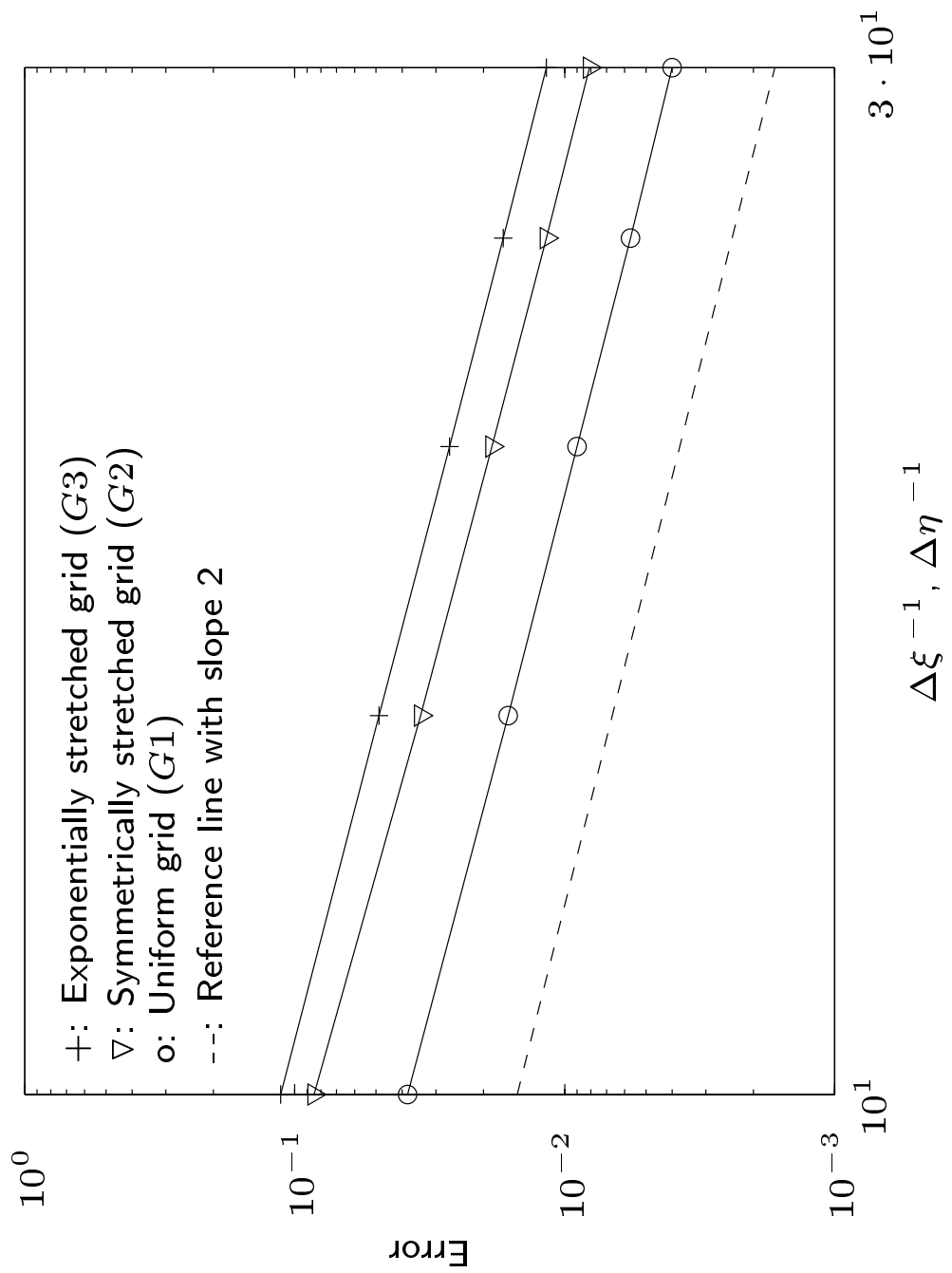


Figure 2: Errors at $t=1$ for varying $\Delta\xi$ and $\Delta\eta$, cell centered approximations.

1D systems of equations

Consider,

$$v_t + v_x = 0, \quad w_t - w_x = 0, \quad v(0, t) = w(0, t), \quad w(1, t) = v(0, t),$$

A strictly stable cell centered finite volume approximation can be written,

$$\vec{W}_t + (P^{-1}Q \otimes I_2)(\Lambda \vec{W}) = (P^{-1} \otimes I_2)S\vec{W},$$

where $\vec{W}_i = (v_i, w_i)^T$ and $\Lambda = I_N \otimes diag(1, -1)$.

The discrete energy rate becomes

$$\frac{d}{dt}(\|v\|_P^2 + \|w\|_P^2) = R$$

where $R = -(v_0 - w_0)^2 - (v_N - w_N)^2$ for $\sigma_L = -1, \sigma_R = 1$.

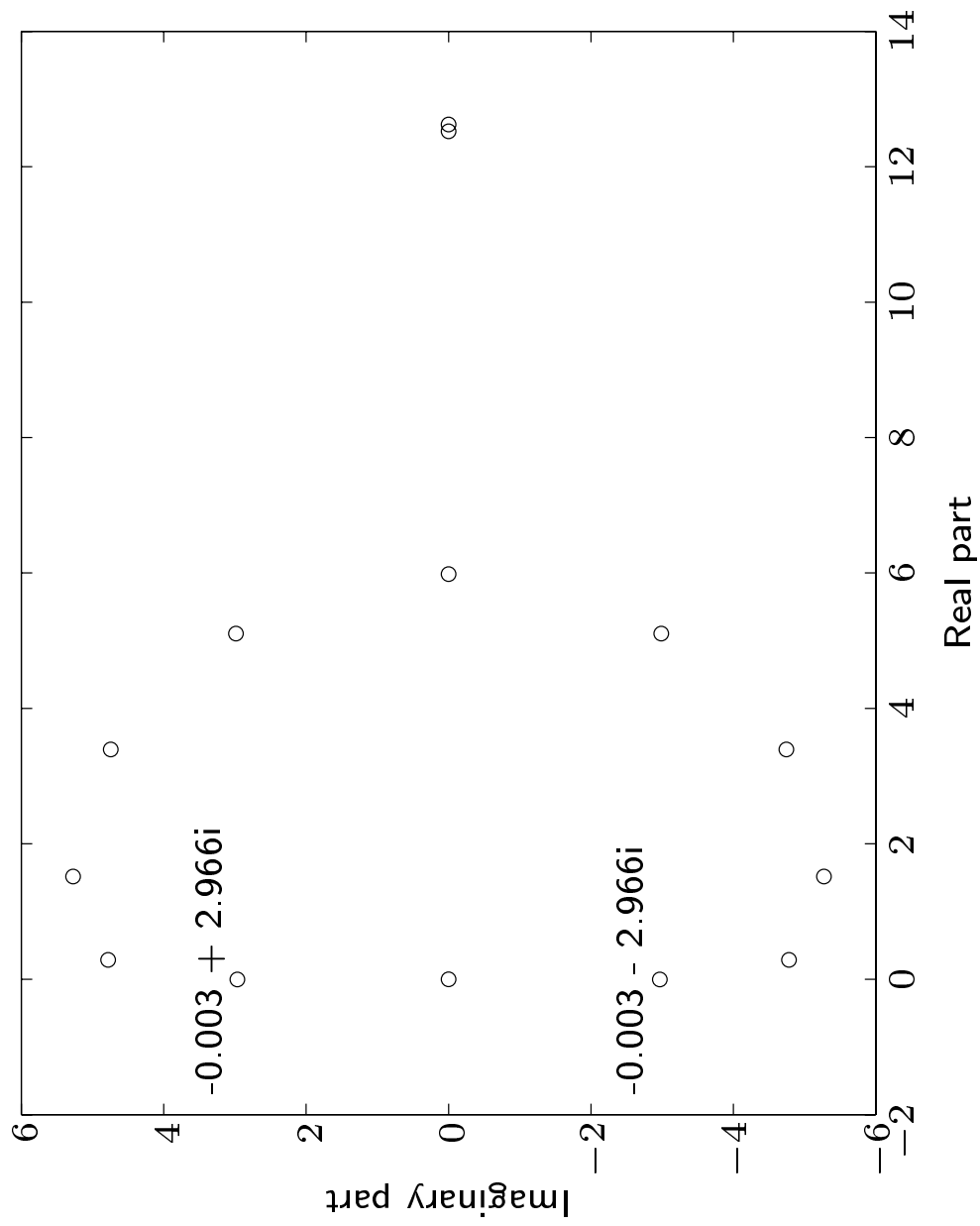


Figure 3: Spectrum of the *usual cell centered difference matrix* for the system problem. *Not strictly stable formulation*, $\Delta \zeta^{-1} = 7$.

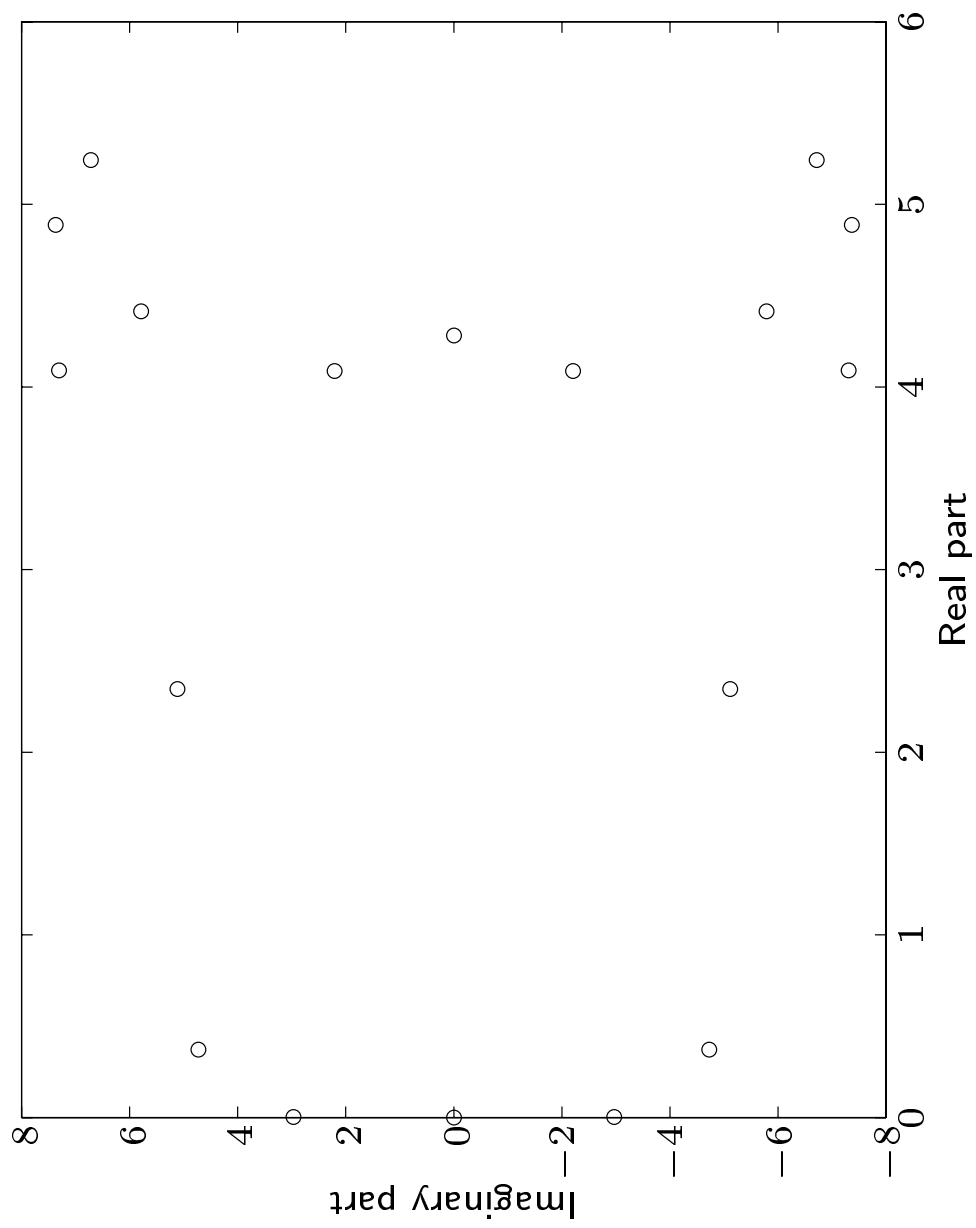


Figure 4: Spectrum of the \mathcal{D} matrix for the system problem. Cell centered strictly stable formulation, $\Delta\xi^{-1} = 7$.

Node centered unstructured approximations (EDGE)

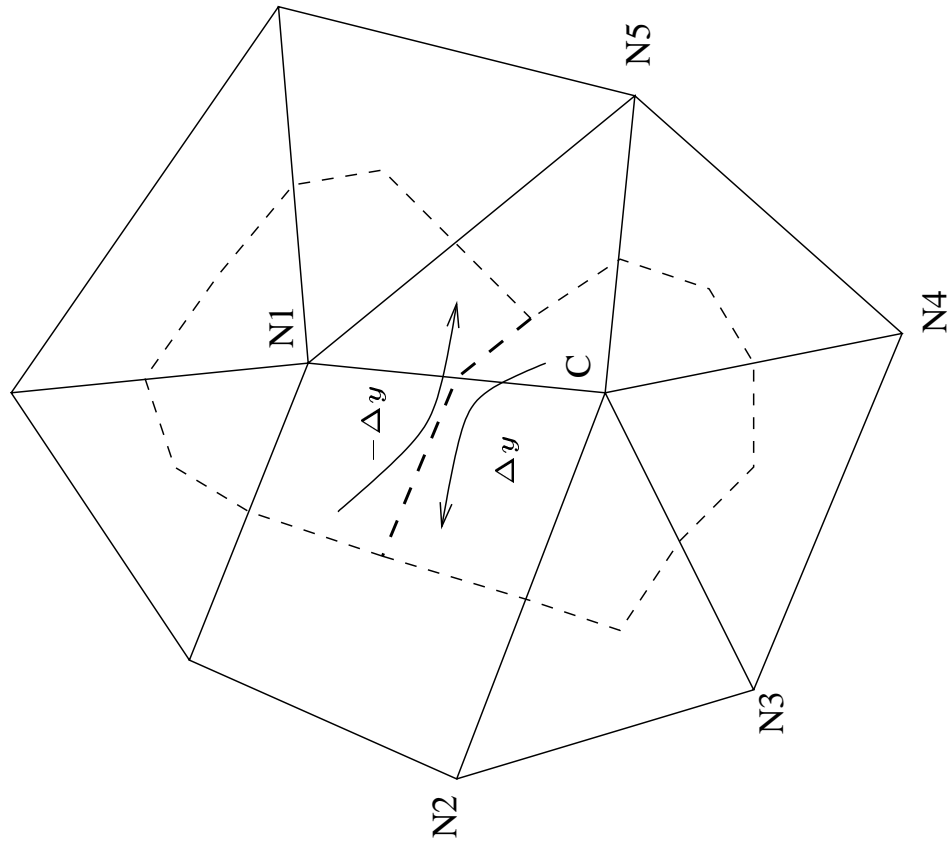


Figure 1: Part of the grid (solid line) and the dual grid (dashed line).

Integration of $u_t + u_x = 0$ over a control volume, Ω_C , leads to

$$\iint_{\Omega_C} u_t dxdy + \iint_{\Omega_C} u_x dxdy = \iint_{\Omega_C} u_t dxdy + \oint_{\partial\Omega_C} u dy = 0.$$

The semi discrete approximation can be written

$$Pu_t + Q_x u = 0.$$

- P is a matrix with the control volumes on the diagonal.
- Q_x approximates the line integral of u around the control volume.

No boundaries

$$\text{flux} = \sum_i \frac{u_C + u_{N^i}}{2} \Delta y_i = \sum_i u_C \frac{\Delta y_i}{2} + \sum_i u_{N^i} \frac{\Delta y_i}{2},$$

where the sum goes over all neighbours to the point C . Not considering the boundary of the domain, this leads to

$$Q_{CC} = \sum_i \frac{\Delta y_i}{2} = 0, \quad Q_{CN^i} = \frac{\Delta y_i}{2} = -Q_{N^i C}$$

i.e the matrix Q is skew symmetric in the interior.

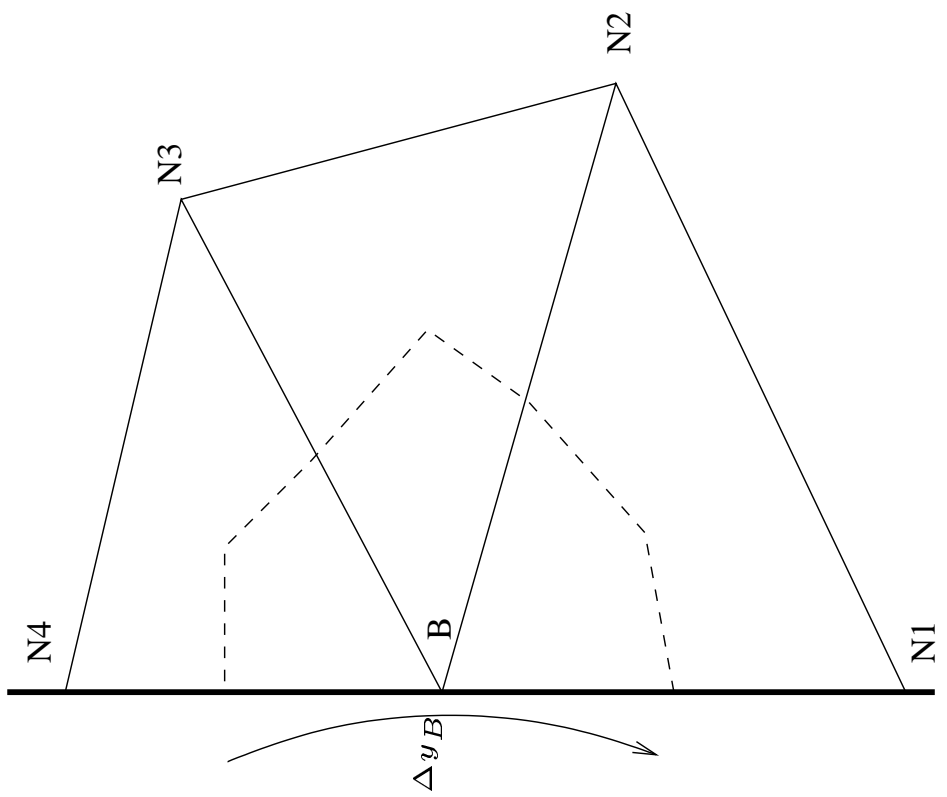


Figure 2: The geometry at the boundary.

Boundaries without boundary conditions

The flux through the boundary edge is calculated as the node value at the boundary node, u_B , times the corresponding Δy_B , i.e.

$$\text{flux} = \sum_i \frac{u_B + u_{N_i}}{2} \Delta y_i + u_B \Delta y_B = u_B \Delta y_B + \sum_i u_B \frac{\Delta y_i}{2} + \sum_i \frac{u_{N_i}}{2} \Delta y_i.$$

Note that sums are not over a closed loop. From the figures we obtain

$$\sum_i \Delta y_i = -\Delta y_B$$

Thus we have

$$\text{flux} = \sum_i u_{N_i} \frac{\Delta y_i}{2} + u_B \frac{\Delta y_B}{2},$$

which leads to

$$Q_{BB} = \frac{\Delta y_B}{2}, \quad Q_{BN_i} = \frac{\Delta y_i}{2} = -Q_{N_i B}.$$

Boundaries with boundary conditions

Let us now consider the case with b.c, $u = g$ at the boundary. We impose the b.c weakly. The fluxes, become:

$$\text{flux} = \sum_i \frac{u_B + u_{N_i}}{2} \Delta y_i + g_B \Delta y_B = \sum_i u_{N_i} \frac{\Delta y_i}{2} + u_B \frac{\Delta y_B}{2} + b,$$

where

$$b = (g_B - u_B) \Delta y_B \quad \text{at the boundary with b.c,} \quad b = 0 \quad \text{otherwise.}$$

Finally we obtain,

$$P\mathbf{u}_t + Q\mathbf{u} + b = 0,$$

which is a penalty formulation.

Numerical Examples

The diagonalized form of Maxwell's equations in 1D with PEC boundary conditions reads

$$\begin{pmatrix} \mu \\ \nu \end{pmatrix}_t + \begin{pmatrix} 1 & 0 \\ 0 & -1 \end{pmatrix} \begin{pmatrix} \mu \\ \nu \end{pmatrix}_x = 0, \quad (x, y) \in \Omega \subset \mathbb{R}^2, \quad (\mu - \nu)|_{\partial\Omega} = 0.$$

The discrete approximation is

$$\begin{pmatrix} P & 0 \\ 0 & P \end{pmatrix} \begin{pmatrix} \mu \\ \nu \end{pmatrix}_t + \begin{pmatrix} Q & 0 \\ 0 & -Q \end{pmatrix} \begin{pmatrix} \mu \\ \nu \end{pmatrix}_x + b = 0,$$

where

$$b = (\sigma_1, \sigma_2)^T (\nu_i - \mu_i) \Delta y_i.$$

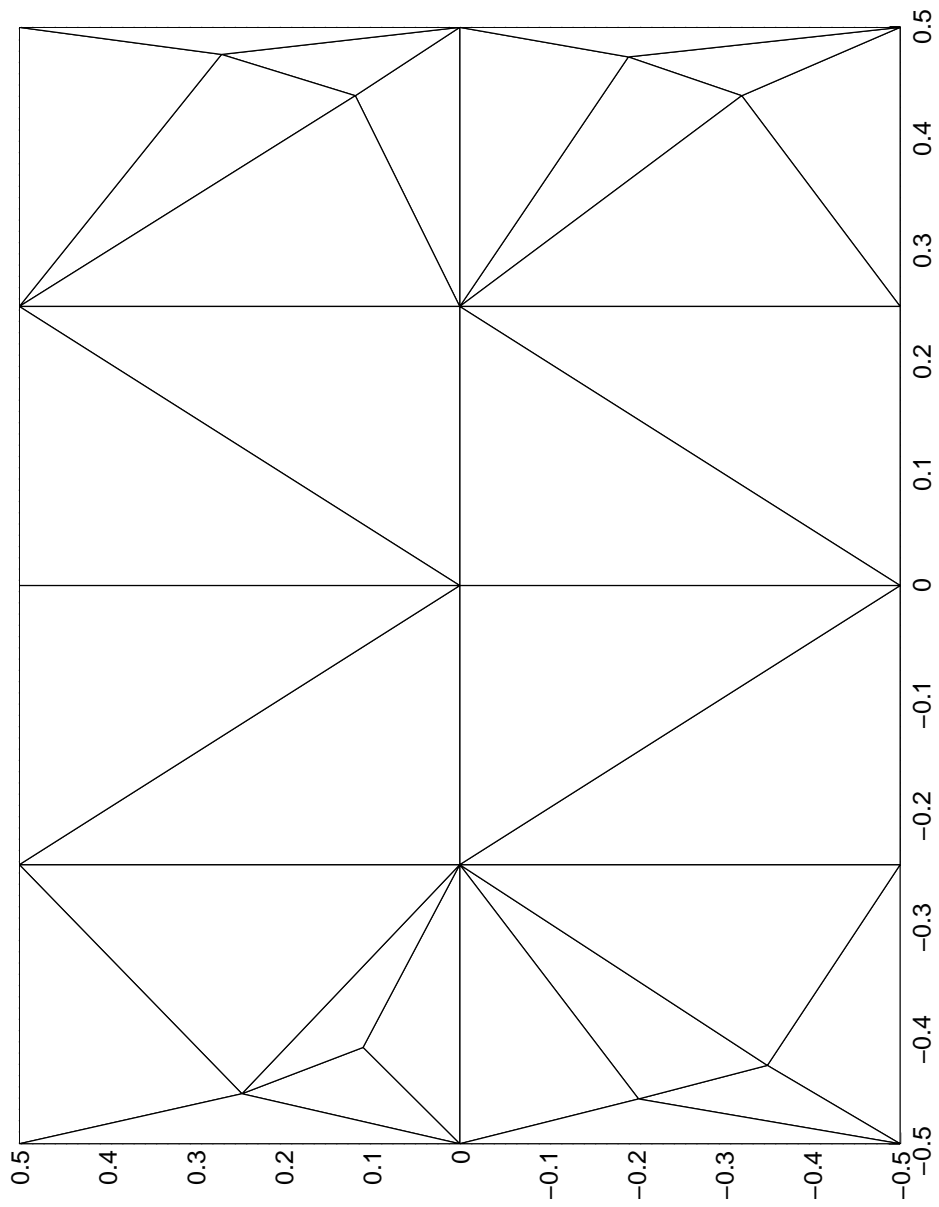


Figure 3: A highly irregular mesh with 23 nodes.

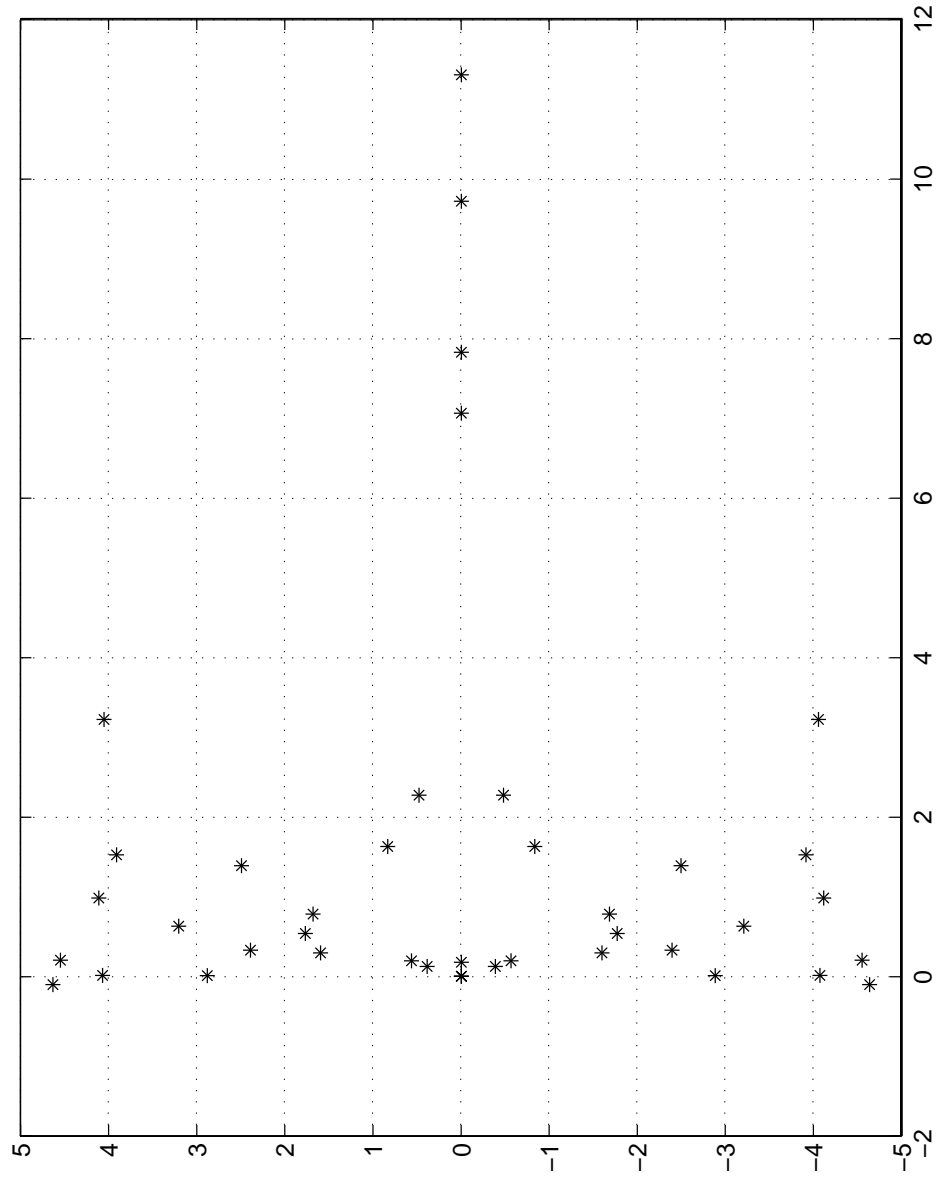


Figure 4: The spectrum for injection on a mesh with 23 nodes. $\min(\text{Re}(\lambda_i)) = -0.105$

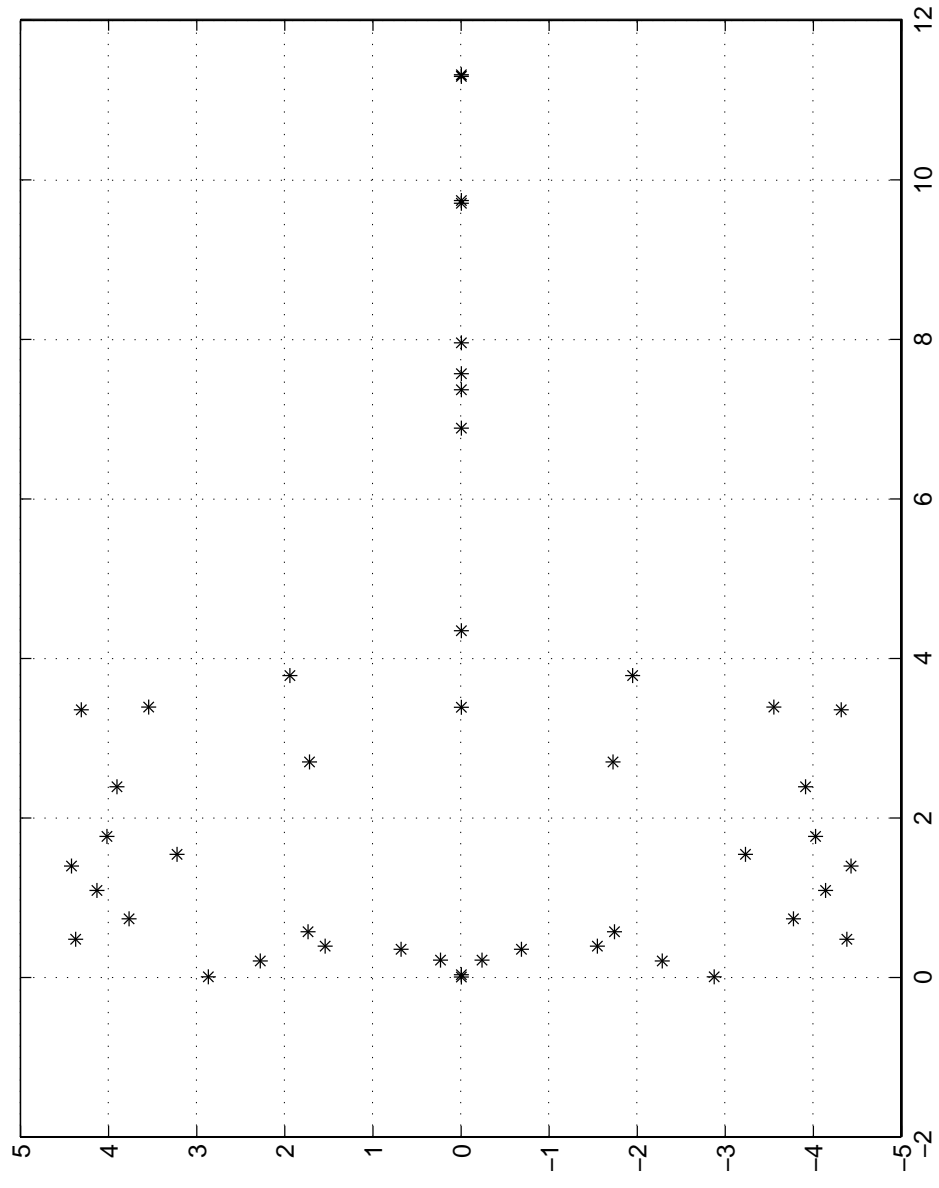


Figure 5: The spectrum of a strictly stable method on a mesh with 23 nodes. $\min(\operatorname{Re}(\lambda_i))=0$

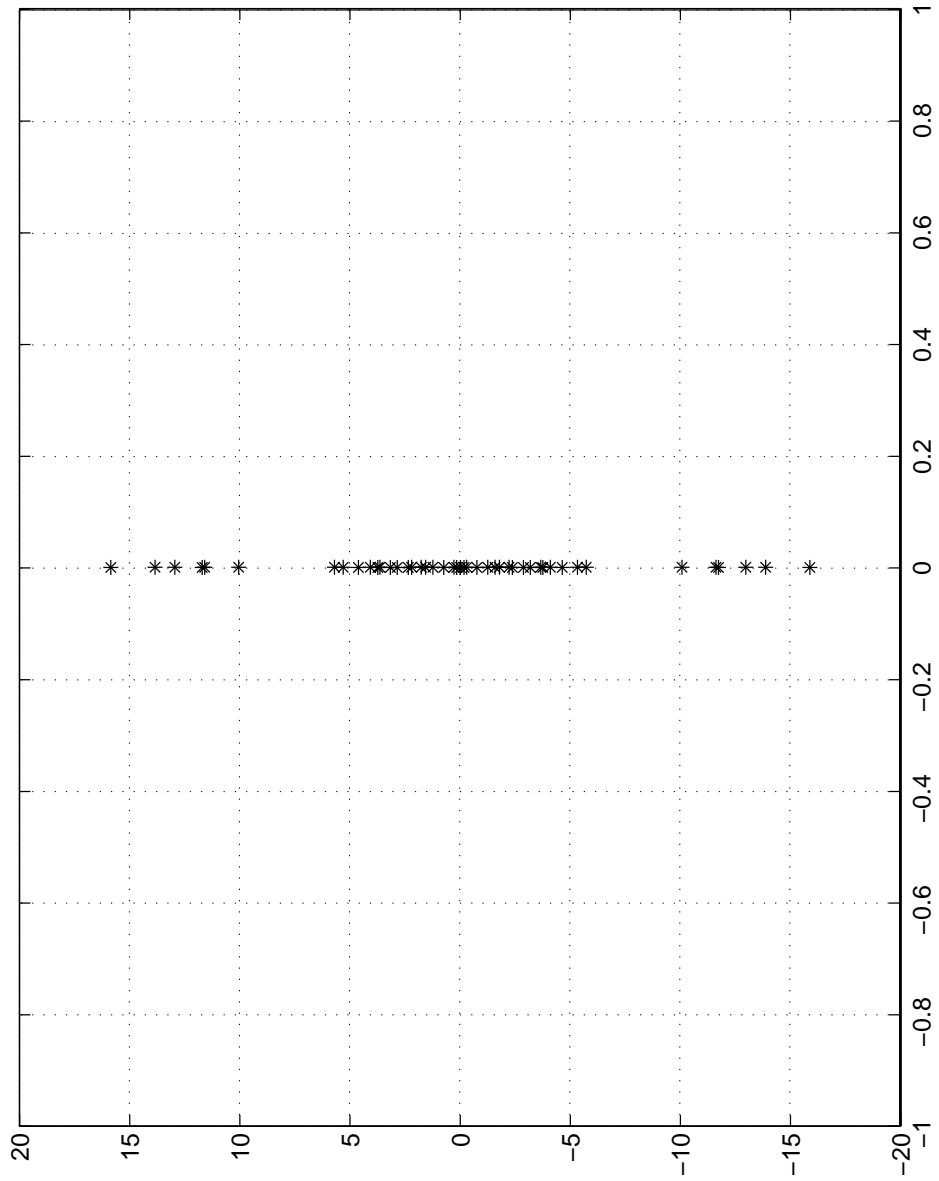


Figure 6: The spectrum of a strictly stable method on a mesh with 23 nodes. $\min(\operatorname{Re}(\lambda_i))=0$

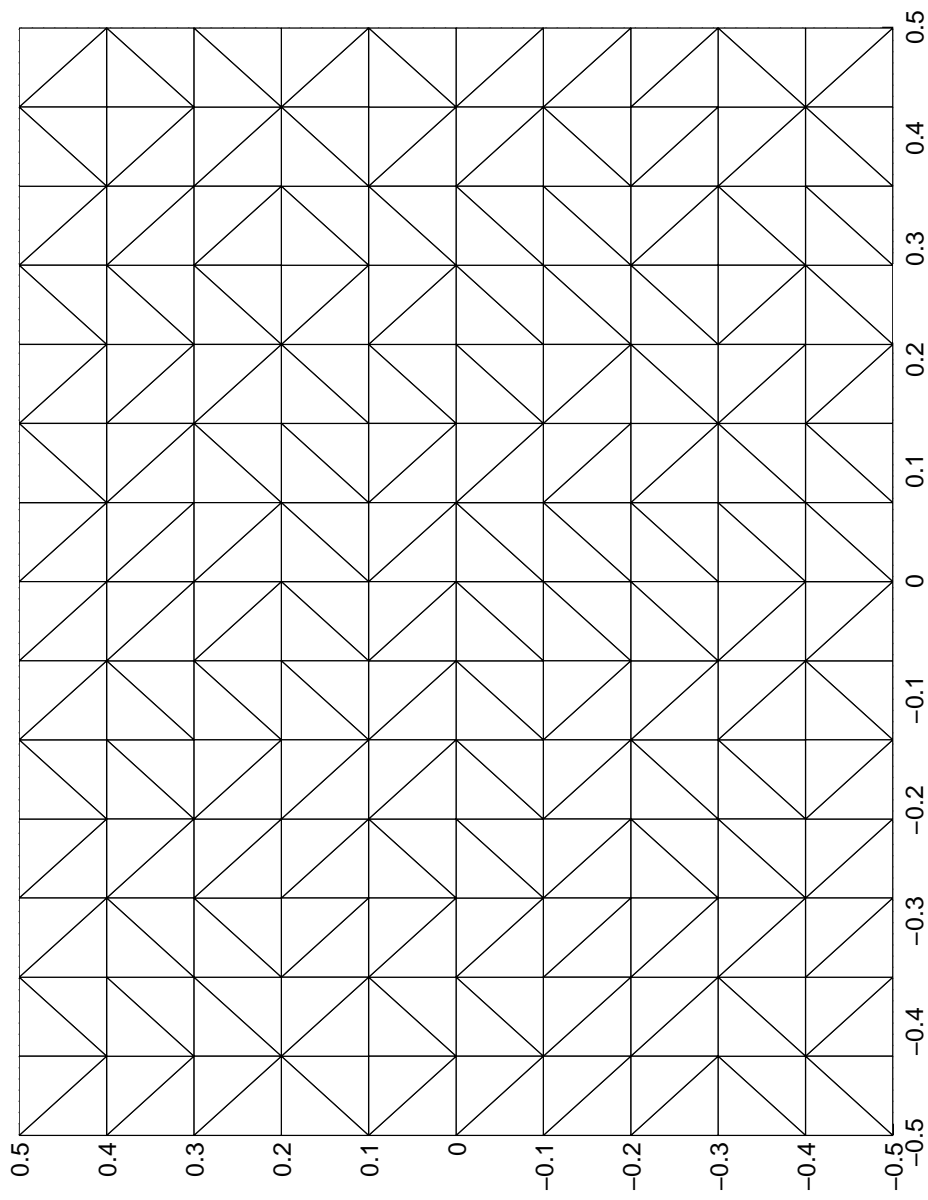


Figure 7: A mesh with almost equally sized volumes.

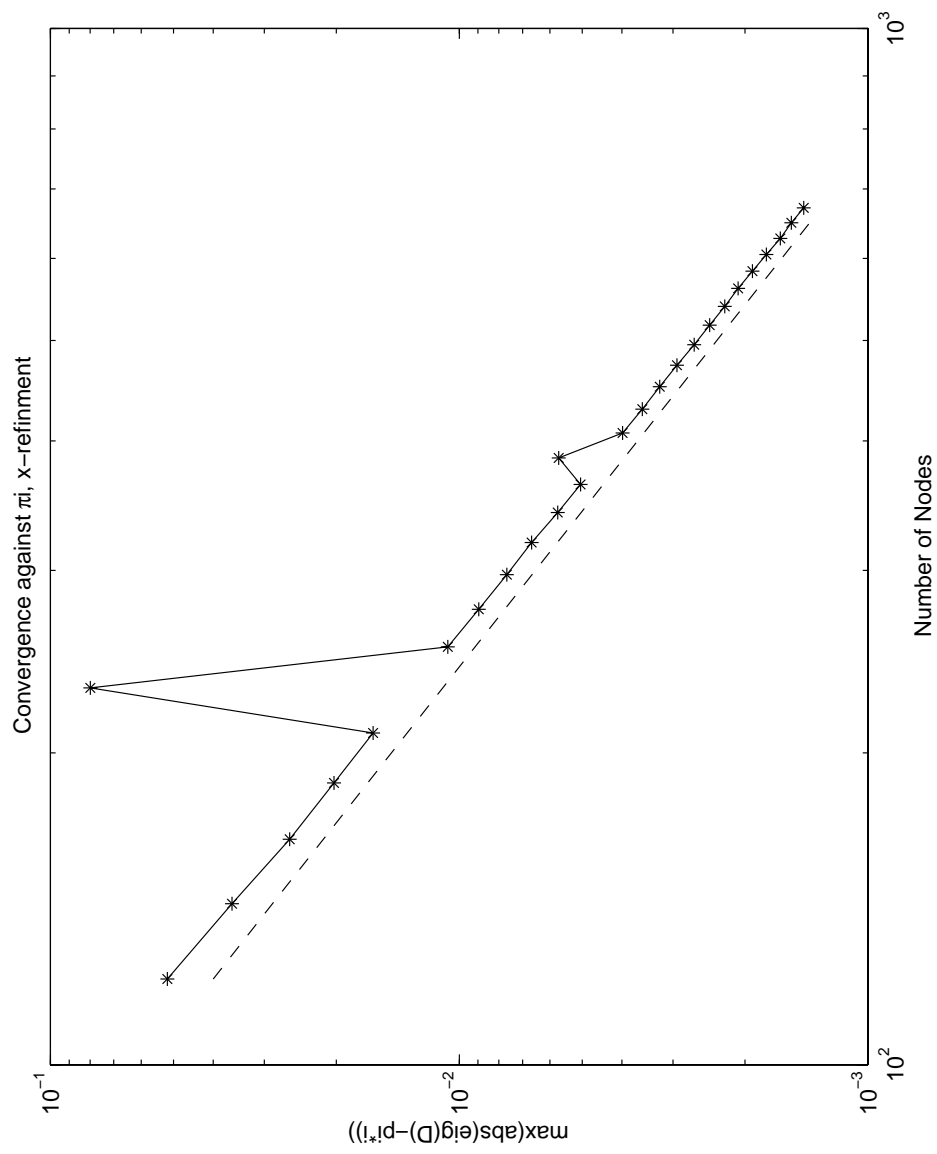


Figure 8: Convergence against the point π_i . New nodes are introduced in the x-direction. The dashed line is a reference line with slope -2.

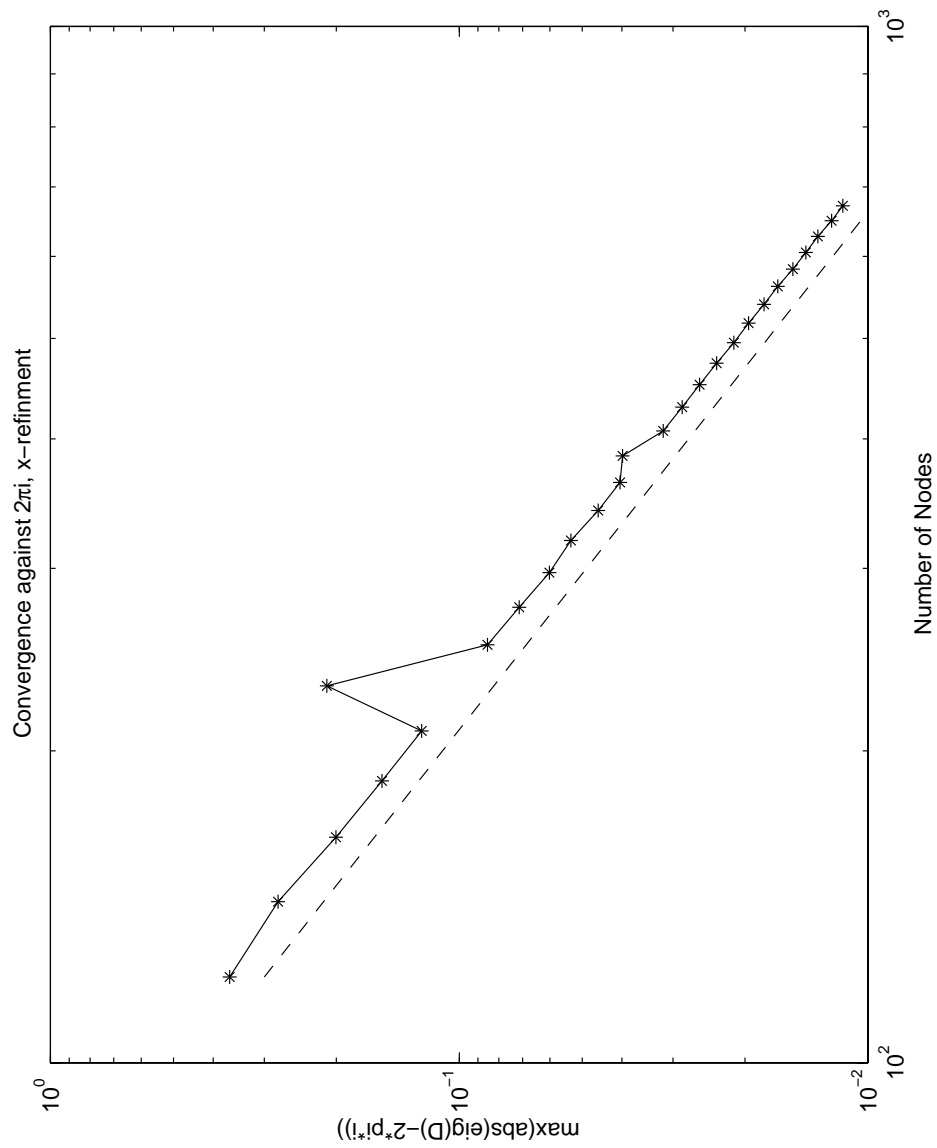


Figure 9: Convergence against the point $2\pi i$. New nodes are introduced in the x-direction.

The dashed line is a reference line with slope -2.

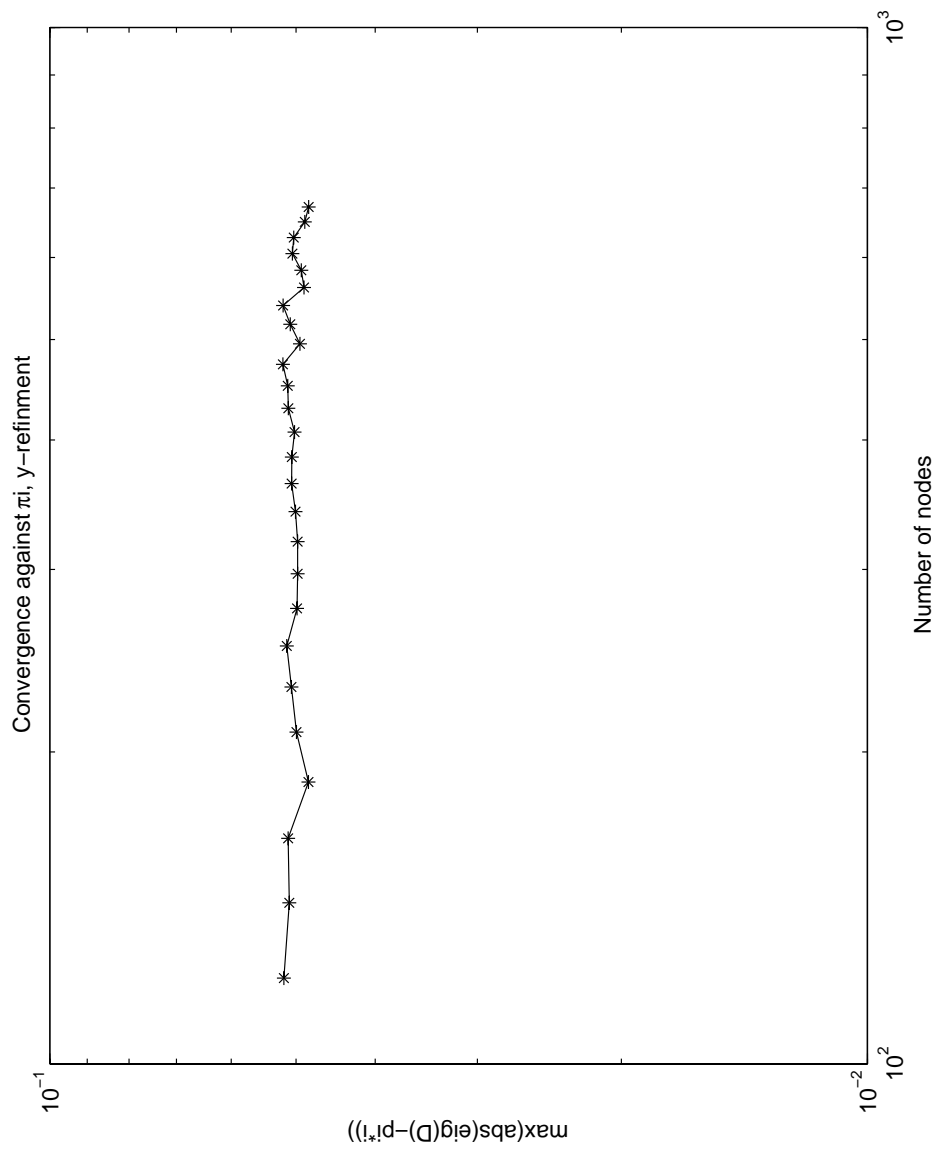


Figure 10: Convergence against the point π_i . New nodes are introduced in the y-direction.

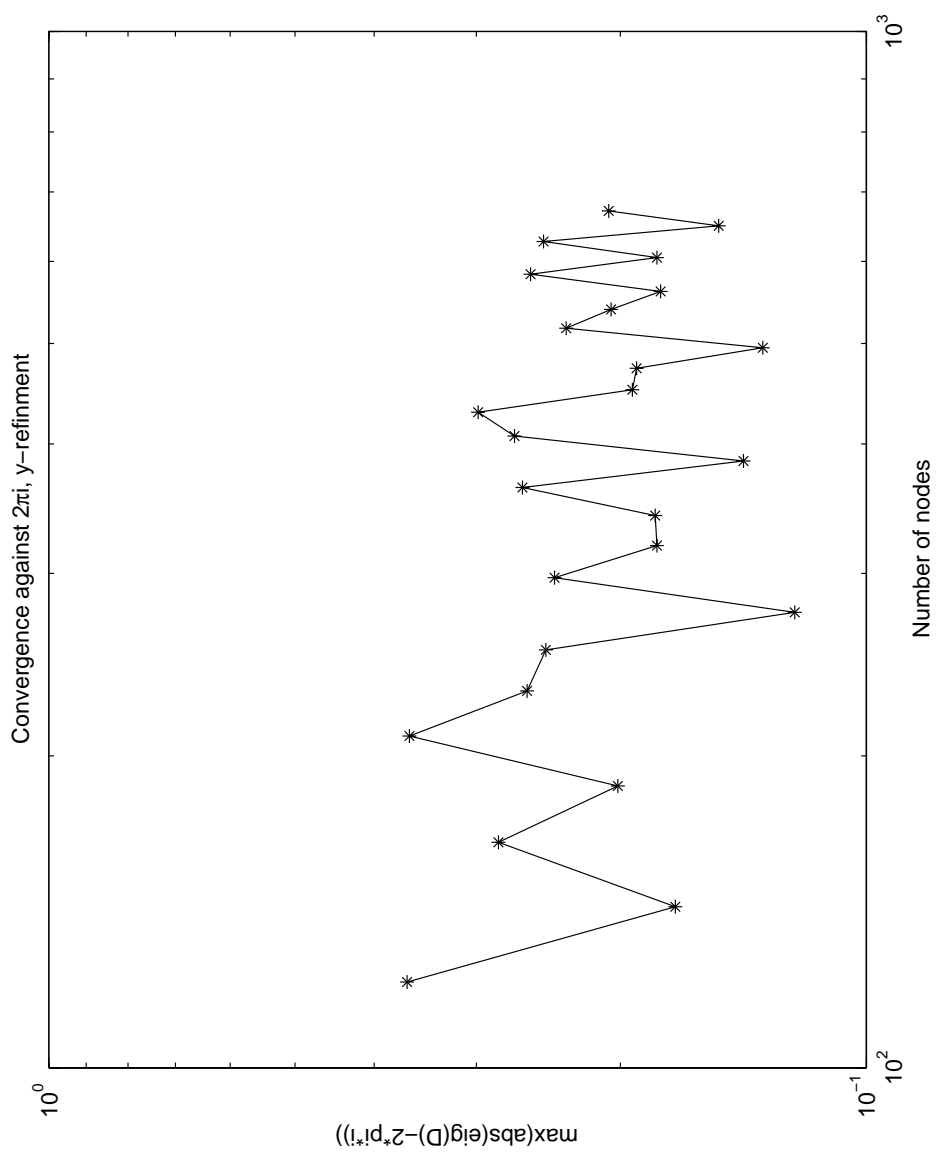


Figure 11: Convergence against the point $2\pi i$. New nodes are introduced in the y-direction.

G. Efraimsson

Aeroacoustics

AKUSTIK

Nuvarande och tidigare verksamhet

- Ljudutbredning kring propeller
- Ljudgenerering i turbo fläkt-motor
- Högre ordningens noggranna metoder

Framtida intresseområden

- Ihopkoppling av lägre ordningens metoder med högre ordningens metoder.
- Ljud genererat av turbulens i ett kompressibelt medium.

Ljudutbredning kring propeller

- Icke-linjär inviskös lösning närmast propellern. Kirchhoffmetod för akustiska signalen i fjärrfältet.

Meijer S., Lindblad I, *Prediction of Noise Variations with Helical Tip Mach Number for the SR3 Propeller*, CEAS/AIAA-95-167

- Icke-linjär inviskös lösning i hela fältet.

Eliasson P., Wang D., Meijer S., Nordström J., *Unsteady Euler Computations through Non-matching and Sliding-Zone Interfaces*, AIAA-98-0371

Ljudgenerering i turbo fläkt-motor

EU-projekt TurboNoiseCFD

- Reducera buller från rotor/stator interaktion med befintliga CFD-metoder.
- Viskösa beräkningar med Euranus.
- Industri, forskningsinstitut och universitet från 6 länder (16 partners).
- 3 år, 16 manmånader (1.7 Mkr)

Ihopkoppling av lägre och högre ordningens metoder

- Ide': Använd robust andra ordningens noggrann lösare i ljudgenereringsområdet. Använd en högre ordningens noggrann metod i propageringsområdet.
- Svårighet: Att få ihopkopplingen både noggrann och stabil.

Ljud genererat av turbulens

DNS eller LES beräkning i det turbulentta området. Högre ordningens metoder i fjärrfältet.

Exempel:

- Ljud genererat av en turbulent jet
- Ljud genererat av t. ex. ett gränsskikt på en yta eller en del av en flygplanskropp.

The interaction between a lightning flash and an aircraft in flight

Anders Larsson

FOI – Swedish Defence Research Agency
Grindsjön Research Centre
Weapons and Protection Division
Warheads and Propulsion



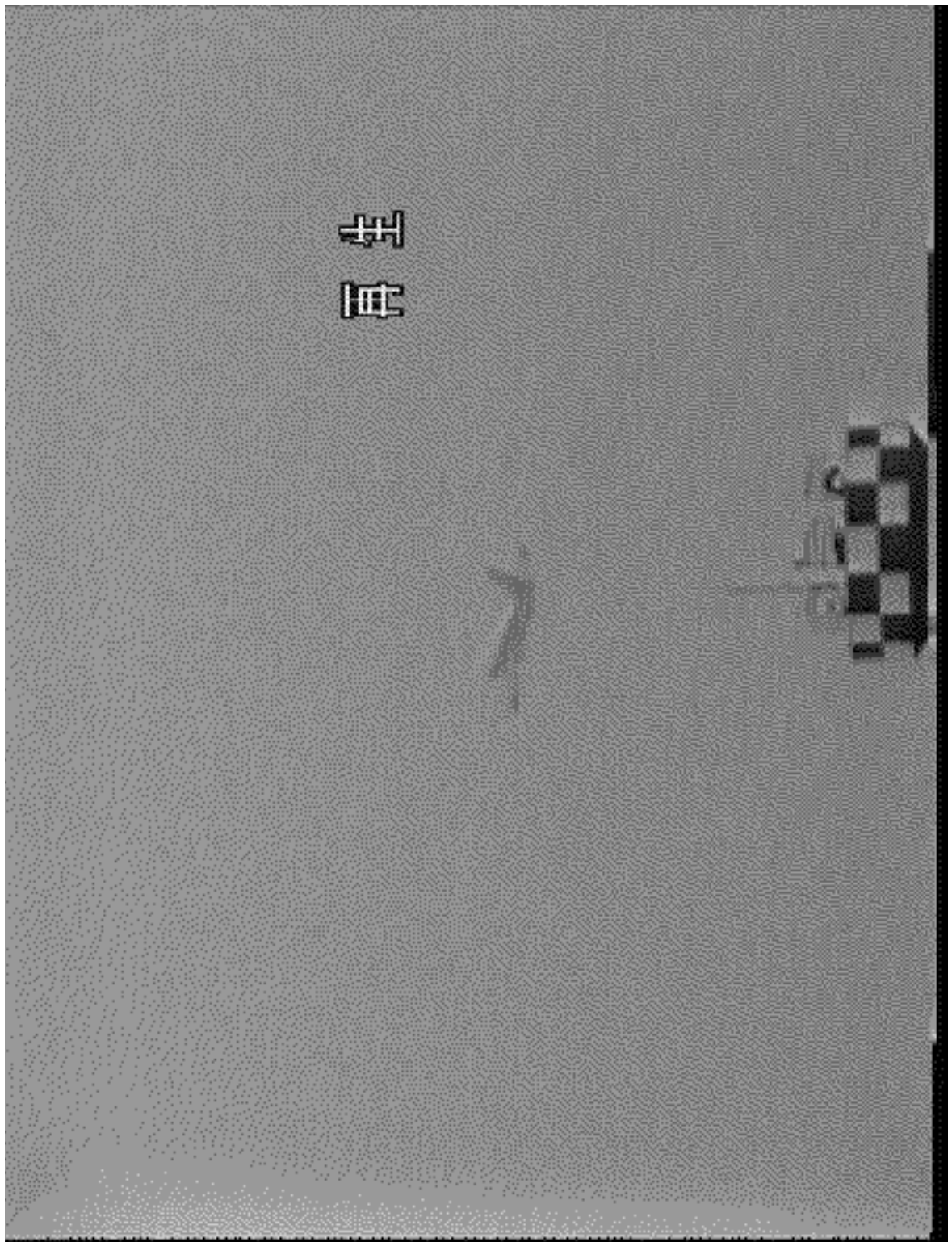
Methods and Technologies for Aircraft Safety and Protection against Electromagnetic Hazards (EM-Haz)

EU-project within Key Action "New Perspectives in Aeronautics"

P	Saab Avionics (S)	DaimlerChrysler Aerospace Dornier (D)
a	AEA Technology (UK)	Eurocopter Deutschland (D)
r	Aerospatiale-Airbus (F)	Eurocopter France (F)
t	British Aerospace (UK)	ONERA (F)
n	CEAT (F)	Aerospatiale CCR (F)
e		
r		
s		



FOI, subcontractor to ONERA

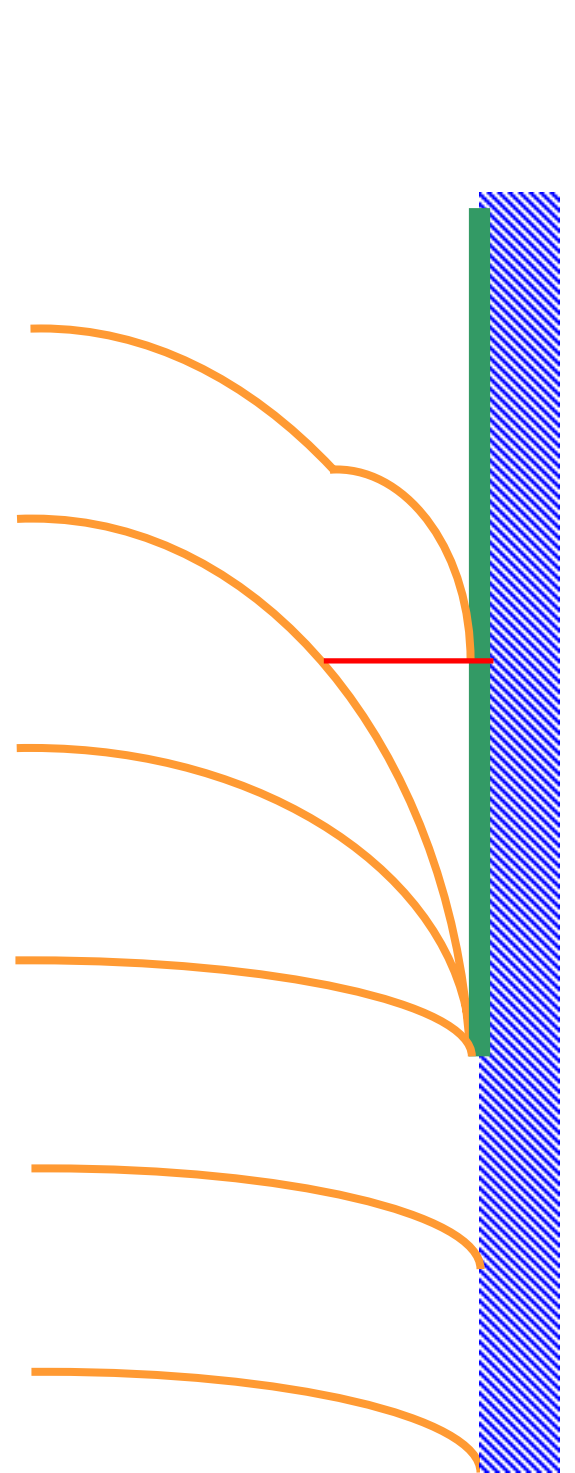


By courtesy of Prof. Zen Kawasaki, Osaka, Japan

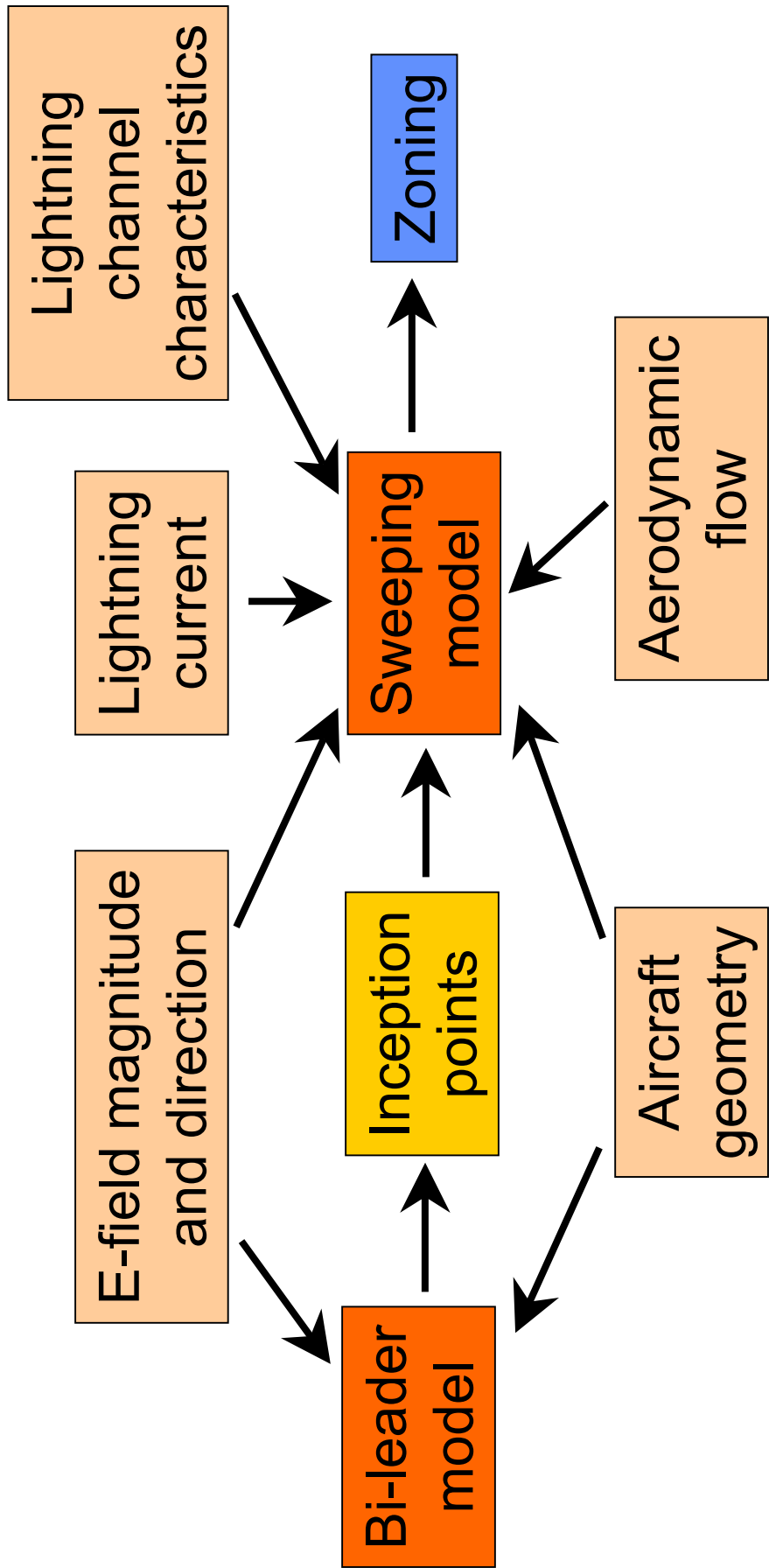


Illustration of swept stroke phenomena

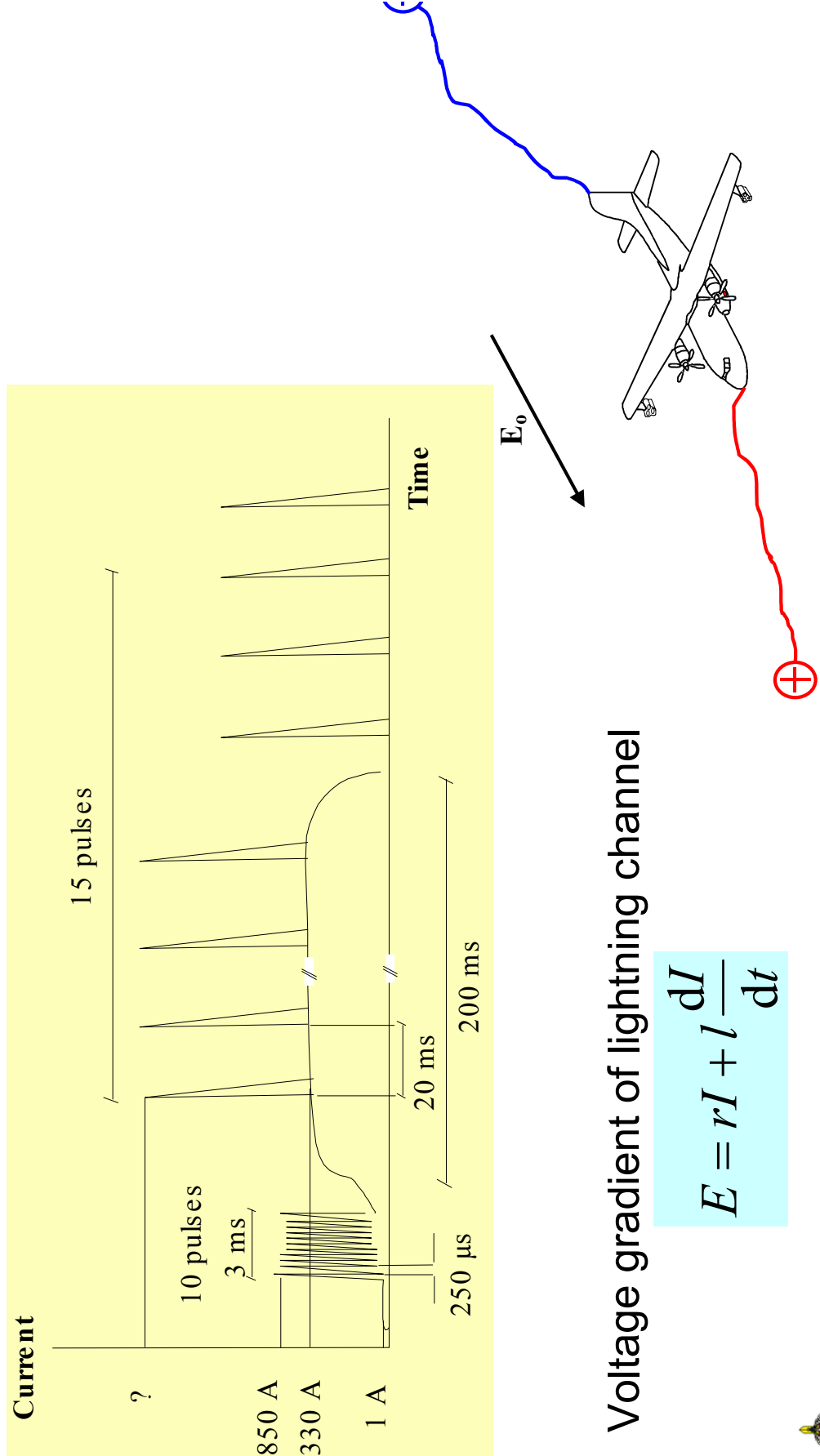
Direction of aerodynamic flow



Zoning strategy

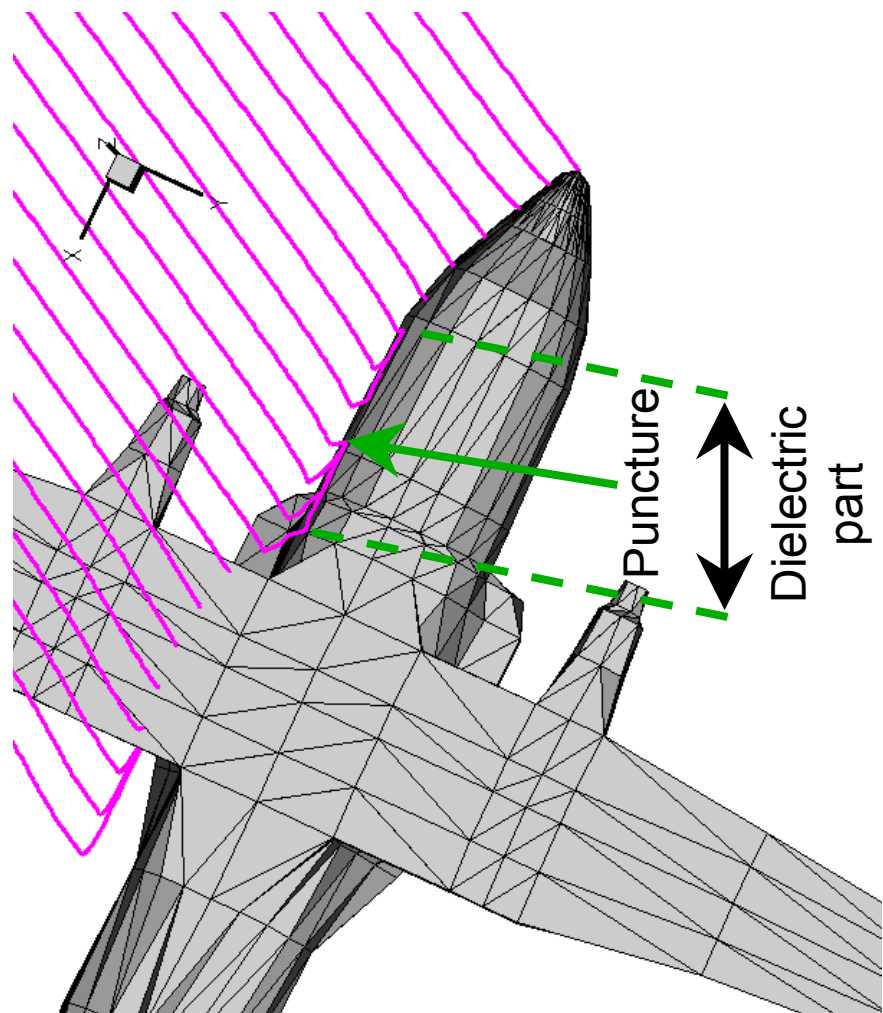


Typical lightning current



Voltage gradient of lightning channel

Example of swept stroke simulation



Future challenges

- Detailed modelling of the lightning channel
 - Transient currents
 - Turbulence and 3D dynamics
- Arc root phenomena
 - Influence of rivets, joints etc.
- Experimental validation

FoI

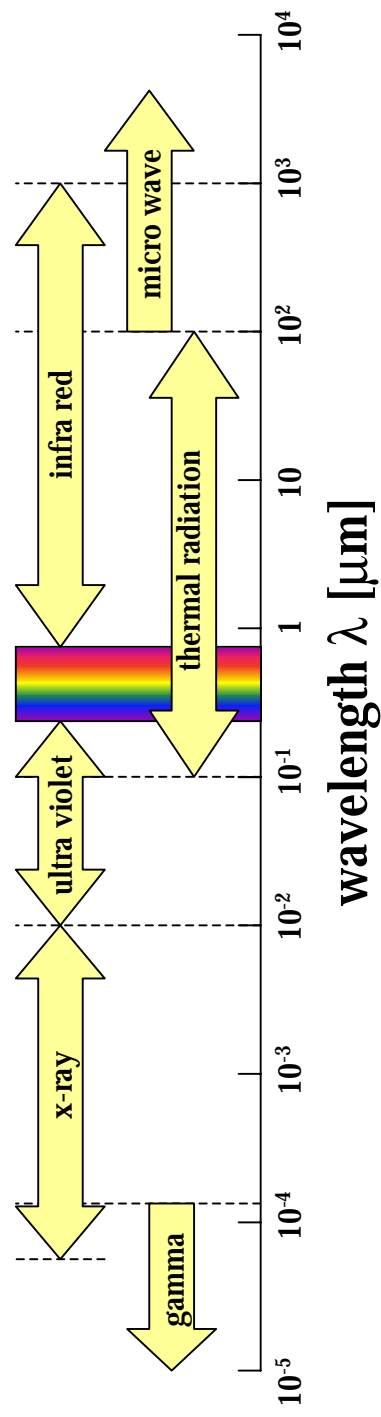
M. Andersson

IRR Calculations

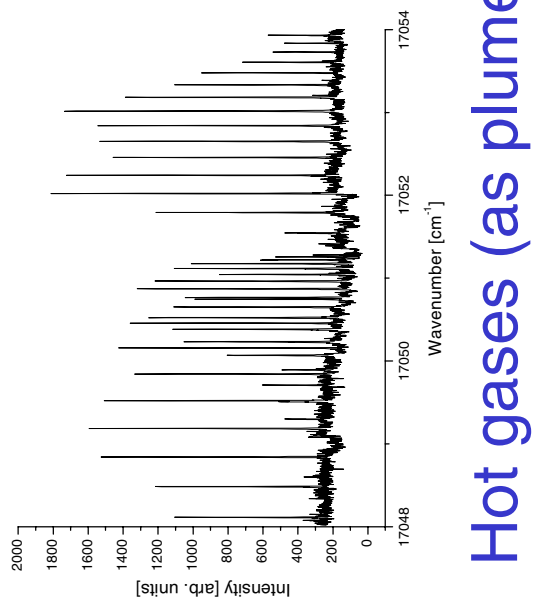
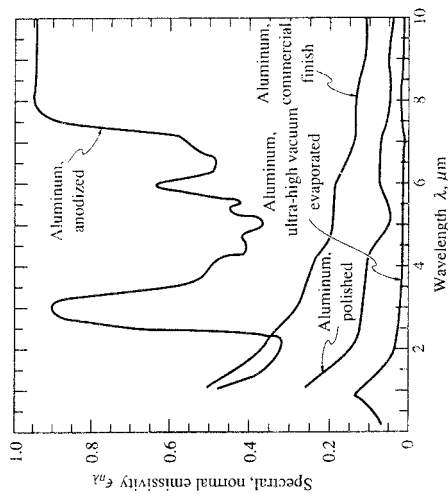
IR CALCULATIONS

Marlene Andersson and Ingmar Karlsson

- Radiative heat transfer
- Wavelengths: $\lambda \approx 0.7 - 14 \mu\text{m}$



Sources of IR Radiation



- Hot gases (as plumes)
- A body with $T > 0 \text{ K}$
- Gives an IR signature
- For some military vehicle a low IR signature is important

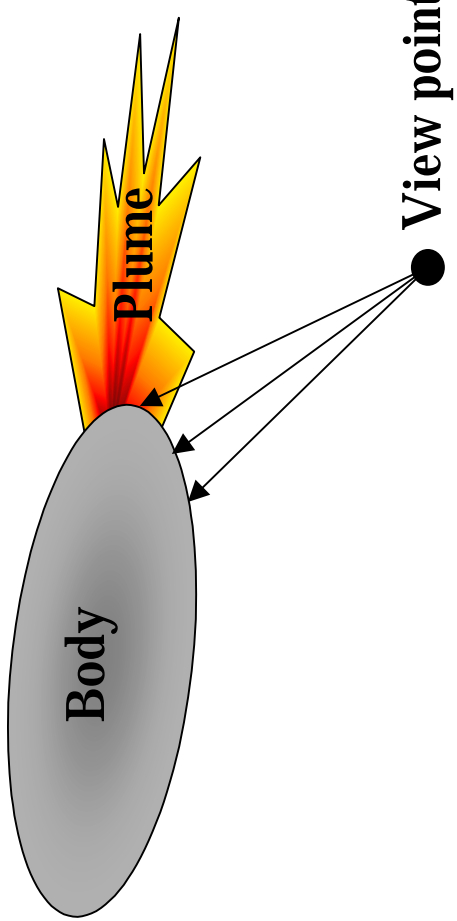
FOI

Calculation of IR Signature

- Intensity given by the equation of heat transfer:

$$I_\eta = I_\eta(0) e^{-\int_0^s \kappa_\eta ds'} + I_{b\eta} \left(1 - e^{-\int_0^s \kappa_\eta ds'} \right)$$

- Ray tracing:



FOI

The Module Based Code SIGGE

- Under development
- Calculate the IR signature
- Uses the CFD solution and mesh as input data
- Uses ray tracing
- Needs a database of gas data (i.e. absorption coefficients)
- Extendable software design
- Visualisation of the result

Local Preconditioning for Low-Speed Compressible and Incompressible Turbulent Flows

Shia-Hui Peng

FFA/FOI, SE-172 90 Stockholm
(E-mail: peng@foi.se)

• Motivation

- ▷ Improve convergence rates for low-speed flow computations
 - robustness of compressible codes for general configurations
 - coupled with time-marching algorithms, where the local time step is inversely proportional to the largest eigenvalue of the equation system
 - improve convergence for multigrid
- ▷ Improve convergence rates for high-speed flow computations
 - ▶ Use the same code for compressible and incompressible flows
 - ▶ Handle low-speed flows with local compressible effects
 - ▶ Handle wall-bounded, incompressible viscous flows
- ▷ ...

- Basic principle of local preconditioning

- ★ Diminish the large disparity between the eigenvalues of the equation system (u and $u \pm c$) at low Mach numbers
 - the time derivative terms in the equation system are premultiplied by a preconditioning matrix to re-scale the eigenvalues (and brings down the condition number to the order of unity)
 - the transient nature of the system is thus changed, but the converged steady solution should not be modified (for stationary flow computations)
- ★ For time-accurate computations, the dual time stepping method is used, where a pseudo-time derivative is introduced into the system, and the solution at each physical time step is treated as being "steady"

- **Preconditioning methodology**

- * The governing equations

$$\frac{\partial U}{\partial \tau} + \frac{\partial f}{\partial x} + \frac{\partial g}{\partial y} + \frac{\partial h}{\partial z} = L(Q) + S$$

where

$$U = \begin{pmatrix} \rho \\ \rho u \\ \rho v \\ \rho w \\ \rho E \end{pmatrix}, \quad f = \begin{pmatrix} \rho u \\ \rho u^2 + p \\ \rho uv \\ \rho uw \\ \rho uH \end{pmatrix}, \quad g = \begin{pmatrix} \rho v \\ \rho vu \\ \rho v^2 + p \\ \rho vw \\ \rho vH \end{pmatrix}, \quad h = \begin{pmatrix} \rho w \\ \rho ww \\ \rho wv \\ \rho w^2 + p \\ \rho wH \end{pmatrix}$$

- * The preconditioned system

$$P_c^{-1} \frac{\partial U}{\partial \tau} + \frac{\partial f}{\partial x} + \frac{\partial g}{\partial y} + \frac{\partial h}{\partial z} = L(Q) + S, \quad \text{or equivalently,}$$

$$P_c^{-1} \frac{\partial U}{\partial \tau} + A \frac{\partial U}{\partial x} + B \frac{\partial U}{\partial y} + C \frac{\partial U}{\partial z} = L(Q) + S$$

- ★ The preconditioning matrix, P_c^{-1} , must
 - be positive definite
 - not introduce time reversal into the diffusive terms
 - maintain well-conditioned inviscid eigenvalues (based on P_cA , P_cB and P_cC)
- ★ The preconditioning-based variables are not necessary to be a conservative set. For primitive variables, V , e.g. in a non-conservative system

$$P^{-1} \frac{\partial V}{\partial \tau} + \tilde{A} \frac{\partial V}{\partial x} + \tilde{B} \frac{\partial V}{\partial y} + \tilde{C} \frac{\partial V}{\partial z} = L_v(Q_v) + S_v$$

- ★ Retaining the conservative fluxes in the system, we employ a selected set of solution variables, W ,

$$\Gamma^{-1} \frac{\partial W}{\partial \tau} + \frac{\partial f}{\partial x} + \frac{\partial g}{\partial y} + \frac{\partial h}{\partial z} = L(Q) + S$$

- ★ Transformation of preconditioning matrices based on different dependent variables

$$P^{-1} = \frac{\partial V}{\partial U} P_c^{-1} \frac{\partial U}{\partial V}, \quad \Gamma^{-1} = P_c^{-1} \frac{\partial U}{\partial W}, \quad \Gamma^{-1} = \frac{\partial U}{\partial V} P^{-1} \frac{\partial V}{\partial W}$$

- ★ Local preconditioning is essentially to precondition the spatial residuals using local information from the node,

$$\frac{\partial W}{\partial \tau} + \Gamma(W) \text{Res}(W) = 0$$

- ★ Comparing to the eigenvalues $(\vec{v} \cdot \vec{n} \pm c)$ of the unpreconditioned system, the preconditioned acoustic eigenvalues may typically read

$$\begin{aligned} \lambda_{\pm} &= \frac{1}{2} \left\{ z \vec{v} \cdot \vec{n} \pm \sqrt{\left(z \vec{v} \cdot \vec{n} \right)^2 + 4 \left[\vec{n}^2 - \left(\frac{\vec{v} \cdot \vec{n}}{c} \right)^2 \right] \beta^2} \right\}, \quad \text{with} \\ z &= \left(1 - \alpha + \omega \frac{\beta^2}{c^2} \right) \end{aligned}$$

- Main consequences due to local preconditioning

- ★ Local time step ⇒ based on the preconditioned eigenvalue (becomes larger)
- ★ Scaling of artificial viscosity ⇒ rescaled (may become smaller)
- ★ Characteristic based boundary conditions ⇒ Riemann invariants are reformulated for the pseudo-acoustic waves
- ★ Solution updating ⇒ based on the selected variable set, W , and the conservative variables, U , are indirectly updated from W
- ★ Time-accurate computation ⇒

$$\frac{\Delta W}{\Delta \tau} \delta V + \Gamma \left(R_c - R_v - R_d - S \delta V + \frac{\Delta U}{\Delta t} \delta V \right) = 0$$

- Implemented preconditioning methods

- ★ Turkel's preconditioner, $W = (p, u, v, w, s)^T$ system
low-Mach number external aerodynamic flows
- ★ Choi-Merkle's preconditioner, $W = (p_g, u, v, w, T)^T$ system
low-Mach number external flows and low-Re number internal flows
- ★ Hakimi's preconditioner, $W = (p_g, u, v, w, H_g)^T$ system
low-Mach number compressible flows
- ★ Hakimi's preconditioner, $W = (p_g, u, v, w, E_g)^T$ system
low-Re number flows and non-Newtonian fluid flows
- ★ Weiss-Smith preconditioner, $W = (p, u, v, w, T)^T$ system
low-speed compressible and incompressible flows, available for $\rho = \rho(T)$

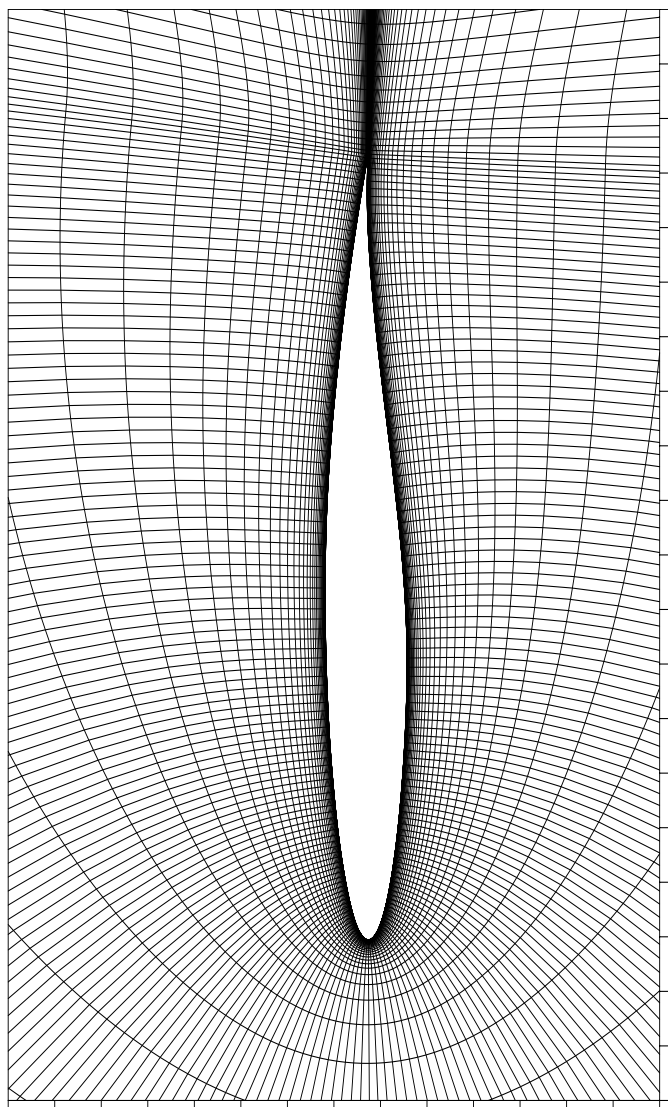
④ The gauge quantities are defined by

$$p_g = p - p_0, \quad H_g = H - \frac{\gamma p_0}{(\gamma - 1)\rho_0}, \quad E_g = c_p(T - T_0) - \frac{p - p_0}{\rho} + \frac{q^2}{2}$$

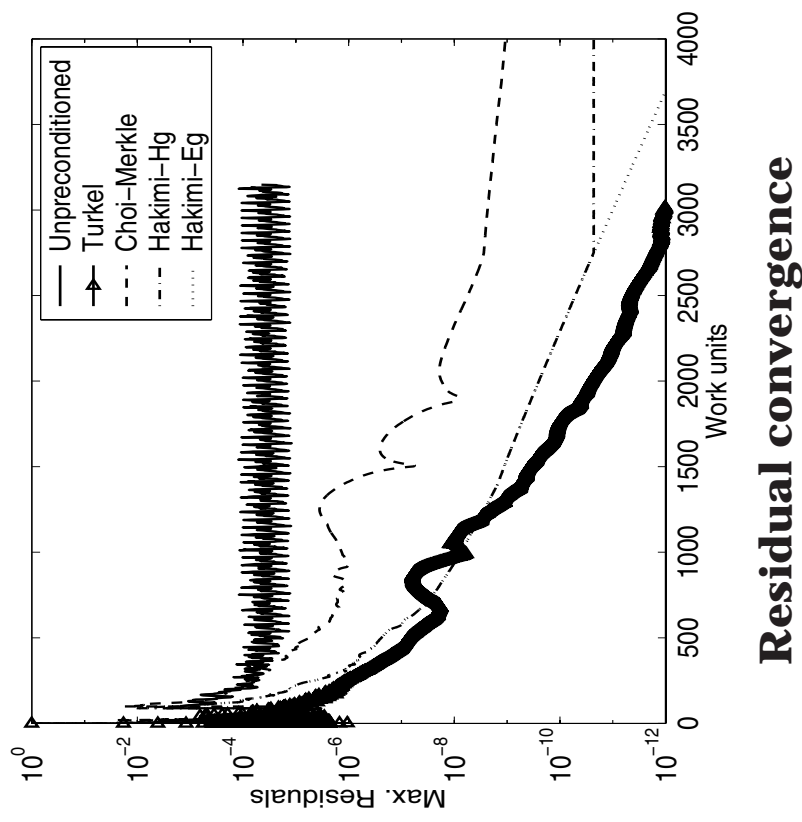
Example - Viscous flow over a RAE 2822 airfoil

$$M_\infty = 0.01, \alpha = 1.89^\circ, Re = 5.7 \times 10^6$$

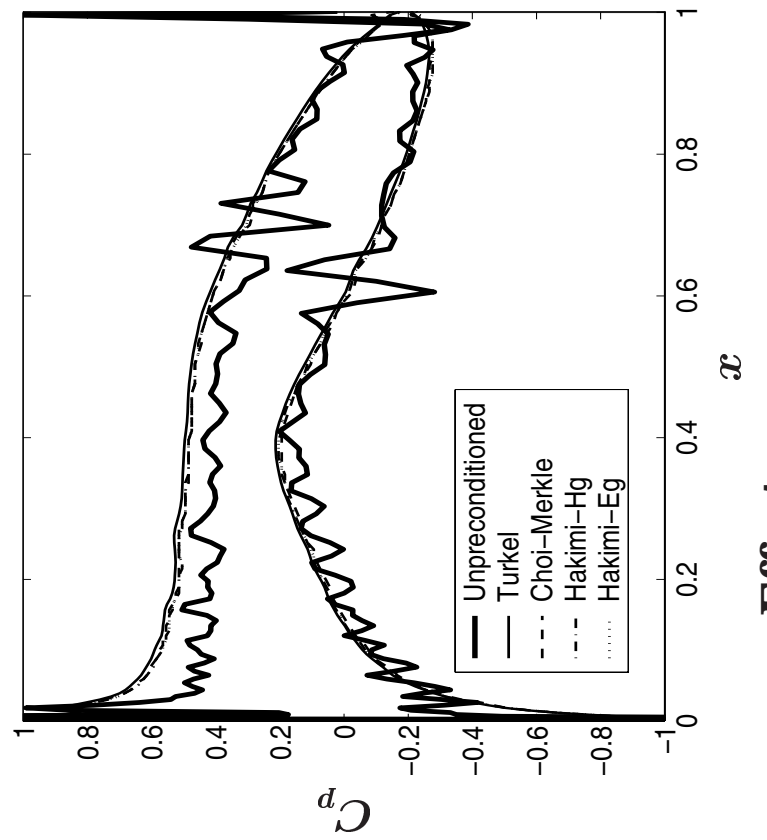
Standard $k - \omega$ turbulence model, C-type mesh with 257×65 nodes.



RAE 2822 airfoil: Residual convergence and preconditioning effect



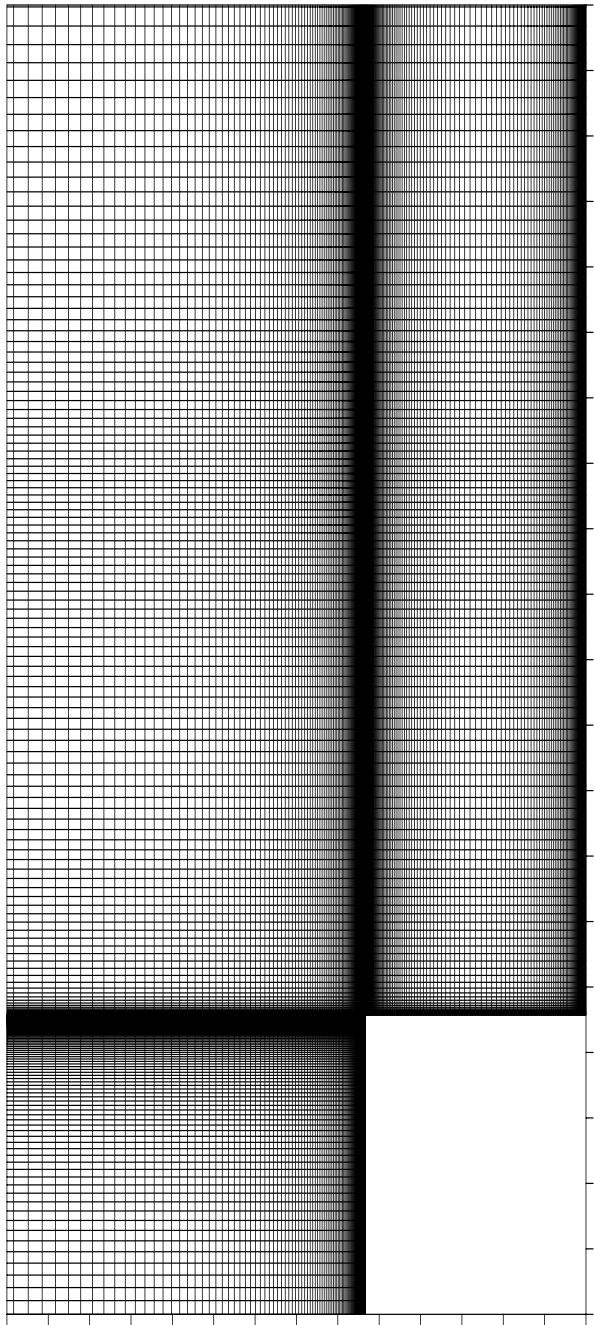
Residual convergence



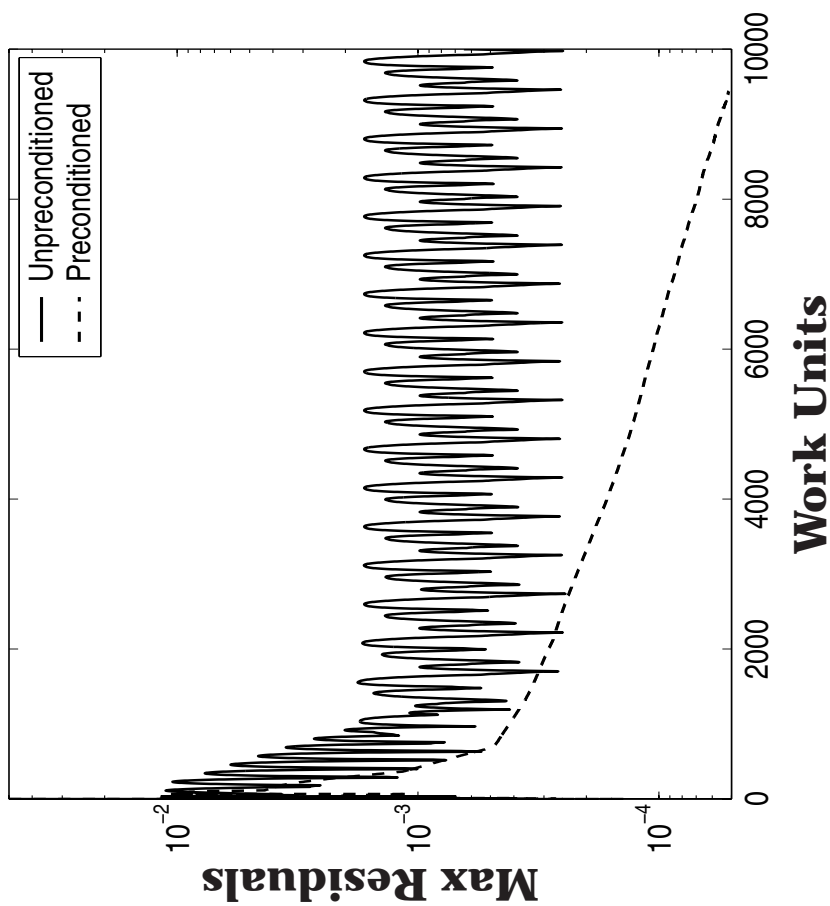
Effect on pressure

Example - Incompressible flow over a backward-facing step

$M_\infty = 0.128$ (normalized: $M_\infty = 0.003$), $Re = 3.75 \times 10^4$, $Re_\theta = 5000$
 $5h \times 44h$ domain, low-Re number $k - \omega$ model, with 241×225 nodes.

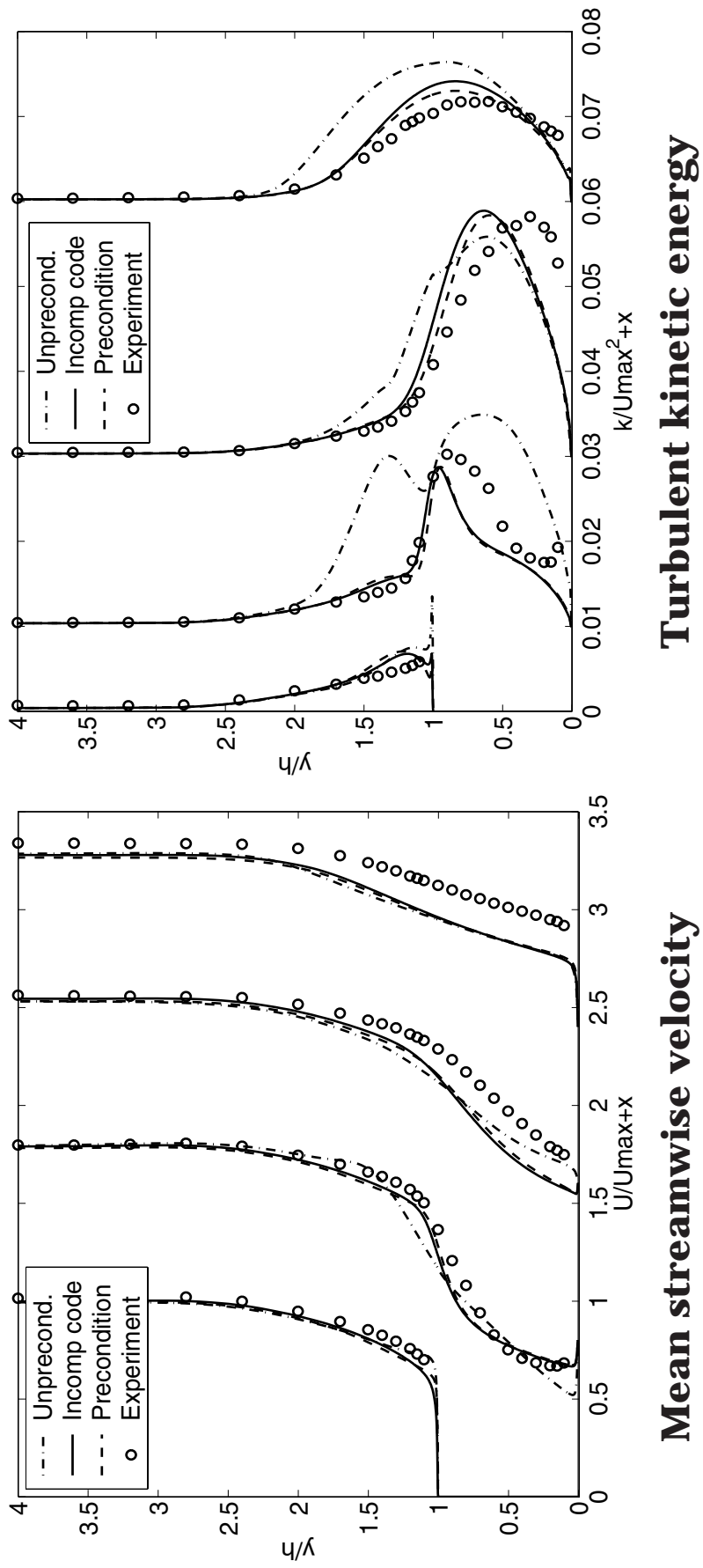


Backward-facing step flow: Residual convergence



Backward-facing step flow: Profiles at $x/h = 0, 2, 6, 16$ (from left to right)

(Compared with an incompressible code)

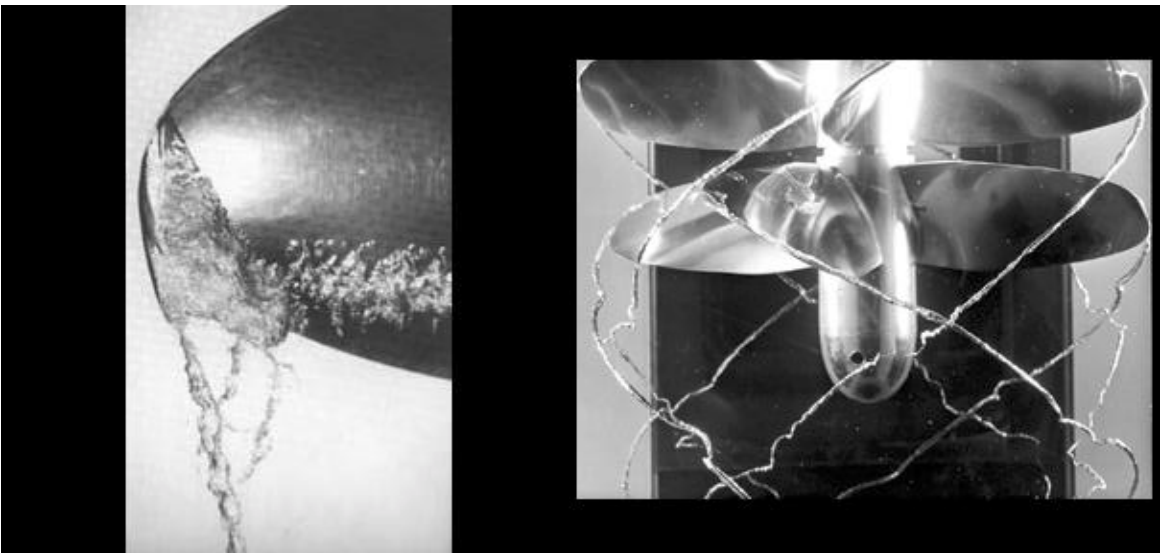


Mean streamwise velocity

Turbulent kinetic energy

- Some remarks

- ★ It is promising to use preconditioning for both inviscid and viscous low-speed external flows, and is very encouraging for internal viscous flows;
- ★ In spite of the same (or very similar) preconditioned eigenvalue, various preconditioners enjoy different degrees of success when dealing with different type of flows;
- ★ The parameter chosen in the preconditioning system plays a significant part in the convergence acceleration;
- ★ Comprehensive evaluation and comparison are being made on several typical preconditioners in applications to a wide range of flows;
- ★ Extensive validations and effort are on progress to implement preconditioning for time-accurate computations of incompressible flows in unsteady RANS and LES.



Utsikter för
kavitationsmodellering

Niklas Wikström
& Göran Bark

FOI

Vattenturbin & Fartygspropeller

För att förstå vad som hänt.

Spetsvirvelkavitation avslöjar Ubåt.

Buller redan vid låg propellerbelastning.

FOI

Något om kavitation

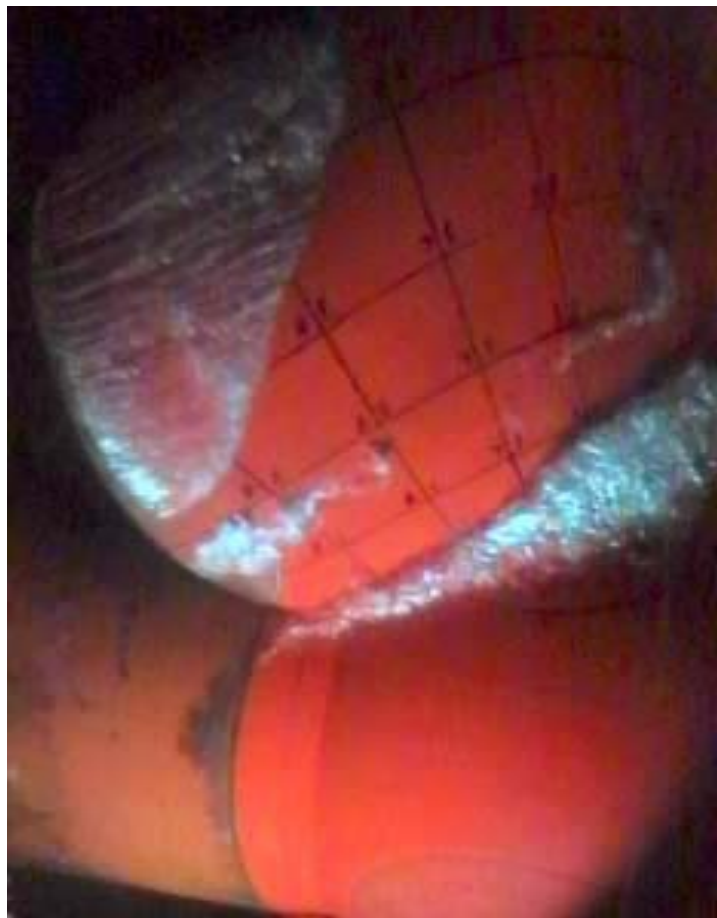
Gasblå sor skapas i lågtrycksområde, ofta invid struktur.
Konvekteras till region med högre tryck där kollaps påbörjas
och bubblan förintas.

Snabb kollaps kan skapa mycket höga tryckpulser, som i sin tur accelererar kollaps hos grannbubblor; Bubblesnöjd kollapsar ofta mycket våldsamt.

Vid ej våldsam kollaps - fluktuation lägre men hörbara tryckpulser. Skrovinteraktion - Taxfree-klirr.

Skikt kavitation

Bildas från bladets
framkant, på sugsidan.
Större skikt som stundom
beter sig mycket våldsamt i
olika kollapsförlopp...

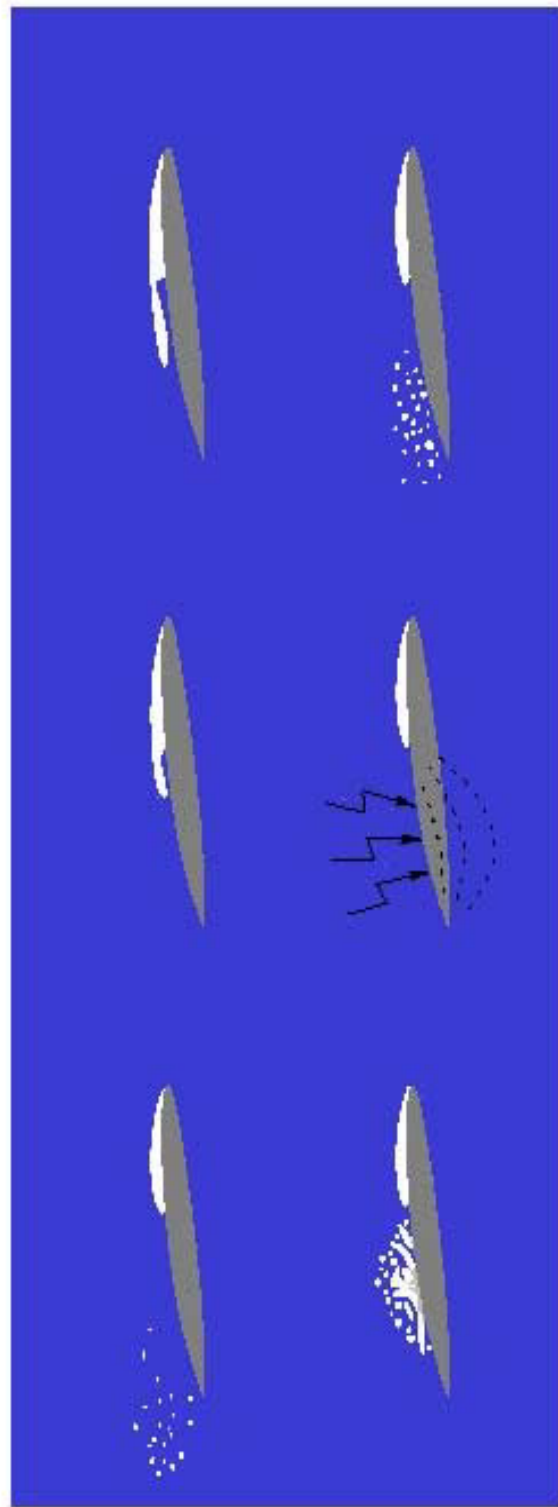


...Skiktkav. Två viktiga förlopp

Hela skiktet kollapsar som en bubbla.

Returstråle: Del snörps av och kollapsar. (Bild.)

Ofta flera återstudsar, molnkavitation

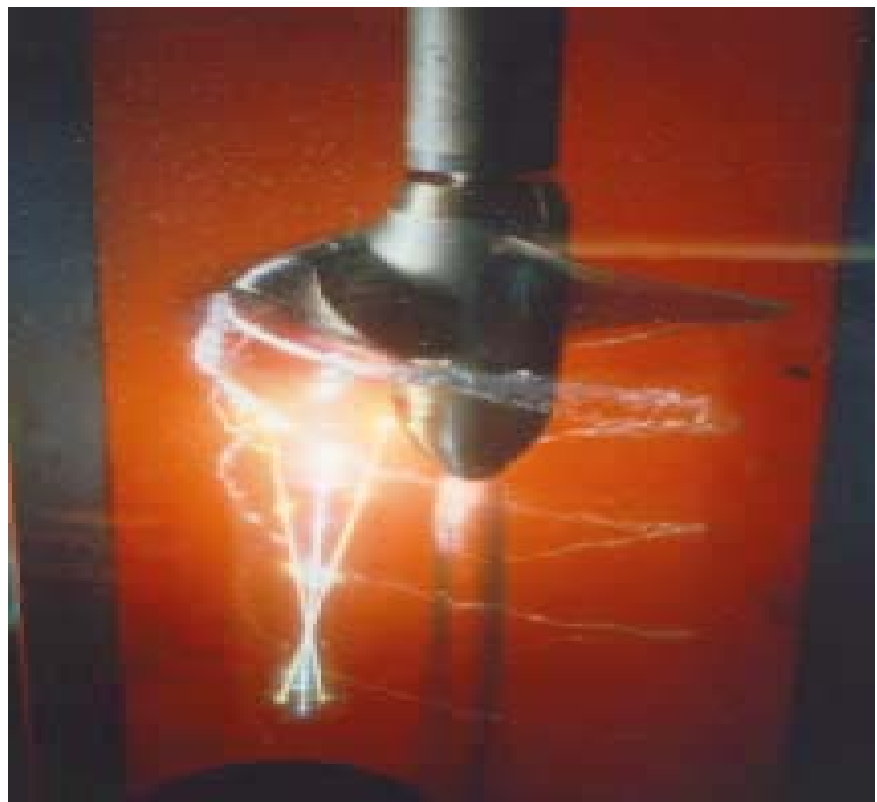


Erosionsskada från molnkavitation



FOI

Spetsvirvelkavitation...



Kraftiga virvlar rullas upp från bladspets och nav. Löst gas faller ut, och förångning av virvelkärnan. Skiktkavitet sugsin.

Cylindrisk pulserande kavitet.

Numerisk simulering för förståelse

Utveckla modell för kavitation i Navier-Stokeslösare.

Vi siktar inte på att lösa upp kollapsförloppens oerhört korta tidsskalor.

Kännedom om storskaligt förlopp kan ge ledtrådar om fortsatt utveckling.

FOI

Krängligheter

Två fasproblem (minst), med skarp fasgräns.

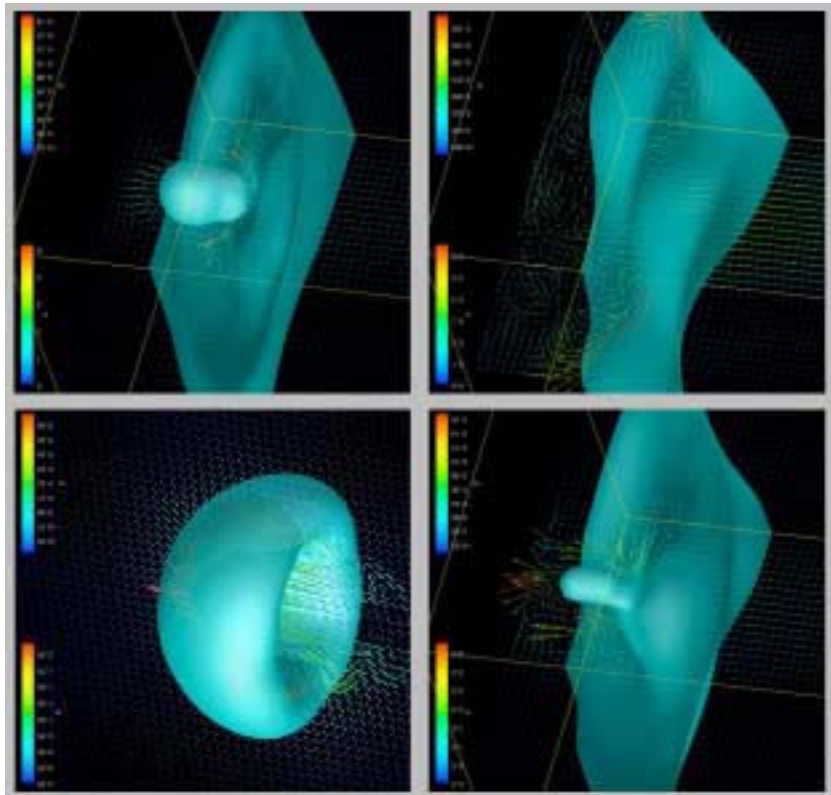
Kraftig krökning - ytspänning elak.

Komplex strömming.

Fasövergång som funktion av trycket.

FOI

Fri vätskeyta.



Lagrange vs. Euler

"Interface capturing"

Level Set & VOF

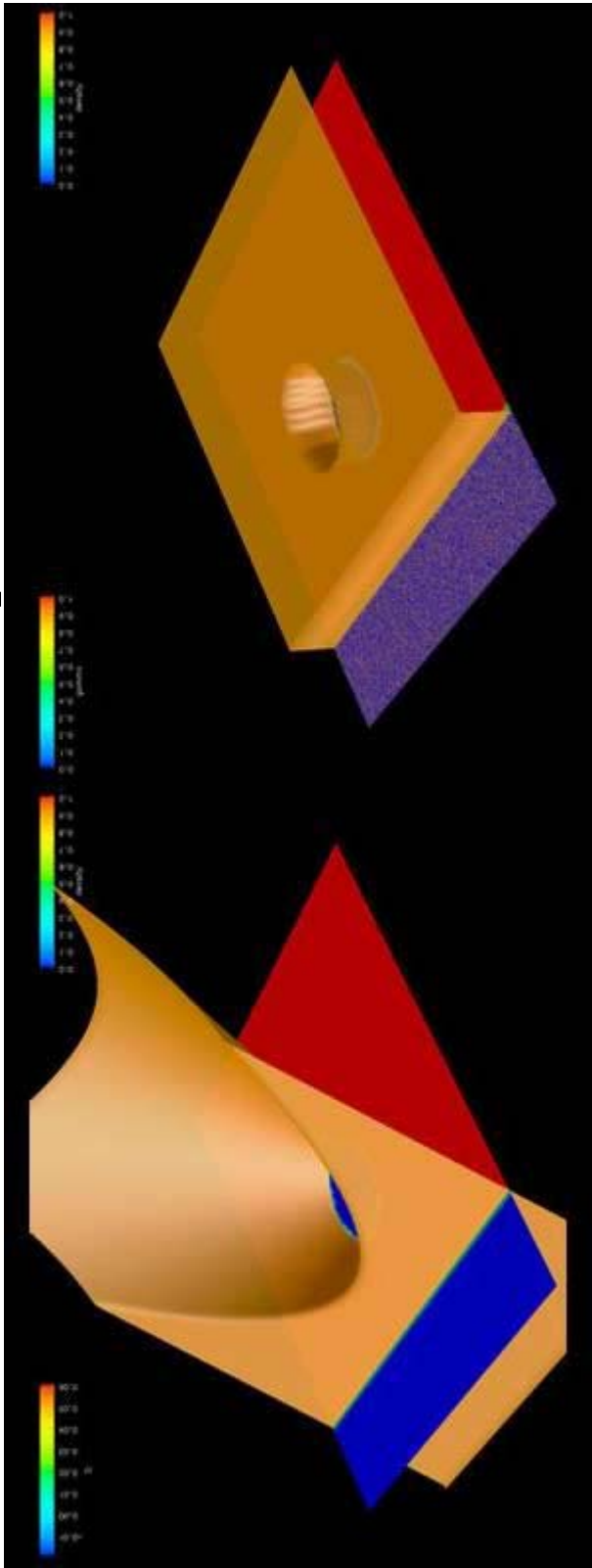
FOI

Level Set & Volume of Fluid

$$\frac{\partial \phi}{\partial \tau} + \nabla \cdot (\phi U) = S$$

Level Set:
Avståndsfunktion

VoF: Proportionell mot
fluidparametrar



FOI

Exempel på modell av fasövergång

$$\frac{\partial(\rho U)}{\partial t} + \nabla \cdot (\rho U U) = \nabla \cdot \tau - \nabla p + F$$

$$\nabla \cdot U = m \left(\frac{1}{\rho l} - \frac{1}{\rho v} \right)$$

$$\frac{\partial \phi}{\partial t} + \nabla \cdot (\phi U) = m \frac{1}{\rho l}$$

$$m = C^- \phi * \min(0, p - p_v) + C^+ \phi^2$$

FOI

Level Set, med gasfasen exkluderad?

Panelmetoder är långt utvecklade för kavitation.
Nästan uteslutande skikt-kaviteter. Enkel topologi.
Goda resultat. Tittar på dem.

Randvilkor för fri vätskeyta inne i domänen. Ångtryck
på bubbeldanden driver expansion/ kollaps.

Slipper empiriska källtermer.
Hittills blott endimensionell implementering.

FOI

UNDERWATER VEHICLE HYDRODYNAMICS

Niklas Alin, Urban Svennberg & Christer Fureby
Totalförsvarets Forskningsinstitut, FOI
Vapen & Skydd
Grindsjöns forskningscentrum



Introduction and Motivation

When designing submarines and UV vehicles hydrodynamic studies are needed to

- estimate performance characteristics
- examine and predict signatures (flow, pressure, noise, EM, internal waves, ...)
- help optimize tactical behaviour
- study manouevring characteristics
- study launch and recovery of torpedo, UUV, etc.
- hull-propulsor coupling

Potential flow, RANS and LES methods

$$\left. \begin{array}{l} \text{Re} = O(10^6) - O(10^{10}) \Rightarrow \text{resolution problems} \\ \Rightarrow \text{Improved turbulence and SGS models} \\ \Rightarrow \text{Basic research in turbulence necessary for applied research} \end{array} \right\} \begin{array}{l} \text{Homogenization} \\ \text{MILES} \end{array}$$

Interest in simulations of global and detailed flow features

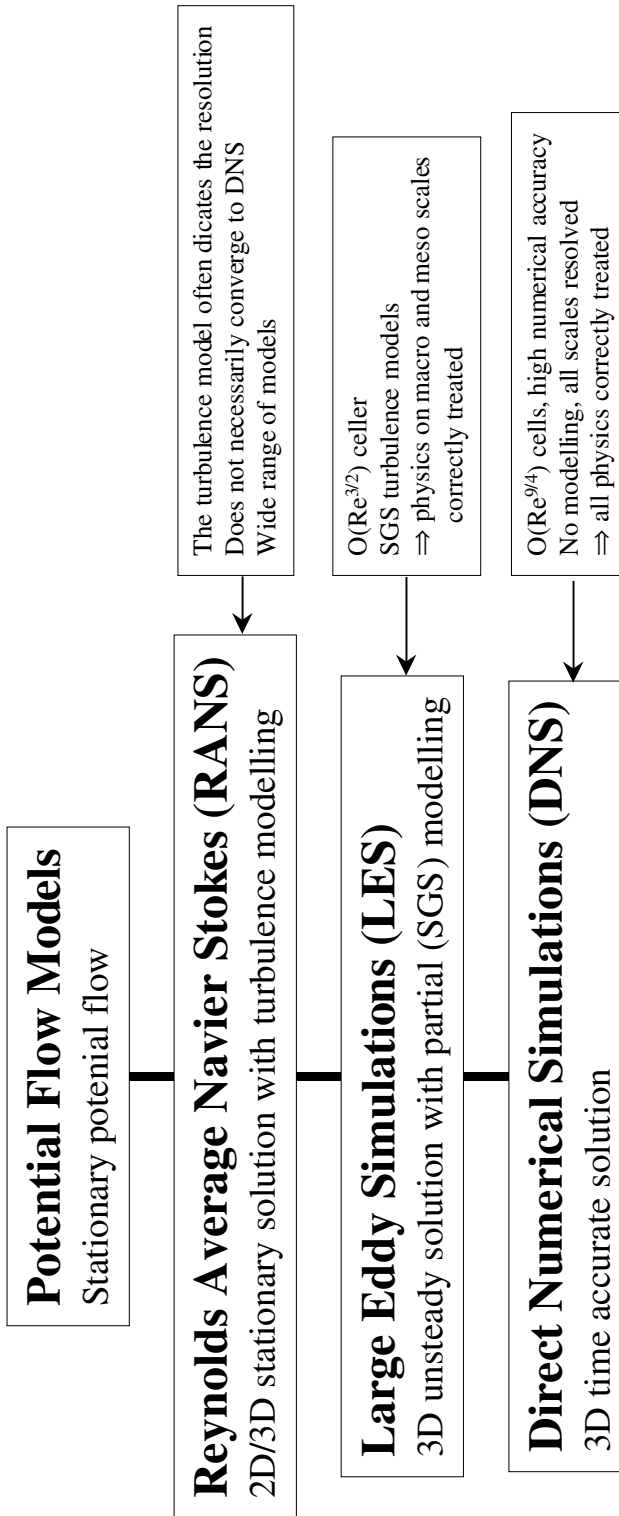
Need to study a wide range of problems (sphere – fully appended submarine)

- some examples will be presented

Overview of CFD methods

For naval applications we utilize the incompressible NSE

$$\partial_t(\mathbf{v}) + \nabla \cdot (\mathbf{v} \otimes \mathbf{v}) = -\nabla p + \nabla \cdot (2\mathbf{v}\mathbf{D}) + \cancel{\mathbf{f}}; \quad \nabla \cdot \mathbf{v} = 0$$



RANS & LES useful at different stages in the ship design chain

- RANS first order statistics & parameter studies
- LES second order statistics & flow dynamics

Summary of RANS and LES

RANS Time or ensemble averaged NSE

$$\nabla \cdot (\langle \mathbf{v} \rangle \otimes \langle \mathbf{v} \rangle) = -\nabla \langle p \rangle + \nabla \cdot (\mathbf{v} \nabla \langle \mathbf{v} \rangle - \mathbf{R})$$

- Model the Reynolds stresses $\mathbf{R} = \langle \mathbf{v}' \otimes \mathbf{v}' \rangle$
- Two-equation models (variants of the k- ϵ model)
- Differential stress models

LES Low-pass ‘spatially’ filtered NSE

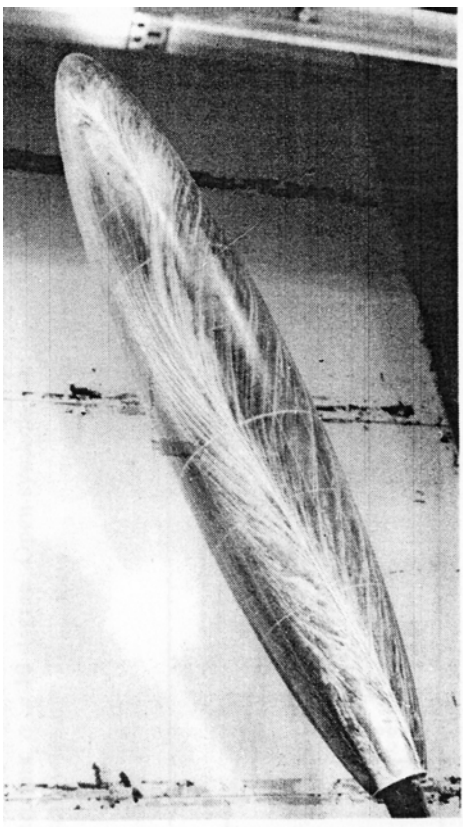
$$\partial_t \bar{\mathbf{v}} + \nabla \cdot (\bar{\mathbf{v}} \otimes \bar{\mathbf{v}}) = -\nabla \bar{p} + \nabla \cdot (\mathbf{v} \nabla \bar{\mathbf{v}} - \mathbf{B})$$

- Model the subgrid scale stresses $\mathbf{B} = (\overline{\mathbf{v} \otimes \mathbf{v}} - \bar{\mathbf{v}} \otimes \bar{\mathbf{v}})$
- Eddy-viscosity subgrid models $\mathbf{B} \approx -2\nu_k \bar{\mathbf{D}}$ with $\nu_k = c_k \Delta \sqrt{k}$
- Wall models

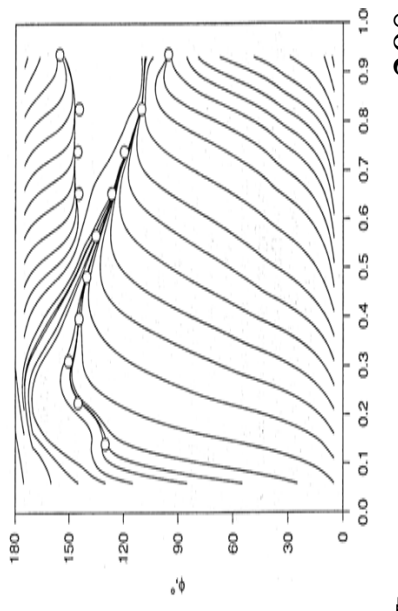
Numerics

- FV-discretization, CD for momentum, no additional diffusion
- 3pt backward differencing in time
- PISO-type algorithm for the pressure-velocity coupling
- Segregated approach with $C_o < 0.4$

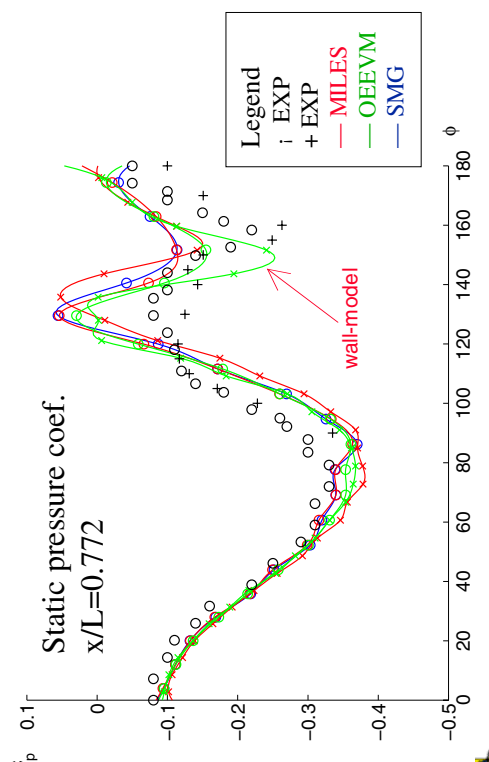
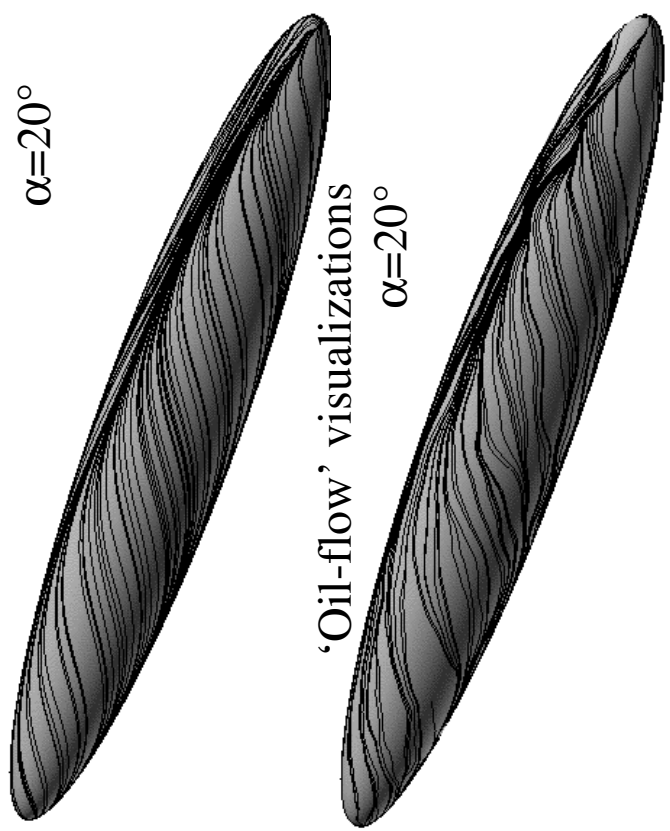
Flow Around a 6:1 Prolate Spheroid cont.



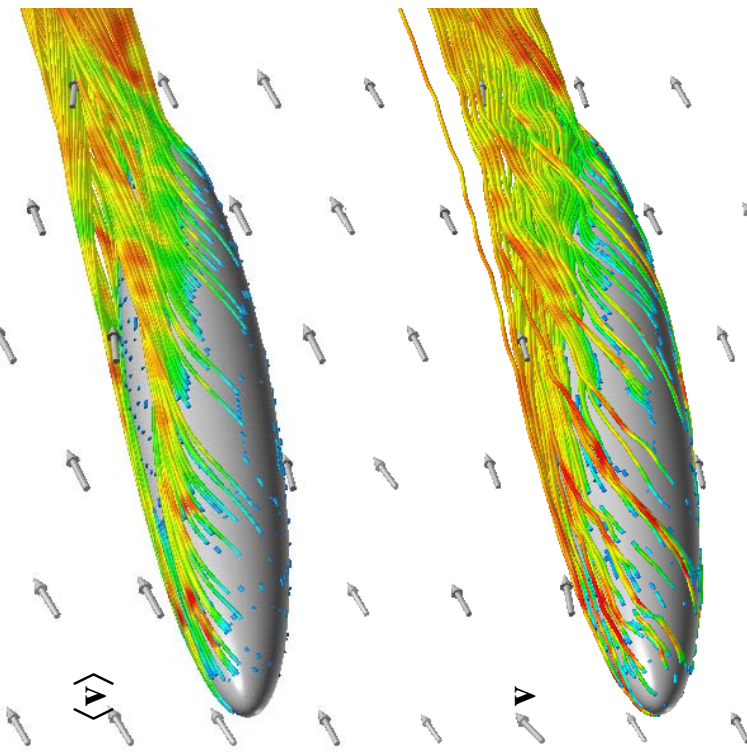
'Oil-flow' Simpson *et al.*, 1998, AIAA J., 36, p 557



$\alpha=20^\circ$

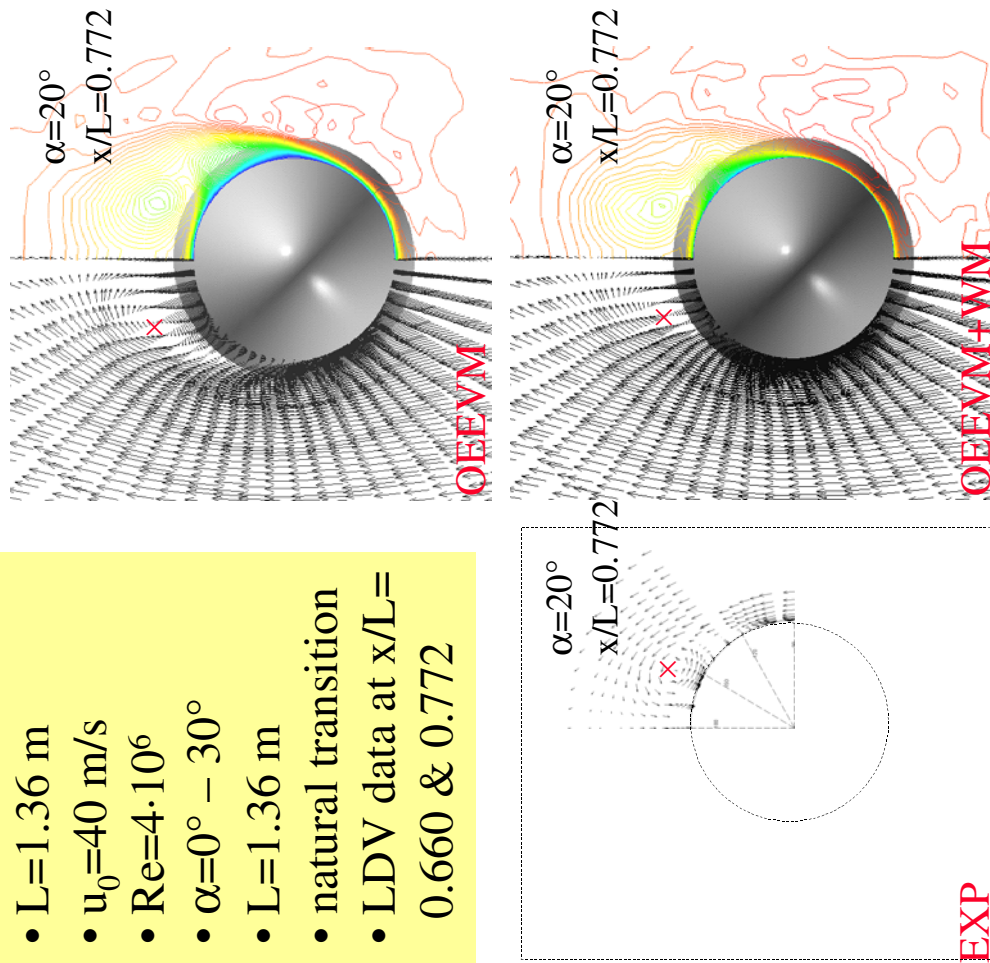


Flow Around a 6:1 Prolate Spheroid

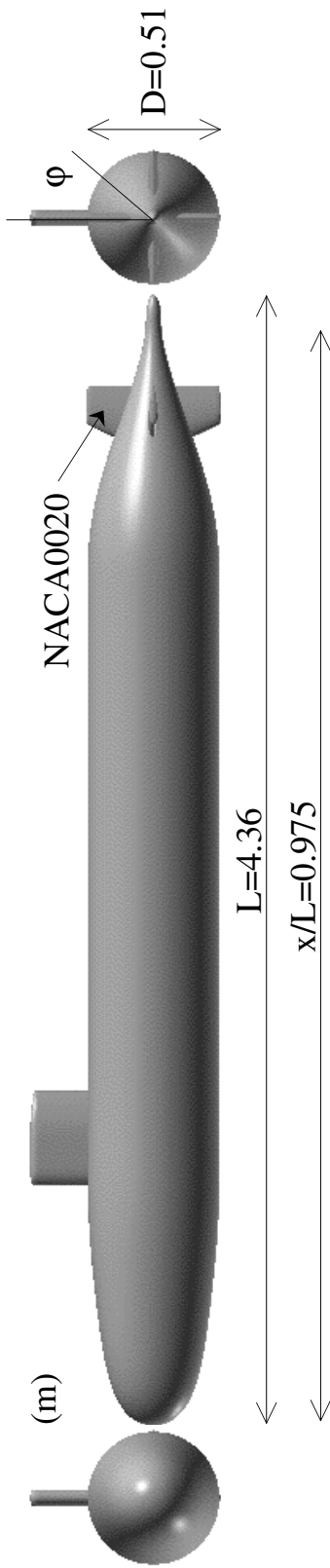


Exp. by
Chesnakkas, C.J. & Simpson, R.L.; 1996, J. Fluids
Eng., 118, p 268.

- $L=1.36$ m
- $u_0=40$ m/s
- $Re=4 \cdot 10^6$
- $\alpha=0^\circ - 30^\circ$
- $L=1.36$ m
- natural transition
- LDV data at $x/L=0.660$ & 0.772

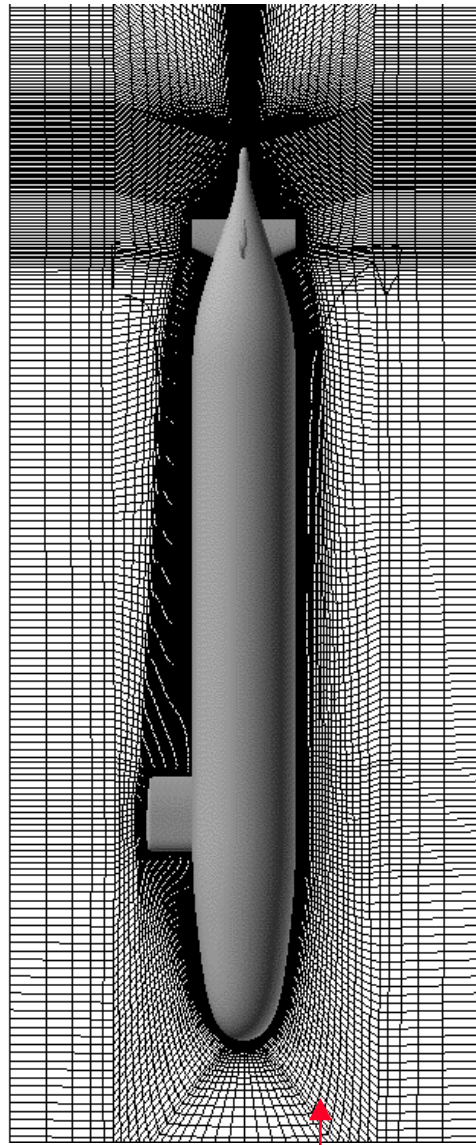


The DARPA Suboff Studies



DARPA AFF 8 Configuration

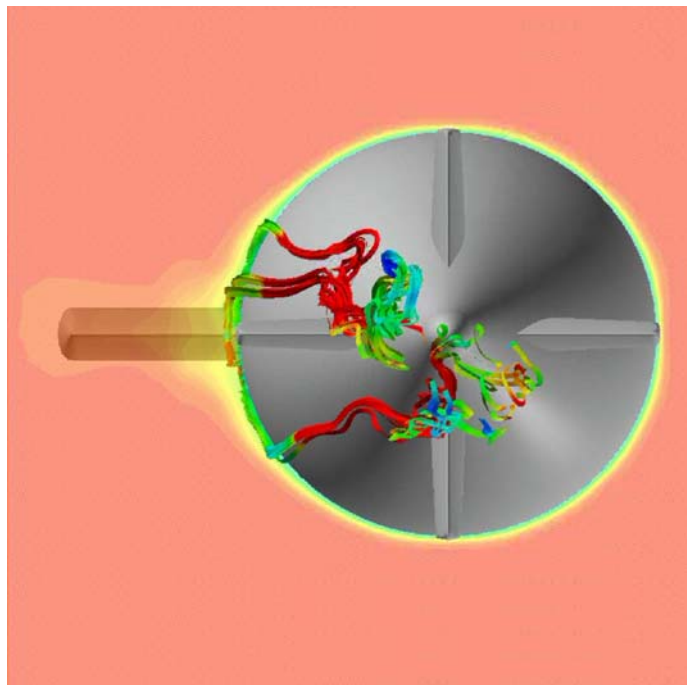
$Re = u_0 L / \nu = 12 \cdot 10^6$
 $u_0 = 43 \text{ m/s}$
Grid 1: $7.4 \cdot 10^5$ RANS
Grid 2: $1.1 \cdot 10^6$
Grid 3: $1.4 \cdot 10^6$ LES
Grid 4: $2.1 \cdot 10^6$
 $y^+ \approx 20-50$



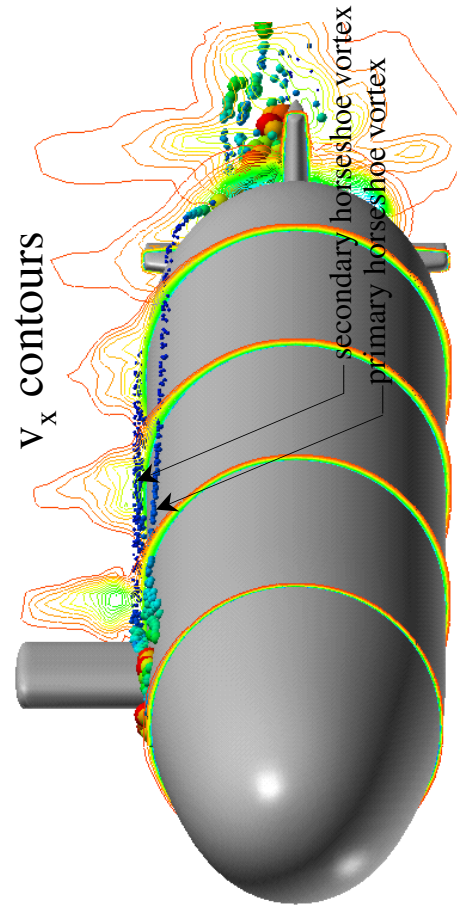
Groves, N.C. *et al.*, Report DTRC/SHD-1298-01, 1989
Huang, T.T., *et al.*, Proc. 19th Symp. on Naval Hydrodynamics, Seoul, Korea, 1992

The DARPA Suboff Studies cont.

Flow Physics



Hydrogen bubbles and
 V_x contours



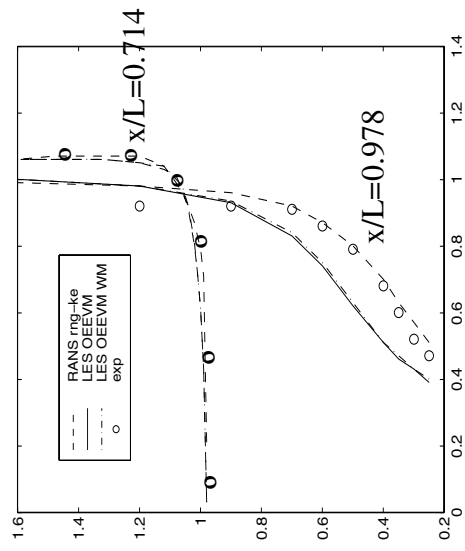
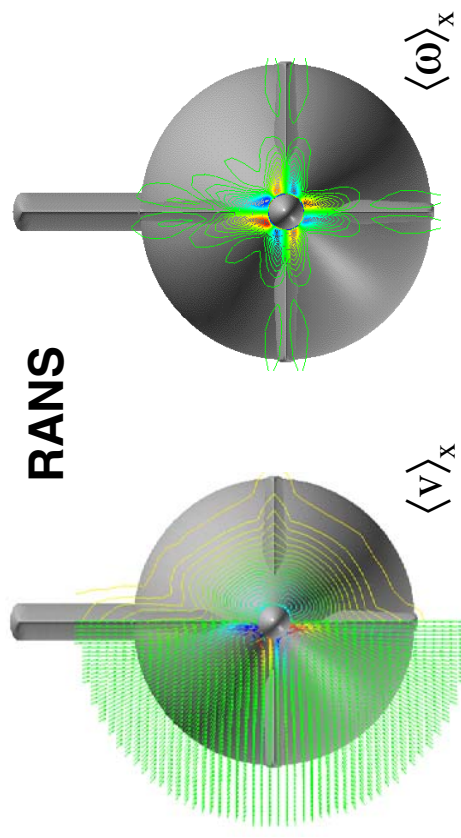
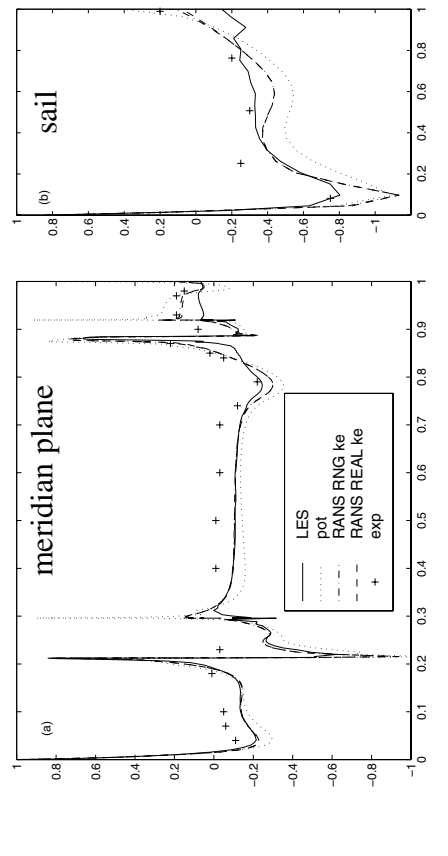
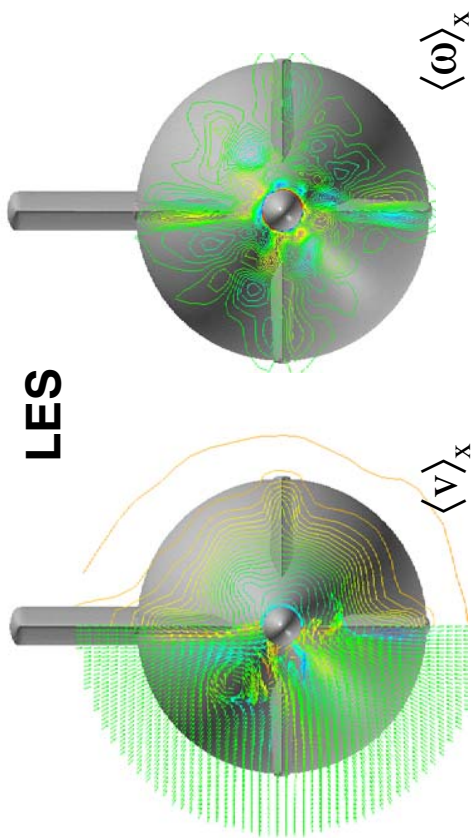
'Oil-flow' visualizations colored by $|\tau_w|$



Animation of V_x in a
plane moving aft and
instantaneous stream-
lines

The DARPA Suboff Studies cont.

Comparison between LES and RANS



Concluding Remarks

- RANS is a well-established method from which $\langle v \rangle$ and $\langle p \rangle$ can be predicted
- LES is a more recent method that predicts not only $\langle v \rangle$ and $\langle p \rangle$ but also the dynamics of the flow
- Both methods are needed in the field of naval hydrodynamics
- Vital to study the flow around naval ships to determine their hydrodynamic and acoustic signatures

Numerical Methods

Finite Volume discretization of RANS and LES equations

$$\begin{cases} \frac{\beta_i \Delta t}{\delta V_p} \sum_f [F_f^{C,p}]^{n+i} = 0 \\ \sum_{i=0}^m (\alpha_i (\bar{v})_p^{n+i} + \frac{\beta_i \Delta t}{\delta V_p} \sum_f [F_f^{C,v} + F_f^{B,v}]^{n+i}) = -\beta_i (\nabla \bar{p})_p^{n+i} \Delta t \end{cases}$$

- Crank-Nicholson time-integration
- Linear reconstruction of convective fluxes
⇒ 2nd order central scheme
- Central difference approx. for inner derivatives in $F_f^{D,v}$ and $F_f^{B,v}$
⇒ 2nd order central scheme

PISO pressure-velocity decoupling algorithm

Segregated approach with Co<0.3

The modified equations

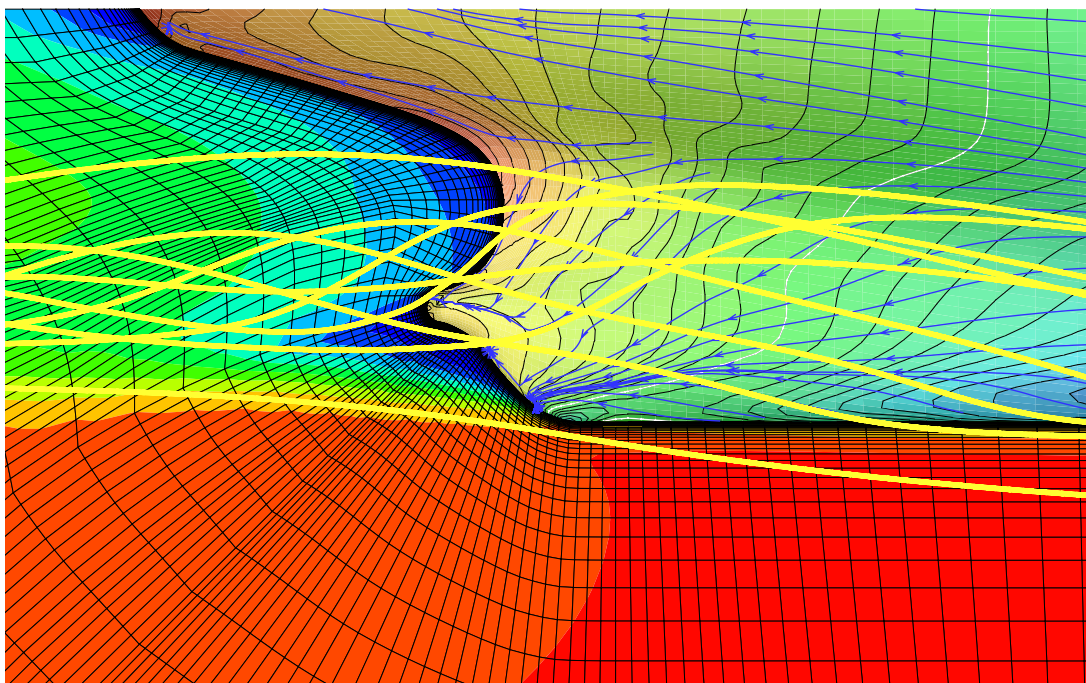
$$\begin{cases} \nabla \cdot (\bar{v}) = 0 \\ \partial_t (\bar{v}) + \nabla \cdot (\bar{v} \otimes \bar{v}) = -\nabla \bar{p} + \nabla \cdot (V_{eff} \nabla \bar{v}) + \nabla \cdot \{ (d \otimes d) [-\frac{1}{8} \nabla^2 \bar{v} + \frac{1}{6} \nabla \nabla^3 \bar{v}] + \dots \} \end{cases}$$

SGS term leading order truncation error

Surface Ship HYDRODYNAMICS

Urban Svennberg & Eric Lillberg
Totalförsvarets Forskningsinstitut, FOI
Vapen & Skydd
Grindsjöns forskningscentrum



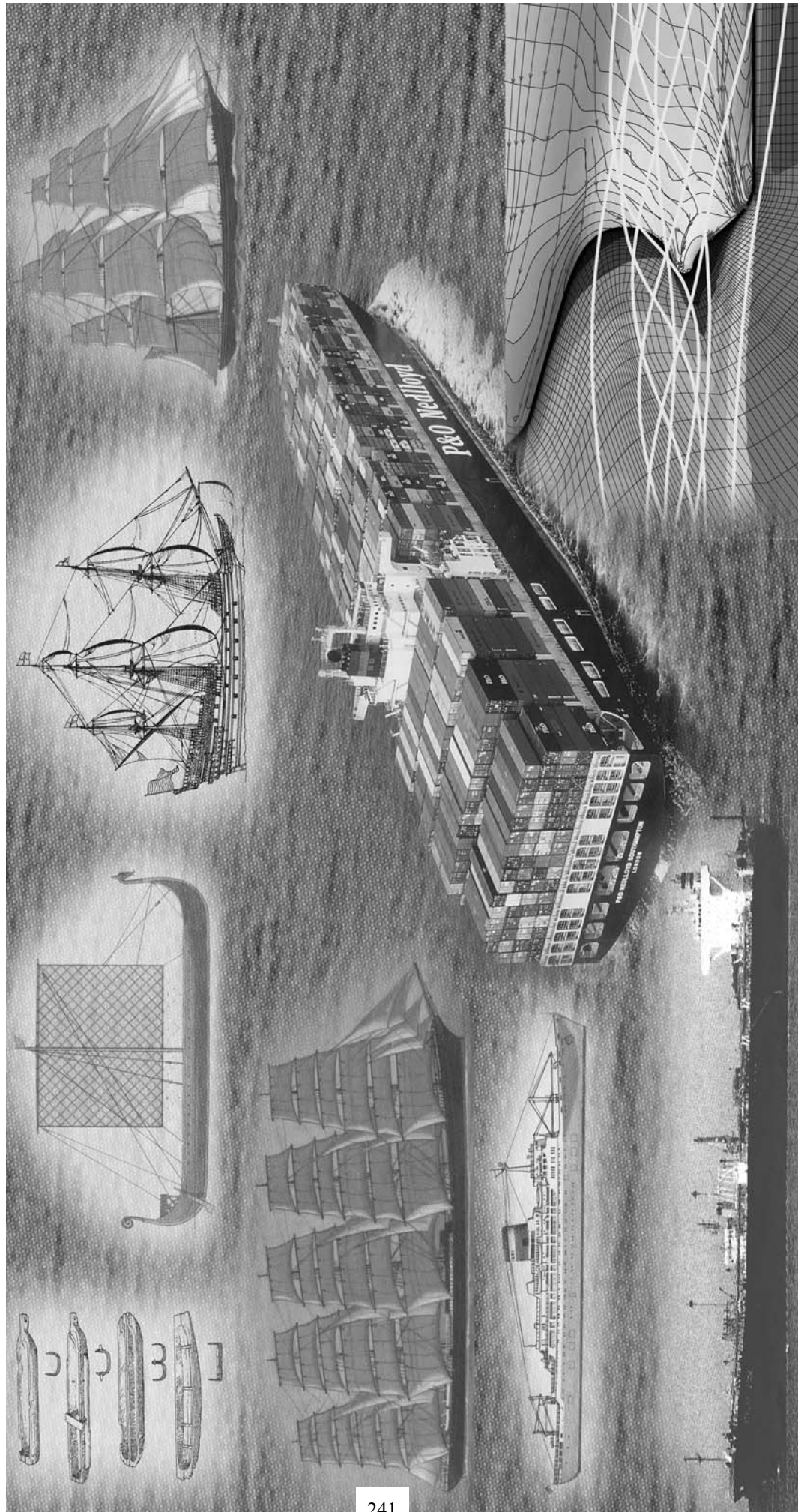


On Turbulence Modelling for Bilge Vortices: A Test of Eight Models for Three Cases

S. Urban Svennberg

Department of Naval Architecture and Ocean Engineering
CHALMERS UNIVERSITY OF TECHNOLOGY
Göteborg, Sweden, 2001

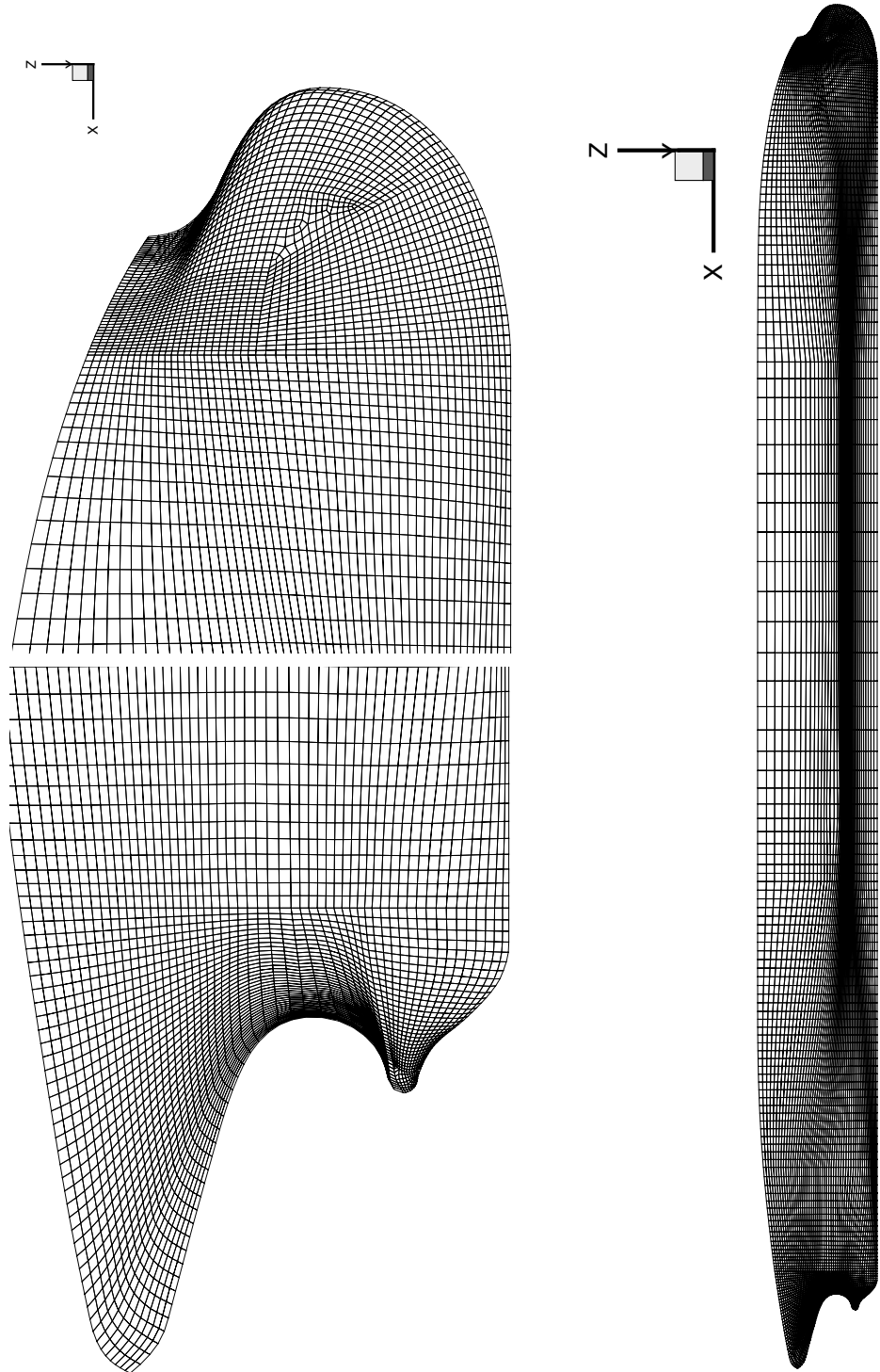
Introduction



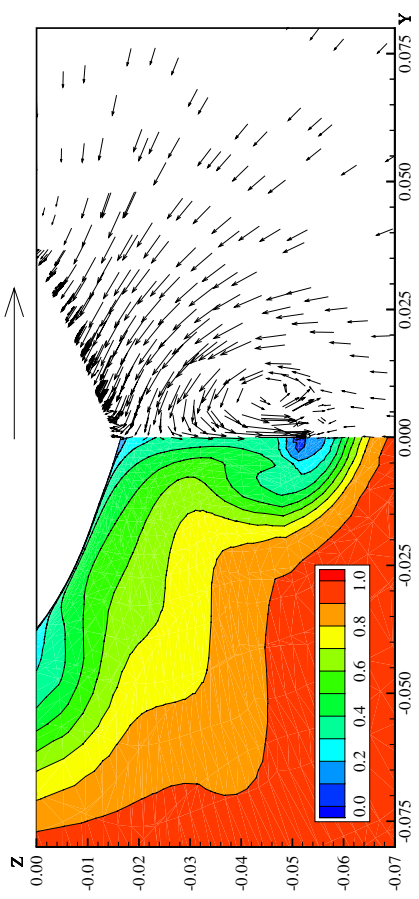
Characteristic Problems

1. **High Reynolds number:** $10^6 - 10^9$
 - Large interval of length scales
 - Thin boundary layers → Resolution problems
2. **Free water surface**
 - Robust algorithms for generic free-surface representation
 - Mesh topology and refinement issues
3. **Three dimensional curved surfaces**
 - Grid generation problems
 - Pressure gradients
 - Vortex separation and decay
4. **Moving geometries (propellers, rudders)**
 - Grid generation problems, complex geometries, moving grids and huge number of cells

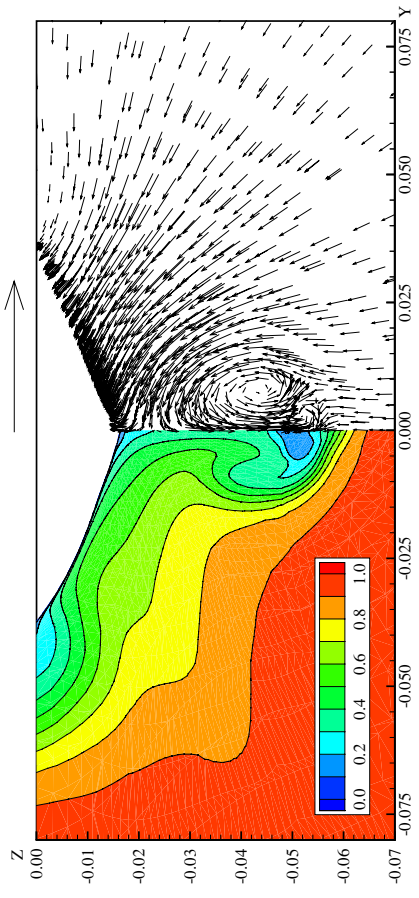
Surface Grid, KVLC2



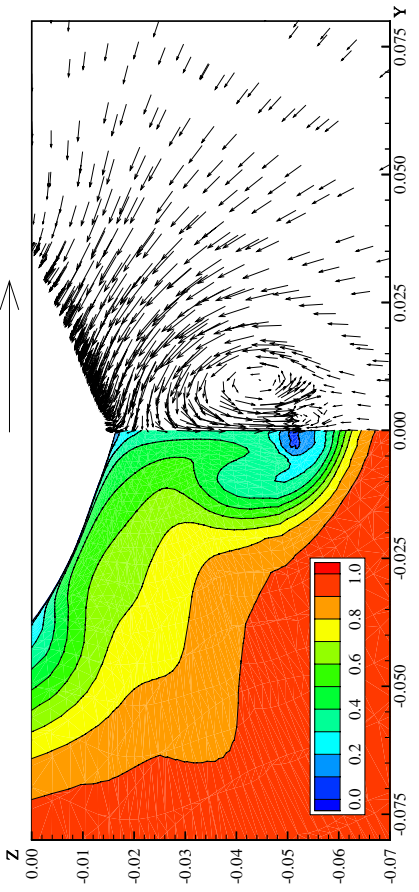
RSM model, four grids



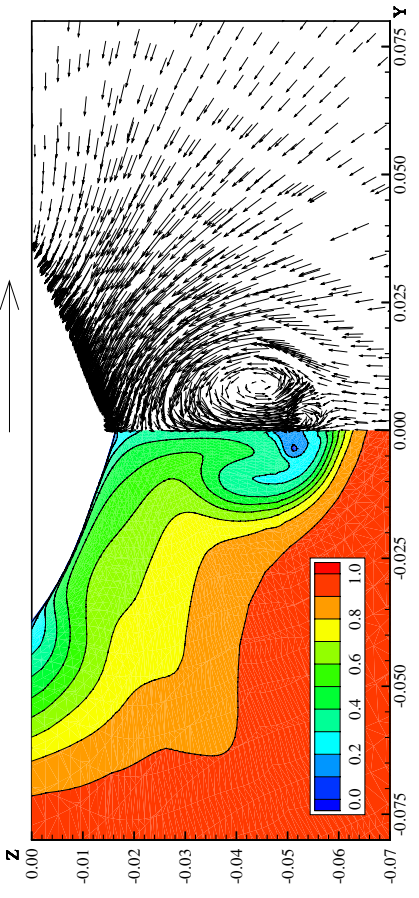
Coarse



Fine



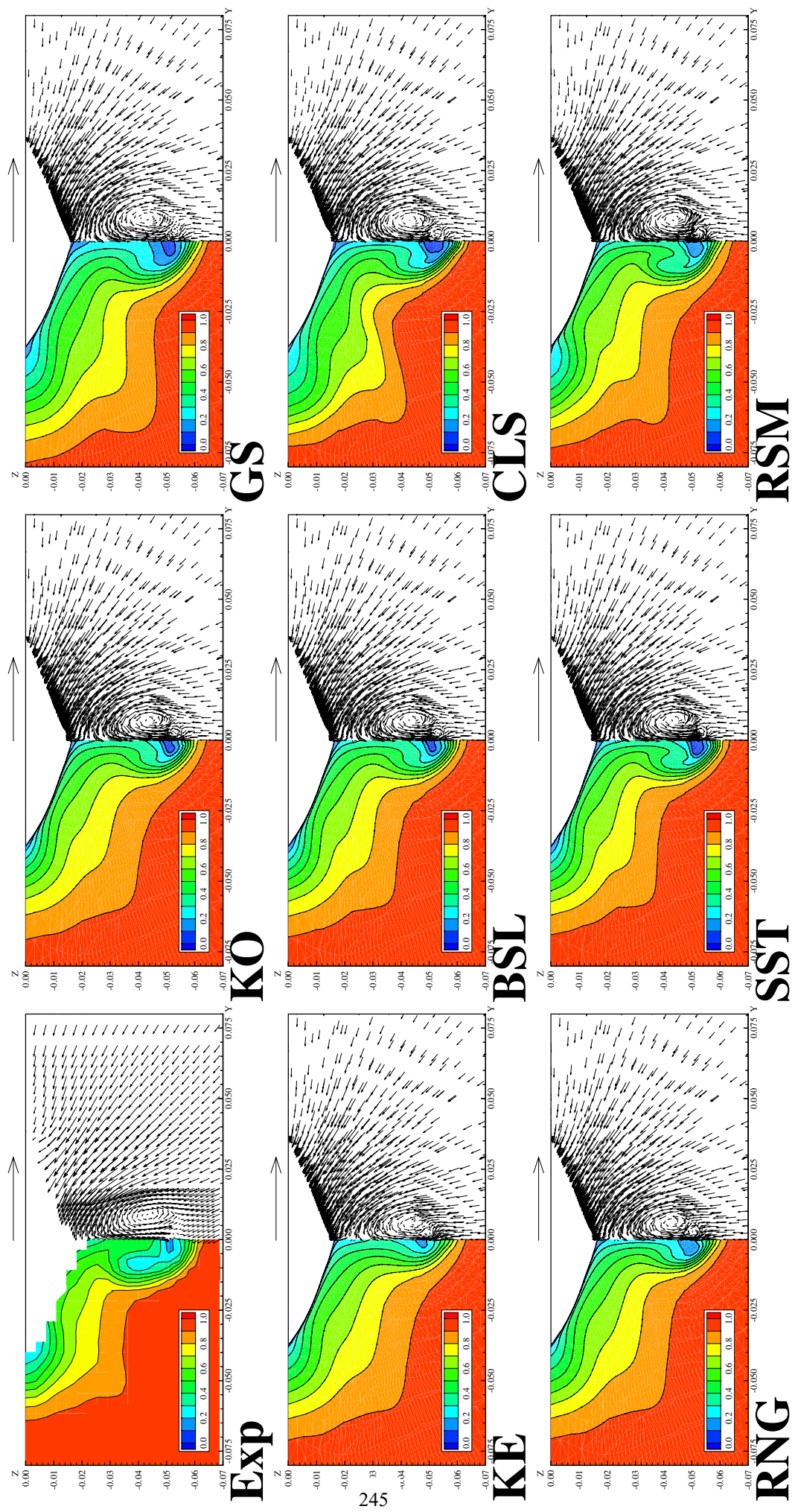
Medium



Extra Fine



Velocity Field, Propeller Plane



Velocity Field, X=0.5226

